SUPPLEMENTO
AL VOLUME IV, SERIE X, DEL
NUOVO CIMENTO
A CURA DELLA SOCIETÀ ITALIANA DI FISICA

1956 2° Semestre N. 4

ATTI
DEL
CONVEGNO INTERNAZIONALE
SULLA
PROPAGAZIONE DELLE RADIOONDE NELLA IONOSFERA
ORGANIZZATO DALLA SOCIETÀ ITALIANA DI FISICA

VENEZIA

OSPITE LA FONDAZIONE "GIORGIO CINI"

18-21 AGOSTO 1955

Indice generale

F. Carnelutti – Parole di saluto . . . . . pag. 1345
G. Polvani – Discorso inaugurale . . . . . » 1346
D. Graffi – Introduzione al Convegno . . . . . » 1349

* * *

T. Kahan – Turbulence ionosphérique et propagation des ondes électromagnétiques . . . . . » 1352
S. Chapman – The Electrical Conductivity of the Ionosphere: a Review » 1385
R. Naismith – Some Properties of the Meteoric E-Layer Used in Radio Wave Propagation . . . . . » 1413
M. Carlevaro – Some Remarks on the Theory of Self-Demodulation . . » 1422

V. A. Bailey – On the Interaction of Radio Waves . . . . . pag. 1430
M. Cutolo, G. C. Bonghi, F. Immirzi and P. Cachon – Ionospheric Self-modulation of Radiowaves . . . . . » 1450
K. Rawer – L'occultation des parcours phénomène important de la propagation ionosphérique . . . . . » 1460
E. Argence – Sur l'absorption des ondes courtes dans un milieu ionisé isotrope . . . . . » 1478
E. Argence et K. Rawer – Sur la détermination du nombre de chocs relatif à la région F_2 de l'ionosphère . . . . . » 1511
W. Dieminger and H. G. Möller – Echo Sounding experiments with Variable Frequency at Oblique Incidence . . . . . » 1532
A. Napoletano – On a Correlation between the Electronic Density of the E-Layer and the 500 mb Surface Position . . . . . » 1546
H. Bremmer – Remarks on the Connection between Mode Theory and Ray Theory . . . . . » 1552
I. Ranzi – On Some Characteristics of the F_2 Region in South America » 1559
N. C. Gerson – The Ionized Aurora . . . . . » 1562
P. Dominici – Some Observations on the Influence of a Solar Eclipse upon the Ionosphere . . . . . » 1572
F. Mariani – Some Considerations on Temperature Effects in the Upper Atmosphere . . . . . » 1579
F. Mariani – Diffusion in a Not-Isotherm Ionosphere . . . . . » 1586
P. Dominici and F. Mariani – Some Critical Considerations on the Parameters h' and f_0 of the Ionospheric Layers . . . . . » 1589
N. Carrara – Problemi sulla spettroscopia con microonde molecolari dell'ossigeno. Misura della larghezza delle righe di assorbimento. . . . . » 1593

La Direzione del Nuovo Cimento *ringrazia vivamente il dott.* L. Caprioli *per l'aiuto dato nella raccolta dei testi e delle discussioni seguite alle Relazioni e Comunicazioni presentate al Convegno e per tutta la compilazione e sistemazione di questo fascicolo.*

SUPPLEMENTO AL VOLUME IV, SERIE X
DEL NUOVO CIMENTO

N. 4, 1956
2° Semestre

Parole di saluto.

F. CARNELUTTI

Presidente del Centro di Cultura e Civiltà della Fondazione « G. Cini » - Venezia

Il Centro di Cultura e Civiltà della Fondazione « Giorgio Cini » non desidera essere ringraziato, ma al contrario ringrazia per aver avuto l'occasione di offrire ospitalità nella sua sede a una delle manifestazioni più importanti dello sforzo che mira a procurare agli uomini una più ampia e profonda conoscenza della natura. Tale manifestazione ha il suo posto nel quadro dei mezzi idonei ad accrescere la civiltà la quale non è altro che la misura della loro capacità di vivere in pace.

Noi non siamo di quelli che considerano i rapporti tra scienza e civiltà con un ottimismo superficiale. Al contrario noi pensiamo che la scienza, e in particolare la scienza della natura, non sia l'ultima responsabile della crisi che, secondo l'unanime riconoscimento, la civiltà sta attraversando. Ci si può facilmente rendere conto che, fino ad un certo punto, quelle che si chiamano le vittorie dell'uomo sulla natura, hanno aperto le vie dell'orgoglio, che sta sempre in agguato nell'animo umano. E questo è il bacillo della crisi. Non sarebbe difficile dimostrare che proprio dalla scoperta della legge, che è un vanto della fisica, anzi di quella che allora si chiamava la fisica celeste, ha preso l'abbrivio quello slancio della filosofia, nella quale la crisi trova non tanto la causa quanto il sintomo manifesto. Ma non c'è miglior rimedio per combattere questo virus di quello che la scienza continui imperterrita la sua strada. La crisi, dopo tutto, è un fenomeno di adolescenza. È una mezza scienza quella che cagiona all'uomo l'illusione del dominio. Man mano che la scienza si dilata e si approfondisce, essa gli procura, accanto al sapere, quella forma superiore del sapere, che è il sapere del non sapere. Man mano che egli si immerge nella scienza dell'universo non tanto si addensano intorno a lui le ombre quanto sempre più l'abbaglia la luce del mistero.

Allora io penso che voi mi potete permettere di offrirvi quale augurio, anzi quale auspicio per i vostri lavori, il nostro emblema: San Giorgio, a cavallo, che trafigge il drago, è il simbolo della Scienza che, infaticata e infaticabile, consapevole che il suo traguardo non è l'irraggiungibile verità, ma lo sforzo inesausto per raggiungerla, sgombra non tanto dall'ignoranza, quanto dalla superbia l'animo dell'uomo.

SUPPLEMENTO AL VOLUME IV, SERIE X
DEL NUOVO CIMENTO

N. 4, 1956
2° Semestre

Discorso inaugurale.

G. POLVANI

Presidente della Società Italiana di Fisica

Nella seduta inaugurale di un qualsiasi convegno scientifico — grosso o piccolo che sia, nazionale o internazionale, di ampio o ristretto tema — tre sono in generale i punti che vengono trattati: si porge da parte dell'ospitante il benvenuto e l'augurio all'ospite; si parla del convegno stesso definendone gli scopi, precisando la situazione delle conoscenze che si hanno circa l'argomento o gli argomenti che verranno trattati, presentando, per così dire, le « dramatis personae »; si entra infine nel vivo delle questioni scientifiche con una prolusione specifica che dia il via alle discussioni.

Ora il primo punto voi avete sentito con quanta squisita cortesia sia stato svolto dal Presidente del Centro di Cultura e Civiltà della Fondazione Cini, il prof. CARNELUTTI, il quale ne ha tratto occasione per esprimere il suo giudizio — giusto giudizio — sulle finalità e possibilità della scienza. Al secondo punto si volgerà tra un momento il prof. GRAFFI, Presidente del nostro Convegno, parlando con tutta la perizia scientifica, che gli proviene dai suoi studi e dalle sue ricerche, e con tutta la conoscenza minuta della organizzazione del Convegno da lui pensata, diretta ed attuata. Al terzo punto infine provvederà il prof. KAHAN dell'Istituto Poincaré di Parigi, trattando il tema fondamentale della turbolescenza ionosferica e degli effetti che essa può produrre sulla propagazione delle onde elettromagnetiche.

Francamente quindi non si vede — almeno a prima giunta — la necessità o l'opportunità che altri prenda la parola e s'inserisca, col suo dire, tra il Presidente del Centro, il prof. CARNELUTTI e il Presidente del Convegno, il professor GRAFFI.

Tuttavia mi si voglia da parte di tutti scusare per questa mia intromissione anche perchè la colpa non è tutta mia. Il prof. GRAFFI accolga il mio più vivo ringraziamento per avermi infatti pregato che anch'io pronunciassi — come si suol dire — due parole all'inaugurazione di questo Convegno; e più ancora per aver voluto reciprocamente accogliere la mia preghiera di cedere a me l'onore di esprimere per primo alla Città di Venezia, e per essa a lei Signor Sin-

daco, la viva gratitudine dei congressisti per la cortese gentile ospitalità con cui siamo stati accolti e i sensi di ammirazione per le bellezze che l'ornano, la storia che la rendono preziosa, la vitalità che tuttora possiede; e ugualmente e ancora i sentimenti di ammirazione e di gratitudine che tutti i fisici italiani nutrono verso il Conte CINI: ammirazione e gratitudine per avere egli costituito questa nobile Fondazione che, intitolata al nome del suo non dimenticato figlio, tanto onora e il fondatore e la città e tutto il nostro paese.

Accanto a questi sentimenti che i fisici italiani, come studiosi e come italiani, indipendentemente dall'essere oggi qui ospiti insieme a colleghi stranieri, porgono al Conte, stanno i sentimenti, anch'essi di gratitudine, che tutti i partecipanti a questo Convegno rivolgono verso la Fondazione « Giorgio Cini » e particolarmente al suo Presidente prof. SPANIO e al suo Segretario generale, prof. BRANCA, e al segretario, sig. TONELLO, e verso il Centro di Cultura e Civiltà e al suo Presidente, prof. CARNELUTTI, per l'ospitalità generosamente concessa.

Personalmente poi un grazie particolarmente caloroso desidero rivolgere ancora al Conte per il colloquio che mi concesse nel passato inverno e per la benevolenza con la quale mi ascoltò, ricevendomi nel suo studio, quando a lui parlai di questo Convegno.

Ma il nostro debito di gratitudine non si arresta qui. La Società Italiana di Fisica è tutt'altro che ricca; e questo Convegno non si sarebbe potuto tenere se la Società Adriatica di Elettricità e la Fondazione « Bordoni » dell'Istituto Nazionale delle Telecomunicazioni non ci avessero aiutato: al Consigliere delegato amministratore della SADE, ing. MARIN, all'ing. ANTONELLO, prezioso demiurgo — dirò così — tra essa e noi, e al prof. GORI, Direttore dell'Istituto delle Telecomunicazioni, giungano pertanto le nostre più vive e cordiali espressioni di gratitudine.

Nè posso omettere di porgere pubblicamente a te, caro amico e collega, prof. GRAFFI, i ringraziamenti miei e dei partecipanti a questo Convegno per tutto quello che hai fatto per attuarlo e superare le difficoltà non piccole, scientifiche ed umane, incontrate. E voglio anche ricordare il tuo efficace collaboratore, il tuo assistente il dott. CAPRIOLI; e qui, della sede, il dott. PILLININI e l'avv. ROSSO MAZZINGHI per l'aiuto dato da loro alla preparazione del Convegno.

Come spesso avviene in simili casi, può darsi che nel citare i nostri collaboratori io abbia omesso qualcuno: se così fosse mi si voglia scusare e ascrivere l'omissione a involontaria dimenticanza, non certo a malvolere o disconoscenza.

* * *

Il mio dire potrebbe qui terminare; ma se Lei, prof. CARNELUTTI, che gentilmente ha accolto la nostra preghiera di presiedere questa prima parte della seduta, me lo permette, vorrei, mosso da quanto Ella ha detto nella sua breve,

ma densamente concettosa allocuzione, rispondere con una parola di assicurazione.

Ella ha accennato al problema morale imposto dalla conoscenza sempre più profonda e sicura delle leggi della Fisica: orbene chi soprattutto sente questo problema sono proprio i fisici; e più essi sono grandi e più lo sentono e lo considerano.

Se una parola è stata detta contro i danni che l'orgoglio d'un sapere incompiuto può portare, questa è stata detta per prima, ed è tuttora ripetuta, dai fisici. I quali — i più, i veri, direi — sapendo e misurando, oggi più che mai con retto giudizio, la sproporzione enorme che v'è tra ciò che si sa e ciò che resta da sapere, sono pervasi nel profondo del loro animo da un vivo sentimento d'umiltà che li guida nello studio, nell'indagine, nella critica, nella scoperta.

Essi possono sperare, e sperano, di potere domani dominare le più intense forze della natura; ma sanno anche che, purtroppo, nulla possono contro la volontà di quanti vivono nell'orgoglio e nella superbia. Per confondere costoro non v'è che isolarli nell'ignoranza. E quindi il compito del fisico è ancora lo studio, l'indagine, la critica, la scoperta.

In questo quadro di nobile e disinteressata attività rientra il nostro Convegno: gli uomini che vi partecipano ne sono sicura garanzia.

Con questa certezza e con questi sentimenti ho l'onore di dichiarare aperto il Convegno Internazionale sulla propagazione delle radioonde nella ionosfera.

SUPPLEMENTO AL VOLUME IV, SERIE X
DEL NUOVO CIMENTO

N. 4, 1956
2° Semestre

Introduzione al Convegno.

D. GRAFFI

Presidente del Convegno

In un discorso, tenuto nel 1926, in occasione del trentennio della Radiotelegrafia, GUGLIELMO MARCONI si esprimeva in questi termini:

« Era stato obiettato che la curvatura della Terra avrebbe inesorabilmente impedito le comunicazioni a distanze superiori a poche decine di chilometri, ma a ciò non credevo e potei ben presto provare con esperienze condotte fra il capo Lizard e l'isola di Wight in Inghilterra che, attraverso una distanza di 300 chilometri, in cui la curvatura terrestre interveniva assai sensibilmente, questa non costituiva alcun ostacolo alle trasmissioni radiotelegrafiche.

« Fu allora affermato che le trasmissioni ad ancora più grande distanza rappresentavano il sogno di un visionario, ma dopo le esperienze da me eseguite nel Dicembre 1901 fra l'Inghilterra e Terranova nel Nord America, durante le quali riuscii a comunicare per la prima volta attraverso l'oceano Atlantico, tutti cominciarono a convincersi che molto probabilmente non vi sarebbe più stata distanza al mondo che avesse potuto fermare la trasmissione delle onde elettriche » (1).

Noi siamo ancora oggi meravigliati dell'intuizione e della genialità di MARCONI, tanto più che le difficoltà prospettate non erano affatto prive di fondamento. Infatti, si osservava, le onde elettromagnetiche a cui erano affidati i segnali da trasmettere non avrebbero superato di molto la curvatura terrestre perchè sarebbero rimaste assorbite o si sarebbero disperse nello spazio; calcoli matematici precisi confermavano e confermano tali previsioni. Gli è che in tutte quelle considerazioni e in tutti quei calcoli non si teneva conto che nell'alta atmosfera vi è una regione, formata da gas ionizzati, e perciò di comportamento elettrico del tutto diverso da quello della bassa atmosfera. Ora è ben noto che tale regione, cioè la ionosfera, gode dell'importante proprietà di funzionare come uno specchio per le onde elettromagnetiche che altrimenti

(1) Cfr. *L'Elettrotecnica*, **13**, 437 (1926).

si disperderebbero nello spazio, a queste ultime infatti si deve la trasmissione a grande distanza; senza quel provvidenziale specchio la radio non avrebbe certamente l'importanza che ha raggiunto nella vita moderna.

Della ionosfera (anche se non chiamata con questo nome, adottato proprio qui, in Venezia, nel 1938 in occasione del Congresso dell'Unione Radioscientifica internazionale) si parla da tempo; già nel 1882, BALFOUR STEWART, per spiegare alcune proprietà del magnetismo terrestre, aveva introdotto l'ipotesi di una regione ionizzata nell'alta atmosfera, ipotesi ripresa da KENNELLY e, indipendentemente, da HEAVISIDE nel 1902, poco dopo le prime esperienze di MARCONI sulla trasmissione a grande distanza, ma solo nel 1924 fu stabilita in modo sicuro la sua esistenza da Sir EDWARD APPLETON, ora Premio Nobel, cui impegni precedenti non hanno permesso di partecipare a questo nostro Convegno. In seguito le ricerche sulla ionosfera si sono moltiplicate molto rapidamente, le pubblicazioni ad essa dedicate si contano già a migliaia e, buona parte, sono già coordinate in importanti trattati. Ciò nonostante numerosi ed affascinanti problemi rimangono aperti, ed è per questa ragione che quasi tutti i cultori italiani di studi sulla ionosfera e alcuni fra i più valenti cultori stranieri sono qui riuniti, sotto gli auspici della Società Italiana di Fisica, grazie ai munifici interventi dell'Istituto superiore delle Telecomunicazioni, della Società Adriatica di Elettricità, e alla signorile ospitalità offerta dalla Fondazione « Giorgio Cini », per esporre e discutere i loro ultimi risultati e per uno scambio di idee che sarà certamente assai proficuo per le ricerche future. Mi si permetta ora di accennare brevemente gli argomenti che verranno esposti nel Convegno.

La ionosfera verrà studiata da alcuni dei partecipanti da un punto di vista che può chiamarsi geofisico, cioè indagheranno la sua struttura, le sue cause, le sue proprietà, le sue relazioni con altri fenomeni terrestri e solari. Il professor CHAPMAN, della Royal Society di Londra, esporrà una sua teoria molto più perfezionata e completa di quella usuale, sulla conduttività della ionosfera. Il prof. ARGENCE, del Servizio militare ionosferico francese, esporrà alcune considerazioni sulla proprietà e sulla misura di una grandezza fondamentale per la ionosfera: il numero degli urti di un corpuscolo elettrico nell'unità di tempo. Il prof. NAISMITH di Slough (Inghilterra) e il prof. GERSON di Cambridge, Mass. (U.S.A.), ci diranno degli strati ionizzati dovuti, rispettivamente ai meteoriti e ai corpuscoli che dànno luogo alla aurora polare; il prof. RANZI, dell'Università di Firenze, parlerà di alcune proprietà della ionosfera osservate nell'America meridionale. Il dott. MARIANI, dell'Istituto Nazionale di Geofisica, esporrà uno studio sull'influenza della temperatura e della diffusione sulla ionizzazione dell'alta atmosfera. Il dott. DOMINICI, dello stesso Istituto, ci dirà di proprietà della ionosfera che si deducono da osservazioni fatte durante le eclissi solari e, in collaborazione con il dott. MARIANI, discuterà alcuni parametri caratteristici della ionosfera.

Il dott. CUTOLO, del Centro studi per la radiodiffusione e radiopropagazione di Napoli, parlerà di ricerche compiute assieme ai suoi collaboratori sulle frequenze utili durante l'eclissi solare. Il dott. NAPOLETANO, dello stesso Centro, accennerà ad una correlazione fra regione E e bassa atmosfera.

Altri partecipanti al Convegno, si proporranno di mettere in luce le leggi con cui le radioonde si propagano nella ionosfera. Il prof. BREMMER, della Philips Company di Eindhoven (Olanda), istituirà un utile raffronto fra due diverse rappresentazioni della propagazione delle onde elettromagnetiche, il prof. ARGENCE, in collaborazione con il prof. RAWER di Friburgo (Germania), studierà la propagazione in un mezzo, come può ritenersi in prima approssimazione la ionosfera, isotropo assorbente e stratificato. Il prof. KAHAN, della Sorbona, ci riferirà sulla teoria delle fluttuazioni ionosferiche e della loro influenza sulla portata delle radioonde. Il prof. RAWER ci proverà come lo strato E può impedire la riflessione delle radioonde sullo strato F e come questo fenomeno, chiamato l'occultazione dei percorsi, può influenzare il valore delle frequenze utili per la trasmissione a grande distanza. Il prof. DIEMINGER, dell'Università di Göttingen, riferirà esperienze condotte con diverse frequenze per ricevitori a differenti distanze, tendenti a stabilire relazioni fra raggi che entrano nella ionosfera con diverse incidenze. Il prof. CARRARA, dell'Università di Firenze, parlerà delle sue ricerche sull'assorbimento delle microonde da parte dell'ossigeno.

Qui presente è il prof. BAILEY, dell'Università di Sidney, al quale si deve la spiegazione del singolare fenomeno dell'interazione delle radioonde per cui il programma di una stazione radio può trasferirsi su un'onda di un'altra stazione; egli ci parlerà delle sue ultime ricerche in proposito. Studiando l'interazione il dott. CUTOLO ha messo in evidenza come una radioonda propagandosi può demodularsi egli e i suoi collaboratori BORGHI, CACHON, IMMIRZI esporranno vari risultati su quest'ultimo fenomeno, mentre l'ing. CARLEVARO lo considererà dal lato teorico.

Ma è ora di concludere. Le onde radio ci hanno rivelato proprietà dell'alta atmosfera, che trent'anni fa non erano neppure sospettate, sicchè oggi siamo in grado di studiarla anche per altra via, cioè con i missili o con quei satelliti artificiali alla cui realizzazione collabora, come hanno riferito i giornali, il prof. CHAPMAN qui presente. A questi metodi di ricerca si aggiungono le nostre conoscenze fisiche e matematiche che ci permettono di interpretare i risultati dell'esperienza, di formulare opportune ipotesi, di controllarle nelle loro conseguenze qualitative e quantitative. Così avanza la scienza e, se al suo progresso si accompagnerà un identico progresso dei valori morali e spirituali, la scienza si manifesterà a tutti qual'è veramente: una delle più alte e delle più nobili espressioni della mente umana.

SUPPLEMENTO AL VOLUME IV, SERIE X
DEL NUOVO CIMENTO

N. 4, 1956
2° Semestre

Turbulence ionosphèrique et propagation des ondes électromagnétiques.

T. KAHAN

Institut Henri Poincaré - Paris

1. – Dans cette conférence d'ouverture je me propose d'exposer l'un des chapitres les plus modernes et les plus fascinants des recherches ionosphériques: la théorie de la turbulence ionosphérique. Elle met en jeu en effet un grand nombre de disciplines fort variées telles que la théorie moderne de la turbulence hydro- et aérodynamique, la théorie moderne des corrélations statistiques, la théorie de la diffusion des ondes électromagnétiques ainsi que la structure fine de l'ionosphère elle-même.

A l'origine des problèmes relatifs à la turbulence ionosphériques se trouve l'observation d'un nouveau mode de transmission de signaux radioélectriques à des distances de l'ordre de 1 000 à 2 000 km, sur des fréquences de l'ordre de 50 MHz. Ce nouveau type de propagation se trouve être indépendant des saisons, de l'heure du jour et des perturbations géomagnétiques. Ces signaux s'observent lorsque toute autre forme de transmission ionosphérique est absente. Divers auteurs ont suggéré, à l'image de ce qui se passe en propagation troposphérique, que ce nouveau type de propagation serait précisement dû à la turbulence ionosphérique de la couche E.

L'ionosphère est en effet le siège, tout comme la plupart des fluides réels dans la nature, d'un état turbulent permanent caractérisé par des mouvements tourbillonaires aléatoires dont le vent représente une sorte de valeur moyenne. L'énergie qui donne naissance à ces tourbillons provient vraisemblablement des radiations solaires et du passage des météores qui donnent lieu à une ionisation correspondante. Cette turbulence donne naissance à des fluctuations dans le temps et dans l'espace de toutes les caractéristiques de l'ionosphère et, en particulier, à des fluctuations de la densité électronique, donc en dernier ressort à des fluctuations de la constante diélectrique: c'est en cela que consiste précisément la turbulence ionosphérique.

2. – Ceci posé, il est indispensable pour aborder la théorie de la turbulence ionosphérique d'analyser de plus près les phénomènes de la turbulence en général. Si le halo de mystère qui entoure le phénomène de turbulence n'a pas encore été entièrement dissipé, il a été néanmoins considérablement éclairci ces dernières années. Le nombre de problèmes en physique où le mouvement turbulentiel joue un rôle va en croissant. L'échange de chaleur dans l'atmosphère, le scintillement de la lumière stellaire, la diffusion des substances radioactives, les courants océaniques, le mouvement des nuages gazeux interstellaires et peut-être jusqu'aux oscillations de plasma sont autant de phénomènes où les caractéristiques de la turbulence interviennent. Il n'est pas surprenant que la turbulence soit omniprésente, car, dans toute matière sous forme liquide ou gazeuse, et pour tout nombre de Reynolds grand (ce qui est toujours le cas dans l'air et dans l'eau pour des mouvements plus étendus que l'échelle du laboratoire) il est inévitable que l'énergie cinétique de la matière se présente sous forme turbulentielle; tout autre forme de mouvement serait presque à coup sûr instable.

La tendance moderne est de regarder en général le mouvement turbulentiel comme un système de mécanique statistique. Cette tendance se justifie par le fait qu'il existe certains traits statistiques communs à tous les types de turbulence.

Imaginons, pour fixer les idées, un volume infini de fluide uniforme susceptible d'être caractérisé de manière classique par une densité ϱ et par des coefficients de transport moléculaire tels que la viscosité μ. Ce volume de fluide peut être le siège de différents modes de mouvement tels que ceux étudiés en hydrodynamique. Sous certaines conditions qui reviennent usuellement à imposer que le coefficient de viscosité cinématique ν $(= \mu/\varrho)$ soit petit, quelques-uns de ces mouvements sont tels que la vitesse en un point et à un instant donnés dans le sein du fluide ne se trouve pas être la même lorsqu'on la mesure à plusieurs reprises dans des conditions apparemment identiques. Dans ces types de mouvement, la vitesse prend des valeurs aléatoires qui ne sont pas déterminés par les données du flux visible ou contrôlable ou « macroscopique » bien que l'on ait l'impression que les propriétés *moyennes* du mouvement soient définies uniquement par ces données. Des mouvements fluctuants de ce type sont dits turbulents. La turbulence est dite homogène quand les propriétés moyennes sont indépendantes de la position dans le fluide. Le problème qui se pose dès lors est de comprendre le mécanisme et de déterminer analytiquement les propriétés moyennes de ces types de mouvement.

Voici comment on arrive à la notion d'échelle de turbulence. Proposons-nous, avec J. Bass, de mesurer, en un point donné, la vitesse d'un écoulement permanent et uniforme à l'échelle macroscopique usuelle, à l'aide d'un instrument de mesure tel qu'un anémomètre (enregistreur de la vitesse du vent) ayant des dimensions et une constante de temps déterminés et d'une nature assez

idéale pour ne pas perturber l'écoulement par sa présence. Si cet anémomètre est suffisamment grand, il mesurera la vitesse d'ensemble du fluide. S'il est extrêmement petit, on peut imaginer qu'il fonctionne d'une façon discontinue, ne subissant jamais l'influence de plus d'une molécule à la fois. Entre ces deux extrêmes, les indications de l'anémomètre dépendront de la structure du fluide. Il peut arriver exceptionnellement que, lorsqu'on diminue progressivement ses dimensions, la vitesse qu'il indique reste immuable, jusqu'au moment où l'influence individuelle des molécules commence à se faire sentir et où les indications perdent toute signification statistique. On dit alors que l'écoulement est *laminaire*. Mais, en général, les choses se passent autrement. Partons d'un premier anémomètre qui, par ses dimensions, nous fixe une certaine *échelle* de mesure. Cet anémomètre mesurera la vitesse moyenne des molécules, dans un certain volume V. Remplaçons-le successivement par des anémomètres plus petits de telle façon que V diminue progressivement. Il arrive que, à partir d'une certaine valeur V_1 de V, l'indication numérique fournie par l'anémomètre change. Si l'on continue à diminuer V, la nouvelle indication reste stable jusqu'à une certaine valeur V_2 puis change à nouveau, et ainsi de suite. Les intervalles (V_1, V_2), (V_2, V_3)... caractèrisent les diverses échelles de turbulence et l'on dit que le mouvement du fluide est *turbulent*. La turbulence implique donc la notion d'échelle.

3. – Equations de Navier (-Stokes).

Si le fluide est en mouvement macroscopique, il convient de définir sa vitesse d'ensemble dans le système des variables d'Euler, c'est-à-dire au voisinage d'un point fixe arbitrairement donné. Dans ce système, la forme la plus générale des équations d'un fluide est, en l'absence d'une force extérieure:

$$\frac{\partial \boldsymbol{v}}{\partial t} + (\boldsymbol{v}\cdot\nabla)\boldsymbol{v} = -\frac{1}{\varrho}\sum_k \frac{\partial T_{ik}}{\partial x_k}\,, \tag{1}$$

$\boldsymbol{v}$ étant la vitesse de la « particule » qui passe à l'instant t au voisinage du point de coordonées $\boldsymbol{r}(x_1, x_2, x_3)$, et le tenseur symétrique T_{ik} étant le tenseur des tensions. Cette particule assez mal définie est un ensemble de molécules contenant suffisamment d'éléments pour que la moyenne de leurs vitesses ait une signification statistique, mais sous un volume suffisamment petit par rapport au volume occupé par le fluide, pour qu'on puisse assimiler son mouvement à celui de son barycentre.

A ces trois équations (1) il s'ajoute l'équation de continuité

$$\frac{\partial \varrho}{\partial t} + \nabla(\varrho \boldsymbol{v}) = 0\,, \tag{2}$$

et, éventuellement, des équations physiques contenant la température et d'autres paramètres physiques.

Dans un fluide en équilibre, les tenseurs se réduisent à une simple pression

$$T_{ik} = p\delta_{ik} . \tag{3}$$

La viscosité, sous la forme des tenseurs obliques, naît du mouvement. On fait l'hypothèse que la vitesse intervient par l'intermédiaire du tenseur des vitesses de déformation $(\partial v_i/\partial x_k) + (\partial v_k/\partial x_i)$, et que les relations entre les deux tenseurs sont linéaires. Si le fluide est incompressible [1]

$$\operatorname{div} \boldsymbol{v} = \nabla \cdot \boldsymbol{v} = 0 , \tag{4}$$

et les équations du mouvement deviennent

$$\frac{\partial \boldsymbol{v}}{\partial t} + (\boldsymbol{v}\cdot\nabla)\boldsymbol{v} = -\frac{1}{\varrho}\nabla p + \nu\nabla^2\boldsymbol{v} , \tag{5}$$

où ∇ est l'opérateur grad [2].

Le seul paramètre qui figure dans (5) est la viscosité ν. Si l'on exprime les longueurs par une unité L, le temps par une unité T, et la vitesse par une unité $V = L/T$, et si l'on pose $t = t'T$, $v = v'V = v'L/T$, $\nabla = \nabla'/L'$, $p = p'V^2\varrho$, où t', v' et p' sont maintenant des grandeurs sans dimension, (5) se transforme en

$$\frac{\partial \boldsymbol{v}'}{\partial t'} + (\boldsymbol{v}'\cdot\nabla')\boldsymbol{v}' = -\nabla' p' + \frac{1}{R_e}\nabla'^2\boldsymbol{v}' , \tag{6}$$

où $\mathrm{Re} = \varrho VL/\mu = VL/\nu$ est un nombre sans dimensions dit nombre de Reynolds. (6) conduit aux lois dites de similitude en hydrodynamique.

Les équations (4) et (5) admettent de nombreuses solutions différentes dont chacune décrit un champ de flux. Bornons-nous à une certaine classe de solutions présentant une variation aléatoire de vitesses par rapport au temps t et par rapport à la variable de position $\boldsymbol{r}$. Le terme « aléatoire » fournit une description nécessaire et suffisante du mouvement turbulentiel. Néanmoins il n'est pas aisé de donner une définition précise d'une variation aléatoire de

---

[1] Les variations de densité se trouvent liées au rapport d'une vitesse de fluide typique (telle que la vitesse efficace) à la vitesse moyenne du son dans le fluide. Lorsque ce rapport est faible devant l'unité, les variations de densité sont négligeables et le fluide se comporte comme s'il était incompressible.

[2] $$(\boldsymbol{v}\cdot\nabla) \equiv (\boldsymbol{i}v_x + \boldsymbol{j}v_y + \boldsymbol{k}v_z)\left(\boldsymbol{i}\frac{\partial}{\partial x} + \boldsymbol{j}\frac{\partial}{\partial y} + \boldsymbol{k}\frac{\partial}{\partial z}\right) = v_x\frac{\partial}{\partial x} + v_y\frac{\partial}{\partial y} + v_z\frac{\partial}{\partial z} .$$

la vitesse. On fait nécessairement appel à l'idée d'un ensemble statistique de solutions qui toutes vérifient les conditions initiales et les conditions aux limites données. Cet ensemble statistique définit la probabilité de trouver $\boldsymbol{v}(\boldsymbol{r}, t)$ compris entre des limites données en même temps qu'il définit la connexion statistique entre les vitesses du fluide en des points et à des instants différents. En d'autres termes, on supposera à titre de définition de la turbulence, que si les données du problème, c'est-à-dire les équations de base et les conditions initiales et aux limites données ne suffisent pas à déterminer $\boldsymbol{v}$ comme fonction de $\boldsymbol{r}$ et t, elles suffisent néanmoins à déterminer les lois de probabilité qui décrivent les valeurs de $\boldsymbol{v}$. Ainsi si l'expérience qui revient à produire le champ de flux avec les conditions initiales et aux limites requises, était effectuée de nombreuses fois, chaque expérience fournissant une « réalisation » du champ de flux, on trouverait que la valeur de $\boldsymbol{v}$, pour des valeurs données de $\boldsymbol{r}$ et t, varierait d'une expérience à l'autre et le collectif des valeurs de $\boldsymbol{r}$ définirait asymptotiquement la distribution de probabilité de $\boldsymbol{v}(\boldsymbol{r}, t)$.

Le champ de vitesse est bien entendu complètement déterminé lorsque l'on a à sa disposition un nombre de renseignements suffisant. L'insuffisance précédente des données tient à ce que nous sommes obligés de négliger les faibles perturbations dans les conditions initiales et aux limites qui échappent au controle expérimental et qui varient d'une expérience à l'autre ([3]).

Comme on ne peut pas se rendre maître de ces perturbations, on les appelle « aléatoires » et on renonce à calculer en détail la turbulence. Heureusement, l'observation montre que les lois de probabilité décrivant la turbulence sont indépendantes des petites perturbations extérieures qui donnent naissance à la turbulence et ne dépendent que des données spécifiées du problème. Ce fait remarquable montre qu'on peut ne pas tenir compte des perturbations extérieures et qu'on peut porter son attention sur la découverte des lois de probabilité de la turbulence comme une fonction univoque des conditions initiales et aux limites du problème. Notre problème s'énoncera dès lors ainsi:

Etant donné un fluide dont le mouvement est régi par les équations (4) et (5), et étant donné que le fluide est mis en mouvement turbulentiel déterminé statistiquement par les conditions initiales et aux limites ainsi que par (4) et (5), trouver les lois de probabilité décrivant la turbulence ainsi que sa variation avec le temps.

([3]) L'idée d'agitation irrégulière en un point en fonction du temps n'est pas suffisante en elle-même. Elle permet en effet de distinguer l'agitation turbulente de l'agitation sonore périodique (son musical), mais pas du bruit qui est une agitation sans période définie; ce qui distingue le bruit de la turbulence c'est qu'il se propage par ondes, qu'il existe des surfaces équiphases et par suite une répartition *spatiale* régulière malgré l'irrégularité dans le temps de la vitesse locale. Chaque composante de la vitesse turbulente $\boldsymbol{v}(\boldsymbol{r}, t)$ est une fonction irrégulièrement périodique à la fois de l'espace $\boldsymbol{r}$ et du temps t.

Quelle forme vont revêtir les lois de probabilité? On fait appel ici à la théorie mathématique des fonctions aléatoires dans laquelle une fonction aléatoire $\boldsymbol{v}(\boldsymbol{r}, t)$ est complètement déterminée statistiquement en se donnant un ensemble de distribution de probabilités liées des valeurs de $\boldsymbol{v}$ pour n paires quelconques de valeurs de $\boldsymbol{r}$ et t, c'est-à-dire pour l'ensemble de toutes les valeurs moyennes de produits qu'on peut former avec les valeurs de $\boldsymbol{v}$ en des points et à des instants différents.

4. – Valeurs moyennes et statistiques.

Proposons-nous de mesurer, sur la Fig. 1 qui donne l'allure dans le temps d'une composante v de la vitesse turbulente, la vitesse moyenne. La méthode la plus naturelle consiste à former l'intégrale ordinaire

$$v_m = \frac{1}{T}\int_0^T v(t)\,\mathrm{d}t\,, \tag{7}$$

étendue à la durée T de l'enregistrement. Cette méthode est en général peu satisfaisante, car l'opération manque de précision dès que la courbe $v(t)$ est compliquée. Un procédé plus précis consiste à découper le graphique par des parallèles à l'axe des t, convenablement rapprochées, d'ordonnées v_1, v_2, v_3, ..., à mesurer le nombre n_i de points où la droite d'ordonnée $\frac{1}{2}(v_i + v_{i+1})$ rencontre la courbe $v(t)$ et à calculer la quantité

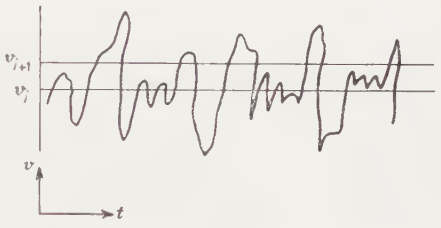

Fig. 1.

$$\bar{v} = \sum_i v_i \frac{n_i}{n}\,, \tag{8}$$

$n = \sum_i n_i$ étant le nombre total de points rencontrés par toutes les parallèles. Or, pour ce calcul, on peut utiliser une première étape qui consiste à construire le graphique donnant, pour chaque vitesse v_i, la fréquence statistique $f_i = n_i/n$ correspondante. Un passage à la limite évident permet de tracer une courbe de fréquence $f(v)$ telle que la proportion des valeurs de la vitesse comprise entre v et $v+\mathrm{d}v$ soit égale à $f(v)\,\mathrm{d}v$, l'intégrale $\int_0^\infty f(v)\,\mathrm{d}v$ qui remplace $\sum n_i/n$, étant égale à 1. L'expression définitive de $\bar{v}$ est alors

$$\bar{v} = \int_{-\infty}^{+\infty} v f(v)\,\mathrm{d}v\,. \tag{9}$$

Elle remplace (8) et doit être comparée à (7). Les opérations pratiques qui permettent de remplacer v_m par $\bar{v}$ correspondent à des opérations mathématiques classiques: le mode de calcul de $\bar{v}$ est celui d'une intégrale de Lebesgue, et v_m est une intégrale du type de Riemann.

A partir de la fonction $f(v)$ on peut calculer d'autres moyennes. On peut, par exemple, chiffrer l'amplitude des écarts de la vitesse par rapport à sa valeur moyenne en calculant la valeur moyenne de $(v - \bar{v})^2$. Plutôt que de définir cette moyenne par l'intégrale de Riemann

$$\frac{1}{T}\int_0^T [v(t) - v_m]^2 \, dt \,, \tag{10}$$

il est plus simple et plus précis d'utiliser la formule:

$$\overline{(v - \bar{v})^2} = \int_{-\infty}^{+\infty} (v - v)^2 f(v) \, dv \,, \tag{11}$$

qui une fois la courbe $f(v)$ tracée, ne fait plus appel qu'à des opérations de nature simple. Ceci montre combien la construction de la courbe $f(v)$ simplifie les calculs numériques relatifs à la turbulence.

5. – Décomposition spectrale de la vitesse.

Ceci posé, nous avons vu que la courbe représentative d'une composante $v(t)$ de la vitesse turbulente en fonction du temps suggère l'idée d'un phénomène périodique irrégulier. La représentation analytique de $v(t)$ n'est pas une série de Fourier périodique, mais plutôt *une série presque périodique* ou une intégrale de Fourier. Dans le premier cas, $v(t)$ est une somme d'harmoniques sans période de base commune, soit en adoptant la notation complexe

$$v(t) = \sum_{-\infty}^{+\infty} A_n \exp[i\omega_n t] \,, \tag{12}$$

les pulsations ω_n forment une suite de nombres réels croissants avec n. On peut toujours supposer que $\omega_{-n} = -\omega_n \cdot v(t)$ est bien une grandeur réelle si $A_{-n} = A_n^*$, la notation A^* désignant l'imaginarie conjuguée de A. La série $|A_n|$ doit être convergente. Dans le second cas

$$v(t) = \int_{-\infty}^{+\infty} A(\omega) \exp[i\omega t] \, d\omega \,, \tag{13}$$

la fonction $A(\omega)$ étant absolument sommable et telle que $A(-\omega) = A^*(\omega)$. Les nombres A_n ou la fonction $A(\omega)$ dépendent de la position de l'appareil enregistreur de la turbulence. Cette représentation est utile lorsque la turbulence est stationnaire dans le temps, ce qui permet d'appliquer en toute rigueur le principe ergodique (4), et de calculer les moyennes attachées à $v(t)$ sur un intervalle de temps aussi grand qu'on le désire.

Ceci étant, l'idée qui est à la base de toutes les théories de la turbulence est que celle-ci résulte de la superposition d'un grand nombre de composantes turbulentes qui diffèrent les unes des autres par leur *échelle* qui a la dimension d'une longueur et qui est associée aux dimensions du tourbillon: elle peut être conçue comme la grosseur moyenne d'un tourbillon.

Or l'équation du mouvement (5) n'étant pas linéaire il en résulte que les diverses composantes du mouvement interagissent, et on attribue les propriétés observées de la turbulence au résultat statistique de cette interaction. Si cette conception de la turbulence ne conduit pas par elle-même immédiatement à des résultats, elle présente l'avantage indéniable de faire appel à des idées intuitives sur le comportement de systèmes dynamiques avec de nombreux degrés de liberté.

La décomposition de la turbulence en un grand nombre de mouvements composants se réduit à la décomposition de la distribution instantanée des vitesses en modes orthogonaux compatibles avec les conditions aux limites. Tout comme la distribution instantanée de vitesse sur une corde élastique tendue entre deux points distants de l peut être conçue comme la somme des composantes d'une série de Fourier qui fournissent des contributions additives à l'énergie cinétique, la longueur d'onde fondamentale étant $2l$, la distribution instantanée de la vitesse du fluide sur un champ tridimensionnel peut être considérée comme la somme des composantes d'une série triple de Fourier. Si le champ s'étend à l'infini, la série correspondante devient une intégrale et si les frontières ont une forme curviligne, une autre suite de fonctions orthogonales, telle que les fonctions de Bessel, ou les fonctions sphériques, etc., sont aptes à représenter la situation physique. Remarquons, sans entrer dans les finesses mathématiques du problème, qu'on pourra toujours utiliser une décomposition de la forme générale

$$\boldsymbol{v}(\boldsymbol{r}) = \int \boldsymbol{A}(\boldsymbol{k}) \exp[i\boldsymbol{k}\cdot\boldsymbol{r}]\,\mathrm{d}\boldsymbol{k}\,, \tag{15}$$

où l'intégration s'étend sur tout l'espace $\boldsymbol{k}$; bien que les coefficients vectoriels $\boldsymbol{A}(\boldsymbol{k})$ divergent dans certains cas, on peut utiliser la fonction sans risque

(4) C'est-à-dire l'égalité des moyennes de phase et de temps.

grave de se tromper. Or

$$\boldsymbol{A}(\boldsymbol{k}) \exp[i\boldsymbol{k}\cdot\boldsymbol{r})\,\mathrm{d}\boldsymbol{k}$$

est la contribution à la vitesse de l'élément de volume $\mathrm{d}\boldsymbol{k}$ de l'espace des nombres d'ondes $\boldsymbol{k}$; ce sera la composante typique de la turbulence et elle représentera une distribution de vitesses sinusoïdales avec la longueur d'onde $2\pi/k$ ($k = |\boldsymbol{k}|$), qui est la mesure de l'échelle de longueur de la composante turbulentielle. L'équation de continuité (4) impose

$$\boldsymbol{k}\cdot\boldsymbol{A}(\boldsymbol{k}) = 0\,, \tag{16}$$

de sorte que les mouvements correspondants sont des « ondes sinusoïdales » avec une vitesse parallèle à $\boldsymbol{A}(\boldsymbol{k})$ et avec une variation spatiale dans la direction du nombre d'onde $\boldsymbol{k}$. Remarquons que ces « ondes », contrairement à celles qui se propagent par exemple sur une corde tendue, ne se propagent pas, en raison de la forme différente de l'équation. Le carré du coefficient de Fourier $\boldsymbol{A}(\boldsymbol{k})$ est proportionnel à la quantité d'énergie cinétique associée à la composante de Fourier du nombre d'onde $\boldsymbol{k}$; c'est aussi la contribution que la composante apporte à l'énergie cinétique de la turbulence. L'analyse de Fourier du champ de vitesse instantanée fournit de la sorte une distribution spectrale d'énergie cinétique; comme la grandeur $\boldsymbol{A}(\boldsymbol{k})$ est fluctuante — c'est-à-dire qu'elle est différente pour des réalisations différentes du champ de vitesses — on prendra la moyenne pour obtenir finalement $A^2(\boldsymbol{k})$ comme mesure de la distribution, dans l'espace des nombres d'onde, de la densité des contributions à l'énergie cinétique de la turbulence.

Si, jusqu'ici, l'idée de l'analyse de Fourier du champ de vitesses ne diffère pas essentiellement de l'analyse de Fourier de la lumière blanche ou du bruit électronique, l'équation fondamentale (5) qui décrit la relation entre les distributions spatiales de vitesse à des instants différents introduit des différences essentielles. On obtient la vitesse de variation du coefficient de Fourier $\boldsymbol{A}(\boldsymbol{k})$ en portant (15) dans (5) et en éliminant le terme de pression à l'aide de (4):

$$\frac{\partial \boldsymbol{A}(\boldsymbol{k})}{\partial t} = i\int \boldsymbol{k}'\cdot\boldsymbol{A}^*(\boldsymbol{k}' - \boldsymbol{k})\left[\boldsymbol{k}\cdot\boldsymbol{A}(\boldsymbol{k}')\,\frac{\boldsymbol{k}}{k^2} - \boldsymbol{A}(\boldsymbol{k}')\right]\mathrm{d}\boldsymbol{k}' - \nu k^2\boldsymbol{A}(\boldsymbol{k})\,. \tag{17}$$

Le second terme du second membre dû à l'effet de viscosité représente une action linéaire d'amortissement comme il fallait s'y attendre, et montre que la dissipation d'énergie est relativement plus rapide pour les composantes de petite échelle ($k \ll$, $1/k \gg$) que pour les composantes de grande échelle ($k \gg$, $1/k \ll$).

D'autre part, le premier terme du second membre, dû aux forces d'inertie et de pression, n'est pas linéaire et met en évidence une interaction incessante, ou modulation, entre les diverses composantes de Fourier. La variation de l'énergie d'une composante de Fourier quelconque est donnée par

$$(18) \qquad \frac{\partial \boldsymbol{A}(\boldsymbol{k})\cdot\boldsymbol{A}^*(\boldsymbol{k})}{\partial t} = i\int[-\boldsymbol{k}'\cdot\boldsymbol{A}^*(\boldsymbol{k}'-\boldsymbol{k})\boldsymbol{A}^*(\boldsymbol{k})\cdot\boldsymbol{A}(\boldsymbol{k}') + \\ + \boldsymbol{k}'\cdot\boldsymbol{A}(\boldsymbol{k}'-\boldsymbol{k})\boldsymbol{A}(\boldsymbol{k}')\boldsymbol{A}^*(\boldsymbol{k}')]\,\mathrm{d}\boldsymbol{k}' - 2\nu k^2\boldsymbol{A}(\boldsymbol{k})\cdot\boldsymbol{A}^*(\boldsymbol{k}),$$

ce qui montre que l'interaction conduit en général à un transfert d'énergie entre deux composantes quelconques. C'est précisément cette interaction cinétique entre les composantes qui est le principal obstacle à la solution du problème de la turbulence. Sauf dans quelques cas simples de mouvement laminaire, la solution de (17) ne semble point être à notre portée pas plus qu'une solution de (5) et l'objet des théories de la turbulence revient précisément et essentiellement à introduire des hypothèses qui permettent d'évaluer quantitativement l'interaction entre les composantes dans des cas bien limités.

Si l'on assimile la turbulence à un système dynamique de caractère statistique où les composantes de Fourier joueraient le rôle des degrés de liberté, l'équation (17) devient le pendant d'une loi de « collision ». L'excitation d'un degré de liberté quelconque conduit en général à l'excitation de tous les autres degrés de liberté, excitation limitée seulement par l'action amortissante de la viscosité. En raison de l'existence de cette dissipation, il ne se produit pas d'équipartition de l'énergie parmi ces divers degrés de liberté.

Tout comme dans (5) le seul paramètre qui figure dans (17) est la viscosité ν ou bien, si l'on veut, en introduisant des grandeurs sans dimension à l'aide d'une vitesse V et d'une longueur L de référence, c'est le nombre de Reynolds $\mathrm{Re} = VL/\nu$.

Il convient de prévoir une turbulence différente pour chaque nombre de Reynolds différent. Du fait que ν figure dans (18) par le produit νk^2, l'effet des forces de viscosité sera toujours prédominant pour des composantes de Fourier ayant des nombres d'onde k suffisamment élevés, mais la région où la viscosité produit une interaction forte se déplacera vers les grandes valeurs de k à mesure que le nombre de Reynolds croîtra, c'est-à-dire à mesure que ν décroîtra. Pour les nombres d'ondes petits, dans la vitesse de variation $\partial\boldsymbol{A}(\boldsymbol{k})/\partial t$ de la composate $\boldsymbol{A}(\boldsymbol{k})$, c'est l'effet d'inertie qui prévaut en vertu de (17). Ainsi donc cette partie du système dynamique n'est pas dissipative, mais elle n'est pas close, et il se produira en général un flux statistique, un échange privilégié d'énergie vers la partie de l'espace du nombre d'onde où l'énergie est absorbée par viscosité. Prenons le cas limite simple de $\mathrm{Re} = \infty$ ou $\nu = 0$. La région de l'espace des k où l'amortissement visqueux joue est alors déplacé vers $k = \infty$ et toute l'énergie finira par être pompée par effet

d'inertie hors de la région où k est fini. Ce cas simple où agissent des forces d'inertie seules, sauf pour $k = \infty$, se prête fort bien à l'utilisation d'hypothèses intuitives sur l'interaction entre les diverses composantes. On peut dès lors présumer que le spectre d'énergie de la turbulence présentera une forme pour les petites valeurs de k qui sera fortement influencée par les conditions aux limites, et que pour les plus grandes valeurs de k l'intensité spectrale décroîtra lorsque k croît, d'une façon qui sera régie par l'échange d'énergie inertielle. Pour un nombre de Reynolds infini, cette chute continue jusqu'à $k = \infty$, mais pour les nombres de Reynolds finis on atteindra une valeur de k où l'effet d'amortissement visqueux deviendra sensible et le spectre tendra vers zéro beaucoup plus rapidement au voisinage de ce nombre d'onde.

L'effet des forces d'inertie est donc d'exciter et de transférer de l'énergie à autant de composantes de Fourier qu'il est compatible avec l'effet d'amortissement de la viscosité. Supposons alors que l'échelle de longueurs représentative des frontières soit L. En général ce sera aussi l'échelle des longueurs des composantes de Fourier de la turbulence qui sont directement excitées par l'action des frontières. Ainsi, par exemple, lorsqu'un fluide passe sous pression à travers un tube de diamètre L, les composantes de Fourier de la distribution des vitesses qui sont directement influencées par les conditions aux frontières auront des nombres d'onde qui seront de l'ordre de grandeur de $1/L$. Une fois ces composantes de la turbulence excitées, les forces d'inertie entrent en jeu pour étaler l'énergie sur un intervalle de spectre plus étendu et pour la transférer de la sorte à des nombres d'ondes plus grands. Ainsi qu'il a été expliqué précédemment, cette tendance ne sera contrariée que si l'énergie atteint des nombres d'onde qui sont si grands que l'amortissement visqueux devient appréciable.

Si maintenant on se propose d'isoler certaines parties d'un système dynamique, en vue d'acquérir par là une intelligence limitée du mouvement, il sera utile d'envisager les composantes de Fourier ayant des nombres d'ondes qui sont grands comparés à $1/L$ puisque ces composantes s'excitent par l'action des forces d'inertie seules et ne sont pas assujetties à l'action directe des frontières. Si, comme cela paraît probable, l'influence des conditions aux frontières se perd progressivement au cours du processus statistique du transfert d'énergie aux nombres d'onde plus grands — ce qui correspond à l'idée intuitive qu'un transfert statistique doit s'accompagner d'une perte d'information, c'est l'hypothèse du désordre de v. Weizsäcker — la turbulence due aux compostantes de Fourier de nombre d'onde suffisamment grand sera statistiquement indépendante des conditions aux limites ainsi que de la source de l'énergie cinétique. Cette région du spectre devrait donc correspondre à un problème relativement simple qui ne serait pas compliqué par la donnée de la forme et de l'état de mouvement exacts des frontières. Les composantes de Fourier avec des nombres d'onde k tels que $k \gg 1/L$ font l'objet de la

théorie dite de la similitude ou de l'équilibre universel (KOLMOGOROFF, OBUKHOFF, ONSAGER, v. WEIZSÄCKER, etc.) [5].

Il est nécessaire que le nombre d'onde (appelons le $1/\eta$, η étant une longueur caractéristique des plus petits tourbillons — mouvements composants — existants dans la turbulence) pour lequel l'amortissement visqueux produit une décroissance rapide dans la distribution spectrale de l'énergie, vérifie également cette condition, car autrement les composantes de Fourier auxquelles s'applique l'hypothèse du désordre ne s'exciteraient pas. Comme, ainsi que l'on l'a vu plus haut, l'accroissement du nombre de Reynolds VL/ν a pour effet de diminuer η, il convient de restreindre notre discussion aux cas de la turbulence pour lesquels $\mathrm{Re} = VL/\nu$ est si grand que

$$\eta \ll L\,, \tag{19}$$

c'est-à-dire que les tourbillons les plus petits de la turbulence soient très petits comparés aux tourbillons les plus grands.

De manière générale, dans l'état turbulent, les grandeurs statistiques qui décrivent le mouvement telles que vitesse quadratique moyenne, etc., varient d'un point à l'autre au sein du fluide. L'échelle de cette non uniformité est déterminée par la géométrie des frontières et, en général, elle est de l'ordre de grandeur de L. Il s'ensuit que la variation des grandeurs statistiques dans une région dont les dimensions linéaires sont petites comparées à L est négligeable et on peut considérer la turbulence comme étant homogène dans l'espace à l'intérieur de cette région. Si l'on analyse la distribution des fluctuations de vitesses autour de la moyenne spatiale, dans cette région, on obtient une suite de coefficients de Fourier qui ont une signification locale et dont chacun correspond à des nombres d'onde grands par rapport à $1/L$.

Tout ce qui a été dit jusqu'à présent des coefficients de Fourier à grand nombres d'onde s'applique à un champ de vitesse local ou à tout le champ, mais il est plus commode de porter maintenant notre attention sur les coefficients de Fourier de grand nombre d'onde de la distribution de vitesse au voisinage d'un point arbitraire dans le fluide. De même, la turbulence peut être considérée comme statistiquement uniforme sur de faibles intervalles de temps. Avec l'hypothèse (faible) que les coefficients de Fourier de faible échelle possèdent des temps caractéristiques relativement faibles — c'est-à-dire que les petits tourbillons ont de faibles périodes — on voit que les composantes de Fourier de faible échelle ne seront pas affectées par les variations lentes dans le temps des grandeurs moyennes décrivant la turbulence et ne dépendront

---

[5] L'interprétation numerique du signe $\gg$ depend de la rapidité avec laquelle l'influence des conditions aux frontières s'amortit dans le processus de transfert d'énergie à travers le spectre.

que de leur valeur instantanée. Dynamiquement parlant, on peut dire que les degrés de liberté correspondant à des grandes valeurs de k sont toujours en équilibre statistique en raison de leur réponse rapide à des conditions extérieures. Les composantes de plus petit k cèdent de l'énergie, mais cette énergie est perdue à son tour par transfert à des composantes ayant de plus grands nombre d'onde — et peut-être par dissipation — avec une vitesse égale.

On parvient ainsi à cette conclusion utile que lorsque le nombre de Reynolds est tel que la condition (19) se trouve vérifiée, les coefficients de Fourier — de la distribution des vitesses en un point quelconque — appartenant à des nombre d'ondes $k \gg 1/L$, sont statistiquement indépendantes des conditions aux limites et sont déterminés par les propriétés moyennes locales dans l'espace et dans le temps de la turbulence.

Remarquons en particulier que les propriétés directionnelles imposées à la turbulence prise dans son ensemble par les conditions aux frontières ne peuvent pas être transmises aux composantes de petite échelle, d'après l'hypothèse du désordre, de sorte que le mouvement associé à ces composantes de petite échelle doit être statistiquement isotrope. L'on aura donc affaire à une turbulence homogène, stationnaire et isotrope.

Le raisonnement peut maintenant se retourner et on peut définir les grandeurs dont dépendent les composantes de Fourier de petite échelle. Ces composantes de petite échelle (que nous désignerons avec BATCHELOR sous le nom d'intervalle d'équilibre des nombres d'ondes) doivent leur excitation au transfert inertiel d'énergie provenant des composantes de grande échelle de la turbulence et l'intensité de cette excitation dépendra naturellement de la vitesse avec laquelle ce transfert d'énergie a lieu.

En raison du fait que toute la dissipation visqueuse a lieu dans l'intervalle d'équilibre — c'est là la signification de la condition (19) imposée au nombre de Reynolds — la vitesse de transfert d'énergie des composantes de grande échelle aux composantes comprises dans l'intervalle d'équilibre doit être égale à la vitesse de dissipation d'énergie ε. Cette grandeur ε doit être locale dans l'espace, et seul le temps parait être nécessaire pour exprimer l'influence du champ de turbulence pris dans son ensemble sur l'intervalle d'équilibre des composantes de Fourier au voisinage d'un point quelconque dans le fluide.

Une fois la valeur locale de ε spécifiée, les composantes de petite vitesse s'ajustent d'abord pour recevoir de l'énergie à cette vitesse et ensuite pour la dissiper. Le mécanisme du processus de dissipation dépendra bien entendu de la valeur de ν. Abstraction faite de la dépendance de ces deux paramètres ε et ν, le mouvement associé à l'intervalle d'équilibre des nombres d'onde — c'est-à-dire le mouvement relatif au voisinage de tout point — sera statistiquement universel. Là est la prévision majeure de la théorie.

Lorsque le nombre de Reynolds est supérieur par un ordre de grandeur à

celui qui est nécessaire pour que les remarques précédentes puissent s'appliquer, on peut pousser la théorie plus loin. Le plus petit nombre d'onde dans l'intervalle d'équilibre est vraisemblablement déterminé par les détails du processus de désordre qui accompagne le transfert d'énergie à travers le spectre, et il est indépendant du nombre de Reynolds. L'accroissement du nombre de Reynolds entraîne un accroissement du nombre d'onde (à savoir $1/\eta$) maximum dans l'intervalle d'équilibre, et par conséquent, un accroissement correspondant de l'étendue de l'intervalle d'équilibre. Lorsque le nombre de Reynolds est si grand que les coefficients de Fourier à l'une des extrémités de l'intervalle d'équilibre sont statistiquement indépendants de ceux de l'autre extrémité, la condition pour qu'il en soit ainsi est qu'il soit possible de trouver des nombres d'ondes k tels que

$$1/L \ll k \ll 1/\eta \; ; \tag{20}$$

les coefficients de Fourier des nombres d'ondes les plus petits ne seront plus influencés par la dissipation visqueuse et ne dépendront pas du paramètre ν. Le flux statistique d'énergie vers une partie quelconque de ce sous-intervalle d'inertie provenant des nombres d'ondes plus petits est composé par un flux s'effectuant vers des nombres d'onde plus élevés à une vitesse ε égale; et le mouvement associé au sous-intervalle est uniquement déterminé statistiquement par l'unique paramètre ε.

Toute valeur moyenne déterminée par la composante de Fourier de l'intervalle d'équilibre doit dès lors présenter une forme isotrope déterminée uniquement par les paramètres ε (dimensions: L^2T^{-3}) et ν (dimensions: L^2T^{-1}). Ainsi par exemple, la densité spatiale relative au nombre d'onde k, d'énergie cinétique $E(k)$ constituerà dans les portions de l'espace k correspondant à l'intervalle d'équilibre une telle valeur moyenne et sera justifiable de la théorie. Des arguments dimensionnels montrent que $E(k)$ revêtira en fonction de ε et ν la forme suivante

$$E(k) = \varepsilon^{\frac{1}{4}}\nu^{\frac{5}{4}}G(k\nu^{\frac{3}{4}}/\varepsilon^{\frac{1}{4}}) \, , \tag{21}$$

G étant une fonction de forme universelle et indéterminée. (21) s'applique à des valeurs de k satisfaisant à $k \gg 1/L$, indépendamment des propriétés à grande échelle de la turbulence pourvu que la condition $\eta \ll L$ soit vérifiée.

Remarquons que la longueur η qui mesure l'échelle des tourbillons les plus petits existants doit être de l'ordre de grandeur de $(\nu^3/\varepsilon)^{\frac{1}{4}}$, car aucune autre longueur caractéristique ne saurait exister dans l'intervalle d'équilibre. Comme η n'est défini que par son ordre de grandeur, on peut écrire

$$\eta = (\nu^3/\varepsilon)^{\frac{1}{4}} \tag{22}$$

de sorte que (21) devient

$$F(k) = \varepsilon^{\frac{1}{4}} \nu^{\frac{5}{4}} G(k\eta) , \tag{23}$$

pourvu que $k \gg 1/L$ et pourvu que le nombre de Reynolds soit tel que la condition

$$L\eta = L\varepsilon^{\frac{1}{4}} \nu^{-\frac{3}{4}} \gg 1 . \tag{24}$$

soit vérifiée.

6. – Fluctuations de densité dans la turbulence homogène.

Ces généralités étant posées, recherchons les lois qui vont gouverner la turbulence ionosphérique. Les ondes électromagnétiques étant censées être diffusées par les fluctuations aléatoires de l'indice de réfraction, nous nous proposons de calculer la diffusion des ondes élémentaires pour ces fluctuations aléatoires dues aux perturbations ionosphériques turbulentes. Nous verrons par la suite que, dans certaines conditions, la diffusion produite par ces fluctuations peut s'exprimer en fonction d'un seul paramètre, l'énergie turbulente dissipée par cm^3 par seconde et que les conditions de validité de cette relation sont bien vérifiées dans le cas de la diffusion des ondes radioélectriques métriques dans la couche E de l'ionosphère.

Relions d'arbord les fluctuations de densité aux fluctuations de vitesse par la loi de Bernouilli. Des fluctuations Δv locales de vitesse seront accompagnées de fluctuations de pression Δp ainsi que de fluctuations de densité $\Delta \varrho$ en vertu de

$$\frac{\Delta \varrho}{\varrho} \simeq \frac{\Delta p}{p} = \frac{(\Delta v)^2}{v_M^2} , \tag{28}$$

v_M^2 étant le carré moyen de la vitesse moléculaire. Etudions alors de plus près les fluctuations de vitesse dans les conditions de turbulence homogène. Cette situation peut se représenter ainsi. Il existe des causes externes qui produisent sans cesse de gros tourbillons d'une certaine dimension L_0 et d'une certaine vitesse v_0. Ces tourbillons se subdivident aussitôt en tourbillons plus petits, de dimension $L_1 = \alpha L_0$ avec $\alpha < 1$. Soit v_1 la vitesse de ces tourbillons plus petit noyés dans les plus gros (v_1 étant la vitesse par rapport à l'entourage, c'est-à-dire relativement aux gros tourbillons qui leur donnent naissance). Ces tourbillons se diviseront à leur tour en tourbillons plus petits $L_2 = \alpha L_1 = \alpha^2 L_0$, avec v_2 pour vitesse relative à leur voisinage. Dans ce processus de subdivision, l'énergie fournie au plus gros tourbillon se trouve transférée aux plus petits, et ainsi de suite. On supposera qu'une quantité d'énergie constante par volume

et par seconde est fournie aux gros tourbillons par une source externe. Le processus de subdivision s'achèvera lorsque la dimension du tourbillon final atteinte est telle que la viscosité moléculaire devient suffisamment grande pour dissiper l'énergie en chaleur.

Voyons avec v. Weizsäcker quelles sont les relations quantitatives qui apparaissent dans ce processus. L'énergie par unité de volume contenue dans un tourbillon est de l'ordre de $\varrho v_n^2/2$. Si la durée de vie d'un tel tourbillon est de l'ordre $t_n = L_n/v_n$, les tourbillons de dimensions L_n fourniront de l'énergie aux plus petits (de grosseur L_{n+1}) avec une vitesse (énergie/temps·volume)

$$S_n \sim \varrho v_n^2/t_n \sim \varrho v_n^2/L_n \,. \tag{29}$$

Comme on supposera le processus stationnaire, l'enérgie S_{n+1} des tourbillons d'une grandeur supérieure transmise à ceux de dimension n doit être égale à S_n. Il en résulte que S_n sera une constante indépendante de n:

$$\varrho v_n^3/L_n = S \,. \tag{30}$$

S est l'énergie transmise aux tourbillons par la source d'énergie (gros tourbillon) puis aux tourbillons plus petits. L'ordre de grandeur de S est donnée par l'énergie fournie aux plus gros tourbillons:

$$S \cong \varrho v_0^3/L_0 \,. \tag{31}$$

On peut utiliser la valeur de S pour déterminer les dimensions des tourbillons les plus petits. L'énergie par cm³ et par seconde dissipée par viscosité moléculaire est par définition $\sim \eta(\mathrm{d}v/\mathrm{d}x)^2$ où $\mathrm{d}v/\mathrm{d}x$ est la vitesse de variation de v par unité de longueur. Les plus petit tourbillon sera celui dans lequel cette énergie prend la valeur S. Comme $\mathrm{d}v/\mathrm{d}x \sim v_n/L_n$, l'on obtient pour le tourbillon minimum de vitesse v_s et de dimension linéaire L_s,

$$nv_s^2/L_s^2 \cong S \,.$$

En vertu de (30) et de (31) il vient alors

$$L_0/L_s = (\varrho v_0 L_0/\eta)^{\frac{3}{4}} \,. \tag{32}$$

En termes physiques: le rapport des dimensions des tourbillons maxima à celles des tourbillons minima est égal au nombre de Reynolds élevé à la puissance $\frac{3}{4}$.

On peut identifier les vitesses v_n avec la grandeur Δv figurant dans (28). Considérons des régions de l'espace de dimension linéaire L satisfaisant à la

relation

$$L_s < L < L_0 \,, \tag{33}$$

et supposons que $L_n = L$. Alors $\Delta v = v_n$, l'écart moyen par rapport à l'entourage, de la vitesse dans cette région. On tire alors de (28) l'écart de densité moyen $(\Delta\varrho)_L$ dans la région L:

$$(\Delta\varrho)_L = \varrho(v_n/v_M)^2 = \varrho(v_0/v_M)^2(L/L_0)^{\frac{2}{3}} \,. \tag{34}$$

Illustrons ce résultat par un exemple. Dans la couche E de l'ionosphère, à une altitude de 100 km, l'on a $\varrho = 2\cdot10^{-9}$ g cm^{-3}. La viscosité est indépendante de la pression et est égale à $\eta = 2\cdot10^{-4}$ g cm^{-1} s^{-1}. Les données fort vagues sur les vitesses et les dimensions des tourbillons permettent de conclure grossièrement:

$$v_0 = 5\cdot10^3 \text{ cm s}^{-1} \,, \qquad L_0 = 5\cdot10^5 \text{ cm} \,, \tag{35}$$

d'où

$$\text{Re} = \frac{\varrho v_0 L_0}{\eta} = 2.5\cdot10^4, \qquad L_0/L_s = 2\cdot10^3 \,, \tag{36}$$

donc $L_s = 2.5\cdot10^2$ cm, et enfin

$$S = 0.5\cdot10^{-3} \text{ erg cm}^{-1} \text{ s}^{-1} \,. \tag{37}$$

Développons maintenant la densité $\varrho(\boldsymbol{r})$ en série de Fourier à l'intérieur du volume diffusant V supposé cubique:

$$\varrho(\boldsymbol{r}) = \frac{1}{V}\sum_i \varrho(\boldsymbol{k}_i)\exp\left[-i\boldsymbol{k}_i\cdot\boldsymbol{r}\right] \,, \tag{38}$$

avec la forme réciproque

$$\varrho(\boldsymbol{k}_i) = \int_V \mathrm{d}\boldsymbol{r}\varrho(\boldsymbol{r})\exp\left[-i\boldsymbol{k}_i\cdot\boldsymbol{r}\right] \,. \tag{39}$$

Nous écrirons sans ambiguité indifféremment $\varrho(\boldsymbol{k}) = \varrho_{\boldsymbol{k}} = \varrho_k = \varrho(k)$. De même

$$\boldsymbol{v} = \sum_{\boldsymbol{k}} \boldsymbol{v}_{\boldsymbol{k}}\exp\left[-i\boldsymbol{k}\cdot\boldsymbol{r}\right] \,, \tag{40}$$

avec $k_x = (2\pi/L)n_x$, ..., n_x, n_y, n_z nombres entiers et $\boldsymbol{v}_{\boldsymbol{k}} = \boldsymbol{v}^*_{-\boldsymbol{k}}$. Le nombre de vibrations propres entre k et $k+\Delta k$ sera donné par $4\pi k^2\cdot\Delta k\cdot V/(2\pi)^3$.

Alors

$$\frac{\overline{v^2}}{2} = \frac{1}{2}\sum_k |\boldsymbol{v}_k|^2 = \frac{1}{2}\int 4\pi k^2\,\mathrm{d}k\,\frac{V}{(2\pi)^3}|\boldsymbol{V}_k|^2 = \int F(k)\,\mathrm{d}k\,, \tag{41}$$

donc

$$F(k) = \frac{1}{(2\pi)^2}\,k^2 V |\boldsymbol{v}_k|^2\,. \tag{42}$$

On peut dès lors mettre l'équation de Navier (5) sous la forme

$$\frac{\hat{c}\boldsymbol{v}_k}{\hat{c}t} + i\sum_{k'}(\boldsymbol{k}\cdot\boldsymbol{v}_{k'})\boldsymbol{v}_{k-k'} = -\frac{\eta}{\varrho}\,k^2\boldsymbol{v}_k - i\,\frac{\boldsymbol{k}}{\varrho}\,p_k\,, \tag{43}$$

en développant aussi la pression p en série de Fourier

$$p = \sum_k p_k \exp[-i\boldsymbol{k}\cdot\boldsymbol{r}]\,, \qquad p_{-k} = p_k^*\,. \tag{44}$$

Comme on supposera le milieu incompressible (4)

$$\boldsymbol{k}\cdot\boldsymbol{v}_k = 0\,. \tag{45}$$

Ceci peut paraître paradoxal en raison de notre tentative de calculer la fluctuation de densité $\Delta\varrho$. En fait, cette hypothèse implique seulement que la partie sans divergence du champ de vitesse est dynamiquement beaucoup plus importante que les composantes irrotationnelles. Cela revient ainsi à admettre que l'énergie potentielle stockée dans les variations de densité est beaucoup plus petite que l'énergie cinétique des tourbillons. Ayant présent cela dans l'esprit, calculons maintenant les fluctuations de pression Δp et ensuite $\Delta\varrho$ à l'aide de

$$p(\boldsymbol{r}) = p_0[\varrho(\boldsymbol{r})/\varrho_0]^\gamma\,, \tag{46}$$

ϱ_0, p_0 étant les valeurs moyennes de la densité et de la pression, et $\gamma = C_p/C_v = 1.4$ pour des molécules diatomiques. En multipliant (43) par $\boldsymbol{k}$ et comme pour $k \neq 0$, $p_k = \Delta p_k$, il vient

$$\Delta p_k = -\frac{\varrho_0}{k^2}\sum_{k'}(\boldsymbol{k}\cdot\boldsymbol{v}_{k'})(\boldsymbol{k}'\cdot\boldsymbol{v}_{k-k'})\,,$$

d'où

$$\Delta\varrho_k = -(\varrho_0/\gamma p_0)^2 k^{-2}\sum_{k'}(\boldsymbol{k}\cdot\boldsymbol{v}_{k'})(\boldsymbol{k}\cdot\boldsymbol{v}_{k-k'})\,. \tag{47}$$

Ceci nous ramène au champ de vitesse $\boldsymbol{v}(\boldsymbol{k})$.

En multipliant (43) par $\boldsymbol{v}(-\boldsymbol{k})$

$$-\frac{\varrho}{2}\frac{\mathrm{d}}{\mathrm{d}t}(\boldsymbol{v}_k, \boldsymbol{v}_{-k}) = i\varrho \sum_{k'} (\boldsymbol{k}\cdot\boldsymbol{v}_{k'})(\boldsymbol{v}_{-k}\cdot\boldsymbol{v}_{k-k'}) + \eta^2 k^2 (\boldsymbol{v}_k\cdot\boldsymbol{v}_{-k}) . \tag{48}$$

Comme

$$\overline{\tfrac{1}{2}\varrho \boldsymbol{v}^2(\boldsymbol{r})} = \tfrac{1}{2}\varrho \sum_k \boldsymbol{v}_k\cdot\boldsymbol{v}_{-k} ,$$

$\frac{1}{2}\varrho \boldsymbol{v}(\boldsymbol{k})\cdot\boldsymbol{v}(-\boldsymbol{k})$ est la densité d'énergie cinétique portée par le nombre d'onde $\boldsymbol{k}$ En sommant sur tous les k dans (48), on obtient le bilan de puissance totale

$$S = -\frac{\mathrm{d}}{\mathrm{d}t}\left(\frac{\varrho}{2}\sum_k \boldsymbol{v}_k\cdot\boldsymbol{v}_{-k}\right) = i\varrho \sum_{k,k'} (\boldsymbol{k}\cdot\boldsymbol{v}_k)\cdot(\boldsymbol{v}_{-k}\cdot\boldsymbol{v}_{k-k'}) + \eta \sum_k k^2 (\boldsymbol{v}_k\cdot\boldsymbol{v}_{-k}) . \tag{49}$$

Le premier terme du second membre décrit le transfert d'énergie cinétique aux divers nombres d'ondes k; le second terme, la dissipation visqueuse d'énergie. Définissons maintenant une situation stationnaire dans une région $(L_0)^3$ complètement enfermée dans le domaine où (49) est valable. Cette région contiendra alors un tourbillon maximum de dimensions L_0 et de vitesse caractéristique v_0. Ce tourbillon sera couplé à l'extérieur de cette région en raison du terme du transfert dans (49). On suppose que l'effet de ce couplage est de maintenir la vitesse moyenne v_0 de ce tourbillon moyennant une fourniture de puissance S_0. Pourvu que S_0 soit constant dans le temps, un état d'équilibre finira par s'établir dans lequel le $\boldsymbol{v}(\boldsymbol{k})$ moyen sera aussi indépendant du temps. On peut alors faire l'hypothèse que

$$S_0 = \varrho v_0^3/L_0 . \tag{50}$$

Si le nombre de Reynolds $\mathrm{Re} = \varrho v_0 L_0/\eta$ est assez grand, le terme dissipatif ne jouera que pour des nombre d'ondes $k \gg 1/L_0$. Il affectera les tourbillons de dimension L_s et de vitesse v_s pour lesquels le nombre de Reynolds « local » est tombé à 1:

$$\varrho L_s v_s/\eta = 1 . \tag{51}$$

Les nombres d'ondes de l'ordre $1/L$ une fois atteints, la dissipation de puissance par frottement remplace le transfert de puissance aux nombres d'ondes plus élevés. On parvient ainsi à une autre équation caractérisant v_s et L_s:

$$S_0 = \eta(v_s/L_s)^2 . \tag{52}$$

Nous nous servirons de (51) et de (52) pour définir les deux grandeurs

$$v_s = (S_0\eta/\varrho^2)^{\frac{1}{4}}, \qquad L_s = (\eta^3/S_0\varrho^2)^{\frac{1}{4}}. \tag{53}$$

On voit que les trois paramètres « externes » S_0, η, ϱ définissent une échelle de longueur et de vitesse absolue pour le problème de transfert d'énergie et de dissipation dans le flux turbulent.

Pour mettre à profit cette idée d'une manière quantitative, partons de la définition (41) de la distribution d'intensité spectrale $F(k)$ pour les vitesses, définition où l'isotropie du spectre de vitesse a été admise,

$$\frac{1}{2}\sum_k \boldsymbol{v}_k \cdot \boldsymbol{v}_{-k} = \int_0^\infty F(k)\,\mathrm{d}k\,. \tag{54}$$

Le terme dissipatif dans (49) sera dès lors

$$2\eta \int_0^\infty k^2 F(k)\,\mathrm{d}k\,. \tag{55}$$

Comme (54) représente la puissance totale absorbée, l'on a avec $y = kL_s$,

$$S_0 = (2\eta/L_s^3)\int_0^\infty y^2 F(L_s^{-1}y)\,\mathrm{d}y\,. \tag{56}$$

En vertu de (52), $F(L_s^{-1}y) = v_s^2 L_s E(y)$ définit une fonction universelle $E(y)$ normée à 1:

$$1 = \int_0^\infty 2y^2 E(y)\,\mathrm{d}y\,. \tag{57}$$

7. – Détermination de $F(k)$.

A condition que $L_s \ll L_0$, il existe une région $k \ll L_s$ dans laquelle la forme du spectre de vitesse $F(k)$ est déterminée par le mécanisme de transfert et n'est pas affectée par la dissipation visqueuse. Dans cette région $F(k)$ devrait être indépendant de η, ou $v_s^2 L_s E(kL_s)$ indépendant de η. Cela ne peut visiblement avoir lieu qu'avec une loi de puissance pour E puisque L_s renferme η. En posant

$$E(kL_s) = \text{const} \cdot (kL_s)^n\,,$$

l'on obtient, moyennant (53)

$$k^n r_s^2 L_s^{n+1} \sim k^n \eta^{\frac{1}{2}+\frac{3}{4}(n+1)}.$$

où l'indépendance par rapport à η exige $\frac{1}{2} + 3(n+1)/4 = 0$, $n = -\frac{5}{3}$.

Pour normer F de manière approchée, on peut faire l'hypothèse que ce spectre vaut pour toutes les valeurs de k comprises entre $1/L_0$ et $1/L_s$, et qu'au delà de ces limites, le spectre est coupé. Du côté des grands nombres d'ondes, on l'a vu, la viscosité agit certainement comme une coupure, tandis que du côté opposé la source de puissance produit naturellement des tourbillons d'une certaine grosseur maximum L_0. Moyennant ces hypothèses la condition de normalisation (57) nous donne

$$\text{const} \cdot (2\eta/S_0) \int_{1/L_0}^{1/L_s} k^{\frac{1}{3}} \, dk = 1;$$

l'on en tire

$$\text{const} \simeq \tfrac{2}{3}(S_0 \eta) L_s^{\frac{1}{3}} = \tfrac{2}{3}(S_0 \varrho)^{\frac{1}{3}}$$

et

$$F(k) = \tfrac{2}{3}(S_0/\varrho)^{\frac{2}{3}} k^{-\frac{5}{3}}. \tag{58}$$

8. – Ailes du spectre des vitesses.

Aucune solution réellement satisfaisante n'existe pour cette région. La manière la plus simple d'aborder ce problème est de considérer le transfert d'énergie cinétique des petits nombres d'onde aux grands nombres d'onde comme un effet d'amortissement sur le mouvement des gros tourbillons. On est ainsi amené à introduire la notion d'une viscosité tourbillonnaire $\eta'(k)$ pour décrire l'absorption de l'énergie d'un tourbillon de dimension k^{-1} par des tourbillons de dimension $< k^{-1}$. Si l'on admet qu'on peut exprimer $\eta'(k)$ moyennant $F(k')$ $(k' < k)$, l'on obtiendra par des arguments de dimensions

$$\eta'(k) = \text{const} \cdot \varrho \int_k^\infty dk' [F(k')/k'^3]^{\frac{1}{2}}. \tag{59}$$

La constante s'évalue en remarquant que $\eta'(k)$ devrait être grand comparé

à η pour $k < 1/L_s$ et lui devrait être égal pour $k = 1/L_s$; d'où

$$\eta = \text{const} \cdot \varrho \int_{1/L_s}^{\infty} \mathrm{d}k' [F(k')/k'^3]^{\frac{1}{2}} .$$

Moyennant (58) cela donne

$$\text{const} \cdot \tfrac{4}{3} \sqrt{\tfrac{3}{2}} \simeq 1 .$$

On peut dès lors représenter notre transfert de puissance stationnaire comme un processus de dissipation où l'énergie S_k dissipée dans les tourbillons $k' < k$, ou transférée aux composantes de vitesse $\boldsymbol{v}_k$, avec $k' > k$, est donnée par

$$S_k = 2[\eta'(k) + \eta] \int_0^k k'^2 F(k') \, \mathrm{d}k' . \tag{60}$$

La condition de transfert stationnaire entraîne que l'énergie ne s'accumule dans aucun intervalle donné de nombre d'onde et que, par suite, S_k est indépendant de k et égal à S_0. On obtient de la sorte, avec (59), l'équation suivante pour $F(k)$:

$$S_0 = 2 \left[\varrho \int_k^{\infty} [F(k')k'^3]^{\frac{1}{2}} \, \mathrm{d}k' + \eta \right] \int_0^k k''^2 F(k'') \, \mathrm{d}k'' . \tag{61}$$

La solution, due à J. Bass, se met sous la forme

$$F(k) = (8S_0/9\varrho)^{\frac{2}{3}} k^{-\frac{5}{2}} [1 + (k/k_s)^4]^{-\frac{1}{3}} \tag{62}$$

avec $k_s = (3S_0\varrho^2/8\eta^3)^{\frac{1}{4}}$

Pour $k \ll k_s$, on retombe bien sur (58), à un changement dépourvu d'importance près de la constante de normalisation. En outre, la valeur k_s est essentiellement identique à $1/L_s$ donné par (53). Pour $k \gg k_s$, $F(k)$ se comporte comme k^{-7}

$$F(k) \cong 8^{-\frac{2}{3}} (S_0\varrho/\eta)^2 k^{-7} . \tag{63}$$

Il y a intérêt à comparer ici k_s avec $k_0 = 1/L$ et $k_M = 1/L_M$, L_M étant le libre parcours moyen des molécules du gaz. La théorie cinétique des gaz nous fournit

$$\eta/\varrho = (2\pi/3) v_M/k_M , \qquad \text{et} \qquad R = v_0 L_0 / v_M L_M$$

(nombre de Reynolds).

On tire de (53)

$$k_S = R^{\frac{1}{3}} k_0 \,, \tag{64}$$

(cf. aussi (32)) et

$$k_M (S_M / S_0) k_S \,, \tag{65}$$

où l'on a introduit $S_M = \varrho v_M^3 k_M$, par analogie avec S_0. (64) montre que $k_S \gg k_0$, si seulement le nombre de Reynolds est suffisamment grand. L'équation (61) tranche la question plus subtile de savoir si les notions hydrodynamiques s'appliquent au fond dans la discussion du processus de dissipation. $k_M \gg k_S$ est une condition nécessaire pour cela, et elle n'est valable qu'à la condition que la puissance fournie S_0 ne soit pas trop grande. Nous reviendrons sur les aspects numériques de ces conditions dans les applications à la diffusion ionosphérique.

Notre analyse du spectre de vitesse étant maintenant achevée dans ses grandes lignes, nous allons passer à l'établissement des lois régissant la diffusion des ondes électromagnétiques.

9. – Diffusion électromagnétique et son calcul.

Calculons la diffusion que subit une onde électromagnétique de vecteur de propagation $\boldsymbol{k}_0$ dans une région de l'espace de volume V qui contient un milieu dont la constante diélectrique ε subit des fluctuations $\varepsilon = \varepsilon_0 + \Delta\varepsilon$, où $\Delta\varepsilon$ est une fonction aléatorie de $\boldsymbol{r}$, $\Delta\varepsilon = f(\boldsymbol{r}')$. Nous admettrons que les variations dans le temps sont suffisamment lentes et qu'elles n'affectent pas la diffusion.

L'onde diffusée par la matière est liée aux fluctuations du moment electrique $\boldsymbol{P}$ par cm³ autour de sa valeur moyenne $\boldsymbol{P}$. Les ondes électromagnétiques couplées avec cette valeur moyenne $\overline{\boldsymbol{P}}$ ($\boldsymbol{P} - \sum \boldsymbol{p} = N\boldsymbol{p}$, $\boldsymbol{p}$ = moment électrique d'un dipôle et la sommation s'étendant sur l'unité de volume, N = nombre de dipôles par cm³) se composant pour restituer une onde cohérente regulière transmise. Les excès

$$\boldsymbol{P} - \overline{\boldsymbol{P}} = \Delta\boldsymbol{P} \qquad (4\pi\boldsymbol{P} = \boldsymbol{D} - \boldsymbol{E}) \tag{66}$$

produisent par contre des ondes sphériques incohérentes qui ne se détruisent pas complètement par interférence, mais se propagent, bien au contraire, sous forme d'onde diffusée de tous les côtés. Si le dipôle est un oscillateur harmonique, le champ ainsi produit aura pour forme classique ($r \gg \lambda$)

$$\boldsymbol{E} = \frac{\omega^2 \boldsymbol{P}}{c^2 \lambda^2 r} \sin\chi \exp\left[i(\omega t - \boldsymbol{k}\cdot\boldsymbol{r})\right] , \tag{67}$$

(χ étant l'angle de polarisation).

L'intensité des ondes diffusées par ces dipôles dans l'élément de volume $\mathrm{d}V = \mathrm{d}\boldsymbol{r}$ sera

$$\overline{\Delta \sum E}^2 \, \mathrm{d}V = I \,, \tag{68}$$

où Δ représente la fluctuation par rapport à la moyenne de la grandeur (67) et la somme étant prise sur toutes les ondes sphériques issues des divers dipôles (molécules) situés dans $\mathrm{d}\boldsymbol{r}$. En portant (67) dans (68), l'on obtient l'intensité du rayonnement diffusé par $\mathrm{d}V$

$$I = \frac{\omega^4}{c^4} \frac{1}{r^2} \overline{\Delta \sum_i p_i|^2} = \frac{(2\pi)^4}{r^2 \lambda^4} \overline{\sum_i p_i}^2 \mathrm{d}\boldsymbol{r} \,. \tag{69}$$

où p_i est le moment instantané du i-ème dipôle (molécule).

Les fluctuations de la quantité $\sum_i p_i$ sont dues à deux causes:

a) fluctuation du nombre $N\mathrm{d}V$ des molécules dans $\mathrm{d}V$

$$N = \overline{N} + \Delta N \,; \tag{70}$$

b) fluctuation des divers moments

$$p_i = \overline{p}_i + \Delta p_i \,.$$

Si l'on néglige ce dernier type de fluctuation, l'on aura:

$$\sum \boldsymbol{p}_i = \boldsymbol{p}(N + \Delta N) \qquad \text{et} \qquad \Delta \sum \boldsymbol{p}_i = \overline{\boldsymbol{p}}_i \, \Delta N = N \boldsymbol{p}_i \, \Delta V \,.$$

Or, comme $P = (\varepsilon - 1)E/4\pi$, $\sum p_i = (\varepsilon - 1)E/4\pi$ et $\Delta \sum p_i \approx \Delta\varepsilon \cdot E/4\pi$.

Finalement l'élement de volume $\mathrm{d}V$ devient un dipôle de moment $P = (\varepsilon - 1)E/4\pi$ et

$$\Delta P = \Delta\varepsilon \, E \cdot V \, 4\pi$$

la fluctuation sera donc

$$\Delta\varepsilon = 4\pi \, \Delta P / V \cdot E \,.$$

Nous supposerons dans cette première partie un milieu dans lequel la diffusion est assez faible pour qu'il ne soit pas nécessaire de considérer qu'un seul pinceau diffusé. Les résultats peuvent alors s'exprimer moyennant une fonction de distribution radiale (6). La considération de diffusion multiple

(6) Si la fonction $n^{(2)}(\boldsymbol{r}_i, \boldsymbol{r}_j) \, \mathrm{d}\boldsymbol{r}_i \, \mathrm{d}\boldsymbol{r}_j$ est la probabilité d'avoir une molécule dans l'élément de volume $\mathrm{d}\boldsymbol{r}_i$ et une autre dans $\mathrm{d}\boldsymbol{r}_j$ et si $N \gg 1$, on définit la fonction de distribution radiale $g(\boldsymbol{r}_i, \boldsymbol{r}_j)$ par $n^{(2)}(\boldsymbol{r}_i, \boldsymbol{r}_j) = n(\boldsymbol{r}_i) n(\boldsymbol{r}_j) g(\boldsymbol{r}_i, \boldsymbol{r}_j)$. $n(\boldsymbol{r}_i)$ étant la densité au point $\boldsymbol{r}_i$. $g(\boldsymbol{r}_i, \boldsymbol{r}_j) \to 1$ lorsque $r_{ij} = |\boldsymbol{r}_i - \boldsymbol{r}_j| \to \infty$, et les écarts à l'unité mesurent les corrélations dans les positions de paires de molécules.

introduit des fonctions de distribution d'ordre plus élevé. Soit $\boldsymbol{k}_0$ le vecteur de propagation de l'onde avant la diffusion et $\boldsymbol{k}$ le même après diffusion. Comme la présente analyse se borne à la diffusion élastique

$$k_0 = k = 2\pi/\lambda ,$$

λ étant la longueur d'onde radioélectrique. Les directions de vecteurs $\boldsymbol{k}_0$ et $\boldsymbol{k}$ indiquent les directions des ondes incidentes et des ondes diffusées.

Si

$$E_i = E_0 \exp [i(\omega t - \boldsymbol{k}_0 \cdot \boldsymbol{r})]$$

est le champ de l'onde incidente et

$$E = E_d \exp [i(\omega t - \boldsymbol{k}_1 \cdot \boldsymbol{r})]$$

celui de l'onde diffusée, l'amplitude E_d de l'onde diffusée sera d'après ce qui précède ($R \gg \sqrt[3]{V}$)

$$E_d = \frac{\pi E_0}{\lambda^2 R} \left| \int_V \Delta\varepsilon(\boldsymbol{r}) \exp [i\boldsymbol{k} \cdot \boldsymbol{r}] \, \mathrm{d}\boldsymbol{r} \right| \sin \chi , \tag{70}$$

χ étant l'angle entre la direction de l'onde incidente et la direction de la diffusion.

D'autre part

$$K = |\boldsymbol{K}| = |\boldsymbol{k}_0 - \boldsymbol{k}_1| = 2k \sin \theta/2 \tag{71}$$

avec $k = |\boldsymbol{k}_0| = |\boldsymbol{k}_1| = 2\pi\lambda^{-1}$.

En introduisant la section efficace $\sigma \, \mathrm{d}\Omega$ pour la diffusion par unité de volume du volume diffuseur dans l'angle solide $\mathrm{d}\Omega$

$$\sigma \, \mathrm{d}\Omega = (R^2/V)(E_d^2/E_0^2) ,$$

l'on obtient

$$\sigma \, \mathrm{d}\Omega = \pi^2 |M|^2 \sin \chi^2 \, \mathrm{d}\Omega / V\lambda^4 , \tag{72}$$

avec

$$M = \int \Delta\varepsilon(\boldsymbol{r}) \exp [i\boldsymbol{K} \cdot \boldsymbol{r}] \, \mathrm{d}\boldsymbol{r} . \tag{73}$$

Pour l'ionosphère

$$\varepsilon = \varepsilon_0 (1 - \omega_N^2/\omega^2) \tag{74}$$

avec

$$\omega_N^2 = Ne^2/m ,$$

N étant la densité d'électrons libres dans le milieu. Par conséquent

$$\frac{\Delta\varepsilon}{\varepsilon_0} = -\frac{\omega_N^2}{\omega^2}\frac{\Delta N}{N} = -\frac{\omega_N^2}{\omega^2}\frac{\Delta\varrho}{\varrho} = g\frac{\Delta\varrho}{\varrho} , \tag{75}$$

où $g = -\omega_N^2/\omega^2$.

On voit que l'amplitude des fluctuations décroît en raison inverse du carré de la fréquence ω: elles n'affecteront donc ni les ondes décimétriques, ni les ondes centimétriques. Passons maintenant au calcul de M (73) qui figure dans (70) en tenant compte de (75)

$$M = g/\varrho_0 \int \Delta\varrho(\boldsymbol{r}) \exp[i\boldsymbol{k}\cdot\boldsymbol{r}]\,\mathrm{d}\boldsymbol{r} , \tag{76}$$

où ϱ_0 est la densité moyenne. Notre propos est de calculer cette grandeur en nous appuyant sur la théorie de la turbulence homogène. Ces concepts ne s'appliqueront que si la longueur K^{-1} est comprise entre L_s et L_0:

$$L_0^{-1} < 2k \sin\theta/2 < L_s^{-1} . \tag{77}$$

L'intégrale figurant dans (76) est le coefficient de Fourier des fluctuations de densité. Reprenons le développement de la densité en une série de Fourier dans le volume diffuseur V supposé cubique

$$\varrho(\boldsymbol{r}) = \frac{1}{V}\sum_i \varrho(\boldsymbol{k}_i) \exp[-i\boldsymbol{k}_i\cdot\boldsymbol{r}] , \tag{78}$$

avec sa transformée de Fourier

$$\varrho(\boldsymbol{k}_i) = \int_V \varrho(\boldsymbol{r}) \exp[i\boldsymbol{k}_i\cdot\boldsymbol{r}]\,\mathrm{d}\boldsymbol{r} . \tag{79}$$

Il est alors évident que M défini par (76) n'est autre chose que

$$M = \frac{g}{\varrho_0}\varrho(\boldsymbol{K}). \tag{80}$$

Recherchons maintenant une relation entre $\varrho(\boldsymbol{k})$ et la grandeur $(\Delta\varrho)_L$ définie par (34). Cette quantité $(\Delta\varrho)_L$ est constituée par des fluctuations dont la période spatiale est de l'ordre de L. En vertu de la nature aléatoire de ces fluc-

tuations, les différentes longueurs d'ondes n'interféreront pas et l'on aura

$$(\Delta\varrho)_L^2 = \frac{1}{V^2}\sum_{k\sim 1/L}{}^{k}|\varrho(\boldsymbol{k})|^2 \cong \frac{1}{V^2}\left(\frac{V}{2\pi^2}\right)\int_{k'}^{k''} k^2|\varrho(\boldsymbol{k})|^2 .$$

L'intervalle est de l'ordre de L lui-même et centré sur $k \sim 1/L$. $(V/2\pi)^2$ est le nombre de composantes de Fourier ayant des nombres d'ondes compris entre k et $k+\mathrm{d}k$. Cela fournit approximativement

$$(\Delta\varrho)_L^2 \cong \frac{1}{6\pi^2}\frac{1}{VL^3}|\varrho(1/L)|^2 , \tag{81}$$

et par suite,

$$|M|^2 = 6\pi^2(g/\varrho_0)^2 V L^3 (\Delta\varrho)_L^2|_{L=1/K} ,$$

et en y portant (34):

$$|M|^2 = 6\pi^2 g^2 V\left(\frac{v_0}{v_M}\right)^4 \frac{L^{13/3}}{L_0^{4/3}}\Bigg|_{L=1/K} .$$

En substituant cela dans (72), l'on obtient

$$\sigma\,\mathrm{d}\Omega \cong 16\pi^4 g^2\left(\frac{v_0}{v_M}\right)^4 \frac{L^{13/3}}{L_0^{4/3}}\frac{\sin^2\chi}{\lambda^4} , \tag{82}$$

en omettant le facteur 3/8. En posant $L \sim K^{-1}$ et compte tenu de (71), l'on a finalement

$$\sigma = \frac{1}{3\sqrt{2\pi}}\frac{g^2}{L_0}\left(\frac{v_0}{v_M}\right)^4\left(\frac{\lambda}{L_0}\right)^{1/3}(2\sin\theta/2)^{-13/3}\sin^2\chi . \tag{83}$$

La validité de cette expression est restreinte par la condition (33). Elle ne s'applique que tant que

$$L_0^{-1} < 2k\sin\theta/2 < L_s^{-1} . \tag{84}$$

On voit que les conditions de turbulence ne figurent dans la section de choc que sous la forme v_0^4/L^4. Il s'ensuit que la section efficace est proportionnelle à $\mathcal{N}^{\frac{4}{3}}$ et ne dépend que de la dissipation d'énergie $\mathcal{N}$. Remarquons la dépendance angulaire caractéristique en $(\sin\theta/2)^{-13/3}$. En outre, σ varie avec la longueur d'onde comme $\lambda^{13/3}$. Si les conditions (84) ne sont plus vérifiées, on doit s'attendre à des écarts par rapport à (83). Le cas où $L = (2k\sin\theta/2)^{-1}$ est comparable ou inférieur à L_s est d'un intérêt particulier. Dans ce cas les

tourbillons de cette dimension sont atténués par dissipation moléculaire, et $(\Delta\varrho)_L$ est alors plus petit que (34). En particulier $(\Delta\varrho)_L$ diminuera plus rapidement que $L^{\frac{5}{3}}$ lorsque L décroît.

Si l'on prend, au lieu de (11), par exemple

$$(\Delta\varrho)_L = \varrho(v_0/v_M)^2(L/L_0)^{\frac{2}{3}}\, F(L/L_s)\,, \tag{85}$$

où $F(x)$ est une fonction égale à l'unité pour $x \gg 1$, et qui décroît rapidement pour $x < 1$, on obtient alors un facteur $F(\lambda/4\pi L_s \sin\theta/2)^2$ qui figurera dans l'expression de la section efficace (83). Il s'ensuit que la diffusion décroît plus rapidement lorsque λ décroît ou θ décroît si $(2k\sin\theta/2)^{-1} < L_s$. (70) et (71) permettent de mettre la section efficace sous la forme

$$\sigma\,\mathrm{d}\Omega = \frac{\pi^2 g^2}{\lambda^4 \varrho^2 V}\left|\int_V \Delta\varrho(\boldsymbol{r})\exp[i\boldsymbol{k}\cdot\boldsymbol{r}]\,\mathrm{d}\boldsymbol{r}\right|^2 \sin^2\chi\,\mathrm{d}\Omega\,. \tag{86}$$

Or

$$\frac{1}{\varrho^2}\left|\int_V \Delta\varrho(\boldsymbol{r})\exp[i\boldsymbol{K}\cdot\boldsymbol{r}]\,\mathrm{d}\boldsymbol{r}\right|^2 = \int \exp[i\boldsymbol{K}\cdot\boldsymbol{r}]\frac{\mathrm{d}\boldsymbol{r}}{\varrho^2}\int \Delta\varrho(\boldsymbol{R})\Delta\varrho(\boldsymbol{R}+\boldsymbol{r})\,\mathrm{d}\boldsymbol{R} = \tag{87}$$

$$= \int \exp[i\boldsymbol{K}\cdot\boldsymbol{r}]\; V\frac{\overline{\Delta\varrho^2}}{\varrho^2}\, C(\boldsymbol{r})\,\mathrm{d}\boldsymbol{r}\,,$$

en définissant une fonction d'autocorrélation par

$$C(\boldsymbol{r}) = \frac{1}{\overline{\Delta\varrho^2}}\int \mathrm{d}\boldsymbol{R}\,\Delta\varrho(\boldsymbol{R})\Delta\varrho(\boldsymbol{R}+\boldsymbol{r}). \tag{88}$$

Si l'on définit maintenant la transformée de Fourier $C(\boldsymbol{k})$ de $C(\boldsymbol{r})$ par

$$C(\boldsymbol{r}) = \left(\frac{1}{2\pi}\right)^3 \int \exp[-i\boldsymbol{k}\cdot\boldsymbol{r}]C(\boldsymbol{k})\,\mathrm{d}\boldsymbol{k}\,, \tag{89}$$

l'on obtient

$$\sigma\,\mathrm{d}\Omega = \frac{\pi^2 g^2}{\lambda^4}\left(\frac{\overline{\Delta\varrho^2}}{\varrho^2}\right) C(\boldsymbol{K})\sin^2\chi\,\mathrm{d}\Omega\,, \tag{90}$$

avec $K = 2k\sin\theta/2$.

Exprimons maintenant la fonction de corrélation $C(\boldsymbol{r})$ moyennant les ϱ_k définis par (39) avec $\varrho_k = \Delta\varrho_k$ pour $k \neq 0$:

$$C(\boldsymbol{R}) = \overline{\Delta\varrho(\boldsymbol{k})\Delta\varrho(\boldsymbol{R}+\boldsymbol{r})} = \frac{1}{V}\int_V \Delta\varrho(\boldsymbol{R})\Delta\varrho(\boldsymbol{R}+\boldsymbol{r})\,\mathrm{d}\boldsymbol{R} = \sum_k \varrho_k\varrho_{-k}\exp[i\boldsymbol{k}\cdot\boldsymbol{r}]\,.$$

Avec $\overline{\varrho^2} \cong \varrho_0^2$ et moyennant (47), il vient

$$C(\boldsymbol{r}) = \left(\frac{\varrho_0}{\gamma p_0}\right)^2 \sum_k k^{-4} \exp[i\boldsymbol{k}\cdot\boldsymbol{r}] \sum_{k'} \sum_{k''} (\boldsymbol{k}\cdot\boldsymbol{v}_{k'})\overline{(\boldsymbol{k}\cdot\boldsymbol{v}_{k-k'})(\boldsymbol{k}\cdot\boldsymbol{v}_{k''})(\boldsymbol{k}\cdot\boldsymbol{v}_{k-k''})} .$$

Les seules contributions différentes de zéro à la valeur moyenne proviennent des combinaisons

(*a*) $\qquad \boldsymbol{k}' = \boldsymbol{k}'' , \qquad \boldsymbol{k} - \boldsymbol{k}' = \boldsymbol{k} - \boldsymbol{k}'' ,$

(*b*) $\qquad \boldsymbol{k}' = \boldsymbol{k} - \boldsymbol{k}'' , \qquad \boldsymbol{k} - \boldsymbol{k}' = \boldsymbol{k}'' .$

Ainsi $\sum_{k'} \sum_{k''}$ se réduit à

$$2 \sum_{k'} \overline{(\boldsymbol{k}\cdot\boldsymbol{v}_{k'})(\boldsymbol{k}\cdot\boldsymbol{v}_{-k'})} \times \overline{(\boldsymbol{k}\cdot\boldsymbol{v}_{k-k'})(\boldsymbol{k}\cdot\boldsymbol{v}_{k'-k})} .$$

En outre, comme la condition d'incompressibilité entraîne $(\boldsymbol{k}\cdot\boldsymbol{v}_k) = 0$, l'on a

$$\overline{(\boldsymbol{k}\cdot\boldsymbol{v}_{k'})(\boldsymbol{k}\cdot\boldsymbol{v}_{-k'})} = \overline{(\boldsymbol{k}_\perp\cdot\boldsymbol{v}_{k'})(\boldsymbol{k}_\perp\cdot\boldsymbol{v}_{-k'})} = \tfrac{1}{2}|\boldsymbol{v}_{k'}|^2 k_\perp^2$$

avec

$$\boldsymbol{k}_\perp = \boldsymbol{k} - \boldsymbol{n}'\cdot(\boldsymbol{k}\cdot\boldsymbol{n})' , \qquad \boldsymbol{n}' = \boldsymbol{k}'/k,$$

et par suite

$$k_\perp^2 = [k^2 k'^2 - (\boldsymbol{k}\cdot\boldsymbol{k}')]/k'^2 .$$

Cela donne

$$\frac{\overline{\Delta\varrho^2}}{\varrho^2} C(\boldsymbol{r}) = 2(\varrho_0/\gamma p_0)^2 \sum_k k^{-4} \exp[i\boldsymbol{k}\cdot\boldsymbol{r}] \sum_{k'} |\boldsymbol{v}_{k'}|^2 \overline{|\boldsymbol{v}_{k-k'}|^2} [k^2 k'^2 - (\boldsymbol{k}\cdot\boldsymbol{k}')]/4k^2(\boldsymbol{k}-\boldsymbol{k}')^2 .$$

Comme en vertu de (89) et (90) on n'a besoin que de la transformée de Fourier $C(\boldsymbol{k})$ de $C(\boldsymbol{r})$, mettons les sommes relatives aux $\boldsymbol{k}$ sous forme d'intégrales de Fourier moyennant la substitution

$$\sum_k \to V(2\pi)^{-3} \int \mathrm{d}\boldsymbol{k} .$$

En faisant appel en même temps à $F(k)$ défini par (54) l'on obtient

$$\frac{\overline{\Delta\varrho^2}}{\varrho^2} C(\boldsymbol{r}) = \pi(\varrho_0/\gamma p_0)^4 (2\pi)^{-3} \int \mathrm{d}\boldsymbol{k} k^{-4} \exp[i\boldsymbol{k}\cdot\boldsymbol{r}] \cdot$$
$$\cdot \int \mathrm{d}\boldsymbol{k}' F(k') F(|\boldsymbol{k}-\boldsymbol{k}'|) \left[\frac{k^2 k'^2 - (\boldsymbol{k}\cdot\boldsymbol{k}')^2}{k^2(\boldsymbol{k}-\boldsymbol{k}'')^2}\right]^2 ,$$

soit, en vertu de (90),

$$\frac{\overline{\Delta\varrho^2}}{\varrho^2}\, C(\boldsymbol{k}) = \pi(\varrho_0\gamma' p_0)^2 k^{-4} \int \mathrm{d}\boldsymbol{k}' F(k') \cdot F(\boldsymbol{k} - \boldsymbol{k}') \left[\frac{k^2 k'^2 - (\boldsymbol{k}\cdot\boldsymbol{k}')^2}{k^2(\boldsymbol{k}-\boldsymbol{k}')^2}\right]^2 . \tag{91}$$

Calculons d'abord (91) pour le cas

$$k_0 \ll k \ll k_s . \tag{92}$$

VILLARS et WEISSKOFF emploient dans ce cas le spectre $F(k)$ donné par (58), en utilisant un cut-off à $k \geqslant k_s$ et à $k \leqslant k_0$. Il se trouve toutefois qu'avec les hypothèses de (92), l'intégrale sur k' — appelons-là $J(k)$ — est essentiellement indépendante des deux limites. On trouve:

$$\frac{\overline{\Delta\varrho^2}}{\varrho^2}\, C(\boldsymbol{k}) \cong 2\pi^2(\varrho_0/\gamma p_0)^2 (S_0/\varrho)^{4/3} k^{-13/3} H , \tag{93}$$

où la valeur approchée de H est

$$H = 1.2 + 1.6(k/2k_s)^{\frac{7}{3}} + \ldots . \tag{94}$$

A la limite de nombres d'ondes très élevés

$$k \gg k_s , \tag{95}$$

$H(k_s/k)$ est égal à $8/5(k_s/k)^{20/3}$, comparé à 1.2 pour le cas $k \ll k_s$.

Les sections efficaces pour les deux cas $k \ll k_s$ et $k \gg k_s$ sont

$$\sigma \cong 0.6 g^2 (v_0/v_M)^4 (\lambda/2\pi)^{1/3} L_0^{-4/3} [2 \sin\theta/2]^{-13/3} \sin^2\chi , \qquad 2k \sin\theta/2 \ll k_s . \tag{96}$$

$$\sigma \cong 0.8 g^2 (v_0/v_M)^9 (\lambda/2\pi)^7 L_0^{-3} L_M^{-5} [2 \sin\theta/2]^{-11} \sin^2\chi , \qquad 2k \sin\theta/2 \gg k_s . \tag{97}$$

Appliquons maintenant la formule de diffusion (83) aux observations de BAYLEY *et al.*, au cours desquelles un pinceau de 50 MHz était diffusé par la couche E. Les conditions géométriques de ces auteurs étaient celles représentées sur la Fig. 2. On obtient alors pour le rapport P_r/P_e de la puissance reçue à la puissance émise

$$\frac{P_r}{P_e} = 4\sigma \frac{bA}{\sin(\theta/2)\, d^2} , \tag{98}$$

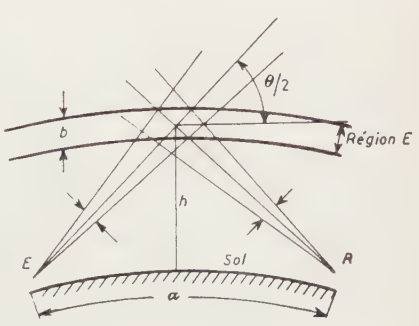

Fig. 2.

où b est l'épaisseur de la couche diffusante et A est la surface d'aperture équivalente de l'antenne réceptrice définie par $G = 4\pi A/\lambda^2$, G étant le gain de l'antenne, et où d est la distance de transmission.

Dans les expériences ed BAILEY *et al.*, les données étaient les suivantes

$$\lambda = 10^2 \text{ cm}, \quad A = 3 \cdot 10^6 \text{ cm}^2, \quad d = 1.2 \cdot 10^8 \text{ cm}, \quad b = 5 \cdot 10^5 \text{ cm}, \quad \theta = 24^\circ.$$

En substituant dans (98) ces valeurs, avec g correspondant à $\omega_N = 1.5$ MHz, ainsi que les constantes de turbulence données par (35), l'on obtient la valeur théorique

$$\frac{P_r}{P_e} = 1.0 \cdot 10^{-18}, \tag{99}$$

alors que l'expérience fournit

$$\frac{P_r}{P_e} = 0.36 \cdot 10^{-18}.$$

Théorie et expérience sont donc en accord remarquable.

Deux hypothèses implicites se trouvent à la base de ces théories de la diffusion turbulente. En premier lieu on ne tient pas compte des diffusions multiples, ce qui peut se légitimer dans certaines parties, de petite densité électronique ou ionique, de l'ionosphère. Il n'en est plus de même dans les plasmas plus denses et de caractère plus général. Il sera donc intéressant de reprendre ces calculs dans le cadre plus large des diffusions multiples.

Une seconde hypothèse conduit à admettre la théorie de la turbulence isotrope, homogène et stationnaire [1-15]. Or, le point de départ de la théorie de la turbulence est lié à l'équation de Navier mise sous la forme

$$\frac{\partial \boldsymbol{v}}{\partial t} + (\boldsymbol{v} \cdot \nabla)\boldsymbol{v} = -\frac{\nabla p}{\varrho} + \nu \Delta \boldsymbol{v}. \tag{100}$$

Or, dans les plasmas de nature et de propriétés plus générales, sièges de champs électromagnétiques rapidement et lentement variables, et rendus biréfringents par l'effet des champs magnétiques, il apparaît que la force de Lorentz est susceptible de modifier profondément, entre autre, le caractère isotrope de la turbulence, ce qui amène à mettre les équations de Navier sous la forme

$$\frac{\partial \boldsymbol{v}}{\partial t} + (\boldsymbol{v} \cdot \nabla)\boldsymbol{v} = \frac{1}{\varrho}(\varrho_e \boldsymbol{E} + \mu \boldsymbol{j} \wedge \boldsymbol{H}) - \frac{1}{\varrho} \nabla p + \nu \Delta \boldsymbol{v}, \tag{101}$$

ϱ_e et $\boldsymbol{j}$ étant définis par les équations de Maxwell

$$\operatorname{div} \varepsilon \boldsymbol{E} = 4\pi \varrho_e, \qquad 4\pi \boldsymbol{j} = -\frac{\varepsilon}{c} \frac{\partial \boldsymbol{E}}{\partial t} + \operatorname{rot} \boldsymbol{H}, \qquad \text{avec } \operatorname{div} \boldsymbol{H} = 0,$$

et

$$\frac{\mu}{c}\frac{\partial \boldsymbol{H}}{\partial t} \qquad \text{rot } \boldsymbol{E} ,$$

ε étant en général un tenseur du second ordre.

Dans ces plasmas, de caractère très général, le champ électrique $\boldsymbol{E}$ et le champ magnétique $\boldsymbol{H}$ sont susceptibles de comporter des composantes fluctuantes. Ces composantes $\boldsymbol{E}_f$ et $\boldsymbol{H}_f$ doivent être à leur tour développées en séries de Fourier

$$\boldsymbol{E}_f(\boldsymbol{r}) = \int \boldsymbol{E}(\boldsymbol{k}) \exp[i\boldsymbol{k}\cdot\boldsymbol{r}]\,\mathrm{d}\boldsymbol{r}, \qquad \boldsymbol{H}_f(\boldsymbol{r}) = \int \boldsymbol{H}(\boldsymbol{k}) \exp[i\boldsymbol{k}\cdot\boldsymbol{r}]\,\mathrm{d}\boldsymbol{r} ,$$

à la manière du champ de vitesse $\boldsymbol{v}$ et de la pression p. Il apparait dès lors nécessaire, dans la théorie générale de la diffusion turbulente des ondes électromagnétiques, de prendre pour base des calculs les équations de Navier modifiées (101), tout en tenant compte de la diffusion multiple.

RÉFÉRENCES

[1] L. Agostini et J. Bass: *Les théories de la turbulence* (Paris, 1950).
[2] J. Bass: *Les méthodes modernes du calcul des probabilités et leur application au probléme de la turbulence* (Paris, 1946).
[3] J. Bass: *Compt. Rend. Paris*, **228**, 22 (1949).
[4] G. K. Batchelor: *Turbulent motion*, in *Rep. Progr. Phys.*, **15**, 101 (1952).
[5] D. K. Bayley, R. Bateman, H. G. Booker, L. V. Berkner, E. M. Purcell, G. F. Montgomery, W. W. Salisbury et J. B. Wiesner: *Phys. Rev.*, **86**, 141 (1952).
[6] H. G. Booker et W. E. Gordon: *Proc. Inst. Rad. Eng.*, **38**, 401 (1950).
[7] W. Heisenberg: *Zeits. f. Phys.*, **124**, 628 (1948).
[8] T. Kahan: *Compt. Rend. Paris*, **241**, 1726 (1955).
[9] T. Kahan: *Diffusion multiple, etc.* (inédit).
[10] A. N. Kolmogoroff: *Compt. Rend. Acad. Sci. Moscou*, **30**, 301 (1941).
[11] E. C. S. Megaw: *Nature*, **166**, 1100 (1950); *Proc. Inst. Electr. Eng.*, **100**, 7 (1953).
[12] H. Staras: *Zeits. Appl. Phys.*, **23**, 1152 (1952).
[13] F. Villars et V. F. Weisskopf: *Phys. Rev.*, **94**, 232 (1954).
[14] J. Voge: *Onde Electrique*, **35**, 564 (1955).
[15] C. F. V. Weizsäcker: *Zeits. f. Phys.*, **124**, 614 (1948).

OSSERVAZIONI ED INTERVENTI

— H. BREMMER:

Est-ce-que le spectre $F(k)$ de la fonction de correlation (r) employée par Weisskopf et Villars diffère essentiellement de celui dérivé par Kolmogoroff et Heisenberg?

— T. KAHAN:

Le modèle de Kolmogoroff et Heisenberg constitue la base du travail de WEISSKOPF et VILLARS.

— K. RAWER:

Si l'on compare cette belle théorie aux résultats des expériences on retrouve deux difficultés: la première est donnée par le fait que l'altitude de « réflexion est nettement au dessous de celle de maximum de l'ionisation de la région E (120 km). La différence est de l'ordre de 40 km. A priori on dirait que l'effet de diffusion du rayonnement était maximum au maximum d'ionisation. Il s'agit donc de trouver la raison pourquoi cette diffusion a lieu vers 80 km. Il est possible qu'il y ait là une très forte turbulence qui devrait être expliquée.

La deuxième difficulté est due aux météores qui n'ont pas seulement un effet direct d'ionisation. Cette ionisation assez forte concentrée dans une trace mince donne certainement lieu à une reflexion partielle du rayonnement. L'influence des météores semble d'ailleurs se retrouver dans les courbes obtenues par la variation journalière de l'effet où l'on observe le maximum dans la nuit connu de la statistique des météores.

— D. GRAFFI:

Con la teoria che Lei ha esposto si calcolano le variazioni della costante dielettrica dovute alle fluttuazioni di densità. È possibile calcolare il campo elettromagnetico in corrispondenza di queste variazioni di costante dielettrica?

— T. KAHAN:

È possibile, mediante un metodo del tipo di quello delle perturbazioni.

SUPPLEMENTO AL VOLUME IV, SERIE X
DEL NUOVO CIMENTO

N. 4, 1956
2° Semestre

The Electrical Conductivity of the Ionosphere: a Review.

S. CHAPMAN

Geophysical Institute - University of Alaska
High Altitude Observatory - Boulder, Colorado (*)

1. – Introduction.

BALFOUR STEWART [1] was the first to infer, in 1882, that the upper atmosphere must include a region with significant electrical conductivity. He drew this conclusion from a discussion of S, the solar daily geomagnetic variation. This variation is decidedly greater in years of high than in years of low sunspot number; he considered that the cause must be electrical currents in the *upper* atmosphere, not in the lower atmosphere or within the earth, because these regions show no appreciable change associated with the sunspot cycle. He suggested also that the currents are produced by dynamo action, that is, by movement of conducting air across the lines of force of the geomagnetic field.

In 1889 SCHUSTER [2] established Stewart's inference that S originates *above* the earth. This he did by spherical harmonic analysis, in the manner introduced in 1839 by GAUSS [3]. In 1908 SCHUSTER [4] gave mathematical form to Stewart's dynamo theory of S. Electromotive forces (e.m.f.) arise wherever air moves across the geomagnetic field, but they will be effective only in the supposed conducting region. The air motion must be mainly horizontal; the induced e.m.f. may have a vertical component, but the current flow was ascribed solely to the horizontal component e.m.f. This sets up electrical currents and also a distribution of electric charge in the conducting layer, such that the combined e.m.f. and electrostatic field impel closed and nearly steady electric current flow.

The magnetic observations of S indicate the pattern of the electric current flow, and also its intensity, integrated over the thickness of the current layer;

(*) Now engaged in a joint research program with the High Altitude Observatory and the National Bureau of Standards, Boulder, Colorado.

they do not determine the height h at which the currents flow; on this account the current pattern and intensity are subject to a slight uncertainty, of proportional amount h/a, where a denotes the radius of the earth.

The current intensity inferred from the magnetic data for S gives the order of magnitude of the product Kv; here K denotes the electrical conductivity integrated over the thickness of the current layer, and v denotes the magnitude of the daily-varying vector departure $\boldsymbol{v}$ of the air velocity from the daily mean air velocity. The data for S indicate that Kv is greater by day than by night, in summer than in winter, and at sunspot maximum than at sunspot minimum.

Schuster [4] calculated K on the assumption that $\boldsymbol{v}$ is the same as for the daily wind variations at ground level. His value, for the maximum K at places where the sun is overhead, was $1.1 \cdot 10^{-5}$ e.m.u. This value implied considerable ionization of the upper atmosphere. Chapman [5] in 1919 inferred an even higher value, $2.5 \cdot 10^{-5}$ e.m.u. (on the same assumption as to $\boldsymbol{v}$), from new investigations of the current flow and the dynamo theory of S, and also of L, the lunar daily geomagnetic variation.

In 1902 Heaviside and Kennelly independently inferred the existence of an ionized layer in the upper atmosphere, from quite different evidence, concerning radio propagation. During the years following 1920 this layer, later known as the *ionosphere*, on the proposal of Watson Watt, was explored by radio experiments made by Appleton, Breit and Tuve and other pioneers. They were able to determine the amount and the daily and other variations of the maximum values of the electron density n_e, at the peaks of the E and F ionospheric layers, distinguished and so named by Appleton; like S, the electron density is greater by day than by night, in summer than in winter (at least in the E and F_1 layers), and in years of high than of low sunspot number. From the radio measurements of n_e it was possible to estimate the specific electrical conductivity k_0, from the formula (derived from the simple mean-free-path theory)

$$k_0 = e^2 \left(\frac{n_e}{m_e \nu_e} + \frac{n_+}{m_+ \nu_+} + \frac{n_-}{m_- \nu_-} \right). \tag{1}$$

Here e denotes the (positive) magnitude, $1.60 \cdot 10^{-20}$ e.m.u., of the unitary electrical charge; m_e, m_+, m_- denote the masses of electrons and of positive and negative ions respectively; n_e, n_+, n_- denote their number densities (or numbers per cm^3), and ν_e, ν_+, ν_- their collision frequencies. (The ions are supposed to be only singly charged). The corresponding total conductivity of the ionosphere is given by

$$K_0 = \int k_0 \, dh , \tag{2}$$

integrated throughout the thickness of the ionosphere.

In 1927 PEDERSEN [6] pointed out, in connection with the radio measurements of n, and the dynamo theory of S, that the geomagnetic field renders the electrical conductivity anisotropic. The above values of k_0 and K_0 are valid in the absence of a magnetic field, and also, when a magnetic field $\boldsymbol{F}$ is present, for the component electric field along $\boldsymbol{F}$; but for the electric component normal to $\boldsymbol{F}$ the specific conductivity is reduced to k_1, given by the formula (derived from the mean-free-path theory)

$$k_1 = e^2 \left\{ \frac{n_e \nu_e}{m_e(\omega_e^2 + \nu_e^2)} + \frac{n_+ \nu_+}{m_+(\omega_+^2 + \nu_+^2)} + \frac{n_- \nu_-}{m_-(\omega_-^2 + \nu_-^2)} \right\}, \tag{3}$$

where, with suffix e, $+$ or $-$ added to the symbols ω and m,

$$\omega = \pm eF/m \ ; \tag{4}$$

here ω is the angular speed, in radians per second, with which the charges spiral round the lines of magnetic force, in opposite directions for the opposite charges; the sign in (4) is opposite to that of the charge, if the right-handed spiral motion of the charges, relative to the direction of $\boldsymbol{F}$, is reckoned positive. Thus ω is $1.76 \cdot 10^7 F$ for the electrons, and $-9.57 \cdot 10^3 F/W_i$ for a positive ion of molecular weight W_i. At the magnetic equator, taking F there to be 0.3 gauss, ω_e is $5.28 \cdot 10^6$; at the geomagnetic pole, taking $F = 0.6$ gauss, ω_e is $1.055 \cdot 10^7$; the corresponding values of ω_i are $\pm 2.90 \cdot 10^3/W_i$ and $\pm 5.79 \cdot 10^3/W_i$, the sign being opposite to that of the ion.

The direction of the current flow in the S system is in many places normal or oblique to the geomagnetic field $\boldsymbol{F}$; hence it seemed that the effective specific conductivity k at such places must be equal or similar to k_1, the «transverse» or «Pedersen» conductivity. The corresponding integrated conductivity K_1, as inferred from the radio data, was estimated by APPLETON [7] to be much less than the value of K inferred from S by SCHUSTER and CHAPMAN, on the assumption that the ionospheric motion $\boldsymbol{v}$ is the same as that at ground level.

The discrepancy was reduced, but not removed, when it came to be considered likely that the ionospheric $\boldsymbol{v}$ exceeds the ground value by a factor of order 100, thus reducing the S estimate of K in the same ratio. This new light on the magnitude of $\boldsymbol{v}$ was given by the theoretical investigations of atmospheric oscillation, by TAYLOR [8] and by PEKERIS [9], and by the radio determination by APPLETON and WEEKES [10] of the very considerable lunar tidal rise and fall of the E layer; later MARTYN [11] showed that the tidal rise and fall of the F layer is even greater (the range being a few km). Meanwhile the accurate kinetic theory of the electrical conductivity of an ionized gas in a magnetic field [12, Ch. 18] had been further developed by COWLING [13].

The remaining discrepancy between K as inferred from S and from the radio data was of order 10; it also has now been removed, by considerations essentially due to COWLING [14]. In the presence of a magnetic field $\boldsymbol{F}$, a transverse component $\boldsymbol{E}$ not only produces a current $k_1\boldsymbol{E}$ in its own direction; it also impels a « Hall » current $k_2 E$ in the direction of the vector product $\boldsymbol{F} \times \boldsymbol{E}$, perpendicular both to $\boldsymbol{F}$ and to $\boldsymbol{E}$: where (according to the mean-free-path theory)

$$k_2 = e^2 \left\{ \frac{n_e \omega_e}{m_e(\omega_e^2 + \nu_e^2)} + \frac{n_- \omega_-}{m_-(\omega_-^2 + \nu_-^2)} + \frac{n_+ \omega_+}{m_+(\omega_+^2 + \nu_+^2)} \right\} . \tag{5}$$

Thus this current has the direction of $\boldsymbol{E} \times \boldsymbol{F}$ for the positive ions, and the opposite direction, that of $\boldsymbol{F} \times \boldsymbol{E}$, for the negatively charged particles. It is appropriate to call k_2 the Hall conductivity.

This current may be inhibited partly or wholly, when the boundaries of the conducting region are normal or oblique to the Hall current, by the field of an electrostatic charge distribution set up in the region. COWLING [14] showed that this will cause the effective conductivity k to exceed k_1, and it may even approach k_0.

The proper application of his ideas to the theory of the geomagnetic variations S and L was rather long delayed. Successive approaches to the application were made by MARTYN [15], HIRONO [16], K. MAEDA [17], BAKER and MARTYN [18] and FEJER [19]. As a result, the dynamo theory of S and L no longer seems at variance with the radio data; moreover the theory of k is found to give a satisfactory explanation of a peculiarity [20, Ch. 7] of S, first discovered at Huancayo in 1922, and later at other stations near the magnetic equator, where the daily variation of the horizontal magnetic component H is at least twice as great as in nearby latitudes. An investigation by A. A. GIESECKE has shown that the abnormality is confined to a belt of magnetic latitude only a few degrees wide. This indicates a local intensification (called by CHAPMAN [21] an electrojet) of the S current system, during the day, along the magnetic equator. This is accounted for by a peculiar enhancement of k in that region, associated with another conductivity coefficient k_3, defined by

$$k_3 = k_1 + k^2/k_1 . \tag{6}$$

It is appropriate to call k_3 the Cowling conductivity.

2. – The Standard Conductivities k_0 to k_3.

At each point the ionosphere must be almost exactly neutral electrically; hence

$$n_e + n_- = n_+ . \tag{7}$$

Let the suffix i refer to ions of either kind, of total number density n_i: then

$$n_i = n_+ + n_- . \tag{8}$$

In the present state of knowledge it is appropriate to ignore the differences between the masses of the (+ and —) ionic and neutral particles, and to write

$$m_+ = m_- = m_i = m , \tag{9}$$

where m denotes the (mean) mass of the neutral particles. Hence also

$$\omega_+ = -\omega_- = \omega_i . \tag{10}$$

Let the positive magnitudes X_e, X_+, X_-, X_i be defined by

$$X = |\nu/\omega| = m\nu/eF , \tag{11}$$

with suffix e, $+$, $-$ or i to all four symbols X, m, ν, ω. Then (1), (3), (5), (6) may be re-written in the form

$$k_0 = \frac{e}{F}\left\{\frac{n_e}{X_e} + \frac{n_i}{X_i}\right\} = \frac{n_e e}{F}\left\{\frac{1}{X_e} + \frac{1}{X_i}\right\} + \frac{2n_- e}{FX_i} , \tag{12}$$

$$k_1 = \frac{e}{F}\left\{\frac{n_e}{X_e + 1/X_e} + \frac{n_i}{X_i + 1/X_i}\right\} = \\ = \frac{n_e e}{F}\left\{\frac{1}{X_e + 1/X_e} + \frac{1}{X_i + 1/X_i}\right\} + \frac{2n_- e}{F(X_i + 1/X_i)} , \tag{13}$$

$$k_2 = \frac{n_e e}{F}\left\{\frac{1}{1 + X_e^2} - \frac{1}{1 + X_i^2}\right\} , \tag{14}$$

where it has been assumed that

$$\nu_+ = \nu_- = \nu_i . \tag{15}$$

Baker and Martyn [18] ignored the presence of any negative ions, that is, they took

$$n_- = 0 , \tag{16}$$

in which case the last terms in (12), (13) would vanish, and k_3 can be expressed by

$$k_3 = \frac{n_e e}{F}\,\frac{X_e + X_i}{1 + X_e X_i} = \frac{X_e X_i}{1 + X_e X_i}\,k_0 < k_0 ; \qquad (n_- = 0), \tag{17}$$

they discussed the height-distribution of the conductivities k_0 to k_3 on the basis of the formulae (1), (3), (5), (6), and on the supposition, suggested as « reasonable » (l. c., p. 287), « throughout the important conducting regions of the ionosphere », that the ratio of the (positive) magnitudes of ω_e/ν_e and ω_i/ν_i is independent of height. In the notation of (11), this means that X_i/X_e is independent of height; throughout much of the ionosphere it is a large number, for which they adopted the value 1650; but actually it decreases greatly from 80 km, where it is about 3000, to 300 km.

Let s be defined by

$$s = \tfrac{1}{2}\ln(X_i/X_e) = \tfrac{1}{2}\ln(m_i\nu_i/m_e\nu_e)\,, \qquad \text{or} \qquad X_i = X_e e^{2s}\,. \tag{18}$$

If X_i/X_e has the value 1650 adopted by BAKER and MARTYN, $s = 3.70$.

Let h_e and h_i denote the heights at which X_e and X_i are respectively unity, that is, at which (ignoring signs) $\omega_e = \nu_e$ and $\omega_i = \nu_i$. Let u denote the function of the height h defined by the equation

$$u = -\tfrac{1}{2}\ln(X_eX_i) = \ln(eF) - \tfrac{1}{2}\ln(m_em_i\nu_e\nu_i)\,. \tag{19}$$

Then

$$X_e = \exp[-s-u]\,, \qquad X_i = \exp[s-u]\,; \tag{20}$$

u is zero at the height h_0, at which

$$X_e = \exp[\quad s] = 1/X_i\,, \qquad X_eX_i = 1\,. \qquad (u=0) \tag{21}$$

If the slow upward decrease of F is ignored, ω_e and ω_i are independent of h and u; ω_e is much the greater, in the ratio m_i/m_e; hence X_e and X_i vary with height like ν_e and ν_i, and so long as n_e is much smaller than n_n, the neutral number density, ν_e and ν_i vary as n_n: in an exponential atmosphere this varies as $\exp[-h/H]$, where H is the scale height; in these circumstances, if s is constant, the « level » u can be identified with $(h-h_0)/H$, that is, as the height measured from h_0, in scale-height units; in less special circumstances, u will be a fairly simple increasing function of $h-h_0$.

By means of (20) the equations (12)–(14), (17) can be expressed in terms of the « level » u as follows (n_- being zero):

$$k_0F/n_ee = 2e^u\cosh s \equiv k_0'\,; \tag{22}$$

$$k_1F/n_ee = \tfrac{1}{2}\{\operatorname{sech}(u+s) + \operatorname{sech}(u-s)\} =$$

$$= \frac{2\cosh s\cosh u}{\cosh 2s + \cosh 2u} \equiv k_1'; \tag{23}$$

$$k_2 F/n_e e = \frac{\sinh 2s}{\cosh 2s + \cosh 2u} \equiv k_2' ; \tag{24}$$

$$k_3 F/n_e e = \cosh s/\cosh u \equiv k_3' ; \tag{25}$$

also

$$k_2/k_1 = \sinh s/\cosh u , \qquad k_0/k_3 = 1 + e^{2u} > 1 . \tag{26}$$

These equations are valid (when u is zero) whether or not s varies with height.

The equations (22)-(25) may be regarded as giving the various « standard » conductivities *per ion-electron pair*, k n_e, these having the values $(e/F)k'$, with appropriate suffix 0, 1, 2 or 3 to k and k'.

The quantities k' have the following properties as functions of the « level » u, in the special case when s is independent of the height:

(*a*) k_0' increases upward exponentially, to infinity; at $u = 0$, k_0' is 2 cosh s ($= 40.6$, if $X_i/X_e = 1650$);

(*b*) k_1', k_2', k_3' are even functions of u;

(*c*) k_1' has a minimum value sech s at $u = 0$, and it has equal maxima near $u = \pm s$; as e^{2s} is a large number, the minimum value of k_1' is small (e.g., if $e^{2s} = 1650$, sech $s = 0.049$); the peak values of k_1' occur at $u = \pm (s - e^{-2s})$, and are equal to $\frac{1}{2} + e^{-2s}$, if one ignores e^{-4s} and still smaller terms;

(*d*) k_2' has a single maximum at $u = 0$ (that is, at the height h_0); the peak value is tgh s, or (to the same degree of approximation) $1 - 2e^{-2s}$, almost exactly 1 if $e^{2s} = 1650$;

(*e*) k_3' likewise has a single peak value cosh s (equal to 20.32 if $e^{2s} = 1650$), at the same level $u = 0$ or height h_0;

(*f*) k_2' has a flatter maximum than k_3'; e.g., at $u = \pm s$, k_2' is $\frac{1}{2}$ tgh $2s$ (almost exactly $\frac{1}{2}$), and k_3' is exactly 1; thus the ratio of the peak value at $u = 0$, to the value at $u = \pm s$, is 2 for k_2', and cosh s (or 20.32 if e^{2s} is 1650) for k_3';

(*g*) at levels well below $u = -s$ (or $h = h_e$), k_1' and k_3' tend asymptotically to equality with k_0', whereas k_2' decreases (for large negative values of u) much more rapidly;

(*h*) at levels well above $u = s$ (or $h = h_i$), where k_0' tends to infinity, k_1' and k_3' tend to zero as $2e^{-u}$ cosh s, and k_2' tends to zero much more rapidly, as $2e^{-2u}$ sinh $2s$; hence despite the flat maximum of k_2', the range of u over which k_2' exceeds any chosen small value is more restricted than it is for k_1'

and k_3'; if for the latter the range is beween $\pm u_1$, and for k_2' it is between $\pm u_2$, then approximately

$$u_2 = \tfrac{1}{2}(u_1 + s) ;$$

the error here (to be subtracted from the right-hand side) is $e^s - u$; this result is a good approximation when $u_1 > 3s$, $u_2 > 2s$; at $u_1 = 3s$ and $u_2 = 2s$ the functions k_1' and k_2' respectively have the values $e^{-2s}(1 \pm e^{-2s})$, which are both very small and very nearly equal;

(*i*) the indefinite integrals $\int k' \, du$ have the following values;

$$\text{for } k_0', \quad 2e^u \cosh s ;$$

$$\text{» } k_1', \quad \mathrm{tg}^{-1} e^{u+s} + \mathrm{tg}^{-1} e^{u-s} = \cot^{-1} X_e + \cot^{-1} X_i ;$$

$$\text{» } k_2', \quad \tfrac{1}{2} \ln \frac{\exp[2u] + \exp[-2s]}{\exp[2u] + \exp[+2s]} = \tfrac{1}{2} \ln \frac{1 + X_e^2}{1 + X_i^2};$$

$$\text{» } k_3', \quad 2 \cosh s \, \mathrm{tg}^{-1} e^u = 2 \cosh s \cot^{-1} (X_e X_i)^{\frac{1}{2}} ;$$

(*j*) the complete integrals

$$\int_{-\infty}^{\infty} k' \, du$$

have twice the values of the complete integrals from $-\infty$ to 0 or from 0 to ∞, in the case of the even functions k_1', k_2', k_3': and their values are:

$$\text{for } k_1', \quad \pi ,$$

$$\text{» } k_2', \quad 2s ,$$

$$\text{» } k_3', \quad \pi \cosh s .$$

If $e^{2s} = 1650$, the numerical values of these three complete integrals are 3.14, 7.41, 63.8;

(*k*) the ratio k_2/k_1 given by (26) has a maximum value $\sinh s$ (equal to 20.3 if $e^{2s} = 1650$) at $u = 0$; the ratio k_3/k_1 also has a maximum at $u = 0$, the peak value being $\cosh^2 s$ ($= 413$ if e^{2s} is 1650); for large values of $|u|$ the ratio k_3/k_1 tends to 1; at $u = 0$, $k_0/k_1 = 2 \cosh^2 s$ ($= 826$ if e^{2s} is 1650).

The equivalent of property (*k*) was stated by Baker and Martyn [18], and some of the other properties listed above can be recognized in their Fig. 2; this plots k/u_r (with suffixes 0 to 3) against $1/X_i$ (which they denoted by $\mathrm{tg}\, \alpha_i$), both scales being logarithmic; thus their scale of ordinates is a linear

scale of height logarithmic; thus their scale of ordinates is a linear scale of height, if the atmosphere is exponential, and if the other assumptions above mentioned are adopted.

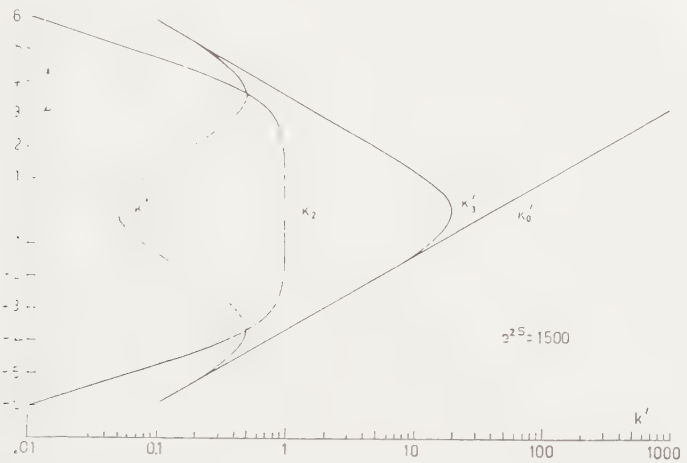

Fig. 1. – The height-distribution of k_0' to k_3'; these numbers, multiplied by $1.60 \cdot 10^{-20}/F$, where F denotes the geomagnetic intensity in gauss, give the electrical conductivity (emu) per electron-ion pair. The graphs refer to a model ionosphere with constant scale height H, in which the ratio ν_e/ν_i of the electronic to the ionic collision frequencies is independent of height. The ordinate u then denotes height measured in units of amount H, from the level where $\nu_e\nu_i = \omega_e\omega_i$, where ω denotes the spiralling frequency eF/m. The ratio ν_i/ω_i is taken to be 1 500 times ν_e/ω_e: The k' scale of abscissae is logarithmic. See equations (22)-(25).

Fig. 1 shows the graphs of the functions $\log_{10} k'$ in terms of the ordinates u, for $X_i/X_e = e^{2s} = 2\,500$.

3. – Discussion of the Conductivity Formulae.

The formulae (1), (3), (5) for k_0, k_1, and k_2 are derived by the crude arguments of the mean-free-path theory [12, Chs. 5, 6; 20, pp. 527-532], whose merits are simplicity and illumination (not always reliable); accuracy it cannot claim. In some cases it gives formulae that are qualitatively correct in important respects, but there remains uncertainty at least as regards a numerical factor. The collision frequency ν that appears in (1), (3), (5) is a conception that has a definite clear meaning only when the particles of the gas are envisaged as rigid elastic spheres. In this case, in a mixed gas in equilibrium, the expression for ν for each kind of particle present (1), (2), ... is known [12, pp. 90, 91].

Let σ_1, σ_2, ,.. denote the diameters of the particles of the kinds 1, 2, ..., and n_1, n_2, ... their number densities, and m_1, m_2, ... their masses. Then ν_1, the collision frequency for a particle of kind 1, can be subdivided into parts,

$$\nu_1 = \nu_{11} + \nu_{12} + \nu_{13} \cdots , \tag{27}$$

where ν_{1s} denotes the average number of collisions per second of a particle of kind 1 with particles of the kind s; and

$$\nu_{11} = 4n_1\sigma_1^2(\pi kT/m_1)^{\frac{1}{2}} , \qquad \nu_{12} = 4n_2\sigma_{12}^2(\pi kTm_0/2m_1m_2)^{\frac{1}{2}} , \tag{28}$$

where

$$\sigma_{12} = \tfrac{1}{2}(\sigma_1 + \sigma_2) , \qquad m_0 = m_1 + m_2 , \tag{29}$$

and k denotes Boltzmann's constant ($1.380 \cdot 10^{-16}$). Note that, in general,

$$\nu_{12} \neq \nu_{21} . \tag{30}$$

Proper quantitative calculation of the electrical conductivity of an ionized gas is attainable only through the method initiateds by Boltzmann and Maxwell, which depend on determining the distribution functions for the velocities of the various kinds of particle present in the gas. The simplest type of ionized gas is a binary mixture of positive ions (all alike) and electrons or negative ions (all alike); this case is discussed in [12], both in the absence of a magnetic field (p. 320) and when such a field is present (p. 335); the results will be briefly indicated.

3·1. *A Neutral Binary Fully Ionized Gas.* – The conductivity of a neutral binary mixture of particles carrying opposite charges e_1, e_2 is given [12, p. 320], in the absence of a magnetic field, by

$$k_0 = -ne_1e_2D_{12}/kT = -\varrho e_1e_2/m_1m_2\nu , \tag{31}$$

where

$$n = n_1 + n_2 , \qquad n_1e_1 + n_2e_2 = 0 , \qquad \nu = \varrho kT/nm_1m_2D_{12} , \tag{32}$$

$$\varrho = n_1m_1 + n_2m_2 = \varrho_1 + \varrho_2 ,$$

and D_{12} denotes the coefficient of diffusion for a binary gas composed only of particles 1, 2. The quantity ν defined by (32) has the dimensions of a collision frequency, and will be called a (conventional) collision frequency.

In the presence of a magnetic field $\boldsymbol{F}$, first approximations to k_1 and k_2

are given by the combined formula (in which i denotes the square root of -1)

$$[k_1 + ik_2]_1 = [k_0]_1/(1 + i\omega/[\nu]_1)\,, \tag{33}$$

where

$$\omega = \omega_1 + \omega_2\,, \qquad \omega_1 = e_1F/m_1\,, \qquad \omega_2 = e_2F/m_2\,. \tag{34}$$

In (33) and later formulae, enclosure in square brackets with exterior suffix 1 denotes the first approximation.

Thus (33) reduces to $[k_0]_1$ when $F = 0$, and when $F \neq 0$ it gives

$$[k_1]_1 = [k_0\nu^2/(\omega^2 + \nu^2)]_1\,, \qquad [k_2]_1 = -[k_0\omega\nu/(\omega^2 + \nu^2)]_1\,. \tag{35}$$

Let the particles 1 be the positive charges, and the particles 2 the negative charges. Suppose that the latter are electrons, so that m_2/m_1 is very small. Then in (1) only the first term need be considered, and $[k_0]_1$ according to (31) is equivalent to $n_e e^2/m_e[\nu]_1$; thus (1) gives the first approximation to k_0, provided that ν_e in (1) is interpreted as being $[\nu]_1$; this depends [12, p. 165 (1)] only on the collisions between the oppositely charged particles. When these are regarded as behaving like rigid elastic spheres [12, p. 245],

$$[D_{12}]_1 = \frac{3}{8n\sigma_{12}^2}\left\{\frac{kTm_0}{2\pi m_1 m_2}\right\}^{\frac{1}{2}}\,, \tag{36}$$

so that (when m_2/m_1 is negligible)

$$[\nu]_1 = \tfrac{4}{3}\nu_{12}\,, \tag{37}$$

where ν_{12} is given by (28). But of course charged particles do *not* behave as rigid elastic spheres; they interact according to the inverse square law of attraction. In this case, using the appropriate expression for D_{12} [12, p. 245 (2)], $[\nu]_1$ is given, when m_2/m_1 is negligible, by

$$[\nu]_1 = \tfrac{2}{3}n_1 A_1(2)\left(\frac{2\pi}{m_e}\right)^{\frac{1}{2}}\frac{e_1^2e_2^2}{(kT)^{\frac{3}{2}}}\,, \tag{38}$$

where $A_1(2)$ is a pure number, whose value will be discussed later (Sect. 3·2). As regards k_1, the accurate first approximation given by (35) reduces to the first term of (3), with ν_e replaced by $[\nu]_1$; thus in a gas consisting only of electrons and positive ions, k_1 will not include the ionic term, which in the conditions discussed in Sect. 2 gives rise to the upper maximum of k_1', corresponding to the term sech $(u - s)$ in (23). Similarly the first approximation to k_2, given by (35), reduces to the first term of (5), so that k_2 does not vary as discussed in Sect. 2.

In the case of an electron-ion mixture, the later approximations to k_1 and k_2 differ notably from the first approximations. COWLING [13, p. 459] indicated that

$$[k_1]_2 = 1.96\,[k_1]_1\,, \qquad [k_2]_2 = 4.88\,[k_2]_1\,, \tag{39}$$

where the suffix 2 outside the square brackets indicates the second approximation. LANDSHOFF [22] and SPITZER and HÄRM [23] made similar estimates of the correction necessary to the first approximation.

These calculations bear on the ionosphere only at levels well above the F_2 peak, where the air may be almost completely ionized. For the major part of the ionosphere the simplest model is a ternary mixture consisting of particles of three kinds, (1) positive ions, (2) electrons, and (3) neutral particles.

3·2. *A Neutral Ternary Partly Ionized Gas.* – The conductivities for a ternary ionized gas have been given, to a first approximation, by COWLING [13, p. 464]. His result, when the particles of kind 3 are neutral, is

$$[k_1 + ik_2]_1 = i\varrho L'/FL\,, \tag{40}$$

where, remembering that

$$n_1e_1 + n_2e_2 = 0\,, \tag{41}$$

L and $i\varrho L'/F$ may be expressed as follows:

$$L = F^2\varrho_3^2 n_1 n_2 e_1 e_2 - iF\varrho\{\theta_{23}n_1e_1(\varrho - 2\varrho_1) + \theta_{12}n_2e_2(\varrho - 2\varrho_2)\} - \\ - \varrho^2(\theta_{12}\theta_{13} + \theta_{21}\theta_{23} + \theta_{31}\theta_{32})\,, \tag{42}$$

$$i\varrho L'/F = -\varrho^2 n_1^2 e_1^2(\theta_{13} + \theta_{23})\,. \tag{43}$$

In these formulae θ_{qr} is defined by

$$\theta_{qr} = \frac{\varrho_q\varrho_r}{\varrho_q + \varrho_r}[\nu_{qr}]_1 = \frac{n_q n_r}{n_q + n_r}\frac{kT}{[D_{qr}]_1} = \theta_{rq}\,, \tag{44}$$

$$[\nu_{qr}]_1 = \frac{8}{3}\,\varrho\sigma_{qr}^2\left\{\frac{2\pi kT}{m_q m_r(m_q + m_r)}\right\}^{\frac{1}{2}}, \tag{45}$$

so that in the case of a binary gas ν_{12} is conformable to the collision frequency defined by (32). Note that

$$\nu_{qr} = \nu_{rq}\,,$$

thus differing from the property (30) for the collision frequencies defined for a gas composed of rigid elastic spheres.

It is not difficult to show that when $n_3 \to 0$, (40) becomes identical with (35).

COWLING showed [13, p. 464] that if (*a*) the neutral particles greatly outnumber the ions and electrons, *and* (*b*) the collisions between the latter are few compared with their collisions with the neutral particles, (40) is closely equivalent to

$$[k_1 + ik_2]_1 = \frac{n_1 e_1^2}{m_1(\nu_{13} + i\omega_1)} + \frac{n_2 e_2^2}{m_2(\nu_{23} + i\omega_2)} . \tag{46}$$

This agrees with (3) and (5), when $n_- = 0$, provided that ν_i and ν_e are interpreted as ν_{13} and ν_{23} respectively, which depend on collisions of the corresponding particle (kind 1 or 2) with the neutral particles (kind 3).

A slight addition is here made to the discussion by COWLING [13], by considering the form taken by the first approximation to $k_1 + ik_2$, when condition (*a*) but *not* condition (*b*) is satisfied.

The laws of force 1, 3 and 2, 3 acting between the neutral particles (3) and the ions (1) or the electrons (2) are not yet known, for encounters with thermal speeds at the temperatures occurring in the ionosphere. Hence it is appropriate to express θ and ν and D in terms of equivalent diameters σ_{13}, σ_{23}, as in (36), remembering, however, that these diameters are merely conventional, and may not be independent of the violence of the encounters, that is, they may vary with T.

As a basis for his brief numerical discussion of the ionospheric conductivity, COWLING [13] adopted the values

$$\sigma_{13} = \sigma_{in} = 5.9 \cdot 10^{-8} (300/T)^{\frac{1}{4}} , \tag{47}$$

$$\sigma_{23} = \sigma_{en} = 2 \cdot 10^{-8} \tag{48}$$

(recognizing their uncertainty). NICOLET [24], followed by H. MAEDA [25], took

$$\sigma_{23} = \sigma_{en} = 1.44 \cdot 10^{-8} ; \tag{49}$$

they both adopted the value (47) for σ_{in}.

By (44), (36), denoting by W the molecular weights of the ions and neutral particles (taking them to be the same) it follows from (47) that

$$\nu_{13} = \nu_{in} = 2.6 \cdot 10^{-9} (n_1 + n_3) W^{-\frac{1}{2}} , \tag{50}$$

and from (49) that, in agreement with NICOLET [24],

$$\nu_{23} = \nu_{en} = 5.4 \cdot 10^{-10} n_3 T^{\frac{1}{2}} . \tag{51}$$

Hence, ignoring n_1 in comparison with n_3,

$$\nu_{13}/\nu_{23} = \nu_{in}/\nu_{en} = 4.8/(TW)^{\frac{1}{2}} . \tag{52}$$

Thus if $W = 25$ and T has the values 300° or 1000°, ν_{23} $(= \nu_{en})$ exceeds ν_{13} (or ν_{in}) in the ratio 17 or 32.

By (38), in which e_1 and e_2 must be given their values in *electrostatic* units,

$$\nu_{12} = \nu_{ei} = \{34 + 4.18 \log (T^3/n_e)\} n_e/T^{\frac{3}{2}} , \tag{53}$$

where the value for A_1 (2) adopted by NICOLET [24] has been used; it is based on the Debye cut-off, but remains uncertain by a factor of order unity. Hence at a level h, (about 120 km), at which we may estimate T as 300 , n_e as 10^5, and n_n (or n_3) as 10^{12},

$$\nu_{13} = \nu_{in} = 520 , \quad \nu_{23} = \nu_{en} = 9350 , \quad \nu_{12} = \nu_{ei} = 850 ; \tag{54}$$

and at a level in the F_2 region where we may estimate T as 1000°, and n_e as 10^6,

$$\nu_{13} = \nu_{in} = 5.2 \cdot 10^{-10} n_n , \quad \nu_{23} = \nu_{en} = 1.7 \cdot 10^{-8} n_n , \quad \nu_{12} = \nu_{ei} = 1470 . \tag{55}$$

Estimates of n_n in the F_2 region have ranged widely; COWLING [13, p. 474] adopted the value $4 \cdot 10^{10}$, MAEDA [25] the value $4 \cdot 10^8$. In either case it is clear that ν_{12} $(= \nu_{ie})$ is large compared with ν_{13} $(= \nu_{in})$ in the F_2 region, and also large compared with ν_{23} $(= \nu_{en})$, if n_n is $4 \cdot 10^8$; but if n_n is $4 \cdot 10^{10}$, ν_{12} $(= \nu_{ei})$ is only about twice as great as ν_{23} $(= \nu_{en})$. Near the E peak ν_{ei} is of the same order as ν_{in}, but it is less than ν_{en} by a factor exceeding 10.

Taking $n_1 = n_2$, and ignoring n_1/n_3,

$$\theta_{23}/\theta_{13} = 1.13 \cdot 10^{-4} (T/W)^{\frac{1}{2}} , \tag{56}$$

so that θ_{23} can be omitted from (43). Omitting also appropriate terms in L, (40) becomes

$$[k_1 + ik_2]_1 = \frac{n_e e}{F} \Big/ \left\{ \frac{\varrho_3 \omega_1}{\varrho \nu_{13}} - \frac{\nu_{12} + \nu_{23}}{\omega_2} - i \right\} . \tag{57}$$

When $F = 0$, the right-hand side reduces to $n_e e^2/m_e \nu_e$, where

$$\nu_e = \nu_{12} + \nu_{23} = \nu_{ei} + \nu_{en} . \tag{58}$$

When n_3 is zero, the term $\varrho_3 \omega_1/\varrho \nu_{13}$ in (57) vanishes, and (57) becomes equivalent to (33).

When n_1/n_3 is small, so that ϱ_3/ϱ can be replaced by unity, (57) may be expressed in the form

$$[k_1 + ik_2]_1 = \frac{n_e e}{F} \Big/ (1/X_i + X_e - i)\,, \tag{59}$$

in the notation of (11), taking

$$\nu_i = \nu_{13} = \nu_{in}\,. \tag{60}$$

In the notation of (20),

$$[k_1 + ik_2]_1 = \frac{n_e e}{F} \Big/ (2\exp[-s]\cosh u - i)\,, \tag{61}$$

so that

$$[k_1]_1 = \frac{n_e e}{F}\,\frac{2\exp[-s]\cosh u}{1 + 4\exp[-2s]\cosh^2 u}\,, \tag{62}$$

$$[k_2]_1 = \frac{n_e e}{F}\,\frac{1}{1 + 4\exp[-2s]\cosh^2 u}\,. \tag{63}$$

These formulae agree with those of Sect. 2 for k_1 and k_2, if e^{-2s} is regarded as negligible compared with unity; this, however, is not the case at the higher levels. Hence it is of interest to indicate the corrections to be applied to the formulae of Sect. 2 for k_1 and k_2, to bring them into accordance with the first-approximation formulae (62), (63). These additive corrections are

$$-\frac{x(3 - x + 4x\cosh^2 u)}{(1 + x)(1 + 4x\cosh^2 u)}\,k_1, \qquad -\frac{2x(1 - x - 2x^2\cosh^2 u)}{(1 - x^2)(1 + 4x\cosh^2 u)}\,k_2\,,$$

where $x = e^{-2s}$.

Thus at $u = \pm s$, these corrections are

$$\frac{x(4 + x + x^2)}{2 + 4x + 3x^2 + x^3}\,k_1, \qquad -\frac{x(2 - 3x + 2x^2 - x^3)}{(1 - x^2)(2 + 2x + x^2)}\,k_2\,.$$

At $u = -s$ (the level h_e where $X_e = 1$), x is very small, and the corrections are respectively $-2xk_1$, $-xk_2$; even at $u = s$ (the level h_i where $X_i = 1$) x is of order 10^{-3}, so that there also the corrections are effectively $-2xk_1$, $-xk_2$, and are negligible; naturally this is so also at the intervening levels—for example, at $u = 0$ they are $-3xk_1$ and $-2xk_2$. But when u/s is large the corrections tend to the values

$$-xk_1/(1 + x) \quad \text{and} \quad x^2 k_2/(1 - x^2)\,,$$

which there may not be negligible.

3·3 *The heights* h_e, h_0, h_i, *and the ratio* X_i/X_e.

The height h_e (at which $u = -s$) is that at which $\nu_e = \omega_e$; at this height is ν_{12} (or ν_{ei}) is negligible compared with ν_{23} (or ν_{en}); hence at h_e, by (51),

$$n_3 = 3.25 \cdot 10^{16} F/T^{\frac{1}{2}} ; \tag{64}$$

that is, taking $T = 230°$, n_3 (or n_n) is $6.4 \cdot 10^{14}$ at the magnetic equator, and $12.8 \cdot 10^{14}$ at the magnetic poles. According to the Rocket Panel (White Sands) atmosphere [26] this corresponds to about 78 km and 73 km. But the atmosphere above the magnetic equator and poles may materially differ in height-distribution from that at White Sands, so these estimates are uncertain by at least 5 km.

The height h_i (at which $u = s$) is that at which $\nu_i = \omega_i$, or, according to (50), neglecting n_1 in comparison with n_3,

$$n_3 = n_n = 3.7 \cdot 10^{12} F/W^{\frac{1}{2}} . \tag{65}$$

Thus, taking $W = 25$, at the magnetic equator n_3 must be $2.2 \cdot 10^{11}$, and at the magnetic poles, $4.4 \cdot 10^{11}$; the heights at which these values are attained are uncertain, because they are determined by the unknown T and W in the ionosphere. According to Maeda [25, Fig. 2] these values of n_3 correspond to heights of about 135 and 130 km respectively; but if T increases upwards more rapidly than he supposed—following Kallmann [27]—namely 2·5 km, the heights would be greater by several km.

Hence h_0 may be estimated as about 105 km (perhaps rather more) at the equator, and 100 km at the poles; these heights are uncertain by at least 5 km.

Between the heights h_e and h_0 the values of n_- may not be negligible, as has been supposed in the preceding discussion. According to Bates and Massey [28], n_-/n_e is not more than unity, and perhaps much less, at $h = 100$ km [29].

The ratio X_i/X_e is given, by (11), (51)–(53), as

$$\frac{X_i}{X_e} = \frac{1837 W \nu_{13}}{\nu_{21} + \nu_{23}} = \frac{1837 W \nu_{in}}{\nu_{ei} + \nu_{en}} . \tag{66}$$

If $W = 25$, at the height (in the E region, at about 120 km) to which the values (54) refer,

$$X_i/X_e = 2350 . \qquad (120 \text{ km}). \tag{67}$$

At the height h_i, taking (as a mean between poles and equator) $n_n = 3.3 \cdot 10^{11}$, and $T = 400°$, $n_e = 2 \cdot 10^5$,

$$X_i/X_e = 1720 . \tag{68}$$

At the level in the F_2 layer to which the values (55) refer, if n_n is taken to be $4 \cdot 10^9$, X_i/X_e is 126; if n_n is taken to be $4 \cdot 10^{10}$, X_i/X_e is 450. Thus, the assumption made by BAKER and MARTYN [18], and followed in Sect. 2, is moderately accurate up to about 150 km, above which X_i/X_e decreases considerably, owing to the high frequency of electron collisions with ions.

4. – Numerical Illustrations.

To calculate the conductivities k_0 to k_3, it is necessary to know the height-distribution of T, W, and n_e. All three are uncertain within limits wide enough to justify, at present, only approximate illustrative calculations. It seems useful, however, to give these in some numerical detail, as being helpful in estimating how far the results for other data would differ from those here obtained. Such calculations will be described here, for the height-range 80 to 300 km, taking $n_- = 0$ over this range.

Two model T-distributions are considered, both alike from 80 to 90 km, where they agree with the Rocket Panel data [26] for White Sands. Above this level T is taken to increase uniformly by either 3° or 6° per km; at 300 km the temperatures attained are respectively 850° and 1480 °K, giving a cooler or hotter F layer; the values of various characteristics of these two model ionospheres are given in Table I in pairs of rows, marked respectively c (cooler) and h (hotter). The mean molecular weights of the ions and neutral particles are taken to be the same at each level (though this may actually not be so), and to be 29 from 80 to 100 km; then they lapse uniformly to 25 at 150 km, and again uniformly, but more slowly, to 19 at 300 km. The value 23 at 200 km would correspond to complete dissociation of O_2 at this level, and the value 19 at 300 km would correspond to the dissociation at this level of 7/19 of the nitrogen. The adopted lapse rate of W in the interval 100 to 200 km may be too small, though turbulent mixing will tend to maintain some undissociated O_2 at levels where in a static atmosphere it would be almost wholly dissociated. The same distribution of n_n, the neutral particle number density, would be obtainable with a more rapid lapse of W by adopting lower values of T in the region affected.

Taking the variation of gravity into account, n_n was calculated for each height 80, 90, 100 km, and thence at 25 km intervals to 300 km.

The adopted distribution of n_e is a smoothed version of that given in a graph of n_e as a function of h by SEDDON, PICKAR and JACKSON [30], for the atmosphere over White Sands; it is based on rocket measurements up to 219 km, and from thence to 300 km on vertical-incidence radio-sounding from the ground. The minor fluctuations in the graph are disregarded, and also the existence of any negative ions above 80 km. The electron density n_e is

TABLE I. *Collision frequencies, electric conductivities and other characteristics of two model ionospheres above White Sands, New Mexico; the rows of data are marked h or c according as they refer to the model with a hotter (h) or cooler (c) F layer. The data in rows 1 to 3 are common to both models. In this table numbers expressed as N^m signify $N \cdot 10^m$.*

Number of row		Height in km										
		80	90	100	125	150	175	200	225	250	275	300
1	g	955.4	952.4	949.5	942.2	935.0	927.4	920.8	913.6	907.0	899.7	893.4
2	W	29	29	29	27	25	24	23	22	21	20	19
3	n_e	1^3	1^4	1^5	1.5^5	2^5	2^5	2^5	2.25^5	2.5^5	2.75^5	3^5
4*h*	T °K	205	220	280	430	580	730	880	1 030	1 180	1 330	1 480
4*c*	»	»	»	250	325	400	475	550	625	700	775	850
5*h*	H km	6.15	6.62	8.46	14.05	20.6	27.3	34.6	42.6	51.5	61.5	72.5
5*c*	»	»	»	7.55	10.62	14.2	17.7	21.6	25.9	30.6	35.8	41.6
6*h*	n_n	4.38^{14}	8.53^{13}	1.78^{13}	1.23^{12}	2.16^{11}	6.03^{10}	2.23^{10}	9.98^9	5.12^9	2.92^9	1.80^9
6*c*	»	»	»	1.83^{13}	8.97^{11}	9.75^{10}	1.72^{10}	4.16^9	1.28^9	4.70^8	2.00^8	9.55^7
7*h*	ν_{ei}	1.72^1	1.43^2	9.35^2	7.63^2	6.66^2	4.84^2	3.74^2	3.36^2	3.08^2	2.86^2	2.68^2
7*c*	»	»	»	1.09^3	1.12^3	1.11^3	8.77^2	7.16^2	6.72^2	6.36^2	6.05^2	5.79^2
8*h*	ν_{en}	3.39^6	6.83^5	1.61^5	1.38^4	2.81^3	8.80^2	3.57^2	1.73^2	9.50^1	5.75^1	3.74^1
8*c*	»	»	»	1.56^5	8.73^3	1.05^3	2.02^2	5.17^1	1.73^1	6.72	3.01	1.50
9*h*	ν_e	3.39^6	6.83^5	1.62^5	1.45^4	3.47^3	1.36^3	7.31^2	5.09^2	4.03^2	3.44^2	3.05^2
9*c*	»	»	»	1.57^5	9.86^3	2.16^3	1.08^3	7.68^2	6.90^2	6.43^2	6.08^2	5.81^2
10*h*	ν_{in}	2.11^5	4.12^4	8.59^3	6.16^2	1.12^2	3.20^1	1.21^1	5.53	2.90	1.70	1.08
10*c*	»	»	»	8.84^3	4.49^2	5.07^1	9.11	2.26	7.07^{-1}	2.67^{-1}	1.16^{-1}	5.70^{-2}
11*h*	$X = \nu/\omega$	3.93^{-1}	7.93^{-2}	1.88^{-2}	1.69^{-3}	4.03^{-4}	1.58^{-4}	8.48^{-5}	5.91^{-5}	4.68^{-5}	3.98^{-5}	3.54^{-5}

13*h*	$X_i/X_e=e^{2s}$	3.33^{3}	3.22^{3}	2.83^{3}	2.10^{3}	1.48^{3}	1.04^{3}	6.99^{2}	4.39^{2}	2.78^{2}	1.82^{2}	1.23^{2}
13*c*	»	»	»	3.00^{3}	2.26^{3}	1.08^{3}	3.72^{2}	1.24^{2}	4.15^{1}	1.60^{1}	7.02	3.43
14*h*	s	4.05	4.03	3.97	3.82	3.65	3.46	3.26	3.04	2.81	2.60	2.41
14*c*	»	»	»	4.00	3.86	3.48	2.96	2.41	1.86	1.39	0.97	0.62
15*h*	u	-3.11	-1.50	0.00	2.55	4.16	5.28	6.10	6.69	7.15	7.53	7.84
15*c*	»	»	»	0.00	2.91	4.80	6.02	6.90	7.57	8.10	8.58	9.00
16*h*	k_0	8.32^{-17}	4.12^{-15}	1.74^{-13}	2.91^{-12}	1.62^{-11}	4.14^{-11}	7.72^{-11}	1.25^{-10}	1.76^{-10}	2.27^{-10}	2.79^{-10}
16*c*	»	»	»	1.79^{-13}	4.29^{-12}	2.60^{-11}	5.22^{-11}	7.40^{-11}	9.42^{-11}	1.16^{-10}	1.44^{-10}	1.88^{-10}
17*h*	k_1	1.12^{-17}	2.70^{-17}	1.23^{-16}	1.29^{-15}	2.88^{-15}	1.04^{-15}	3.87^{-16}	1.91^{-16}	1.07^{-16}	6.54^{-17}	4.31^{-17}
17*c*	»	»	»	1.19^{-16}	1.66^{-15}	1.65^{-15}	2.99^{-16}	7.29^{-17}	2.50^{-17}	9.75^{-18}	4.40^{-18}	2.26^{-18}
18*h*	k_2	2.83^{-17}	3.25^{-16}	3.27^{-15}	4.54^{-15}	1.72^{-15}	1.71^{-16}	2.29^{-17}	4.95^{-18}	1.38^{-18}	4.70^{-19}	1.87^{-19}
18*c*	»	»	»	3.27^{-15}	4.26^{-15}	4.45^{-16}	1.39^{-17}	8.00^{-19}	8.10^{-20}	1.16^{-20}	2.18^{-21}	5.26^{-22}
19*h*	k_3	8.30^{-17}	3.93^{-15}	8.70^{-14}	1.73^{-14}	3.91^{-15}	1.07^{-15}	3.88^{-16}	1.91^{-16}	1.07^{-16}	6.54^{-17}	4.31^{-17}
19*c*	»	»	»	8.95^{-14}	1.26^{-14}	1.77^{-15}	3.06^{-16}	7.30^{-17}	2.50^{-17}	9.75^{-18}	4.40^{-18}	2.26^{-18}

taken to increase uniformly, though at different mount (*) rates, between 80, 90, 100 and 150 km, at which its adopted values are 10^3, 10^4, 10^5 and $2 \cdot 10^5$; it is taken to remain at this last value up to 200 km, and then to increase uniformly to $3 \cdot 10^5$ at 300 km. This was the peak value above White Sands at the time, 10 a.m. Mountain Standard Time, of the rocket launching on May 7, 1954. The peak F_2 values, $3 \cdot 10^5$, may be exceeded at other times and places; estimates have ranged up to 10^6 or even $2 \cdot 10^6$. The model distribution of n_e here adopted, being a smoothed version of the one given in [30], does not indicate the E peak or any lapse of n_e above the E peak and the F_1 « shelf »; provided that n_e at the E-pause, above the E peak, does not fall much below the E peak value (and this is the implication in the graph quoted from [30]), this smoothed version of n_e is adequate for illustrative calculations such as are here presented.

At the ground the magnetic intensity F at White Sands is 0.53 gauss. In the ionosphere F is taken to have the constant value 0.49, which is its approximate value at 150 km. Thus ω_e is taken to have the constant value $8.62 \cdot 10^6$, and ω_i is $4.69 \cdot 10^3/W$.

These data enable the collision frequencies, the ratios X_e, X_i, X_i/X_e, and the conductivities k_0 to k_3 to be calculated; Table I gives the results. To save space in printing the Table, numbers of the form $N \cdot 10^m$ are given in the form N^m.

The conductivity k_0 increases upwards, over the range considered, though with a varying mount rate. The conductivities k_1, k_2, k_3 each have one peak in the range considered. The heights considered are too few to enable the peak values and levels to be adequately inferred: hence additional calculations were made at appropriate intervening heights.

The peak values and peak levels of k_1, k_2, k_3 for the two model ionospheres are approximately as follows in Table II.

TABLE II. – *Peak Levels and Values for the Electric Conductivities k_1 to k_3 for Two Model Ionospheres above White Sands, New Mexico, one (h) with a hotter F layer, the other (c) with a cooler F layer* (see TABLE I).

Model	Peak Level		Peak Value	
	h	*c*	*h*	*c*
k_1	147 km	136 km	$2.9 \cdot 10^{-15}$	$2.8 \cdot 10^{-15}$
k_2	127 km	126 km	$4.5 \cdot 10^{-15}$	$4.3 \cdot 10^{-15}$
k_3	102 km	102 km	$8.7 \cdot 10^{-14}$	$9.0 \cdot 10^{-14}$

(*) The term mount rate, the antithesis of lapse rate, is used in reference to the height gradient of any property that increases with height.

The distributions of the conductivities near their peak levels are shown in Fig. 2; the layer in which the Cowling conductivity k_3 exceeds a tenth of its maximum value is much thinner than the corresponding layers for k_1 and k_2.

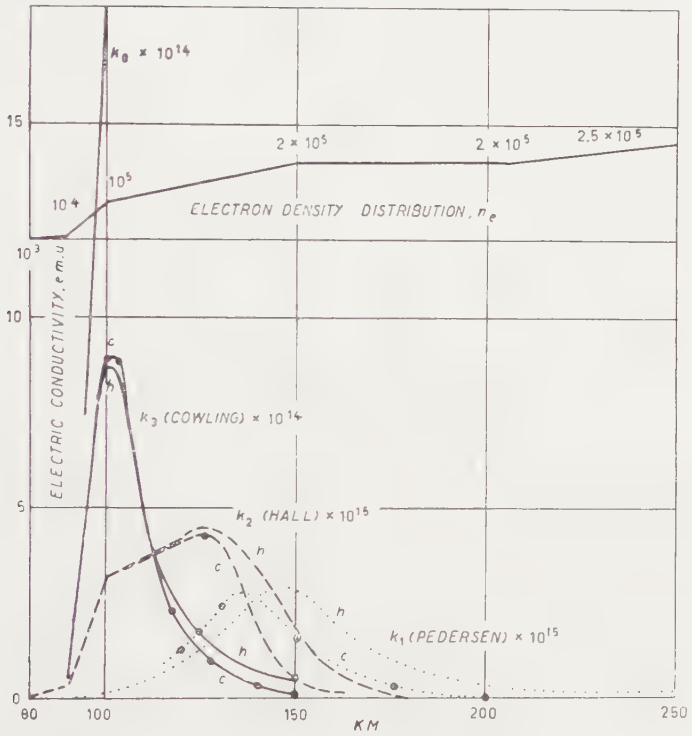

Fig. 2. – The height-distribution of the standard electrical conductivities k_0 to k_3, in two model ionospheres over White Sands, New Mexico, from 80 to 250 km height. The adopted electron density distribution is shown in the upper part of the diagram. The scales for k_1 and k_2 differ by a factor of 10 from those for k_0 and k_3: Of the two curves for each k, the one for the ionosphere with the cooler F layer (see Table I) is distinguished by a few dot marks, *e.g.*, at 150 km.

The integrated conductivities in the ranges between the heights in Table I are approximately as follows in Table III.

The total integrated conductivities K_1, K_2, K_3 are estimated to be as follows in Table IV. The values obtained by BAKER and MARTYN [18], H. MAEDA [25] and J. A. FEJER [19] are given for comparison. These values show as good agreement as could well be expected in view of the different bases of the calculations.

Table III shows that the ionospheric conditions above 200 km have little influence on the results. The present calculations confirm the conclusions

reached in the earlier discussions cited, especially the conclusion that for the Cowling conductivity k_3 the effective layer is the lower part of the E region, and is thin.

TABLE III. *Contributions of Different Layers of the Ionosphere to the Integrated Electric Conductivities for the Model Ionospheres (h, c) of Table I.*

Limits of interval: km.		80 ÷ 90	÷100	÷ 125	÷150	÷175	÷200	÷225	÷250	÷275
1*h*	$10^9 \int k_1 \, dh$	—	.07	1.13	6.00	4.50	1.50	.70	.35	.12
1*c*	$10^9 \int k_1 \, dh$	—	.07	1.50	6.00	1.88	.30	.10	.05	—
2*h*	$10^9 \int k_2 \, dh$	.17	1.80	9.75	8.75	1.75	.22	.03	—	—
2*c*	$10^9 \int k_2 \, dh$	.17	1.80	9.50	5.75	.50	.03	—	—	—
3*h*	$10^8 \int k_3 \, dh$	.20	4.55	13.00	2.25	.62	.17	.05	—	—
3*c*	$10^8 \int k_3 \, dh$	.20	4.65	12.75	1.37	.25	.05	—	—	

TABLE IV. — *Various Estimates of the Integrated Electric Conductivities.*

	$10^9 K_1$	$10^9 K_2$	$10^8 K_3$
Model *h*	14.4	22.5	20.8
Model *c*	9.9	17.8	19.3
BAKER and MARTYN	6.4	13.6	16.4
H. MAEDA	6.7	9.8	7.75
J. A. FEJER (*) (equator)	6	— 21	18

(*) This author expressed the Hall current as $k_2 \boldsymbol{E} \times \boldsymbol{F}$, so that his k_2 is negative.

The value of K_3 is much influenced by the height of the level $u = 0$ in relation to the n_e distribution; $u = 0$ is defined as the level where $X_e X_i = 1$. In the model ionospheres here adopted, this level is 100 km, below which n_e rapidly decreases; the contribution to K_3 from below this level is about a third of the whole. Owing to the flatter peak of the k_2' graph (Fig. 1) the proportion of the contribution to K_2 from below $u = 0$ is still less, only about 10%. Almost the whole contribution to K_1 comes from above $u = 0$, as might be expected from Fig. 1, because the electronic contribution associated with the lower peak of k_1', where n_e is extremely small, is negligible.

The graph of ν_e given by H. MAEDA [25] shows a minimum value (about $7 \cdot 10^2$) at 170 km, above which ν_e increase to about $2 \cdot 10^3$ at 300 km, where his value of n_e is 10^6; his model atmosphere corresponds roughly, as regards n_n, with the *c* model here considered; if for this model n_e were taken to increase to 10^6 at 300 km, ν_e here also would have a minimum value below this level.

MAEDA adopts another (partly rocket-measured) version of the height-

distribution of n_e, showing as many as 6 peaks; these are reflected to some extent in his graphs of the height-distribution of the conductivities.

5. – Horizontal Electric Current Flow in the Ionosphere: the Layer Conductivities.

In the ionosphere the electric current flow must be almost exactly horizontal except at special points. Vertical component electric currents tend to produce opposite charge distributions in the upper and lower parts of the ionosphere, thus polarizing the layer, and adjusting the vertical electric field to a value that stops further vertical flow. In the ionosphere the electric fields change throughout the day, and the polarization also changes, so as to limit the vertical current flow to the almost zero value needed to adjust the polarization.

At any point in the ionosphere let right-handed axes be taken along the unit vectors $\boldsymbol{i}, \boldsymbol{j}, \boldsymbol{k}$, in the magnetic south, magnetic east and upward vertical directions. Let $\boldsymbol{f}$ denote the unit vector along the local magnetic intensity $\boldsymbol{F}$ $(= F\boldsymbol{f})$; if I denotes the magnetic dip or inclination, reckoned positive where the north end of a magnet dips below its south end,

$$\boldsymbol{f} = -C\boldsymbol{i} - S\boldsymbol{k}\,, \tag{69}$$

where

$$C = \cos I\,, \qquad S = \sin I\,. \tag{70}$$

The components $\boldsymbol{E}_f$, $\boldsymbol{E}_n$ of the electric field, along and normal to $\boldsymbol{F}$, are given by

$$\boldsymbol{E}_f = (\boldsymbol{E}\cdot\boldsymbol{f})\boldsymbol{f}\,, \qquad \boldsymbol{E}_n = \boldsymbol{E} - \boldsymbol{E}_f\,, \tag{71}$$

and the electric current intensity $\boldsymbol{J}$ is given by

$$\begin{aligned} \boldsymbol{J} &= k_0\boldsymbol{E}_f + k_1\boldsymbol{E}_n + k_2\boldsymbol{f}\times\boldsymbol{E} \\ &= k_1\boldsymbol{E} + k_0'(\boldsymbol{E}\cdot\boldsymbol{f})\boldsymbol{f} + k_2\boldsymbol{f}\times\boldsymbol{E}\,, \qquad k_0' = k_0 - k_1\,. \end{aligned} \tag{72}$$

By taking the vertical current component $(\boldsymbol{J}\cdot\boldsymbol{k})\boldsymbol{k}$ to vanish exactly, the resultant vertical component of $\boldsymbol{E}$ is required to have the value given by

$$AE_z = -k_0'SCE_x + k_2CE_y\,, \qquad A = k_0S^2 + k_1C^2\,. \tag{73}$$

Substituting this value in the formula for $\boldsymbol{J}$, the expression for this horizontal

vector becomes

$$\boldsymbol{J} = k_{xx}E_x\boldsymbol{i} + k_{yy}E_y\boldsymbol{j} - k_{xy}\boldsymbol{k}\times\boldsymbol{E} \tag{74}$$

or

$$J_x = k_{xx}E_x + k_{xy}E_y\,, \qquad J_y = -k_{xy}E_y + k_{yy}E_y\,, \tag{75}$$

where

$$k_{xx} = k_0k_1/A\,, \quad k_{yy} = k_1(k_0S^2 + k_3C^2)/A\,, \quad k_{xy} = k_0k_2S/A\,. \tag{76}$$

The conductivities k_{xx}, k_{xy}, k_{yy} may be called the *layer* conductivities. At the magnetic equator ($I = 0$)

$$k_{xx} = k_0\,, \qquad k_{yy} = k_3\,, \qquad k_{xy} = 0\,. \qquad (I = 0). \tag{77}$$

At the magnetic poles ($I = 90^\circ$),

$$k_{xx} = k_{yy} = k_1\,, \qquad k_{xy} = k_2\,. \qquad (I = 90^\circ). \tag{78}$$

The magnitude of the third term of $\boldsymbol{J}$ in (74) is $k_{xy}E_h$, where $\boldsymbol{E}_h$ denotes the horizontal component of $\boldsymbol{E}$; the direction is that attained by turning the vector $\boldsymbol{E}_h$ through 90° clockwise (as seen from above) in the horizontal plane. If k_{xy} much exceeds k_{xx} and k_{yy}, then $\boldsymbol{J}$ is almost perpendicular to $\boldsymbol{E}_h$; in general $\boldsymbol{J}$ is inclined to $\boldsymbol{E}_h$, except when the latter is in an azimuth φ (reckoned eastward from magnetic south or north) satisfying the equation

$$\sin 2\varphi = \frac{2k_{xy}}{k_{xx} - k_{yy}} = \frac{2k_0k_2S}{k_1(k_0 - k_3)C^2}\,. \tag{79}$$

This formula can also be written

$$\sin 2\varphi = \frac{2S(X_i - X_e)}{C^2} = \frac{2(m_1\nu_1 - m_e\nu_e)\,\mathrm{tg}\,I}{eH}\,, \tag{80}$$

where H denotes the *horizontal* component of the magnetic intensity; (80) is valid up to the levels at which (57) begins to differ appreciably from (46) in the value given to $|k_1 + ik_2|_1$, and down to the levels, below h_e (about 75 km), where the magnetic field ceases to influence the conductivity appreciably.

At the magnetic equator, where $I = 0$, $S = 0$, the values of φ at all levels are 0° and 90°: that is, $\boldsymbol{J}$ has the same direction as $\boldsymbol{E}_h$ when $\pm\boldsymbol{E}_h$ is to the magnetic east or south.

At the magnetic poles, where $k_{xx} = k_{yy}$, $\boldsymbol{J}$ is *always* inclined to $\boldsymbol{E}_h$, and (80) has no real solution. At each level in the ionosphere there is a range of lati-

tude, on both sides of the equator, up to which φ has real values; this range is given by the equation

$$\pm S = \pm \sin I = \{(X_i - X_e)^2 + 1\}^{\frac{1}{2}} - (X_i - X_e) . \tag{81}$$

At low levels, where $X_i - X_e$ is large, this range is bounded by the isoclines given approximately by

$$\operatorname{cosec} I = 2(X_i - X_e) . \tag{82}$$

Thus the belt of latitude in which at these levels $\boldsymbol{J}$ and $\boldsymbol{E}_h$ can have the same direction is very narrow. At high levels, where $X_i - X_e$ is very small, the belt extends nearly up to the poles, being bounded by the isoclines given approximately by

$$\cos I = \{2(X_i - X_e)\}^{\frac{1}{2}} . \tag{83}$$

In so far as the geomagnetic field can be represented by that of a dipole, these limiting approximations can be expressed by

$$l = \pm 1/4(X_i - X_e) , \qquad (X_i - X_e \text{ large}) \tag{84}$$

$$\theta = \{(X_i - X_e)/8\}^{\frac{1}{2}} \qquad (X_i - X_e \text{ small} \tag{85}$$

where l denotes the geomagnetic latitude and θ the geomagnetic co-latitude (reckoned from either geomagnetic pole).

6. – Variation of the Conductivities with Latitude.

The standard conductivities k_0 to k_3 each contain the factor n_e/F, which decreases from the equator polewards, because n_e decreases and F increases.

The increase of F reduces ω_e and ω_i, and likewise the values of n_n at the levels h_e and h_i, at which $\nu_e = \omega_e$ and $\nu_i = \omega_i$; the reduction of n_n at the poles at these levels is by a factor of 2, corresponding to a relative rise of about 3/4 of a scale height (the distribution of n_n in the ionosphere above the poles being unknown, the actual relative heights h_e or h_i at the poles and equator cannot be stated at present. Owing to the greater obliquity of the sun's rays (at noon) at higher latitude, the n_n height-distribution is raised relative to the n_n distribution; at the poles (at the equinoxes) the rise is by more than a scale height. The net effect on the integrated conductivities will depend also on the unknown T distribution, which, as Table IV shows, affects K_1 considerably, and K_2 to a less extent. As the T-distribution in the polar ionosphere

is unknown, no precise estimate can at present be made of the latitude variation of the K's, but the preceding considerations suggest that they will materially decline polewards: this is suggested also by the distribution of the S currents.

The layer conductivities k_{xx} and k_{xy} also decline from the equator to the poles, very rapidly at first at the higher levels. The layer conductivity k_{xy}, however, is zero at the equator, and has maxima with respect to latitude, north and south of the equator; at the higher levels these maxima occur very near the equator, so near that the variation of k_{xy} depends mainly on the latitude-variation (there most rapid) of the magnetic dip I, and one can neglect the slow variation of n_e and F near the equator. On this basis the latitudes l of maximum are given by $\mathrm{d}k_{xy}/\mathrm{d}l = 0$ or $\mathrm{d}k_{xy}/\mathrm{d}I = 0$; this indicates that they correspond to

$$\sin I = k_1^{\frac{1}{2}}/(k_0 - k_1)^{\frac{1}{2}},$$

and that the maximum value of k_{xy} is

$$k_0 k_2 / \{2k_1(k_0 - k_1)\}^{\frac{1}{2}},$$

or approximately

$$(k_0 2k_1)^{\frac{1}{2}} k_2 .$$

The following Table V shows the latitudes and values of maximum k_{xy}, thus calculated, at various levels, and illustrates in a striking way the rapidity of the variations of k_{xy} near the equator, from zero there to these maxima. The values refer to the model ionosphere h.

TABLE V. – *Latitudes and values of maximum k_{xy} at various levels.*

Level (km)	80	90	100	125	150	175	200
Latitude l	12°	2.3°	0°.8	0°.6	0°.4	0°.014	0°.006
Maximum k_{xy}	4.6^{-17}	2.9^{-15}	8.7^{-14}	1.5^{-13}	8.9^{-14}	2.3^{-14}	7.2^{-15}

7. – Concluding Remarke.

Up to the level (about 150 km) where ν_{ei} begins to approach equality with ν_{en}, any change of n_e affects all the conductivities (standard and layer) nearly proportionately; hence for White Sands the values k_0 to k_3 for any other distribution of n_e up to this level can readily be found from the values given in Table I. Above this level the values of ν_{ei} have to be modified in proportion to n_e, and the recalculation of the conductivities k is more complicated.

The numerical results given in Table I may be modified by further experimental or other determinations of σ_{en} and σ_{in}; for example, if $\sigma_{en}^2\sigma_{in}^2$ should prove to be (say) 4 times greater than has been assumed, X_eX_i (below 150 km) would be multiplied by this factor, and at 100 km the value of u would be changed from zero to -0.69; more of the peak range of k_3' (Fig. 1) would thus come into the region where n_e exceeds 10^5, and k_3 would be materially increased.

The results here given refer to normal conditions: during a solar flare the electron (and ion) content of the D layer is enhanced, augmenting the S current system and its magnetic effects. This case will be considered in detail in a later paper.

* * *

I am indebted to J. C. Cain of the University of Alaska, and Miss Marion B. Wood of the National Bureau of Standards, for assistance in the computations on which are based the Tables and Figures in this paper; and to D. C. Wilder (University of Alaska) and the drafting staff of the National Bureau of Standards for the preparation of Figs. 1, 2.

REFERENCES

[1] B. Stewart: *Encyc. Britannica*, 9th ed. (1882).
[2] A. Schuster: *Phil. Trans. Roy. Soc.*, A **180**, 467 (1889).
[3] C. F. Gauss: *Resultate magnet. Verein* (1839); *Werke*, **5**, 121.
[4] A. Schuster: *Phil. Trans. Roy. Soc.*, A **208**, 163 (1908).
[5] S. Chapman: *Phil. Trans. Roy. Soc.*, A **218**, 1 (1919).
[6] P. O. Pedersen: *Danm. Naturvid. Samf.*, A **15** *a/b* (1927).
[7] E. V. Appleton: *Proc. Roy. Soc.*, A **162**, 451 (1937).
[8] G. I. Taylor: *Proc. Roy. Soc.*, A **156**, 318 (1936).
[9] C. L. Pekeris: *Proc. Roy. Soc.*, **158**, 650 (1937).
[10] E. V. Appleton and K. Weekes: *Proc. Roy. Soc.*, A **171**, 171 (1939).
[11] D. F. Martyn: *Proc. Roy. Soc.*, A **189**, 241 (1947); A **190**, 273 (1947).
[12] S. Chapman and T. G. Cowling: *Mathematical Theory of Non-Uniform Gases* (Cambridge, 1939, 1952).
[13] T. G. Cowling: *Proc. Roy. Soc.*, **183**, 453 (1945).
[14] T. G. Cowling: *Mon. Not. R. Astron. Soc.*, **93**, 90 (1933).
[15] D. F. Martyn: *Nature*, **162**, 142 (1948); **163**, 685 (1949).
[16] M. Hirono: *Journ. Geomag. Geoelec., Kyoto*, **2**, 1 (1950); **4**, 7 (1952); **5**, 22 (1953).
[17] K. Maeda: *Journ. Geomag. Geoelec., Kyoto*, **3**, 77 (1951).
[18] W. G. Baker and D. F. Martyn: *Nature*, **170**, 1090 (1952); *Phil. Trans. Roy. Soc.*, A **246**, 281 (1953).

[19] J. A. Fejer: *Journ. Atmos. and Terr. Phys.*, **4**, 184 (1953); **5**, 103 (1954).
[20] S. Chapman and J. Bartels: *Geomagnetism* (Oxford, 1940).
[21] S. Chapman: *Archiv Met. Geophys. Bioklim.*, A **4**, 368 (1951).
[22] R. Landshoff: *Phys. Rev.*, **76**, 904 (1949); **82**, 442 (1951).
[23] L. Spitzer jr. and R. Härm: *Phys. Rev.*, **89**, 977 (1953).
[24] M. Nicolet: *Journ. Atmos. Terr. Phys.*, **3**, 200 (1953).
[25] H. Maeda: *Journ. Geomag. and Geoelect.*, **5**, 94 (1953).
[26] Upper Atmospheric Research Rocket Panel: *Phys. Rev.*, **88**, 1030 (1952).
[27] H. H. Kallmann: *Journ. Geophys. Res.*, **58**, 209 (1953).
[28] D. R. Bates and H. S. W. Massey: *Journ. Atmos. Terr. Phys.*, **2**, 1 (1951).
[29] H. S. W. Massey and E. H. S. Burhop: *Electronic and Ionic Impact Phenomena* (Oxford, 1952).
[30] J. C. Seddon, A. D. Pickar and J. E. Jackson: *Journ. Geophys. Res.*, **59**, 521 (1954)

SUPPLEMENTO AL VOLUME IV, SERIE X
DEL NUOVO CIMENTO

N. 4, 1956
2° Semestre

Some Properties of the Meteoric E-Layer Used in Radio Wave Propagation.

R. NAISMITH

Radio Research Station - Slough

1. – Introduction.

During the « Congresso Internazionale per il cinquantenario della scoperta Marconiana della Radio » I described [1] some work on the exploratory properties of radio waves and their application to the detection of Meteor Trails. This work on the ionization produced by the impact of sporadic Meteors on the ionosphere has been continued at the Radio Research Station at Slough and it now seems possible to identify an ionized layer in the upper atmosphere which is caused by these small projectiles. This paper deals with some of the characteristics of this layer and describes its properties for radio wave propagation.

2. – Meteor Ionisation.

The luminous streaks in the night sky caused by the capture of meteors in the earth's atmosphere are phenomena which have been observed for many centuries. This light comes from the luminous gas produced by the hot particle and not from the particle itself. It is because this gas is ionized that we can observe it by radio reflection methods. LOVELL and CLEGG [2] estimate that there are about $8 \cdot 10^9$ sporadic meteors entering the earth's atmosphere each day and that the total mass added to the earth each day is of the order of 1000 kg. This means that on the average, one particle of meteor dust weighs less than a milligram. A study of the velocities of sporadic meteors [3] shows that it is always less than about 72 km/s and it is deduced from this that there is no evidence of any large number of meteors originating outside the solar system. It is the combination of high velocity and enormous numbers

which make meteors one of the important phenomena occurring in the ionosphere. The heights at which the meteor trails are observed visually are consistently near 95 km according to WATSON (1941) [4].

3. – Radio Observations of Meteor Ionisation.

The visual observations therefore suggest that the phenomena occur within the *E*-region of the ionosphere and, as there are already other types of echo obtained from this region it is necessary to devise some means of separating them. Thus, although a number of observers [5, 6] were convinced that meteor type echoes did exist it was not until special types of equipment, generally of the high power radar type, were available that the evidence became sufficiently convincing. It was with such equipment that we were able to show a close association between a sporadic E-layer reflection and a meteor shower associated with the passage of the Giacobini-Zinner comet [6]. Using higher radio frequencies HEY [8] and LOVELL [9] were able to identify various well known meteor showers and the latter was able to show for the first time [10] that a shower of considerable intensity occurred during the daytime in summer.

Although part of the sporadic E-type of reflection was thus identified in association with meteors it was clear that all sporadic E-layer echoes were not due to this cause and the problem of further distinguishing between the various types then arose. Some were associated with magnetic and ionospheric storms, some with reflections from Aurorae which occur about the same height, and it was suggested that some were due to turbulence [11], and some to atmospheric electricity [12] (not necessarily accompanied by lightning flashes) and there is a somewhat elusive increase in summer which is not satisfactorily explained by any of these observations or suggestions.

It is thus fairly clear that the identification of a particular type of echo occurring in this region requires careful planning. A study of the echoes received during the passage of the Giacobini-Zinner comet showed certain characteristics which were exploited to produce the maximum difference between them and the various other types.

4. – Characteristics of Meteor Type Echoes.

In particular, it was noted that, although the meteor echoes included a large range of delay times, there was a consistent lower boundary indicating a height of reflection of just below 100 km at vertical incidence. Apparent heights greater than this were often due to laterally deviated signals from meteor trails not directly overhead. The heights of reflection were therefore

below most of the other types of E-region echoes and accorded well with the visual observations of the same phenomenon. An early observation of a marked diurnal variation in the number of echoes which corresponded to a similar variation in the number of sporadic meteors provided another clear indication of association. The marked intermittent character of the echoes could be clearly demonstrated when observations were made on a suitable radio frequency. Comparatively weak reflections were always observed from these ionized trails and this could be demonstrated again by making observations on a suitable frequency. Thus it is possible to record the higher layers in regions E and F in the presence of meteor-type reflections and the complete blanketing of the upper layers by a certain type of sporadic E-layer is never associated with the meteor-type of reflection. DIEMINGER [13] provides a figure for the reflection coefficient of low echoes of 10^{-3} on frequencies round about 2 MHz and this seems to accord well with our own observations.

5. – The Meteoric E-Layer.

From these and other considerations referred to below it appears that a case has been made for the recognition of a layer in the E-region of the ionosphere and to which we may attach, for convenience, the name of Meteoric E-layer. This leaves the term « sporadic E-layer » to denote ionization in the E-region other than that due to ultra-violet light or meteors. The highest frequencies on which these three types of E-region echoes occur at vertical incidence namely, ultra-violet, meteor and sporadic may then be denoted by the symbols *fE*, *fEm*, and *fEs* respectively. The meteoric E-layer echoes may be observed on normal types of *h'f* record as a lower fringe to either or both the echo traces from the normal and sporadic E-layers as shown in the Fig. 1. (Thanks is due to the *Journal of Atmospheric and Terrestrial Physics* for permission to reproduce the photograph and diagrams). The echoes from the meteoric E-layer may also be observed quite clearly on a record taken on a fixed frequency as shown at (*B*) and (*C*) in photograph 1. The frequencies selected are 4.2 MHz and 4.6 MHz. In the latter case it will be noted that whereas the reflection from the sporadic E-layer is due to the extraordinary component and occurs at a greater height than the reflection of the ordinary component (shown in *B*) the meteoric E-layer reflections continue to be received from the same uniform height in both photographs. This is another distinguishing feature of the meteoric E-layer and may be used with effect in cases where the ordinary component of the sporadic E-layer lies very nearly on top of the meteoric E-layer echoes.

Still another distinguishing feature of the meteoric E-layer reflections is shown on the vertical incidence records by the absence of multiple reflections.

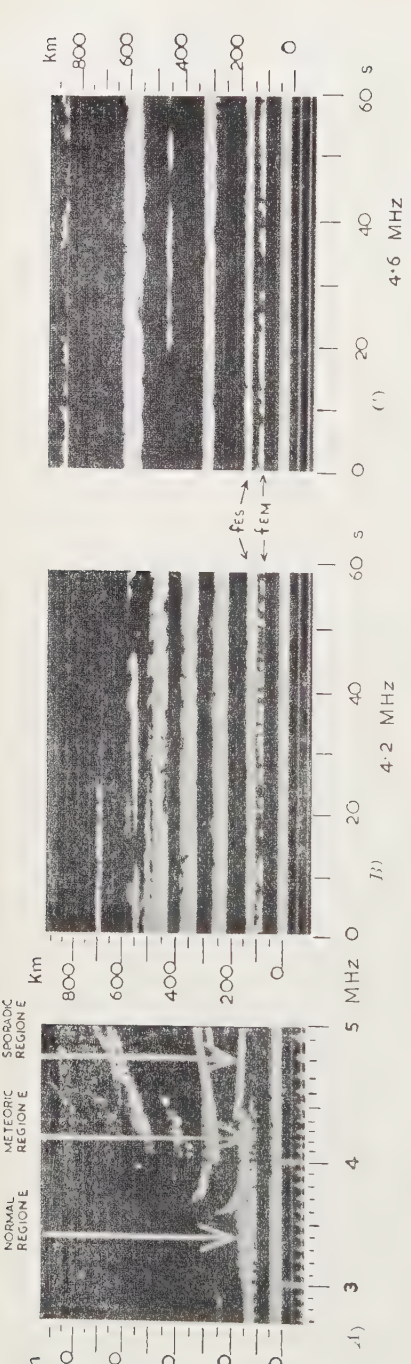

Fig. 1 Meteor type echo.

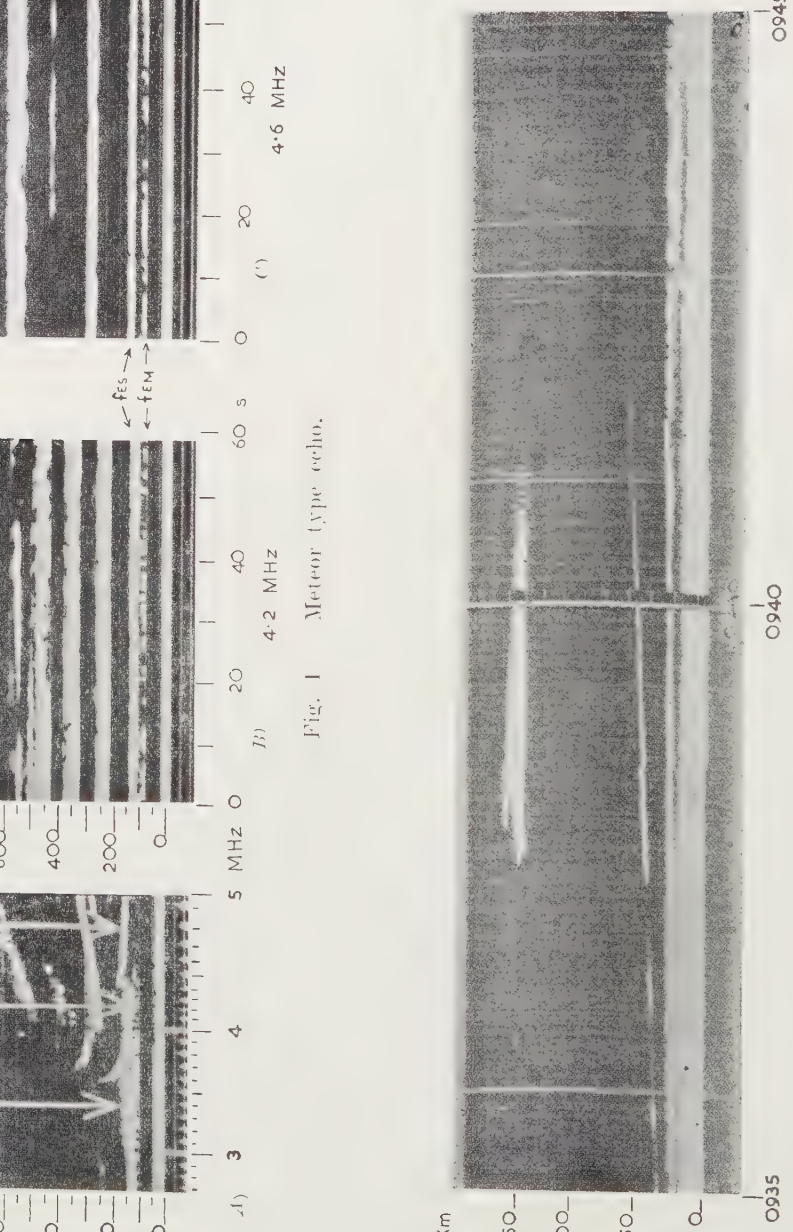

Fig. 2.

This readily distinguishes it from the sporadic E-layer and the absence of any form of critical frequency or cusp such as occurs in the normal E-layer distinguishes it from that layer.

One example of an ionization trail due to the arrival of a meteor is shown in Fig. 2. This observation was made on the relatively high frequency of 30 MHz and the range recorded indicates that the ionization was not produced directly overhead. (The lower echo traces are caused by reflections from aircraft).

6. – Diurnal and Seasonal Variations.

The meteoric E-echoes are observed on higher frequencies than all other forms of sporadic E-echoes for 70% of the time in summer and 95% in winter.

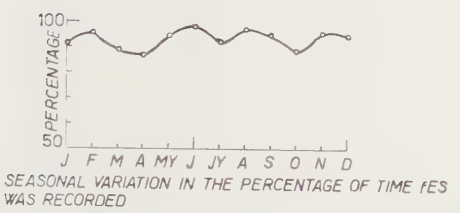

Fig. 3.

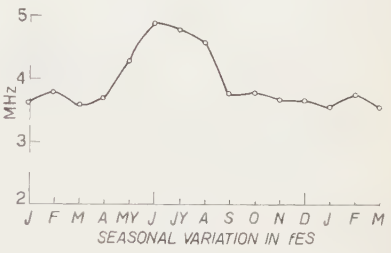

Fig. 4.

On occasions, therefore, when it is impossible to distinguish between them we may use this feature in looking at data produced over long periods. From an analysis of over 25000 hourly measurements made at vertical incidence and using a power in the pulse transmitter of less than 1 kW the seasonal variation has been obtained and plotted in Fig. 3. This shows that the echoes are present for about 90% of the time and that there is no

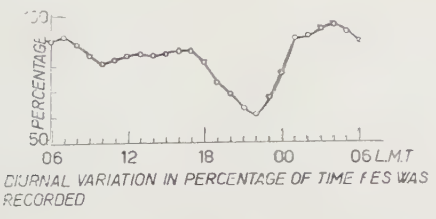

Fig. 5.

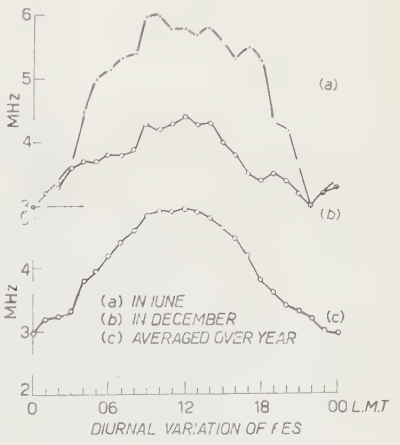

Fig. 6.

marked seasonal variation. There is a variation in the highest frequency on which they are recorded and this is shown in Fig. 4. There is also a marked diurnal variation which is shown in Fig. 5 and which is associated with a somewhat similar diurnal variation in the arrival of sporadic meteors

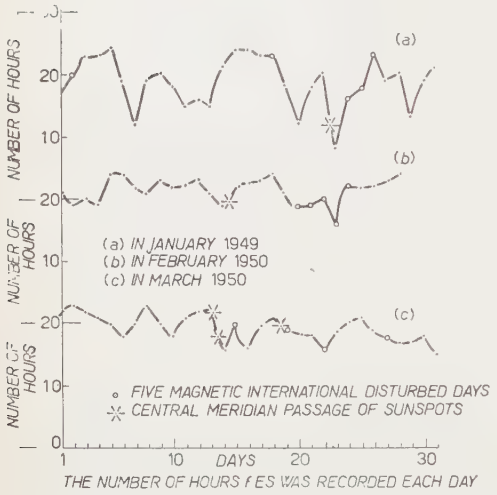

Fig. 7.

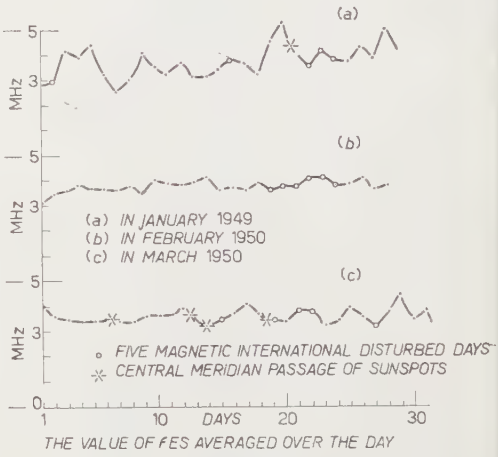

Fig. 8.

in the earth's atmosphere as discussed above. The diurnal variation at various seasons of the year is given in Fig. 6. Comparisons with the central meridian passage of sunspots and with the incidence of magnetic storms are given in Figs. 7 and 8 and these show no association whatever either in the number of hours recorded or in the highest frequency on which the echoes were recorded at vertical incidence.

7. – Oblique Incidence Observations.

There are various types of observation which may be due to reflections from the meteoric E-layer; although they have not so far been identified as such. For example, from a study of the long range navigation system referred to as « LORAN », BRAMLEY and I show [14] that there exists a fairly well-defined layer lying between 90 and 97 km. The frequency used in this case was 2 MHz and the distances over which the measurements were made varied from zero to 1200 km. The fact that it is possible to use a navigation aid on this layer indicates a degree of uniformity in height which is unattainable either with the ultraviolet E-layer or the sporadic E-layer and we may there-

fore attribute this characteristic to indicating that it was the uniform height of the meteoric E-layer which was responsible for the accuracy attainable with this navigation aid.

More recently BAILEY and others [11] have shown that it is possible to maintain communication over distances of 1250 km on a frequency (50 MHz) well above that which is reflected from the more normal layers. Although the authors favour turbulence as an explanation of this phenomenon they remark that the effect of sporadic meteor ionization could explain some of their observations.

The author has also had an opportunity to examine some types of observation over distances of $600 \div 1500$ km on frequencies in the $20 \div 30$ MHz region which appear to be due to reflections from a meteoric E-layer and which will be published in due course [15].

8. – Conclusions.

We may conclude therefore that there is a prima facie case for the separation of the ionization produced in the sporadic E-region by the impact of meteors, from that due to other causes. Reasons and methods of identification have been given for the recognition of the layer of the ionosphere in which the former is produced as the meteoric E-layer.

The characteristics of this layer have been established by vertical incidence sounding methods.

Certain special types of oblique transmission which conform to this idea of a meteoric E-layer are referred to and there should be an increasing amount of information available in the near future because it seems probable that the meteoric E-layer will be used for certain types of intermediate distance transmission (up to distances of 2500 km) using frequencies in the very high frequency (V.H.F.) band.

The low reflection coefficient and the scattered nature of the transmission will place practical limits on the commercial development of this system of communication. On the other hand, the freedom from magnetic and ionospheric storm effects is an attractive feature. The greater aerial efficiency which is possible and more readily attainable directional characteristics add to its attractions. Another advantage is the smaller amount of congestion in the V.H.F. band and, since the area of use is likely to be restricted to 2500 km it is possible to share a common frequency beyond this boundary.

* * *

The work described above was carried out as part of the programme of the Radio Research Board. This paper is published by permission of the Director of Radio Research of the Department of Scientific and Industrial Research.

The author also wishes to acknowledge the assistance rendered by Mr. W. M. CURTIS, who maintained an exceptionally high standard of measurement throughout the whole six-year period of observation.

REFERENCES

[1] R. NAISMITH: *Atti del Congr. Intern. per il cinquantenario della scoperta Marconiana della Radio*, p. 160 (1947).
[2] B. LOVELL and J. A. CLEGG: *Radio Astronomy* (London, 1952), p. 76.
[3] *Occasional Notes Roy. Astr. Soc.*, edit by A. C. B. LOVELL: **3**, 16, 49 (1954).
[4] F. G. WATSON: *Between the Planets* (New York, 1941), p. 93.
[5] A. M. SKELLETT: *Phys. Rev.*, **37**, 1668 (1931).
[6] E. V. APPLETON, R. NAISMITH and J. L. INGRAM: *Phil. Trans.*, A **236**, 191 (1937).
[7] E. V. APPLETON and R. NAISMITH: *Proc. Phys. Soc.*, **59**, 461 (1947).
[8] J. S. HEY and G. S. STEWART: *Proc. Phys. Soc.*, **59**, 858 (1947).
[9] A. C. B. LOVELL and J. A. CLEGG: *Proc. Phys. Soc.*, **60**, 491 (1948).
[10] A. C. B. LOVELL, J. A. CLEGG and V. A. HUGHES: *The Observatory*, **68**, 49 (1948).
[11] D. K. BAILEY, R. BATEMAN, R. V. BERKNER, H. G. BOOKER, G. F. MONTGOMERY, E. M. PURCELL, W. W. SALISBURY and J. B. WIESNER: *Phys. Rev.*, **86**, 141 (1952).
[12] G. A. ISTED: *Nature*, **171**, 617 (1953).
[13] W. DIEMINGER: *Report of Phys. Soc., Conference on The Physics of the Ionosphere*, p. 53 (Sept. 1954).
[14] R. NAISMITH and E. N. BRAMLEY: *Wireless Engineer*, **28**, 271 (1951).
[15] R. NAISMITH: *Wireless Engineer*, **33**, 159 (1956).

OSSERVAZIONI ED INTERVENTI

— S. CHAPMAN:

Can Mr. NAISMITH explain the sharpness of the meteor-ionized layer? One would think that the meteors would have a range of mass, speed and inclination, so that they would form a layer of some thickness.

— R. Naismith:

The sharpness to which I referred is, of course, relative to the comparatively large variations which occur in the lower level of the other ionospheric layers. Some idea of the actual variation in height of the meteoric E-layer may be obtained from the « scatter diagram » given in the paper « Time delay Measurements » which is referred to in the text. It is probable that the Meteoric layer is due mainly to the incidence of enormous numbers of sporadic meteors which, on the average, weigh only a small fraction of a milligram. There is no complete explanation of this relative sharpness of the layer at present. I would prefer to leave the complete explanation open for further discussion.

SUPPLEMENTO AL VOLUME IV, SERIE X
DEL NUOVO CIMENTO

N. 4, 1956
2° Semestre

Some Remarks on the Theory of Self-Demodulation.

M. CARLEVARO

Centro Studi di Radiopropagazione
Istituto di Fisica Tecnica dell'Università - Napoli

1. – Introduction.

Early observations of self-demodulation were reported in papers concerning experimental work on radio-interaction and gyro-interaction.

The new phenomenon was accounted, by analogy, to the same mechanism of interaction, i.e. to a modulation of collision frequency of electrons, caused by the modulated electric field of a wave passing through an ionized layer.

Later, when the interest of a systematic investigation on self-demodulation was recognized, the results of the experiments gave some surprise. In particular, the modulation-frequency dependence of the demodulation was found to be quite opposite to the expected.

Simple analogy with interaction seamed to show an effect decreasing as modulation-frequency increased.

On the contrary the experiments gave generally as result an increase in demodulation as the modulation-frequency increased.

Some times the increase began from a certain low value of modulation-frequency for which a minimum of demodulation was reached.

New hypothesis were advanced to explain the phenomenon and its main experimental features. No entirely satisfactory theory has been proved true till now.

Therefore it appears interesting to evaluate, on the basis of the theory of modulation of collision-frequency, the residual modulation to be expected.

No attempt of this computation was made, as to Author's knowledge.

2. – Computation of Residual Modulation.

The start of Bailey's theory of interaction is the equation of motion of an electron in a gas, under the action of an alternative electric field. The

equation is

$$a\frac{\mathrm{d}\nu}{\mathrm{d}t} + \frac{1}{2}aG(\nu^2 - \nu_0^2) = w_0(t)\,, \tag{1}$$

where: ν is the collision frequency of the electron;

ν_0 is the thermal equilibrium value of ν;

a is the product of the mass of the electron by the square of mean free path;

G is the mean relative energy loss in a collision. G is constant if the temperature of electrons slightly exceeds the temperature of the gas;

$w_0(t)$ is the mean value of the work done by the field on one electron between two consecutive collisions.

Equation (1) cannot be integrated in general, because of its non-linearity.

The Author has already suggested that exact computations, where necessary, were carried out by means of electronic analogical computers.

An obvious solution for (1) can be easily found if $w_0 =$ constant, i.e. if an alternative electric field of constant amplitude is applied to the electron. In this case, the steady state solution in given by

$$\nu_1 = \nu_0 \sqrt{1 + \frac{w_0}{GT}}\,, \tag{2}$$

T beig the thermal equilibrium energy of the electron $= \frac{1}{2}a\nu_0^2$.

If the electric field is modulated with a modulation-frequency $n/2\pi$ and a modulation depth M,

$$\mathcal{E}_i = \mathcal{E}_m(1 + M \sin nt) \tag{3}$$

the work $w_0(t)$ can be expressed by:

$$w_0(t) = w_0(1 + M \sin nt)^2 \tag{4}$$

and an approximate integral of (1) can be calculated assuming that ν varies by a small amount $\Delta\nu$ around the mean value ν_1, corresponding to the mean value of $w_0(t)$, neglecting the second order term $(\Delta\nu)^2$ and the second order harmonics of the development of (4).

The approximate solution is:

$$\Delta\nu = \frac{2Mw_0}{a\sqrt{n^2 + G^2\nu_1^2}} \sin(nt - \psi_1); \qquad \operatorname{tg}\psi_1 = \frac{n}{G\nu_1}\,, \tag{5}$$

which can be written also

$$\Delta\nu = \nu_1 \frac{M w_0}{w_0 + GT} \cos\psi_1 \sin(nt - \psi_1) . \tag{6}$$

The modulation frequency is contained in the factor $\cos\psi_1$ which replaces the factor δ of V. A. Bailey's notation. It must be observed that as n varies from zero to infinity, ψ_1 varies from zero to $\pi/2$ and $\cos\psi_1$ from 1 to zero.

The ratio of amplitude of $\Delta\nu$ to the mean value ν_1 is

$$M' = \frac{M w_0}{w_0 + GT} \cos\psi_1 . \tag{7}$$

The absorption coefficient of an ionized layer, far from gyrofrequency, is proportional to ν. Thus it can be written:

$$K = K_0[1 + M' \sin(nt - \psi_1)] . \tag{8}$$

The field of the wave after passing through the layer is given by:

$$\mathcal{E}_0 = \mathcal{E}_i \exp\left[-\int_0^{\cdot} K \, ds\right], \tag{9}$$

the integral being extended to the entire path of the wave through the layer.

In the case of radio-waves incident on a layer of the ionosphere, the only important terms of the integral are the ones referring to the portion of the path near the vertex of the trajectory of the wave, because there K reaches its maximum value. In this portion of the path M' also may be assumed as constant.

Calling α the mean value of the total absorption, equation (9) may be written:

$$\begin{aligned} \mathcal{E}_0 &= \mathcal{E}_i \exp[-\alpha\{1 + M' \sin(nt - \psi_1)\}] = \\ &= \mathcal{E}_i \exp[-\alpha] \exp[-\alpha M' \sin(nt - \psi_1)] \sim \\ &\sim \mathcal{E}_i \exp[-\alpha][1 - \alpha M' \sin(nt - \psi_1)] , \end{aligned} \tag{10}$$

$\alpha M'$ being in general small as compared to unity.

Neglecting the constant factor $\exp[-\alpha]$ the explicit form of $\mathcal{E}_0$ becomes:

$$\begin{aligned} \mathcal{E}_0 &= \mathcal{E}_m(1 + M \sin nt)[1 - \alpha M' \sin(nt - \psi_1)] = \\ &= \mathcal{E}_m\left[1 - \frac{\alpha M M'}{2} \cos\psi_1 + M \sin nt - \alpha M' \sin(nt - \psi_1) + \frac{\alpha M M'}{2} \cos(2nt - \psi_1)\right] . \end{aligned} \tag{11}$$

The mean value of $\mathcal{E}_0$ is, obviously:

$$\mathcal{E}_{0m} = \mathcal{E}_m \left[1 - \frac{\alpha}{2} \frac{w_0}{w_0 + GT} M^2 \cos^2 \psi_1\right] = \mathcal{E}_m(1 - \varrho M^2 \cos^2 \psi_1) , \tag{12}$$

calling for semplicity ϱ the positive quantity $(\alpha/2)\{w_0/(w_0 + GT)\}$. With the same notation the square of the amplitude of the fundamental oscillating term is

$$\begin{aligned} \mathcal{E}_{0n}^2 &= \mathcal{E}_m^2 M^2[(1 - \varrho)^2 + \varrho^2 - 2\varrho(1 - \varrho) \cos 2\psi_1] = \\ &= \mathcal{E}_m^2 M^2[1 - 4\varrho(1 - \varrho) \cos^2 \psi_1] . \end{aligned} \tag{13}$$

Finally the residual modulation depth, referred to the fundamental oscillating term, can be expressed by the ratio

$$M''^2 = \frac{\mathcal{E}_{0n}^2}{\mathcal{E}_{0m}^2} , \tag{14}$$

or in the form

$$\left(\frac{M''}{M}\right)^2 = \frac{1 - 4\varrho(1 - \varrho) \cos^2 \psi_1}{(1 - \varrho M^2 \cos^2 \psi_1)^2} = \frac{1 - A \cos^2 \psi_1}{(1 - B \cos^2 \psi_1)^2} \tag{15}$$

It must be observed that

$$A \leq 1 , \tag{16}$$

$$B > 0 . \tag{17}$$

3. – Frequency Dependence of M''.

The derivative of M'' is

$$\frac{\mathrm{d}}{\mathrm{d}\psi_1}\left(\frac{M''}{M}\right)^2 = \frac{A - 2B + AB \cos^2 \psi_1}{(1 - B \cos^2 \psi_1)^3} \sin 2\psi_1 . \tag{18}$$

The derivative annullates when ψ_1 is zero or $\pi/2$, n being respectively zero or infinite, where a maximum, or a minimum of M'' must be expected. In the interval $0 < \psi_1 < \pi/2$, $\sin 2\psi_1$ is always positive and the sign of (18) depends on the sign of the fraction only. To discuss this sign, two cases must be distinguished:

(19) *a*) $B < 1$ or $M^2 < \dfrac{1}{\varrho}$.

Then the denominator is positive in the interval and the sign of (18) is the same of the numerator's.

The numerator is always positive, and therefore M'' is a steadily increasing function of n if

$$A - 2B > 0 \qquad \text{or} \qquad M^2 < 2(1-\varrho)\,. \tag{20}$$

The numerator is always negative, and M'' is a decreasing function of n if

$$A - 2B + AB < 0 \qquad \text{or} \qquad M^2 > \frac{2(1-\varrho)}{1 - 2\varrho(1-\varrho)}\,. \tag{21}$$

Finally the numerator may change sign in the interval if there is a value of $\cos^2\psi_1$ for which the numerator annullates.

The conditions are

$$0 \leqslant \frac{2B - A}{AB} \leqslant 1\,, \tag{22}\quad a)$$

or

$$2(1-\varrho) \leqslant M^2 \leqslant \frac{2(1-\varrho)}{1 - 2\varrho(1-\varrho)}\,.$$

In this last case M'' is an increasing function of n in the interval

$$0 \leqslant n \leqslant Gv_1\sqrt{\frac{2\varrho M^2(1-\varrho)}{M^2 - 2(1-\varrho)} - 1}\,,$$

and from this value of n to infinity a decreasing function.

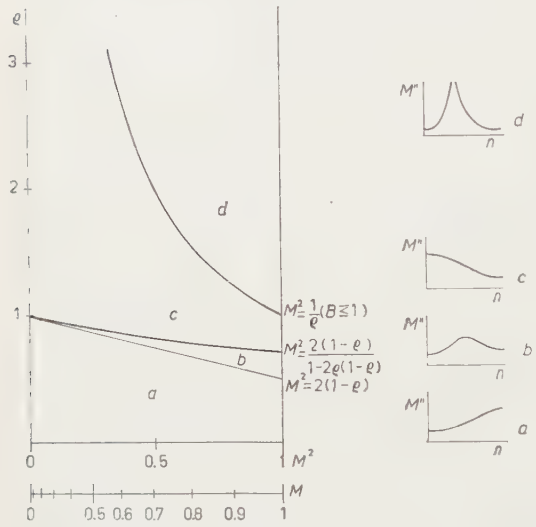

Fig. 1.

In Fig. 1 is represented the plane M, ϱ, limited to the interval of physical significance of M, and are plotted the curves $M^2 = 1/\varrho$; $M^2 = 2(1-\varrho)$ and $M^2 = 2(1-\varrho)/\{1 - 2\varrho(1-\varrho)\}$ that divide the plane in regions corresponding to the behaviours described and to the following one.

$$B > 1 \qquad \text{or} \qquad M^2 > \frac{1}{\varrho}\,. \tag{23}\quad b)$$

In this case the denominator of (18) becomes zero and changes its sign when

$$\cos^2\psi_1 = \frac{1}{B} \qquad \text{or} \qquad n_1 = Gv_1\sqrt{\varrho M^2 - 1}\,. \tag{24}$$

At this frequency the derivative of (15) becomes infinite and changes its sign; M'' must therefore become infinite itself, i.e. the mean value of $\mathcal{E}_0$ must annullate, or, in terms of spectrum, the carrier must vanish.

For $0 \leqslant n \leqslant n_1$ the denominator of (18) is negative. The numerator varies in this interval between $A - 2B + AB$ and $2(A - B)$ and is negative because ϱ is greater than unity and A is negative. Thus the sign of (18) is positive, and M'' is an increasing function of n.

For n increasing from n_1 to infinity the denominator of (18) is positive. The numerator varies between $2(A - B)$ and $A - 2B$ keeping inalterated its negative sign, so M'' decreases.

4. – Effect of the Magnetic Field.

In the neighborhood of gyro-frequency the absorption coefficient of an ionized layer becomes inversely proportional to the collision frequency.

The effect can be approximately taken into account by changing the sign of the oscillating term from + to — in the expression (8).

This change modifies (11) in

$$\mathcal{E}_0 = \mathcal{E}_m \left\{ 1 + \frac{\alpha M M'}{2} \cos \psi_1 + M \sin nt + \alpha M' \sin (nt - \psi_1) - \right. \tag{25}$$

$$\left. - \frac{\alpha M M'}{2} \cos (2nt - \psi_1) \right\},$$

(12) in

$$\mathcal{E}_{0m} = \mathcal{E}_m (1 + \varrho M^2 \cos^2 \psi_1) \tag{26}$$

and (13) in

$$\mathcal{E}_{0n}^2 = \mathcal{E}_m^2 M^2 [1 + 4\varrho(1 + \varrho) \cos^2 \psi_1] . \tag{27}$$

The formula (15) then becomes:

$$\left(\frac{M''}{M}\right)^2 = \frac{1 + 4\varrho(1 + \varrho) \cos^2 \psi_1}{(1 + \varrho M^2 \cos^2 \psi_1)^2} = \frac{1 + C \cos^2 \psi_1}{(1 + B \cos^2 \psi_1)^2}; \tag{28}$$

C is always positive.

The derivative of (28) is

$$\frac{\mathrm{d}}{\mathrm{d}\psi_1} \left(\frac{M''}{M}\right)^2 = \frac{2B - C + BC \cos^2 \psi_1}{(1 + B \cos^2 \psi_1)^3} \sin 2\psi_1 . \tag{29}$$

The denominator of (29) is always positive. The sign of numerator is positive for all values of n if

$$C < 2B \qquad \text{or} \qquad M^2 > 2(1+\varrho)\,. \tag{30}$$

M'' would be an increasing function of n, but this case has no physical possibility, M^2 resulting greater than unity. The sign of numerator is always negative if

$$\begin{cases} C > B(2+C) & \text{or} \\ M^2 < \dfrac{2(1+\varrho)}{1+2\varrho(1+\varrho)}\,, \end{cases} \tag{31}$$

and M'' is a decreasing function of n.

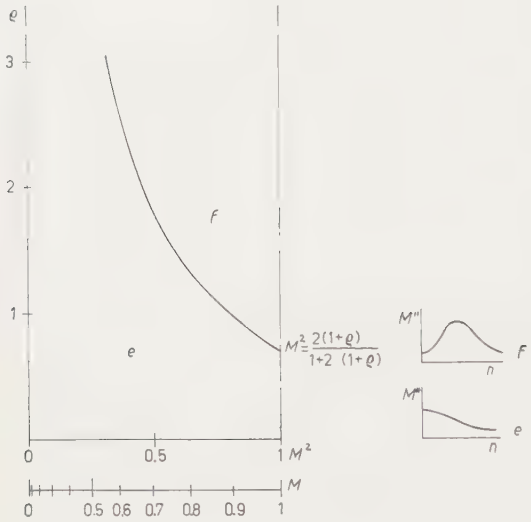

Fig. 2.

The numerator changes its sign if

$$0 \leqslant \frac{C-2B}{BC} \leqslant 1\,, \tag{32}$$

or

$$\frac{2(1+\varrho)}{1+2\varrho(1+\varrho)} \leqslant M^2 \leqslant 2(1+\varrho)\,.$$

In this case M'' increases with n for n increasing from zero to

$$n_2 = Gv_1 \sqrt{\frac{2\varrho M^2(1+\varrho)}{2(1+\varrho)-M^2} - 1}\,, \tag{33}$$

and thereafter decreases.

In Fig. 2 is plotted the curve $M^2 = 2(1+\varrho)\{1+2\varrho(1-\varrho)\}$ that divides the plane in two regions where different behaviours of $M''(n)$ occur.

5. – Final Considerations.

From equation (15) the values assumed by M'' for $n = 0$ and $n = \infty$ can be easily deduced:

$$M''_{n=0} = M \begin{matrix} 1 & A \\ 1 & B \end{matrix}, \tag{34}$$

and

$$M''_{n=\infty} = M\,. \tag{35}$$

This last value, to which M'' tends asymptotically from higher values in all discussed cases but one, may appear to invalidate the explanation of the phenomenon by the theory of the modulation of collision frequency.

Besides it is evident that at high modulation-frequencies the simple theory is not valid, because physically the carrier and side bands become three different waves following very different paths and suffering different absorptions.

Furthermore too many simplifying assumptions were made in developing the previous formulae. However the only interesting conclusion is that the modulation-frequency dependence of residual modulation depth at low values of n cannot be predicted by simple analogy, but a more detailed analysis is always necessary.

If the theory of the modulation of collision frequency will be proved true by experiments, the behaviour of demodulation, depending strongly on α, can give perhaps some information on this parameter up to now not otherwise measurable.

SUPPLEMENTO AL VOLUME IV, SERIE X
DEL NUOVO CIMENTO

N. 4, 1956
2° Semestre

On the Interaction of Radio Waves.

V. A. BAILEY

University of Sydney - Sydney

An account is given of the development of the theory of radio wave-interaction which led to new methods for studying the ionosphere and ionized gases in the laboratory. The concepts and experimental methods of J. S. TOWNSEND relating to the steady motions of electrons in gases are briefly expounded. From these it followed that an alternating electric field increases the collision-frequency of the electrons.

It thus became clear that a powerful radio wave A could increase the collision-frequency ν in the E-region of the ionosphere by an appreciable amount. In order to detect this increase a second wave B was introduced which passes through, and is absorbed by, the region of the ionosphere affected by A; the increase of ν would then cause an increased absorption of B and so any modulation of A would be impressed on B. This conception also automatically explained the « Luxembourg Effect » and successfully predicted that the impressed modulation would decrease as the modulation frequency is increased.

A more rigorous formulation showed later that as the carrier frequency of A is varied about the local gyro-frequency resonance occurs. This was early confirmed by experiments in Europe and more recently by experiments in Italy, Australia and the U.S.A.

The theory also predicted the self-distortion of a powerful wave. This has been confirmed by the recent (unpublished) experiments of L. GOLDSTEIN. It is not certain that the phenomenon of self-demodulation discovered by CUTOLO in 1950 is an example of self-distortion; it is suggested that this question could be resolved by observing the effect on self-demodulation of a change in the radiated power.

Another consequence of the theory is the possibility of generating an artificial aurora (or air glow).

Lastly, the empirical formulae of CROMPTON, HUXLEY and SUTTON, relating to the motions of slow electrons in air, are subjected to a critical analysis.

1. – Introduction.

In order to present any difficult subject in the clearest possible way it is usually best to give it in historical form. For this reason I may be permitted to give a few biographical details.

In the year 1913 I went to the University of Oxford as a Mathematical Scholar. Then after one year I turned to Engineering Science, solely for economic reasons. This course was interrupted by the First World War but was resumed again after my demobilization in 1919. Shortly after my return to Oxford I encountered by chance a remarkable personality who was destined to influence me and my future career in a decisive manner. This was the famous JOHN SEALEY TOWNSEND, the « Father of Electrical Discharges ».

With him I worked for about four years before I departed to a Professorship in Australia. During these four years I learnt to regard the whole of Physics with a *most sceptical* eye and to turn every subject upside-down and inside-out until the lurking defects had been revealed. I also then learned most of what I know about the motions of slow electrons in gases.

2. – The Concepts and Methods of Townsend.

In the Appendix I are set out the main concepts, theoretical formulae and experimental methods of TOWNSEND [1, 2] relating to the study of the *steady motions of electrons in a gas at pressure p, under the influence of an electric field Z and a transverse magnetic field H.*

In this Appendix it is firstly shown that the electrons possess a mean random velocity u while they drift with the mean velocity W in the direction of the electric force Z and simultaneously diffuse in all directions with a coefficient of diffusion K. TOWNSEND proved that the ratio W/K is equal to $Z/40.3\,k$ where k is the ratio of the mean energy (or temperatures) of the electrons to that of the surrounding gas molecules; k is termed Townsend's energy factor.

The theory then shows that the spatial distribution of the electron density n depends only on Z and k. Hence by measuring this distribution k can be determined.

Fig. 1A of the Appendix shows the instrument and method used to determine k. From k we easily calculate the random velocity u.

On applying a suitable magnetic field H perpendicular to the force Z (Fig. 1A) the electron stream is deflected through a known angle θ. Then W is determined from the relation $\operatorname{tg}\theta = WH/Z$.

Theoretically and experimentally k and W are found to be functions of

the ratio Z/p. Hence k and W are always represented in terms of Z/p by means of curves as in Fig. 3A. These always show that k is greater than 1 the value corresponding to equipartition of energy.

Afterwarsds it is shown how from the known values of k and W we can derive the collision frequency ν, the mean free path l and the mean proportion λ of the energy lost by an electron at a collision. For electrons in air, TOWNSEND and TIZARD [3] obtained data in 1913 which yield the curves for l (at 1 mm pressure) and λ shown in the Fig. 4A. The lowest value of the electron's mean velocity u corresponds to $k = 2.6$. (In recent years new measurements on electrons in air have been made by HUXLEY and collaborators, extending down to $k = 4$, and if time permits these will be discussed later.) The curve for l shows that the collision frequency ν $(= u/l)$ increases with u and so at any given pressure ν increases with the force Z.

3. – The Increase of the Collision Frequency Caused by an Alternating Electric Force.

Many years later, in connection with his experiments with high-frequency electrical discharges, TOWNSEND demonstrated that the collision frequency ν of electrons increases also under the influence of an *alternating* electric force E. We show this firstly deriving the mean work P done on an electron per second and then the differential equation (13A) which governs the variation of ν during intervals of time dt large compared with the period of the alternating field. This equation involves the energy η lost in a collision by an electron which possesses the energy U. For perfectly elastic collisions η is equal to $G(U - U_1)$ where U_1 is the mean energy of a molecule and G is a constant equal to $2m/M$ where m and M are the masses of an electron and a gas molecule respectively. For simplicity l is taken as constant.

Then the formulae for P and η are given as well as the equation for ν in terms of η and $w = P/\nu$. From these we deduce the differential equation for ν, which is numbered (15A).

This equation shows that the collision-frequency ν *ultimately increases with the effective value of the alternating electric force.*

4. – Origin of the Theory of Wave-Interaction.

During my first six years in Australia, i.e. from 1924 to 1930, I was engaged in the experimental study of k and W for electrons in gases like air, H_2O, NH_3, HCl etc., in which the electrons tend to form negative ions by their attachment to molecules.

But in 1931 my colleague Professor MADSEN, Chairman of the Australian Radio Research Board, pressed me to collaborate with his newly formed circle of physicists who were engaged in studying the ionosphere by means of the methods of APPLETON and of BREIT and TUVE.

Early in 1933 Professor MADSEN had a tea-party, now memorable for me, in which we discussed for the first time the letter in *Nature* from TELLEGEN [4] which reported his experimental investigation of the newly discovered Luxembourg effect: in this effect a station of power 200 kW and wave-length 1190 m interfered seriously with several different medium-wave broadcasts. The discussion was fruitless and in due course I completely forgot about TELLEGEN's report.

Several months later, while acting as the Official Examiner of the late A. L. GREEN I was engaged in studying his doctoral thesis. It then occurred to me to examine whether a powerful radio wave A, corresponding to an output of 200 kW, could increase *the collision-frequency* ν by an appreciable amount, as illustrated by Fig. 1.

I then introduced a second wave B passing through this region as a *means of detecting* this increase of ν through the resulting effect on the absorption of B.

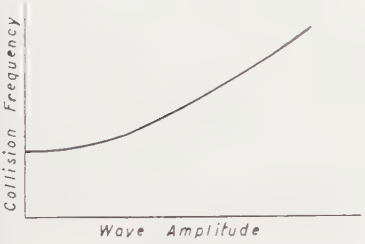

Fig. 1.

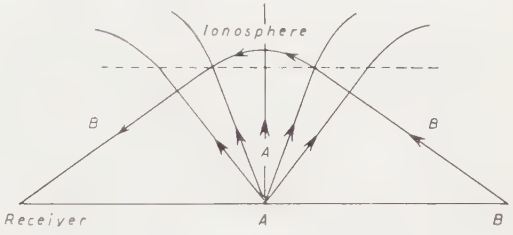

Fig. 2.

It became obvious that in this way any modulation of the amplitude of A could be impressed on B. This arrangement is shown in Fig. 2.

It then dawned on me that I had unwittingly found the explanation of the recently discovered « Luxembourg Effect » or Radio-Wave Interaction.

Further reflection showed that the *impressed modulation* M, *would decrease as the modulation frequency increased*, in the manner shown in Fig. 3 (*).

(*) This prediction was later confirmed by VAN DER POL and VAN DER MARK in Europe; their observations are shown as the four dots in Fig. 3 . It was also thoroughly confirmed by the more recent work of HUXLEY and RATCLIFFE and their collaborators.

I then invited Dr. D. F. MARTYN to assist me in the development of these ideas by means of his knowledge of the current facts about the absorption of the wanted wave *B*. In this initial phase [5] I adopted an approximation in the mathematical theory which seemed reasonable, but which did not yield any resonance effect—contrary to my expectation.

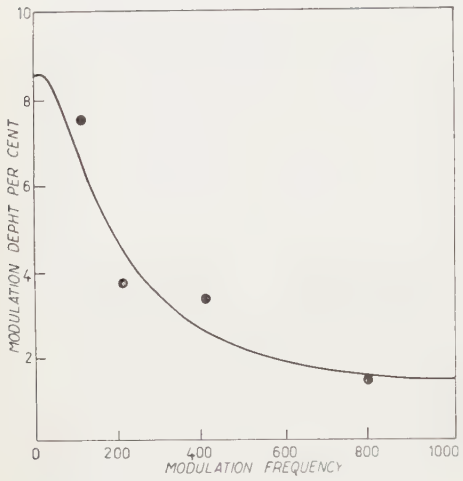

Fig. 3.

A comprehensive but simple account of the state of the subject after this initial phase is given in the *Wireless World* [6].

5. – The New Mathematical Theory of Wave-Interaction.

Three years later I found means to avoid the approximation mentioned and, as a result, discovered that *resonance* may occur in the impressed modulation as the frequency of the disturbing wave *A* passes through the local *gyro-frequency*.

A wave with its frequency near the gyro-frequency is called a « gyro-wave » and interaction caused by such a wave is called « gyro-interaction ».

The theory was now developed [8, 9] so as to take proper account of the propagation of the disturbing wave *A* through the ionosphere. This led to the discovery that at medium or higher latitudes a gyro-wave would act with greatest effect on a « slab » or stratum of the ionosphere which lies approximately between 90 and 95 km above the ground.

The detecting wave *B* was then selected so as to suffer most of its absorption in this slab, as shown by Fig. 4.

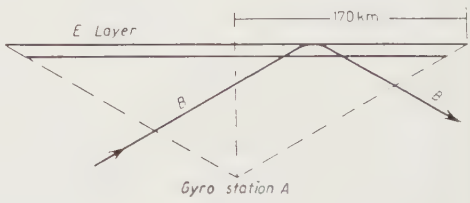

Fig. 4.

It was then found that a gyro-wave *A* of *only* 1 kW of radiated power could impress an observable modulation on the wave *B*. This was about 1 per cent of the lowest powers previously found necessary to produce observed interaction.

This prediction of the theory was substantially confirmed in 1937 by my experiments conducted in Europe with the help of the B.B.C. and other autho-

rities. It was also confirmed about 1946 by M. CUTOLO and colleagues [11] in Italy using powers less than 1 kW.

6. – The Two Forms of Resonance.

Another outcome of the new theory [12] was the discovery that the resonance curve for the impressed modulation would take one of two forms, namely:

One-humped (« dromedarian »), or *Two-humped* (« bactrian »). These are illustrated by the curves shown in Fig. 5 which were published in 1938.

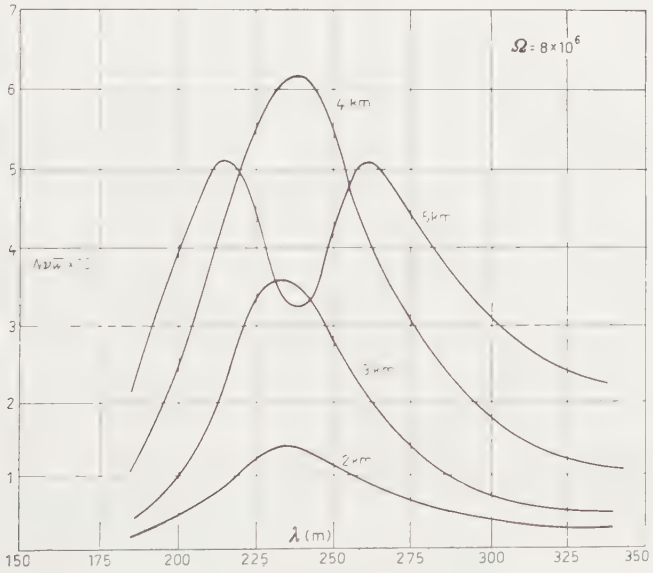

Fig. 5.

Ten years later M. CUTOLO [13] and his colleagues in Italy observed the predicted two-humped curve, (bactrian resonance).

7. – The Australian Experiments on Gyro-Interaction.

During 1950 and 1951 experiments [14] were carried out in Eastern Australia which were planned to conform as closely as possible to the theoretical requirements mentioned earlier.

As illustrated in Fig. 6 the disturbing gyro-wave A was radiated vertically from an aerial at Armidale which lies almost exactly at the mid-point of the 740 km line which joins Brisbane and Katoomba. The wanted wave B was radiated from Brisbane on 590 kHz and received at Katoomba. From the magnetic data for Armidale the local gyro-frequency was estimated to be 1530 kHz.

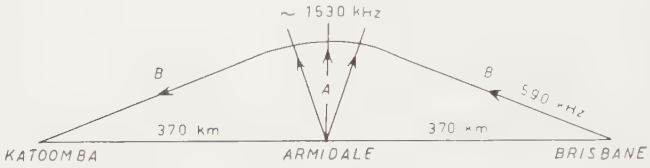

Fig. 6.

Time allows mention of only the results obtained on October 24, 1951 between 0100 and 0220 hours Eastern Standard Time.

The gyro-wave was radiated 40 times per second as a square pulse of length 1 millisecond and power 36 kW. Its frequency f was kept constant for 2 minutes at each of 8 values lying within $\pm$ 23% of the gyro-frequency 1530 kHz.

Each of cycles 1, 2 and 3 ran through the middle *six* frequencies and lasted 17 minutes.

Cycle 4 ran through all the 8 frequencies and lasted 23 minutes.

In order to provide a standard of comparison for the depth of modulation impressed on the wanted wave B the latter was modulated at its source for $\frac{1}{2}$ *minute* in each 2-minute period with a *standard tone of* 80 Hz to a *depth of* 5%.

At Katoomba 2 receivers R_B and R_A were tuned respectively to the wanted wave B and the disturbing wave A. Their rectified outputs were displayed on the screen of a double beam C.R. oscillograph with a time-base frequency of 80 Hz. This display and the time and signal strength were photographed every 10 seconds.

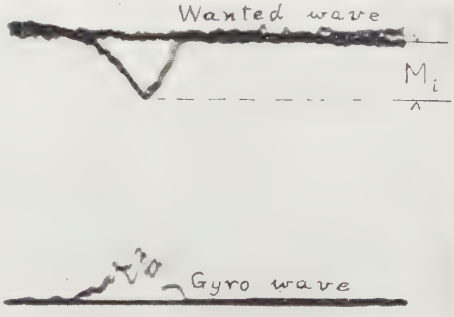

Fig. 7.

Examples of the pulses impressed by A on B are shown by Figs. 7 and 8. In these the *time increases from right to left*. Fig. 7 yields the depth M_i of the impressed modulation and also the relaxation time τ from the rising part of the curve on the left.

Fig. 8 shows the standard tone of 5% depth and the impressed pulse together.

The mean value of M_i corresponding to each frequency in one cycle was plotted and the resulting points were joined by means of a smooth curve as shown in Fig. 9, where cycles 1 and 3 show *2-humped resonance* and cycle 4 shows *1-humped resonance*.

Cycle 3 shows resonance even though the propagation conditions were just then very unsteady.

The *positions* of the 2-humped minima and the 1-humped maximum agree with the gyro-frequency within 3 %.

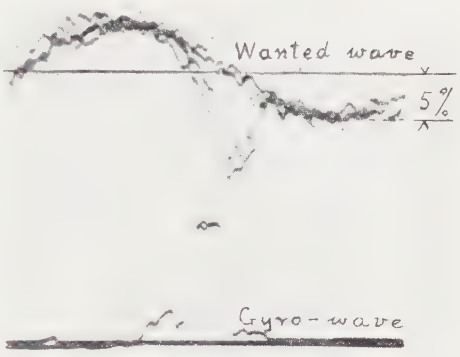

Fig. 8.

The *magnitudes* of the maxima are of the same order as that predicted by the theory.

These experimental curves closely resemble the theoretical curves published thirteen yeard earlier.

From the « free decay » of the impressed pulse we found the *time constant* $\tau = 1/Gv$ to lie between 0.7 and 1 millisecond. This agrees with the values deduced from previous studies of ordinary interaction. The constant G for different gases is known from laboratory experiments.

From such observations of gyro-interaction the following quantities relating to the E-region can be determined:

The field H at the E layer — from the minimum or maxima of the resonance curves depicting M_i;

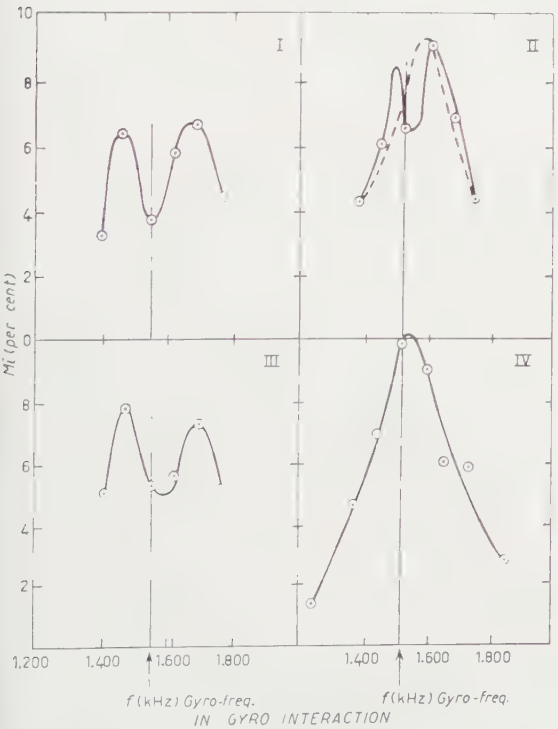

Fig. 1.

The collision frequency ν — from the shapes of the resonance curves (e.g. Ω/ν or p_H/ν behaves roughly like the Q-number of a circuit);

The gas elasticity constant G — from the values of Gv deduced from the free decay of the impressed pulse.

The value of G then allows us to *identify the gas* in the E-layer.

In addition the gas-temperature T and the electron-density gradient b can be determined from the resonance curves, the field vector of the A wave at the E-layer and the detailed theory.

8. – The Reality of Resonance in Gyro-Interaction.

It should be mentioned that about the same time CUTOLO [15] reported that besides bactrian resonance he had also observed dromedarian (one-humped) resonance.

J. A. RATCLIFFE and I. J. SHAW had previously concluded that resonance in wave-interaction near the gyro-frequency does not exist; but their choice of the wanted wave B did not conform to the requirements of the theory and so their observations and deductions cannot be regarded as conclusive.

The Australian and Italian experiments agree in confirming the existence of resonance in gyrointeraction.

9. – Micro-Wave Interaction in Gas-Discharge Tubes.

The theory of interaction, including gyro-interaction, was also confirmed in 1953 by the experiments with micro-waves of GOLDSTEIN, ANDERSON and CLARK [17] in America. In particular they studied the effect of a magnetic field on the interaction between waves of frequencies 8600 and 9400 MHz which passed through a gas-discharge tube inside a wave-guide. They found that a magnetic field of intensity corresponding to 8600 MHz produced observable interaction even when the disturbing signals were too weak to cause it without the magnetic field.

10. - Self-Distortion of Powerful Waves.

Another phenomenon predicted in the early publication [18.20] is the self-distortion of sky-waves received from powerful long-wave stations (*). This should appear as a decrease of the modulation at the low-frequency end.

(*) This phenomenon was later called « self-interaction » by RATCLIFFE and SHAW [16] who did not appear to know of the earlier work.

An opposite behaviour has been reported by CUTOLO [21] to have been observed on gyro-waves radiated with powers of about 5 kW. He also found that this phenomenon is subject to resonance near the gyro-frequency. His conclusions have recently received some support from the work of S. N. MITRA [22] in India and G. J. AITCHISON and G. L. GOODWIN [23] in South Australia. On the other hand in somewhat similar circumstances M. BOELLA [24] of Turin has failed to observe this phenomenon.

In the present state of the theory Cutolo's phenomenon is not easy to explain on the same basis as that of the interaction of two different waves i.e. in terms of an appreciable increase in the collision frequency. For, at (or near) the gyro-frequency only the *ordinary* component of the wave is received and the top of this component's trajectory lies well above the 5 km slab affected by the *extraordinary* component. Hence, in accordance with the numbers in the fifth row of Table V of my publication [8] « Part I » (p. 955) it follows that the modulation impressed by the extraordinary component on the ordinary component must be much less than 0.4 per cent (which is the value there given for a wanted wave of wave-length 625 metres and a power of 10 kW in the gyro-wave). The direct effect of the ordinary wave on itself, even if it were large enough, would not display the resonance observed by CUTOLO.

It therefore seems likely that the explanation of Cutolo's phenomenon is to be sought in another process. One which seems to me worthy of investigation is the increasing difference at the receiver in the phases and amplitudes of the carrier and its two side-bands as the modulation frequency increases. These differences are due to the dispersion of the Ionosphere and these may well become large near the gyro-frequency (*). This process is essentially independent of the power radiated.

The self-distortion of a wave by the change it imposes on the collision frequency will, of course, depend on the power radiated. This dependence may therefore be used as a criterion for inferring the nature of the process involved in any observed distortion of a wave. It is therefore to be hoped that the further study of Cutolo's phenomenon can include the effect of changing the power by a factor of at least 2.

About five weeks ago I wrote to Professor GOLDSTEIN asking whether it might be possible to investigate the phenomenon of self-distortion by means of his micro-wave techniques. His reply reached me at Genoa eight days ago. In this he states that before receiving my letter he had already investigated self-distortion by means of his techniques, using square-pulse modulation.

(*) In the subsequent discussion Dr. T. KAHAN indicated that he had independently arrived at the same conclusion.

His results (the photoprints of the oscillograph displays obtained are in the press) convincingly demonstrate the self-distortion of a wave due to the increase of collision frequency caused by it and also the large distortion caused by relatively much lower powers when the gyrofrequency, corresponding to a slowly varying magnetic field applied to the discharge tube, approximates to the wave-frequency.

It should also be possible to observe the self-distortion of long waves by means of existing powerful stations and perhaps also by observing the radiation from electrical storms (*).

11. – The Artificial Aurora (or Air Glow).

Another consequence of the underlying ideas is the possibility of generating an artificial air glow (or aurora) by means of powerful gyro-waves. It was shown [12, 25] in 1938 that with a suitable system of aerials and a power of 500 kW (**) it would be possible to produce a celestial glow which would allow the gas in the E-region to be studied spectroscopically. This would also allow its motion and temperature to be inferred. It was also shown that with 1 million kW of power the glow would have the same illuminating value as moonlight. (It has even been suggested that this glow would have the same romantic value as moonlight).

12. – The Motion of Slow Electrons in Air.

I have been asked more than once to express an opinion on the conclusions with regard to slow electrons in air which were published in 1953 by Crompton, Huxley and Sutton [26]. The space at my disposal allows only a few critical remarks on their work.

By means of new experiments they obtained fresh data on the collisions of electrons possessing energies corresponding to $k \geqslant 4$. These data they combined with the earlier observations of Nielsen and Bradbury on the drift velocity of electrons in air (which correspond to $k \geqslant 5.4$). From the combined data they derived empirical formulae by means of extrapolations to the range $1 \leqslant k \leqslant 4$. These empirical formulae are here given in Appendix II.

(*) For this purpose it may be sufficient to re-examine old oscillograph records of electrical storms.

(**) A later estimate reduced this to 250 kW.

In Sect. 1 of Appendix II are set out the three classical fundamental relations (A), (B), (C) and the inequality (D) which is a logical consequence of them. In Sect. 3 it is proved by means of (D) (*) that the two fundamental formulae of CROMPTON, HUXLEY and SUTTON are mutually contradictory when k is near 1. It can also be shown that at $k = 4$ their resulting formula for the product λk is not consistent with their own observations. It follows immediately that their formula for λ (given here under (3)) is unacceptable.

But these inconsistencies do not impair the value of their experimental observations. Consequently it is useful to point out that their observations are consistent with the hypothesis that the formula (14.A) in Appendix I, namely

$$, \quad G(U - U_1) ,$$

is valid in the range $1 \leqslant k \leqslant$ about 5.

13. – Conclusion.

In conclusion I would like to pay a tribute to the work of Dr. CUTOLO and his collaborators which constitutes an outstanding and convincing contribution to our knowledge of the behaviour of radio waves in the ionosphere. In particular one must admire the great persistence and ingenuity with which he has organised and successfully performed experiments with the low radiated powers available to him. Lastly I would like to thank the Società Italiana di Fisica for inviting me to Venice and for its hospitality. I can assure it that this invitation is much appreciated in Australia. My thanks are also due to the Cini Foundation for its kind hospitality in this city.

Note Added on June 13, 1956.

The conclusions of Sect. 12 above are now supported by the fact that more recently Prof. HUXLEY (in the *Proc. Roy. Soc.*, A **229**, 405, 1955) has rejected the formula for λk of CROMPTON, HUXLEY and SUTTON.

(*) Or alternatively (C).

Appendix I

(We have omitted numerical factors which depend on the velocity distribution of the electrons, for these factors do not differ much from 1 and their inclusion does not in general affect the conclusions reached).

If U and U_1 are the mean kinetic energies of an electron and a molecule respectively then Townsend's relation between the velocity W and the coefficient of diffusion K is

$$\frac{W}{K} = \frac{Z}{40.3k}. \tag{1A}$$

where

$$k = U/U_1. \tag{2A}$$

The mass flow, or flux, $\boldsymbol{F}$ of electrons through a unit area at a point and the electron number-density n are related by the following two vector equations:

$$\boldsymbol{F} = n\boldsymbol{W} - K \operatorname{grad} n, \tag{3A}$$

$$\operatorname{div} \boldsymbol{F} = 0. \tag{4A}$$

From equations (4A), (3A) and (1A) we obtain

$$\nabla^2 n = \frac{Z}{40.3k} \frac{\partial n}{\partial z}. \tag{5A}$$

when the z-axis of coordinates is parallel to the force Z.

Equation (5A) shows that the spatial distribution of the electron density n depends only on Z and k (and the boundaries). Hence, from measurements of this distribution the value of k can be derived.

Townsend's method for determining the values of the energy factor k and the drift velocity W depends on the instrument schematically illustrated in Fig. 1A.

The principal parts consist of a disc D and the electrodes E_1, E_2, E_3 and guard-ring G which all lie in a plane parallel to D. In D is a straight narrow slit S (shown end-on) and above D is a source of electrons, usually a suitable photo-cathode. The electrodes E_1, E_2, E_3 constitute a disc separated from the guard-ring G by a narrow gap. The middle electrode E_2 is a strip with its edges parallel to the slit S and is separated from E_1 and E_3 by narrow gaps. G is earthed and the electrodes E_1, E_2, E_3 are insulated but maintained (by induction) near earth potential. The disc D and the electron source are maintained at such potentials that everywhere a uniform, constant electric field Z acts downwards on the electrons. The gas-pressure p is maintained constant (at a value of the order of several millimetres of mercury).

The electrons which pass through the narrow slit S diffuse laterally (as

indicated by the broken curves in Fig. 1A) and the resulting currents i_1, i_2, i_3 to the respective electrodes E_1, E_2, E_3 are measured: more precisely the following ratio R is measured:

$$R = \frac{i_2}{i_1 + i_2 + i_3},$$

i.e. the proportion of the total electron stream which falls on the middle electrode E_2 is measured.

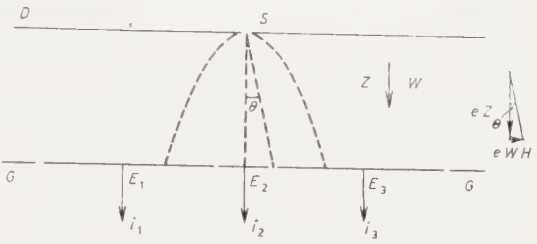

Fig. 1A.

Also, from the partial differential equation (5A) and the boundary conditions appropriate to the instrument used we can determine R as a known function of the ratio Z/k. This function can be represented by means of a curve as in Fig. 2A.

By means of this curve we can easily determine the value of Z/k corresponding to each observed value of R. Since the value of Z is known we can thus determine the corresponding value of the energy factor k.

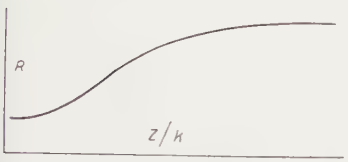

Fig. 2A.

The value of the drift velocity W is determined as follows: A uniform magnetic field of intensity H is applied parallel to the edges of the strip E_2 (and of the slit S), i.e. in a direction perpendicular to the Fig. 1A. Then the value of H is adjusted until $i_1 + i_2 = i_3$. This corresponds to a deflection of the middle of the electron stream to the middle of the narrow gap separating E_2 and E_3. Therefore this value of H corresponds to the known angle of deflection θ shown in Fig. 1A. Also this new direction of the middle of the stream must be the same as the direction of the resultant of the vertical force eZ and the mean horizontal force eWH which act simultaneously on an electron in the stream. The corresponding triangle of forces is shown, at the right side of Fig. 1A.
It follows immediately that

$$\operatorname{tg}\theta = eWH/eZ\,,$$

and so

$$W = (Z/H)\operatorname{tg}\theta\,.$$

The value of W can thus be derived from the known values of θ, Z and H.

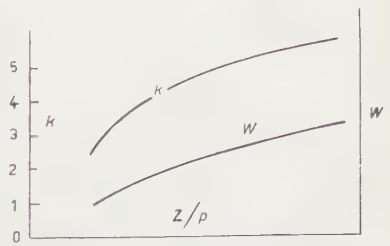

Fig. 3A.

For a given gas k and W are unchanged in value when we change Z and p by the same factor, i.e. k and W are functions of the ratio Z/p alone. Consequently the values of k and W in a given gas can be represented in terms of Z/p by means of curves like those sketched in Fig. 3A.

From the observed values of k and W we can derive the corresponding

values of the mean (*) random velocity u of an electron, its approximate collision-frequency ν and mean free path l and the approximate mean proportion λ of its energy lost at a collision with a molecule.

For a simple calculation based on (2A) and the formula $U = \frac{1}{2}mu^2$ yields the formula

$$u = 1.15 \cdot 10^7 \sqrt{k} \text{ cm/s}, \tag{6A}$$

and from the definitions of l and ν we have

$$\nu = u/l. \tag{7A}$$

Also, on equating the mean loss and gain of *momentum* suffered by an electron per second we obtain

$$\nu(mW) = eZ,$$

and so

$$W = \frac{Ze}{\nu m}. \tag{8A}$$

Finally, on equating the mean loss and gain of *energy* suffered by an electron per second we obtain

$$\nu\lambda(\tfrac{1}{2}mu^2) = eZ \cdot W,$$

and so, on using (8A) to eliminate ν, we have

$$\lambda = 2W^2/u^2. \tag{9A (**)}$$

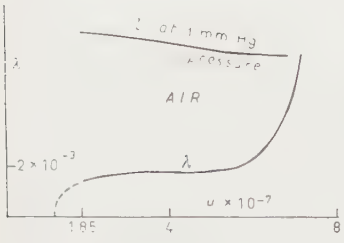

Fig. 4A.

Thus for a given value of Z/p we use the corresponding values of k and W to derive first the value of u from (6A) and that of ν from (8A), then that of l from (7A) and lastly that of λ from (9A).

For electrons in air, TOWNSEND [3] and TIZARD found values of k and W which yield the curves for l and λ sketched in Fig. 4A.

We may now consider the change in the collision-frequency ν which is caused by an alternating electric field $\boldsymbol{E}$ where

$$E = \sqrt{2}Z \sin \omega t. \tag{10A}$$

The equation of mean motion $\boldsymbol{v}$ of an electron is

$$m\frac{d\boldsymbol{v}}{dt} + \nu m\boldsymbol{v} = e\boldsymbol{E}. \tag{11A}$$

(*) More precisely: the root of the mean square velocity.

(**) Whan l varies litle with u.

The mean power impressed on the electron is therefore P where

$$P = e\boldsymbol{E}\cdot\bar{\boldsymbol{v}} = \frac{e^2}{m} Z^2 \frac{\nu}{\nu^2 + \omega^2}. \tag{12A}$$

[This is analogous to the following expression,

$$P = VI = V^2 \frac{R}{R^2 + L^2\omega^2},$$

for the power impressed by an e.m.f. V on an alternating-current circuit of self-inductance L and resistance R.]

We now proceed to find the variation of v in a time $\mathrm{d}t$ much greater than the period $(2\pi/\omega)$ of the alternating field.

If U is the mean kinetic energy of an electron and η is the mean energy lost by it at a collision with a gas molecule then we must have

$$\mathrm{d}U + \eta\cdot\nu\,\mathrm{d}t = P\,\mathrm{d}t,$$

and so

$$\frac{\mathrm{d}U}{\mathrm{d}t} + \eta\nu = P.$$

Since $U = \frac{1}{2}mu^2$, $\nu = u/l$, this yields

$$ml\frac{\mathrm{d}(l\nu)}{\mathrm{d}t} + \eta = w, \tag{13A}$$

where $w = P/\nu$ is the mean work done on an electron over a free path, i.e.

$$w = \frac{e^2}{m} Z^2 \frac{1}{\nu^2 + \omega^2}. \tag{12A.1}$$

Also η is a function of v which is determined by experiments like those of TOWNSEND and his collaborators. For example, with Helium as the gas, we found that

$$\lambda = G\left(1 - \frac{1}{k}\right),$$

where $G = 2m/M$ and M is the mass of a molecule; since η is equal to λU it follows that

$$\eta = G(U - U_1). \tag{14A}$$

Since $U = \frac{1}{2}ml^2\nu^2$ this yields

$$\eta = \tfrac{1}{2}ml^2G(\nu^2 - \nu_1^2), \tag{14A.1}$$

where ν_1 is the value of the unperturbed collision frequency.

On using (14A.1) and (12A.1) the equation (13A) becomes

$$\frac{1}{l}\frac{\mathrm{d}(lv)}{\mathrm{d}t} + \tfrac{1}{2}G(v^2 - v_1^2) = \frac{1}{l^2}\frac{e^2}{m^2}\frac{Z^2}{v^2 + \omega^2}. \tag{15A}$$

Here v_1, Z and ω are constants. When the variation of l with v is such that

$$\left|\frac{\mathrm{d}l}{\mathrm{d}v}\right| \ll \frac{l}{v},$$

then the first term in (15A) may be replaced, with little error, by $\mathrm{d}v/\mathrm{d}t$. It then follows from (15A) that *v will ultimately increase with Z.*

This conclusion is, in effect, due to TOWNSEND and was published by him before 1930.

The value ultimately attained by v is v_0 the positive root of the equation

$$\tfrac{1}{2}G(v^2 - v_1^2) = \frac{1}{l^2}\frac{e^2}{m^2}\frac{Z^2}{v^2 + \omega^2}. \tag{16A}$$

NOTE. – On considering the experiments of TOWNSEND and TIZARD on electrons in air, and from the more recent experiments of HUXLEY and his collaborators, it appears that as a *working hypothesis* the formula (14A) may be applied also to electrons in air in the range of energies corresponding to $1 \leqslant k \leqslant 5$ or so, with G taken as an empirical constant of the order of $2 \cdot 10^{-3}$.

APPENDIX II

(In this Appendix the symbols c_1, c_2, ... c_q represent known positive constants).

1. – The following are classical fundamental relations; the first two, essentially due to TOWNSEND, have already been given in Appendix I as equations (8A) and (9A) respectively.

$$W = c_1 Z/v = c_2 Z l k^{-\frac{1}{2}}, \tag{A}$$

$$\lambda = c_3 W^2/k, \tag{B}$$

$$\lambda \geqslant \lambda_E = G_E(1 - k^{-1}), \tag{C}$$

where $G_E = 2m/M$.

The formula (C) merely states that λ cannot be less than the proportion, λ_E, of energy lost in *perfectly* elastic collisions.

On substituting from (B) and (A) in (C) we obtain the following necessary inequality:

$$Z^2 l^2 \geqslant c_4 k(k - 1). \tag{D}$$

2. – The fundamental empirical formulae of CROMPTON, HUXLEY and SUTTON [26], for the range of energies corresponding to $1 \leqslant k \leqslant 4$, are two in

number. The first is

$$v = c_5 k \,, \tag{17A}$$

which, on account of the relations (6A) and (7A) in Appendix I, is equivalent to the empirical formula

$$l - c_6 k^{-\frac{1}{2}} \,. \tag{17A.1}$$

Their second empirical formula is

$$k = 1 + c_7 Z \,. \tag{18A}$$

On eliminating W, Z and l between the equations (B), (A), (17A.1) and (18A) we obtain the formula

$$\lambda = c_8 (1 - k^{-1})^2 k^{-1} \,. \tag{19A}$$

This formula is also given by Crompton, Huxley and Sutton.

3. – From (18A) and (D) we deduce the inequality

$$l \geqslant c_9 \sqrt{k/(k-1)} \,. \tag{20A}$$

This necessarily leads to the conclusion that as k tends to 1 then l tends to infinity, which clearly contradicts (17A.1) and so also contradicts the first fundamental empirical formula (17A).

Thus we see that *the two fundamental empirical formulae of Crompton, Huxley and Sutton contradict one another when the value of k is near* 1.

Also it can be shown that at the value $k = 4$ their formula (19A) leads to a value of the *slope* of the curve representing $y = \lambda k$ in terms of $x = k$ which is nearly one quarter of the slope, at $k = 4$, of the empirical curve given by Crompton, Huxley and Sutton in their Fig. 7.

We thus conclude that the two fundamental empirical formulae of Crompton, Huxley and Sutton are mutually contradictory when k is near 1 and that their resulting formula for λk is not consistent with their own observations.

REFERENCES

[1] J. S. Townsend: *Electrons in Gases* (London, 1947).

[2] R. H. Healey and J. W. Reed: *The Behaviour of Slow Electrons in Gases* (Sydney, 1940).

[3] J. S. Townsend and H. T. Tizard: *Proc. Roy. Soc.*, A **88**, 336 (1913).

[4] B. D. H. Tellegen: *Nature*, **131**, 840 (1933).

[5] V. A. Bailey and D. F. Martyn: *Phil. Mag.*, **18**, 369 (1934).
[6] V. A. Bailey: *Wireless World*, February 26 and March 5, 1937.
[7] V. A. Bailey: *Phil. Mag.*, **23**, 774 (1937).
[8] V. A. Bailey: *Phil. Mag.*, **23**, 929 (1937).
[9] V. A. Bailey: *Nature*, **139**, 68 (1937).
[10] V. A. Bailey: *Nature*, **139**, 838 (1937).
[11] M. Cutolo, M. Carlevaro and M. Gherghi: *Alta Freq.*, **15**, 2, p. 111 (1946).
[12] V. A. Bailey: *Phil. Mag.*, **26**, 425 (1938).
[13] M. Cutolo: *Nature*, **166**, 98 (1950).
[14] V. A. Bailey, R. A. Smith, K. Landecker, A. J. Higgs and F. H. Hibberd: *Nature*, **169**, 911 (1952).
[15] M. Cutolo: *Nuovo Cimento*, **9**, 391 (1952).
[16] J. A. Ratcliffe and I. J. Shaw: *Proc. Roy. Soc.*, **193**, 311 (1948).
[17] L. Goldstein, J. M. Anderson and G. L. Clark: *Phys. Rev.*, **90**, 151 (1953).
[18] V. A. Bailey: *World Radio*, January 25, (1935).
[19] V. A. Bailey and D. F. Martyn: *Wireless Engineer*, March 1935.
[20] V. A. Bailey: *Wireless World*, February 26, 1937.
[21] M. Cutolo: *Nature*, **167**, 314 (1951).
[22] S. N. Mitra: *Conference on the Physics of the Ionosphere*, Cavendish Laboratory Cambridge (1954), p. 7.
[23] G. J. Aitchison and G. L. Goodwin: *Nuovo Cimento*, **1**, 722 (1955).
[24] M. Boella: *Ricerca Scient.*, n. 6, June, 1955.
[25] V. A. Bailey: *Nature*, **142**, 613 (1938).
[26] R. W. Crompton, L. G. H. Huxley and D. J. Sutton: *Proc. Roy. Soc.*, A **218**, 507 (1953).

OSSERVAZIONI ED INTERVENTI

— I. Ranzi:

Il prof. Bailey ha riferito su di una recentissima esperienza eseguita dal prof. Goldstein e che prova la esistenza di un forte assorbimento di microonde da parte di un gas ionizzato posto in un campo magnetico di valore opportuno. Va ricordato, a tale riguardo, che sin dal 1930, il prof. G. Todesco aveva dimostrato sperimentalmente l'esistenza di tale fenomeno per onde continue di circa 2000 MHz, propagantisi in un gas elettronico; esperienza questa di indubbio valore, quando si tengano presenti le difficoltà sperimentali in quell'epoca nel campo delle microonde.

— K. Rawer:

1) I suppose that the level of interaction is that, where the extraordinary component of the disturbing (gyro-) wave is reflected or absorbed. This corresponds to a very low electron density which should even be zero for the gyrofrequency. This is the result of the usual simplified theory. Or if we have no electrons, there can be no effect. The theory should I feel be made precise for this case.

2) The observations have been made as I suppose during the night. If I have well understood, an exponential law has been supposed for the distribution of the electron density as well as for the collision number. Now I think there is experimental

evidence from routine ionograms that the electron density at the E-level is very variable at night. Even a rather low electron density in this level may be seen from the trace of ionogram. In that case we may observe a v-trace curve in a concave form at low frequencies (about $1.8 \div 2.2$ MHz) thus indicating an effect of retardation in a lower layer. Now this form of ionogram does not always exist there are many cases without retardation of the v-trace. The conditions seem to be rather rapidly variable.

— V. A. Bailey:

1) Regions with few electrons per unit volume (e.g. with zero electron density) can have only a small effect on the extraordinary component of a gyro-wave. It is necessary to consider the effect of *all* the electrons in a unit volume on the gyro-wave and this consideration immediately leads to the emergence of a slab (or stratum) of the E-region as the principal region which is effective in gyro-interaction.

2) For the almost complete absorption of a gyro-wave the electron density need not exceed about 400 electrons per cm^3. Hence it should nearly always be possible to have the slab (referred to before) actually present and so we should nearly always be able to produce gyro-interaction.

SUPPLEMENTO AL VOLUME IV, SERIE X
DEL NUOVO CIMENTO

N. 4, 1956
2° Semestre

Ionospheric Selfdemodulation of Radiowaves.

M. CUTOLO, G. C. BONGHI and F. IMMIRZI

Centro Studi di Radiopropagazione
Istituto di Fisica Tecnica dell'Università - Napoli

and

P. CACHON

Institut de Physique Industrielle - University of Algiers

In 1951 M. CUTOLO published on *Nature* [1], a letter in which he communicated to have observed a new phenomenon that he then called self-gyro-interaction and now refers to as self-gyro-demodulation. This phenomenon consists in the reduction of the modulation depth of a radiowave, modulated for example 80 per cent at 230 Hz (after its passage in the ionosphere), whose carrier frequency is varied around local gyro-frequency of about 500 kHz.

The behaviour of the phenomenon is such that the resonance curve is almost the same as Bailey's curve with two humps in gyro-interaction.

While, in this last case, the parasitic modulation (or better « interaction index ») has the biggest percent on the humps of the resonance curve and the minimum nearly on gyro-frequency, in self-demodulation the maximum of the phenomenon is nearly on gyro-frequency, on the contrary the minima lye on the two peaks of the curve. Which is intuitive by Bailey's theory. That is to say self-gyro-interaction is the contrary of gyro-interaction.

To verify whether self-demodulation also exists on frequencies far removed from local gyrofrequency (1200 kHz) one of us (M.C.) made some experiments in July 1952 using the station Radio Naples I (656 kHz, 80 kW) of the Italian Broadcast (R.A.I.), which for two nights emitted its carrier frequency modulated 80% from 50 to 1000 Hz.

The reception of the waves was made at the Istituto Elettrotecnico Nazionale « G. Ferraris » in Turin.

From the few measurements we were able to make, very little demodulation was apparent. It was greater for higher modulation tones and only occasionally was the effect so great as not to be masked by experimental errors.

A wide program of experiments were proposed to Mr. PICAULT, the Chairman of the Subcommission IIIb of the URSI and these were realized in March 1953 [2], with receiving stations located in many cities of Europe and one in Algiers.

Here we give the results obtained in Naples and in Algiers only.

The receiving station of Naples consisted of a good antenna, a receiver with tuned circuits (3 H.F. circuits) the output being coupled to an oscillograph with a cinematographic apparatus. The envelope of the oscillograph trace gave a measure of the modulation percentage.

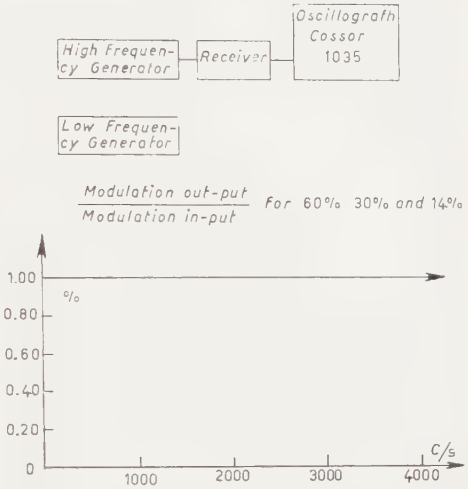

Fig. 1. – Method and curve of calibration of the receiver.

Our receiver was linear as far as 4000 Hz (Fig. 1).

The Algiers receiving station consisted of a superheterodyne equipped for automatic recording of both the field and the modulation percentage.

The transmitting stations were Radio Paris (863 kHz, 150 kW) and Radio Strasbourg (1160 kHz, 200 kW), which emitted their carrier frequency mo-

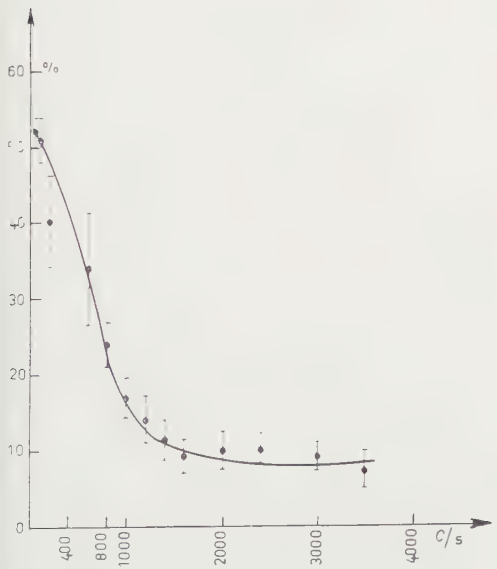

Fig. 2. Experiments of 28 March 1953.

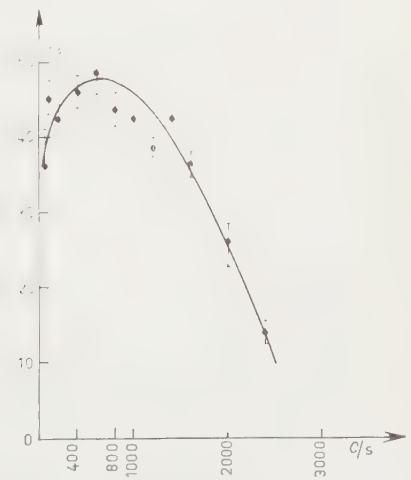

Fig. 3. – Experiments of 27 March 1953. Behaviour of self-demodulation acting as the modulation frequency. Transmitter: radio Paris (863 kHz, 75 kW; 60%). Receiver: Naples.

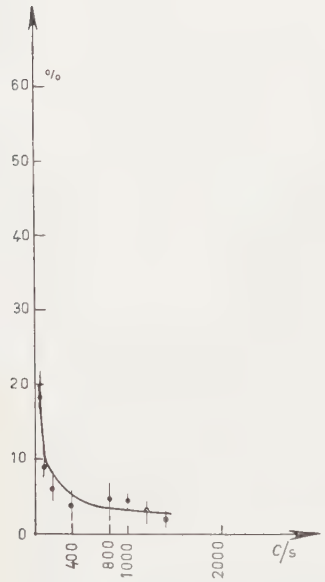

Fig. 4

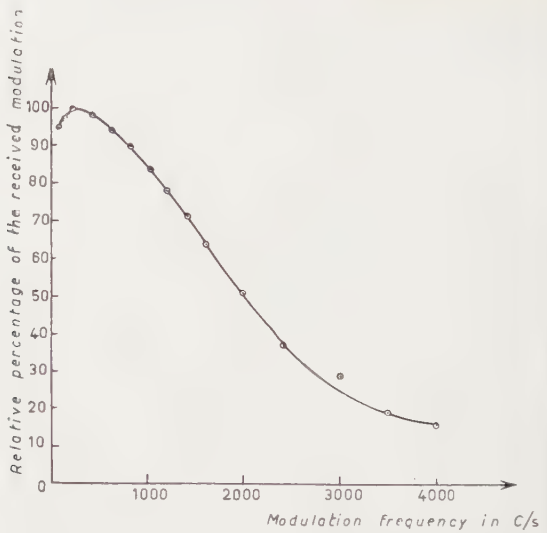

Fig. 5. – Experiments of 26 March 1953. Behaviour of self-demodulation acting as the modulation frequency. Reception in Algier. Transmitter: Radio Paris (863 kHz, 150 kW; 60%).

dulated 60% and 30%, full and half power, at 50, 100, 200, 400, 600, 800, 1000, 1200, 1400, 1600, 2000, 3000, 3500, 4000 Hz.

A study of the diagrams obtained in Naples and Algiers clearly showed at least on night when the ionosphere was indisturbed, a strong demodulation effect which favoured the *lower* tones (Fig. 2, 3, 4, 5, 6, 7). We consider that the results obtained for Naples

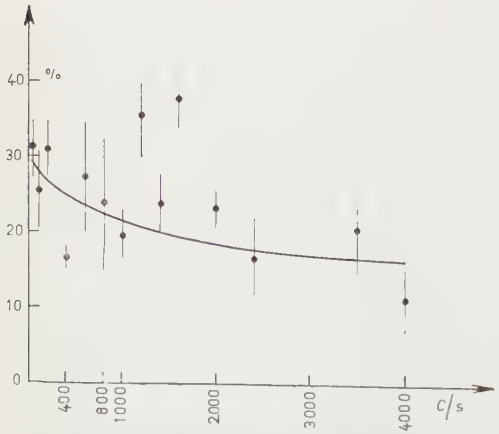

Fig. 6. – Experiments of 28 March 1953; transmitter: radio Strasbourg 1160 kHz, 200 kW; 30%; receiver: Naples.

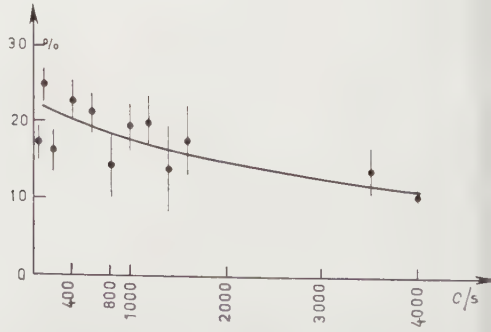

Fig. 7. – Experiments of 28 March 1953; transmitter radio Strasbourg 1160 kHz. 100 kW; 30%; receiver: Naples.

and Algiers confirm the existence of a demodulation effect for frequencies not too far removed from gyrofrequency.

New experiments were carried out in August 1954 with Hilversum I (764 kHz) the carrier wave of which was modulated 60% with modulation frequencies varying from 50 to 4000 Hz. Unfortunately an interference due to Radio Warshaw precluded the possibility of measurable effects except for one night when we could get a curve of the residual modulation depth as function of the modulation frequency similar to the previous ones. The modulation increased as far as 1000 Hz and then remained constant, Fig. 8.

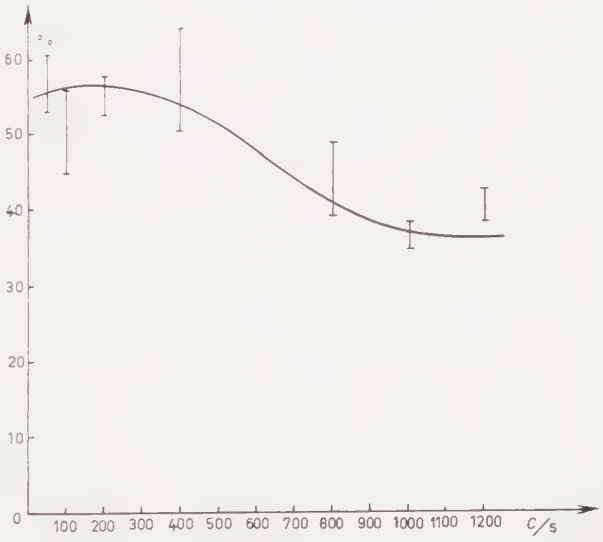

Fig. 8

The last experiments were carried out in March 1955. They were intended to show the dependence of the phenomenon on 1) emitted power, 2) the modulation depth, 3) fading (when present). The transmitter was Radio Paris modulated 60% and 30% with modulation frequencies from 30 to 4000 Hz the transmissions of fixed power modulation frequency and modulation depth lasting one minute each. During two nights Radio Paris transmitted at full and half power at 1000 Hz, with a modulation depth of 60%, 30%, 20%, 15% each transmission lasting two minutes. A 40 minutes transmission at full power, 1000 Hz, was also effectuated.

But this time the experiments were also disturbed by interference from Radio Roma.

Strong demodulation was always observed and was most pronunced at high modulation tones as far as 3000 Hz at least (Figs. 9, 10, 11, 12). On the average the demodulation was stronger in 1953 than in 1955. In 1953, we were not able to follow the phenomenon at full power at 60%. The phenomenon was well observed at full and half power, at 30%; but the results on which we can rely at full and half power respectively, refer to different nights, so that their comparison is scarcely useful.

As far as the dependence of the phenomenon on the power is concerned, no conclusion can be drawn, and new experiments will be necessary.

Each point of the curves shown in the figures represents the median value of several measurements carried out when transmission occurred at a given modulation frequency, the number of each group of measurements ranging from 20 to 50 (for each modulation frequency). Occasionally 200 or more

Table for Fig. 9.

Hz	%	ε	$\varepsilon/\sqrt{n}$
200	41.8	± 3.83	± 0.836
400	46.4	± 3.89	± 0.629
600	46.05	± 3.67	± 0.669
1 000	42.2	± 3.47	± 0.500
1 600	47.7	± 4.26	± 0.906
1 700	35.2	± 3.13	± 0.736
1 800	37.5	± 3.78	± 0.475
1 900	32.7	± 3.45	± 0.811
2 000	29.5	± 3.81	± 0.566

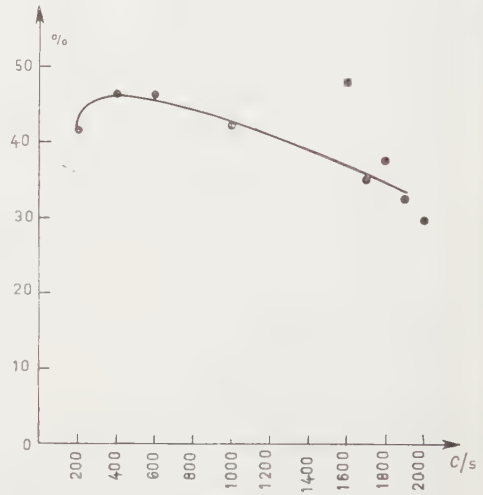

Fig. 9. – Experiments of 10 March 1955. Transmitter radio Paris (863 kHz, 75 kW; 60%)

Table for Fig. 10.

Hz	%	ε	$\varepsilon/\sqrt{n}$
50	22.6	± 6.59	± 0.888
200	24.2	± 3.24	± 0.368
400	23.4	± 4.01	± 0.447
800	16.7	± 4.54	± 0.432
1 000	18.2	± 2.87	± 0.350
1 200	32.3	± 9.59	± 2.260
1 500	17.6	± 6.08	± 1.570
1 600	16.4	± 4.27	± 0.636
1 700	18.9	± 3.72	± 0.522
1 800	22.7	± 5.21	± 0.554
1 900	18.9	± 4.85	± 0.591
2 000	18.8	± 4.10	± 0.639

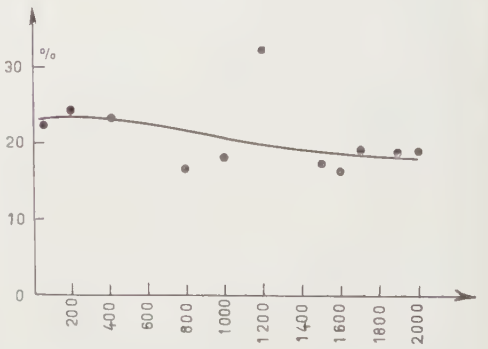

Fig. 10. – Experiments of 10 March 1955. Transmitter radio Paris (863 kHz 75 kW; 30%).

measurements were taken when the signal strength underwent a marked fluctuation. Distorted oscillograms were not taken into account when drawing the curves.

Interesting are Fig. 6 and 7 obtained with radio Strasbourg. The behaviour of the phenomenon is the same but less marked than that with radio Paris.

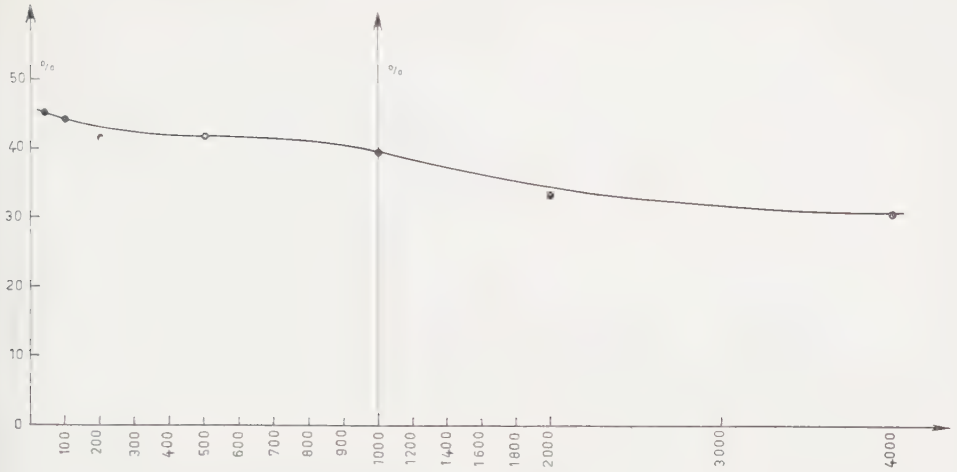

Fig. 11. – Experiments of 20 March 1955. Transmitter radio Paris (863 kHz; 75 kW; 60%).

Probably the sensible dispersion of the points in the diagrams is because the carrier frequency of the station is very near to gyrofrequency ($\sim$ 1200 kHz) where the absorption for the resonance is more critical. Fig. 13 shows an example of fluctuations observed during one minute for each modulation frequency.

The curve of Fig. 5 has been constructed using measurements obtained in Algiers, due account being taken of the amplitude of the signal, of the response of the receiver as well as of the registering equipment.

TABLE FOR FIG. 11.

Hz	%	ε	$\varepsilon/\sqrt{n}$
30	45.25	$\pm$ 3.42	$\pm$ 2.420
40	45.20	$\pm$ 3.23	$\pm$ 0.423
100	44.40	$\pm$ 5.02	$\pm$ 0.626
200	41.67	$\pm$ 3.99	$\pm$ 0.460
500	41.81	$\pm$ 3.47	$\pm$ 0.389
1 000	40.00	$\pm$ 2.74	$\pm$ 0.365
2 000	33.90	$\pm$ 3.62	$\pm$ 0.458
4 000	31.30	$\pm$ 9.20	$\pm$ 1.550

TABLE FOR FIG. 12.

Hz	%	ε	$\varepsilon/\sqrt{n}$
500	23.61	$\pm$ 4.76	$\pm$ 0.584
1 000	23.70	$\pm$ 4.31	$\pm$ 0.786
2 000	25.20	$\pm$ 5.27	$\pm$ 0.929
4 000	17.20	$\pm$ 7.46	$\pm$ 0.954

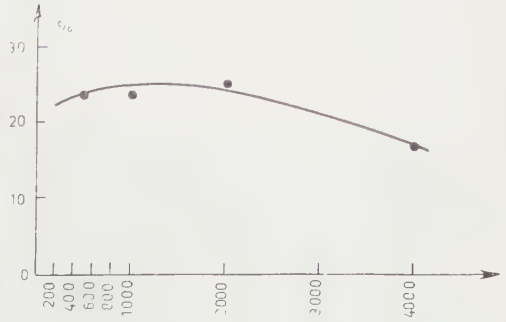

Fig. 12. – Experiments of 20 March 1955. Transmitter radio Paris (863 kHz, 150 kW; 30%).

So far as the dependence of our phenomenon on carrier frequency and power is concerned our results may be so summarized:

1) For carrier frequencies which are very far from gyro frequency demodulation does not exist or at least it is too small to be measurable with the available means (for example our measurements at 656 kHz). The same may be true for powers less than 80 kW.

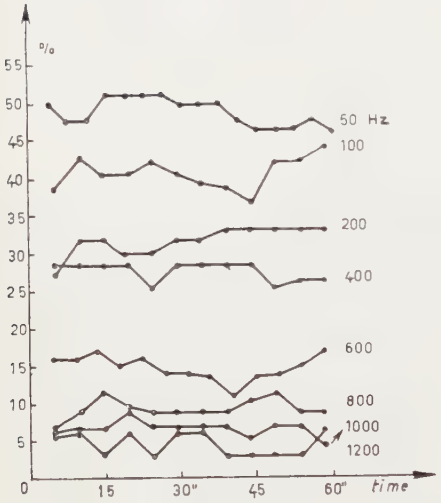

Fig. 13. – Behaviour in Naples of self-demodulation for each frequency of modulation (in Hz). Transmitter: Radio Paris (863 kHz, 150 kW, 60%). The diagram shows that the fluctuations of received percentage for each audio frequency are small and therefore self-demodulation does not depend on fading.

2) For frequencies far from gyro-frequency and for powers of the order of one hundred kW (for example our measurements at 764 kHz), demodulation is apparent.

3) The percentage of demodulation increases rapidly as the carrier frequency approaches gyro-frequency (for example our measurements at 863 kHz).

4) At the gyro-frequency demodulation is so great as to reach 40% of the transmitter modulation depth. This is true for powers as low as 3.3 kW.

Concluding the self-demodulation exists around gyro-frequency only (at least for powers less than 100 kW) *and so it is due to absorption caused by the action of the terrestrial magnetic field.*

So far as the dependence of our phenomenon on the modulation frequency is concerned two different behaviours have been observed:

a) The received depth of modulation is at first a decreasing function of the modulation frequency. When a certain limiting value is attained the received depth of modulation remains constant.

b) The received depth of modulation is already low at low modulation frequencies, it then increases (until say 600 Hz) and eventually follows a behaviour similar to the former case.

The dependence of demodulation on the modulation frequency yields curves

which are similar to those of interaction. The behaviour of the phenomenon on the other hand is opposite, because in the case of interaction the effect becomes less and less important as the modulation frequencies increase whereas in the case of demodulation the contrary is observed.

Our results are fairly well in accordance with the conclusions of M. Carlevaro's [3] mathematical theory of demodulation, based on V. A. Bailey's theory of the motion of electrons [4].

On the other hand the explanation suggested by some one that demodulation should be considered a consequence of selective fading does not conform with our experimental results. We have (indeed) observed demodulations already at very low frequencies (30 Hz) where selective fading plays an insignificant role, nor can selective fading account for the steady behaviour of our experimental curves in the region of high modulation frequencies.

Selectivity as such cannot but grow in importance at high modulation frequencies. *A serious objection is that if self-demodulation were due to fading, then the phenomenon should take place on all frequencies, as fading does, and not on gyro-frequency only.*

Aitkinson and Goodwin [5] have been able to carry out in Australia measurements of demodulation in conditions where the occurrence of any type of fading was out of question. They have, moreover, measured on gyrofrequency percentages of demodulation stronger than those observed by one of us (M.C.). This might suggest that fading, when present, should lower rather than increase demodulation.

Important experiments made in 1953 in India by S. N. Mitra have confirmed self-demodulation around gyrofrequency and indirectly confirm the results obtained by us [6].

A careful examination of Fig. 13, which shows the fluctuations of the depth of modulation received during one minute, for each frequency of modulation shows that such fluctuations can hardly be interpreted as due to interference fading whereas it has been suggested by one of us (M.C.) that they rather appear to be due to fluctuations of ionospheric electron density [7].

Finally, distorted oscillograms were observed most of the time at low modulation frequencies: also this last result cannot be accounted for by selective fading.

All results above illustrated are particularly important for Broadcasting by medium waves.

In fact the existence of a demodulation for the waves between 500 : 1 500 kHz explains the abnormal behaviour of the medium waves.

Further researches shall be realized to explain the mechanism of the phenomenon. New experiments are being carried out.

* * *

We thank very much, Italian Radio Broadcast, France Radio Diffusion, Holland Radio, The Istituto Elettrotecnico Nazionale of Turin, the Istituto Superiore delle Telecomunicazioni of Rome, for their collaboration.

We are particularly very grateful to Mr. E. PICAULT, Chairman of S. Commission IIIb of U.R.S.I. and to Mr. ANGLÉ D'AURIAC, technical director of E.U.R., for the organisation of experiments. We are obliged to U.R.S.I., particularly to Mr. P. LEJAY, Sir. EDWARD APPLETON, Prof. A. BLANC LAPIERRE and Prof. E. CARLEVARO for their valuable interest.

REFERENCES

[1] M. CUTOLO: *Nature*, **166**, 98 (1950); **167**, 314 (1951); *Nuovo Cimento*, **9**, 391, 687 (1952).
[2] E. PICAULT: *U.R.S.I.*, **10**, n. 3, 28 (1954).
[3] M. CARLEVARO: in this issue pag. 1422.
[4] V. A. BAILEY: *Phil. Mag.*, **23**, 929 (1937); **26**, 425 (1938).
[5] G. Y. AITKINSON and G. L. GOODWIN: *Nuovo Cimento*, **1**, 722 (1955).
[6] S. N. MITRA: *Phys. Soc. Report of Cambridge Conf. on the Physics of the Ionosphere*. p. 71.
[7] M. CUTOLO: *Nuovo Cimento*, **1**, 726 (1955).

OSSERVAZIONI ED INTERVENTI

— I. RANZI:

Vorrei suggerire al dr. CUTOLO di eseguire, durante le esperienze di demodulazione, prove con emissione ad impulso, al fine di separare l'effetto di demodulazione dovuto ai cammini multipli (2E, 3E, M, 2F, 3F, ecc.) delle onde riflesse dalla ionosfera; tale effetto può essere tanto forte da mascherare l'eventuale fenomeno di autogirodemodulazione.

— V. A. BAILEY:

In the discussion following the papers by CUTOLO and myself I pointed out the difficulties that exist in explaining Cutolo's observed self-demodulation on the basis of self-distorsion by increase of the electron collision frequency namely: that on the basis of my published calculation of 1937 the observed *amount* of demodulation was

too large for the power radiated (e.g. about 5 kW). I proposed that another process be investigated theoretically to see wether it could account for Cutolo's phenomenon quantitatively: — This is the differential effects caused on the carrier and its two side-bands by a highly dispersive condition of the ionosphere (such as can occur near the gyro-frequency) in which the refractive index and absorption coefficient vary rapidly with the frequency. Lastly I suggested that in all future experiments on self-demodulation, the effect of *changing the* radiated *power* should be examined as this could serve to identify or exclude our phenomenon of self-distortion. (The equivalent of all these comments are also given in Sect. **10** of my manuscript).

— P. Dominici:

Senza entrare in merito alla natura od all'esistenza del fenomeno, è mia opinione che, per stabilire una corretta correlazione fra i dati sperimentali ottenuti in luoghi diversi ed in istanti diversi, occorra riferire i dati, con opportune correzioni nella formula che dà l'assorbimento, a condizioni « standard » di ionizzazione della zona dello strato E in cui ha luogo il fenomeno.

— M. Carlevaro:

I remark that the experiments have always shown a great distortion at low modulation frequencies and almost no distortion over 1 000 Hz.

This experimental result can not be explained by the hypothesis of the multiplicity of paths, for it would be necessary to admit that path-lenghts differencies must never be less than a given amount.

SUPPLEMENTO AL VOLUME IV, SERIE X
DEL NUOVO CIMENTO

N. 4, 1956
2° Semestre

L'occultation des parcours: phénomène important de la propagation ionosphérique.

K. RAWER

Service de Prévision Ionosphérique - Fribourg en Brisgau

Introduction.

Si l'on veut établir la théorie d'un phénomène quelconque on remplace d'abord la réalité qui est d'habitude assez complexe par un modèle simplifié. Cette simplification peut aller très loin à condition que le modèle reste «suffisant et adapté», c'est-à-dire qu'il puisse représenter les caractéristiques essentielles observées dans la réalité.

Pour le cas de la propagation ionosphérique les phénomènes observés sont extrêmement complexes, leur description complète nécessiterait un modèle très compliqué. La théorie de la propagation des ondes dans un milieu inhomogène, biréfringent, anisotrope et absorbant est pratiquement inextricable. Pour les calculs pratiques de nombreuses simplifications sont inévitables, il s'agit de savoir lesquelles peuvent être admises.

Il nous paraît qu'une théorie satisfaisante doit d'abord tenir compte du fait de l'existence de *plusieurs parcours différents*. Ensuite il y a le phénomène de la *réflexion ionosphérique* par réfraction des ondes dans le plasma, donnant lieu au phénomène bien connu de la zone de silence. Il y a encore *l'absorption* des ondes dans les couches basses de l'ionosphère. Enfin il existe encore un phénomène bien important pour une description satisfaisante des faits, c'est l'occultation des parcours qui sont réfléchis sur la région supérieure de l'ionosphère, la région F. Ce dernier phénomène découle directement de l'existence de plusieurs couches réfléchissantes dans l'ionosphère; malheureusement il est moins connu que les deux autres phénomènes dont nous venons de parler.

C'est un phénomène très simple causé par la simple loi de réfraction valable pour un rayon dont le complément de l'angle de départ est α_r

(Fig. 1; μ indice de réfraction):

$$R \cdot \mu(R) \cdot \sin \alpha = R_T \cdot \sin \alpha_T \,. \tag{1}$$

Suivant cette loi on a réflexion totale à l'endroit où $\alpha = \pi/2$, soit pour

$$\mu(R) = \frac{R_T}{R} \cdot \sin \alpha_T \,. \tag{2}$$

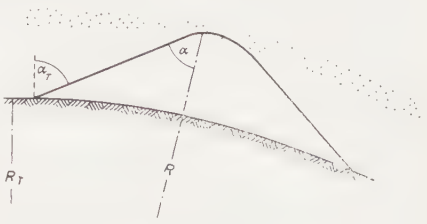

Fig. 1.

Pour une fréquence fixe la fonction $\mu(R)$ est essentiellement donnée par la répartition de la densité électronique. Sur une couche ionisée on a donc réflexion totale de tous les rayons suffisamment inclinés à partir d'une limite α_{T0}. Cette dernière peut être obtenue à partir de l'équation (2) appliquée au centre de la couche en question (μ_c).

Afin que la condition soit satisfaite au moins pour le rayon à *départ rasant* ($\alpha_{T0} = \pi/2$) il faut que

$$\mu_c \leqslant R_T/R \,. \tag{2a}$$

Or en propagation ionosphérique R_T/R est sensiblement inférieur à 1, nous trouvons donc une ionisation minimum nécessaire pour la réflexion d'une fréquence donnée même à départ rasant. Ceci est très différent du cas de la propagation troposphérique ($R_T/R \cong 1$).

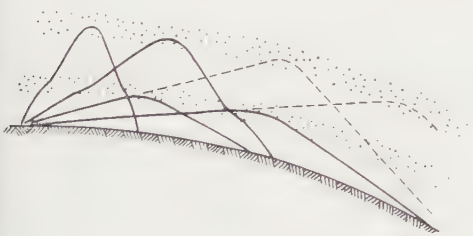

Fig. 2.

Dans le domaine des ondes décamétriques déjà l'ionisation de la région inférieure, E, suffit très souvent à la condition (2a). Les rayons suffisamment inclinés ($\alpha_T > \alpha_{T0}$) ne peuvent donc pas être réfléchis par la région supérieure, F (Fig. 2). Il s'en suit que ces rayons ne peuvent pas être comptés quand les parcours réfléchis par F sont discutés. Un parcours éventuel par réflexion sur une couche supérieure peut donc être coupé à cause d'une réflexion sur une couche inférieure.

Il s'agit d'un effet d'écran qui donne lieu à une troisième condition pour l'existence de ces parcours. Les deux autres conditions, à savoir celle de l'efficacité de la réflexion et celle du champ suffisant, ne font entrer en jeu que l'ionisation de la région F d'une part et l'absorption dans les couches basses (surtout en *D*) d'autre part. Mais notre troisième condition fait encore entrer en ligne de compte l'ionisation de la région E.

1. – Théorie de l'occultation.

Un effet de réfraction dans la couche inférieure existe en principe pour tous les rayons, même ceux qui ne sont pas réfléchis par cette couche. Pour un tel rayon l'effet de réfraction revient essentiellement à un décalage latéral du rayon au passage de la couche inférieure (plus exactement c'est une très faible rotation autour du centre de la terre). C'est le mérite de Bibl d'avoir vu que ce décalage peut devenir très important au cas limite.

1'1. *Cas d'une couche mince.* – Dans ce cas le décalage des rayons traversant la couche inférieure peut être négligé. C'est certainement vrai pour une couche mince du type « *E* sporadique » (E_s) et d'ont l'ionisation est nettement supérieure à celle de la couche épaisse E normale. L'ionisation peut être caractérisée par une fréquence critique, f_{E_s}.

Si nous ajoutons la formule de dispersion à la condition de réflexion (2) nous obtenons au centre de la couche:

$$\mu_c = F(f/f_{E_s}) \leqslant \frac{R_T}{R_c} \cdot \sin \alpha_{T0} \,. \tag{3}$$

Au lieu de considérer différents rayons à fréquence fixe on peut supposer α_T constant tout en faisant varier la fréquence f de l'onde. L'équation (3) nous donne dans ce cas une valeur critique de la fréquence, f_a. Pour des fréquences inférieures à f_a on a réflexion sur la couche E_s, donc occultation des parcours sur F. f_a est appelée la « fréquence d'occultation » correspondant à α_T.

Si nous nous contentons de la simple formule de dispersion de Sellmeier

$$\mu^2 \quad 1 \quad (f_0/f)^2$$

(f_0 fréquence de plasma) nous trouvons

$$f_a/f_{0\max} = \sec \alpha_T / \sqrt{1 + \operatorname{tg}^2 \alpha_T \cdot (R_c^2 - R_T^2)/R_c^2} \,. \tag{4}$$

Si α_T est bien inférieur à $\pi/2$ la valeur de la racine est très peu différente de 1.

Le champ magnétique terrestre (formule d'Appleton-Hartree) complique beaucoup les relations précédentes parce qu'il y faut tenir compte d'un effet dépendant de la direction du rayon: il y a aussi biréfringence. Ces effets sont d'autant plus faibles que le rapport f/f_H (f_H gyrofréquence) est grand; ils sont d'ailleurs négligeables pour le rayon ordinaire dans le cas spécial d'une propagation dans le plan Est-Ouest (coordonnées magnétiques).

En désignant par a (« facteur d'occultation »), le second membre de l'équa-

tion (4) et en négligeant l'influence du champ magnétique. THEISSEN a calculé les valeurs de a données par la Fig. 3. En abscisse il a mis la distance que le rayon avec la même α_T parcourerait en l'absence de toute région E, c'est-à-dire après réflexion sur la région F. Le résultat dépend bien entendu du « facteur de transmission » de cette dernière qui est indiqué comme paramètre des courbes. Pour la répartition de la densité électronique dans la région F un modèle parabolique a été utilisé [1]. Il intervient encore un deuxième paramètre, à savoir le rapport des fréquences critiques des deux régions, b.

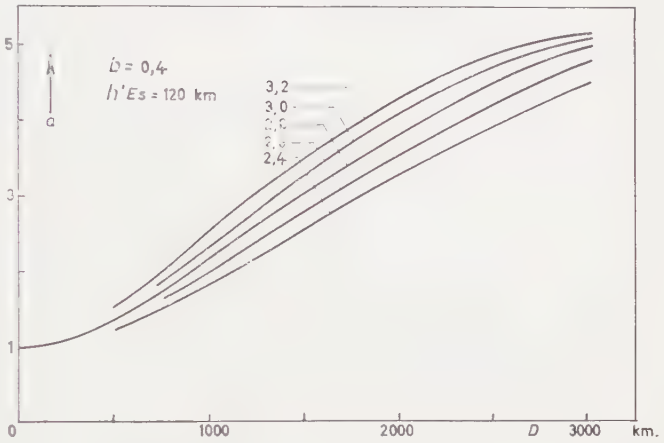

Fig. 3. – Facteur d'occultation a en fonction de la distance.

A l'aide des facteurs d'occultation, a, par multiplication avec la fréquence de plasma au centre de la couche E on obtient la fréquence d'occultation $f_a(D)$ pour la distance D. Or très souvent l'ionisation de la couche E_s n'est pas homogène dans le plan horizontal. Dans ces cas l'occultation efficace correspond à l'ionisation minimum; à celle-ci correspond en incidence verticale la « blanketing frequency », f_{bE_s} (voir Fig. 12).

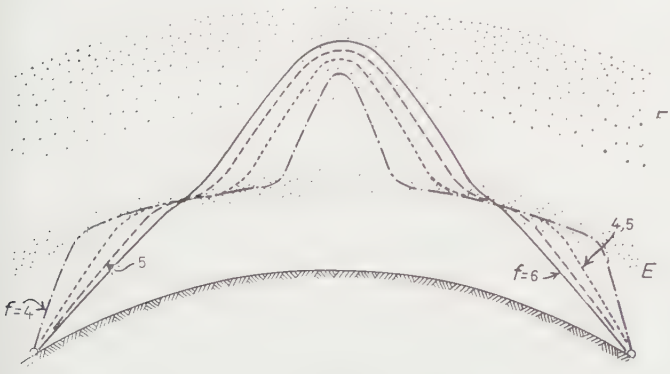

Fig. 4.

1'2. *Cas d'une couche épaisse.* – Supposons maintenant une couche inférieure épaisse et homogène comme c'est le cas de la couche E normale (fréquence critique f_E). Si l'on tient compte de la réfraction dans cette couche un raisonnement géométrique semble montrer que l'occultation proprement dite n'existe pas. Pour une distance donnée on trouve en effet toujours une liaison

géométrique. Plus faible est la fréquence, plus fort devient le décalage latéral dû à la traversée de la couche E, plus petit devient donc l'angle α_T (Fig. 4). Le cas limite correspondant à un départ vertical s'obtient pour $f = f_E$; au voisinage de ce cas limite pour la plus grande partie du parcours le rayon reste dans la région E.

Or ces parcours très déformés malgré leur « existence géométrique », sont effectivement occultés parce que la « perte de transmission » [2] correspondante est très importante. Il y a deux raisons à cette perte très grande au cas limite. Ce sont: la dilution géométrique du rayonnement et l'aborption sélective dans la couche E [1, 3].

Afin d'obtenir la *dilution du rayonnement* nous considérons un faisceau dont l'ouverture est standard au départ. La dilution est d'autant plus forte que le diamètre est plus grand à l'arrivée, c'est-à-dire à l'endroit de réception. Or l'« optique géométrique » de la propagation ionosphérique est très nettement astigmatique [4]. En direction horizontale le diamètre du faisceau correspond simplement à la distance entre deux grands cercles voisins. Par contre dans le plan de propagation la réfraction ionosphérique intervient très nettement. Nous avons appliqué une méthode de calcul dûe à Försterling et Lassen [5]; suivant ces auteurs, le diamètre du faisceau est proportionnel à la dérivée partielle

$$\left(\frac{\partial D}{\partial \alpha_T}\right)_{f=\text{const.}}.$$

Un modèle de l'ionosphère constitué de deux couches « paraboliques » a été introduit [1]. Le calcul numérique a été effectué pour différents choix des

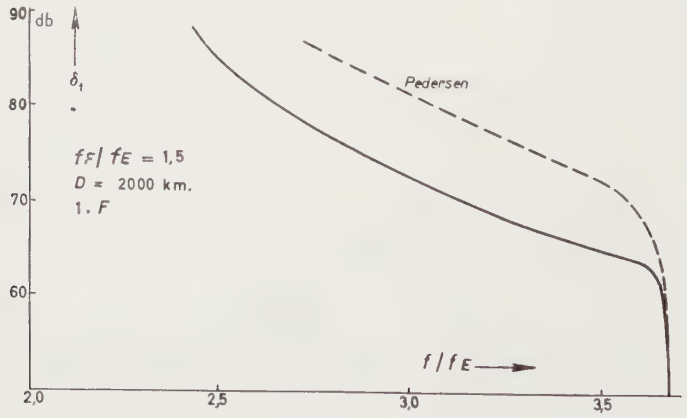

Fig. 5. – Décrément géométrique pour le cas de la Fig. 4.

paramètres [6], l'atténuation est donnée comme d'habitude par le décrément logarithmique du champ, δ_1 en décibels. La Fig. 5 en donne un exemple ($D = 2\,000$ km). Les deux courbes se distinguent par leur comportement dans

la région F; la courbe inférieure correspond au rayon normal, la branche supérieure au rayon dit de Pedersen. Une focalisation (où δ_1 tend vers moins l'infini) existe au point de convergence de ces deux branches, soit à la MUF (« maximal usable frequency ») de la région F. Cette focalisation est bien connue [5] mais elle ne concerne pas notre problème. D'autre part l'augmentation de l'atténuation du côté des basses fréquences est assez bien marquée; ceci est l'effet de dilution dans la région E que nous cherchons.

Les chocs électroniques dans la région E donnent lieu à une *absorption sélective* qui, elle-aussi, a pour effet une atténuation accentuée à la limite d'occultation. Le décrément de l'absorption en incidence oblique, $\delta_{3\wedge}$, peut être obtenu à partir du théorème de Martyn, qui doit être valable dans la région E [7] à condition que l'influence du champ magnétique puisse être négligée.

$$\delta_{3\wedge}\left(\frac{f}{f_E}\right) = \cos\alpha_E \cdot \delta_{3\perp}\left(\frac{f}{f_E \cdot \cos\alpha_E}\right). \tag{5}$$

α_E est l'angle d'arrivée à la couche E; $\delta_{3\perp}$ est le décrément d'absorption en incidence normale:

$$\delta_{3\perp}(\nu) \cong \int_{\mu=1}^{\nu} \frac{\mathrm{d}z}{\mu(z,\nu)} N(z)\cdot\nu(z)\,, \tag{6}$$

N densité électronique, ν nombre de chocs, z altitude.

Des valeurs numériques pour δ_3 se trouvent dans la Fig. 6 ($D = 2\,000$ km; épasseur totale de la région E, 50 km; nombre de chocs à l'altitude de son centre, 10^4 Hz).

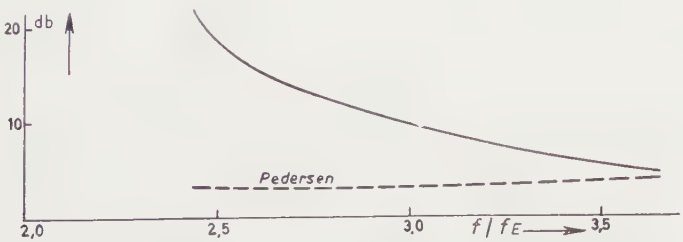

Fig. 6. – Décrément de l'absorption déviative.

On y voit l'augmentation rapide du côté des basses fréquences. Elle devient importante pour $f/(f_E \cos\alpha_E) \cong 1$, soit au voisinage de la « fréquence d'occultation », f_a, donnée par la simple théorie d'une couche inférieure mince.

Ajoutons encore le décrément δ_2 de l'absorption non-sélective qui a lieu

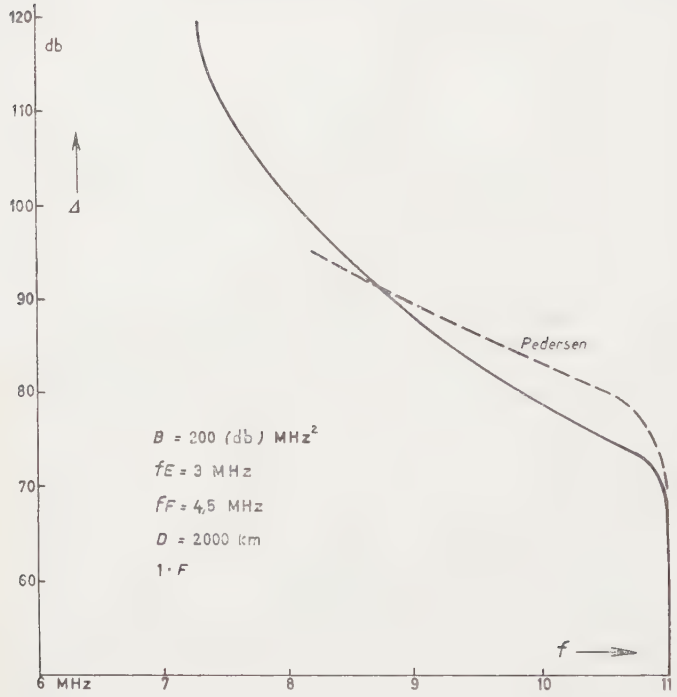

Fig. 7. – Perte de transmission dans le cas de la Fig. 4.

dans la région D (ainsi qu'à la base de la région E) [8]:

$$(7) \qquad \delta_2 = \frac{B \cdot \sec \alpha_D}{(f + f_L)^2} \ .$$

Rayon ordinaire; f_L = = composante longitudinale de la gyrofréquence.

Nous obtenons enfin la « perte totale de transmission » [2]

$$(8) \qquad L = \delta_1 + \delta_2 + \delta_3 \ .$$

La Fig. 7 montre un résultat typique (paramètres: $B = 200$ db, $f_E = 3$ MHz). On y voit qu'une « fréquence d'occultation » ayant le caractère d'une limite précise n'existe plus. Il n'y a qu'une augmentation progressive de la perte de transmission vers les fréquences basses. Notre problème est devenu un problème de calcul du champ. La limite effective est définie par l'égalité de la perte de transmission et du « pouvoir transmissif » [2] qui est un paramètre essentiellement technique. Ainsi la fréquence effective d'occultation, f_A dépend maintenant de la puissance de l'émission ainsi que de la sensibilité du récepteur. La limite donnée par l'absorption dans les couches basses ne peut plus être considérée séparément de l'occultation.

Nous définissons malgré tout un « facteur d'occultation », A, par

$$(9) \qquad f_A = A \cdot f_E \ .$$

A est fonction non seulement de la distance D et des données géométriques des régions mais de plusieurs autres paramètres tantôt physiques (fréquences critiques des régions, nombre de chocs des régions E et D) tantôt techniques (pouvoir transmissif). La variation de A en fonction de la valeur maximum admise pour L correspond à une variation non négligeable en fonction de la puissance de l'émetteur. Ceci est montré par la Fig. 8 (pour la plupart des liaisons les valeurs maxima de L se situent entre 80 et 110 db).

L'influence de la puissance devient encore plus prononcée pour les parcours multiples. Or dans ce cas la variation des paramètres le long du parcours peut jouer un rôle important.

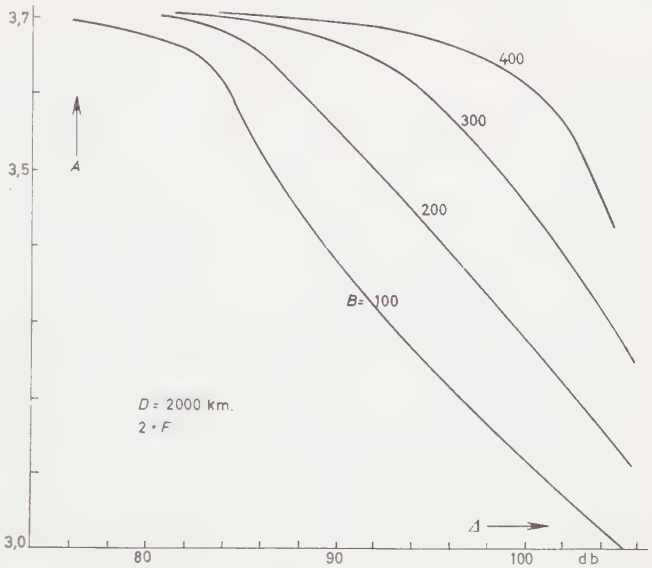

Fig. 8. – Facteur d'occultation A en fonction de la perte de transmission (paramètre des courbes: la constante de l'absorption non-déviative, B).

2. – Expériences.

2·1. *Incidence normale.* – L'occultation par la couche E normale (épaisse) est une caractéristique de chaque ionogramme de jour (*). L'absorption sélective au voisinage de la fréquence critique f_E (où l'on a transition de la trace E à une trace F) est bien visible (Fig. 9).

La présence de la couche E_s n'est pas si régulière. Même si elle existe cette couche est parfois transparente dans toute la gamme d'observation (Fig. 10). Mais, assez souvent, on peut noter une occultation très nette par E_s (Fig. 11). Tenant compte de l'existence des deux composantes magnéto-ioniques nous avons pu montrer que les cas d'une telle couche non-transparente ne sont pas rares [9]. D'autre part il y a aussi des cas où la réflexion est partielle dans une assez grande gamme; dans ces cas on distingue la fréquence d'occultation, f_{bE_s} (« blanketing frequency »), de la « top frequency », f_{E_s} (Fig. 12). Les conditions typiques sont illustrées par la Fig. 13; l'intensité de l'écho F augmente rapidement avec la fréquence tandis que celle de l'écho E_s ne diminue souvent que lentement.

Les fréquences caractéristiques f_{E_s} et f_{bE_s} sont définies par les intersections avec la courbe qui correspond au « pouvoir transmissif » (courbe en traits brisés). Par contre une « fréquence critique » de la couche E_s, f_{cE_s}, peut être definie indépendamment des données techniques par l'intersection des courbes donnant le coefficient de réflexion R et celui de traversée T [10].

(*) Un ionogramme donne la hauteur apparente des échos en fonction de la fréquence de sondage.

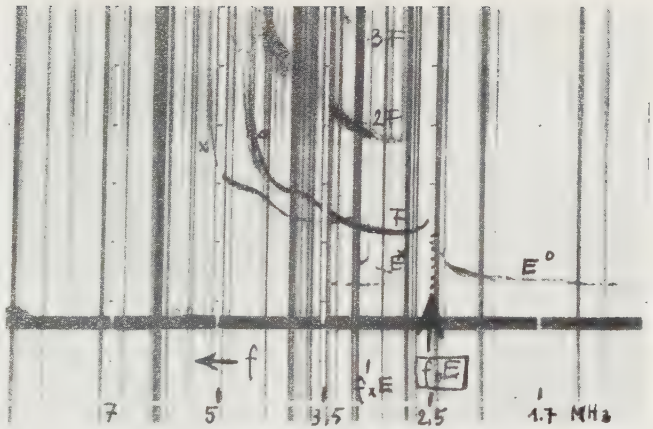

Fig. 9.

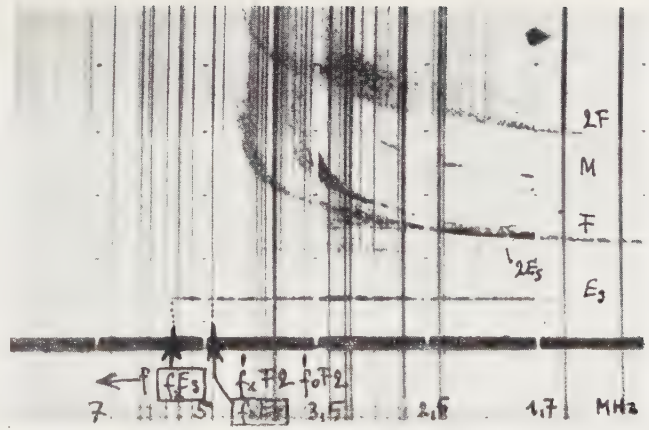

Fig. 10.

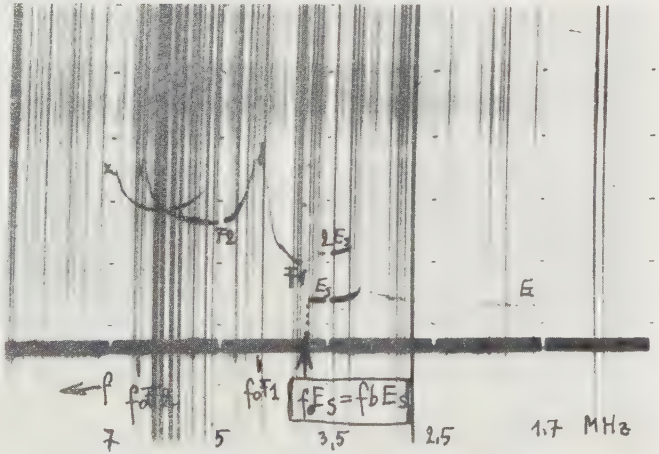

Fig. 11.

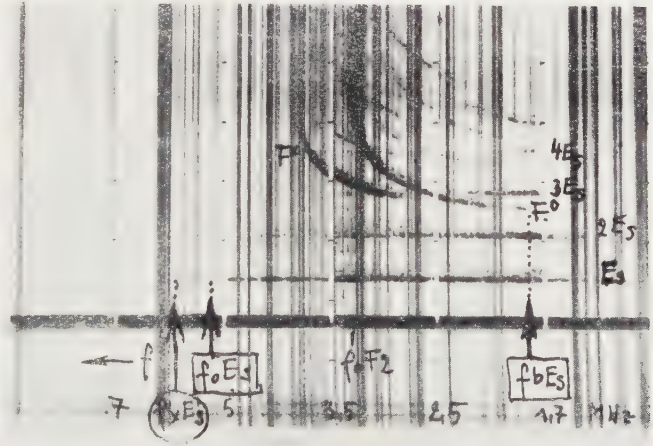

Fig. 12.

Figs. 9-12. – Ionogrammes typiques
(abscisse, la frequence f, sens inverse; ordonnée, hauteur virtuelle; l'identification des traces est indiquée).

Nous avons essayé de préciser l'information en ce qui concerne l'occultation en généralisant cette définition. Le rapport des coefficients, ou mieux la dif-

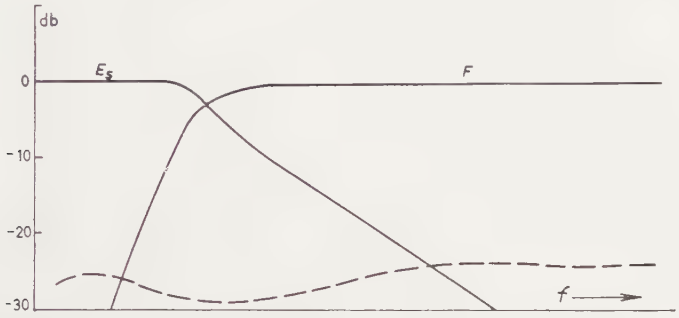

Fig. 13. – Variation typique de l'intensité des échos en provenance de la couche E_s et F (échelle logaritmique; courbe en traits brisés: pouvoir transmissif de l'ionosonde).

férence de leurs logarithmes, doit être généralement une fonction monotone de la fréquence. Cette fonction

$$G(f) = 20 \cdot (\log T - \log R) \tag{10}$$

caractérise les conditions d'une manière complète. Nous avons une longue série d'observations où l'on a essayé de déterminer cinq valeurs de cette fonction [11], à savoir $f_1 \ldots f_5$ avec

$$G(f) = -40\,, \quad -20\,, \quad 0\,, \quad +20\,, \quad +40 \text{ db}\,.$$

Ces observations nous ont montré que d'habitude f_{bE_s} est nettement mieux définie que f_{E_s}, parce que les valeurs f_m sont moins étendues au début de la série (Fig. 14). On en peut conclure que, malgré sa dé-

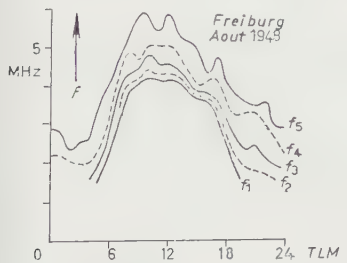

Fig. 14. – Répartition statistique des fréquences $f_1 \ldots f_5$ [voir équation (10)].

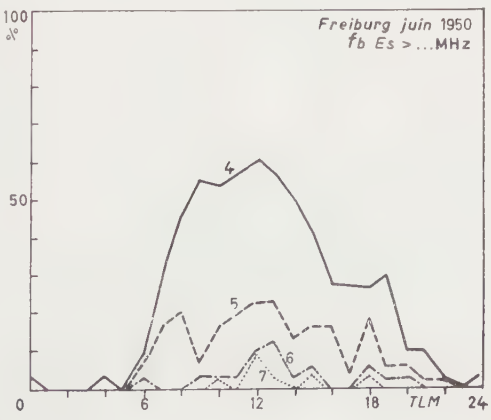

Fig. 15. – Répartition statistique des valeurs de la blanketing frequency », f_{bE_s} (probabilité de dépasser certaines valeurs).

finition insatisfaisante, f_{bE_s} n'est pas tellement dépendante des caractéristiques techniques que ne l'est f_{E_s}.

La statistique des valeurs observées de f_{bE_s} nous montre que les cas d'une forte occultation sont rares. Il y existe une variation journalière (Fig. 15) ainsi que saisonnière (Fig.16) [9].

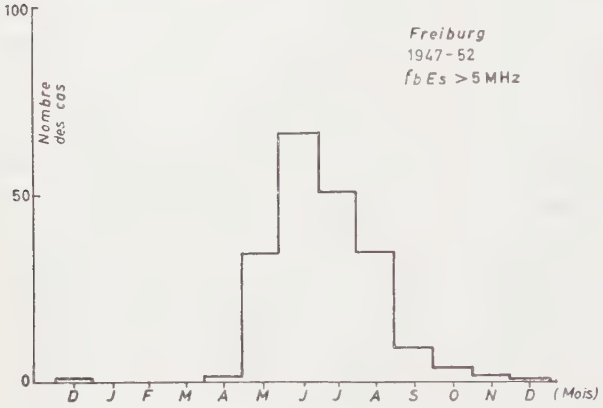

Fig. 16. – Variation saisonnière du nombre d'observations horaires où f_{bE_s} dépassait 5 MHz.

2·2. *Incidence oblique.* – En incidence oblique le nombre des observations est assez limité. Néanmoins nous pouvons donner assez d'exemples d'occultation. L'influence de la couche E normale ne peut se présenter que sur des fréquences relativement basses.

Regardons un enregistrement qui a été obtenu sur fréquence fixe de 1.95 MHz à une distance d'environ 1500 km (*).

La Fig. 17 a été obtenue au lever du soleil. Avant le lever on a les conditions de nuit. Il y a un premier écho en provenance d'une couche E ou plutôt E_s. Derrière cette première trace on voit les échos multiples réfléchis par la région F à partir de 3F. (En incidence oblique, à cause des angles de départ différents des parcours réflechis sur les couches E et

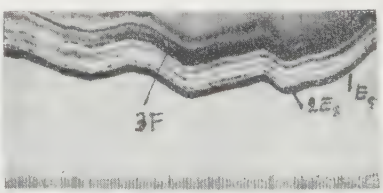

Fig. 17.

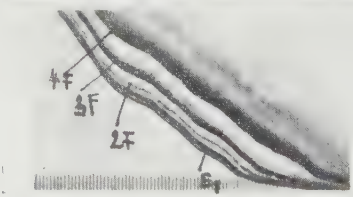

Fig. 18.

Enregistrement des échos d'un émetteur « Loran » á une distance de 1500 km, de nuit.

(*) Les traces sont inclinées parce que la synchronisation entre l'émission et l'enregistreur à la réception n'était qu'approximative. Les déformations visibles p.e. sur la Fig. 18, sont aussi dûes à la synchronisation.

F peuvent exister en même temps sans que la couche E soit transparente). Il y a aussi quelques traces correspondant à des parcours combinés (E+F, etc.). Avec le lever du soleil l'absorption dans les couches basses augmente rapidement; par conséquent les parcours multiples commencent à disparaitre. D'autre part, avec l'augmentation de l'ionisation de la couche E, l'occultation normale coupe d'abord le parcours 3F (à cause de son incidence inclinée). Pendant une courte période, parmi les échos en provenance de la région F le parcours 4F est prépondérant. Puis il disparait aussi et nous n'avons qu'un seul écho venant de la couche E. Ceci est apparamment un cas d'occultation par la couche E normale.

Par contre le premier enregistrement de la Fig. 18 montre un cas d'occultation par E_s; ce fut une observation en pleine nuit. On y a voit les écho E_s et $2E_s$ avec une amplitude importante. Derrière il y a d'abord des traces assez faibles, les parcours 1F et 2F sont pratiquement occultés, les parcours multiples à partir de 3F seulement se présentent avec l'amplitude normale. A titre de comparaison nous reproduisons en dessous de cet enregistrement un cas sans occultation (Fig. 18).

D'autres exemples d'occultation par E_s ont été obtenus sur une fréquence, plus élevée, d'environ 5 MHz à une distance de 1000 km. Sur la Fig. 19 on peut remarquer quatre traces: E_s, F, 2F et 3F. Les deux dernières sont toujours présentes tandis que 1F est coupé pendant la moitié du temps. Il est important de noter que le parcours E_s (première trace) ne remplace pas 1F

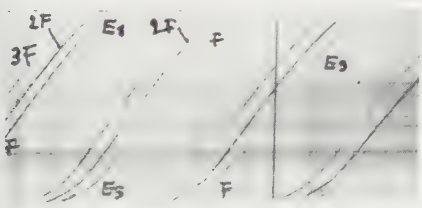

Fig. 19.

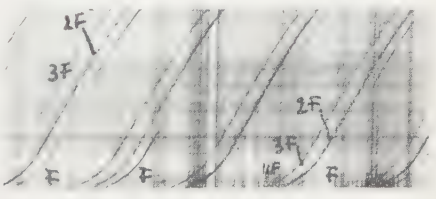

Fig. 20.

Enregistrement des échos d'un émetteur d'environ 5 MHz à une distance de 1 000 km (la trace est répétée deux fois pour être mieux lisible).

durant la période de son occultation. Assez longtemps ni 1F ni $1E_s$ ne sont présents. Ceci s'explique par le fait que la couche E_s a une structure nuageuse et que l'endroit de coupure du parcours 1F est bien différent du mielieu de la distance où le parcours $1E_s$ est réfléchi. Sur la Fig. 20 il n'y a aucune trace E_s mais une forte occultation du parcours 1F, tandis que 2F reste tous le temps.

Par comparaison statistique EYFRIG [12] a pu constater que l'occultation par E_s en incidence oblique se produit moins souvent que le laisseraient sup-

poser les observations en incidence normale. Il semble que ceci soit dû à l'inhomogénéité de la couche E_s qui permet encore le passage d'une onde dont la direction est légèrement différente de celle de la liaison purement géométrique.

3. – Applications pratiques.

Le phénomène de l'occultation joue un rôle important pour le calcul de la LUF (« lowest useful frequency ») [8]. La gamme des fréquences utilisables est limitée vers le haut par la MUF et vers le bas par la LUF. Considérons, séparément pour une distance moyenne, les différents parcours. Des parcours réfléchis par la région F, celui qui fait le minimum de bonds est le plus incliné au départ. En ce qui concerne l'absorption dans les couches basses elle est sans doute minimum pour ce parcours; mais d'autre part l'occultation par la couche E est maximum à cause du départ rasant. De cette façon si le « pouvoir transmissif » n'est pas extrêmement faible la LUF de ce parcours est déterminée par l'occultation. Examinons maintenant un parcours comportant un bond de plus. Il est moins incliné. L'absorption est plus forte, mais l'occultation est plus faible. Si la LUF est toujours déterminée par l'occultation elle est inférieure à celle du parcours précédent, donc plus avantageuse.

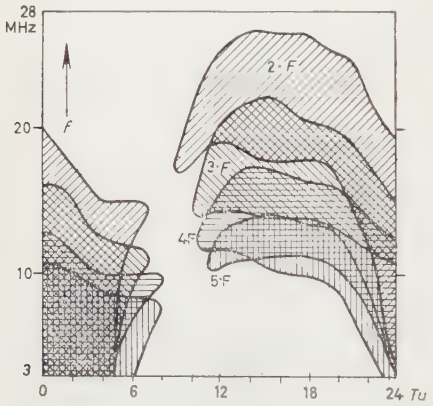

Fig. 21. – Gamme utilisable sur une distance transatlantique en fonction de l'heure (les différents parcours sont séparés).

Dans le cas d'un grand « pouvoir transmissif » (grande puissance) la possibilité d'un certain nombre de parcours est ainsi limitée par l'occultation. Dans un diagramme fréquence/heure (Fig. 21) on a plusieurs régions utilisables qui, de haut en bas, correspondent successivement à des parcours de plus en plus multiples. La LUF effective se trouve enfin déterminée par un parcours où l'occultation et l'absorption sont à peu près équivalentes. (Ceci dépend du pouvoir transmissif). Nous allons examiner quelques applications de ces résultats généraux.

3·1. *Angles de départ et d'arrivée.* – A l'aide de la Fig. 21 les angles peuvent déjà être déterminés grossièrement : α_1 doit augmenter avec la fréquence, l'angle de départ (qui est le complément de α_1) doit diminuer. Pour la fréquence

maximum utilisable on a un parcours presque rasant donc un angle assez faible. (Le minimum réalisable dépend des antennes et du terrain).

De jour on observe en effet une telle variation de l'angle d'arrivée. La Fig. 22 donne des résultats obtenus pour une liaison transatlantique. A cause de l'absorption il exsite presque toujours un parcours dont l'amplitude est prépondérante.

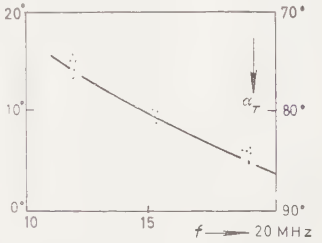

Fig. 22. – Angle d'arrivée en fonction de la fréquence (New York - Berlin, été 1944. de jour).

De nuit les conditions sont différentes. L'occultation par la couche E normale n'existe plus dans la gamme des ondes décamétriques. L'occultation par E_s ne se produit que de temps en temps. L'absorption est presque négligeable. Par conséquent en ce qui concerne les LUF's la limitation des « régions utilisables » que nous avons obtenue de jour n'existe plus. Plusieurs parcours d'amplitudes comparables sont reçus en même temps. Leur coëxistence rend difficile la mesure de l'angle d'arrivée. La seule limitation est dû à la MUF, c'est-à-dire au phénomène de la zône de silence. En effet à proximité de la MUF efficace on n'a qu'un seul parcours. On a pu constater que les angles correspondants sont toujours presque rasants [13].

3·2. *Délai de transmission.* – L'observation à grandes distances des signaux horaires [14] a montré que le délai de transmission varie en fonction de la fréquence; il est minimum pour les fréquences à proximité de la LUF. Ce fait ne peut pas être expliqué sans que l'on fasse intervenir l'occultation. Le parcours ayant le minimum de bonds est sans doute le plus intéressant en ce qui concerne la MUF. On dirait qu'il l'est aussi pour la LUF si cette dernière était déterminée par l'absorption seule. On ne s'attendrait donc pas à une variation systématique. Seulement par l'effet de l'occultation les parcours inclinés sont coupés sur les basses fréquences, d'où suit un délai maximum pour le maximum de l'occultation.

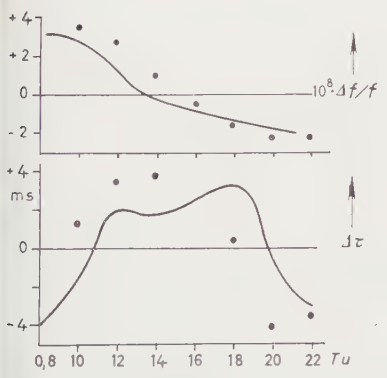

Fig. 23. – Variation moyenne de la fréquence reçue et du délai detrans mission sur la distance Washington-Paris, 20 MHz (courbes calculées à partir des données ionosphériques; points: résultats des observations) [15].

En effet l'explication des observations en termes d'un seul parcours [14] n'a pas donné satisfaction. A. Stoyko a constaté que la vitesse apparente des signaux est plus grande de nuit que de jour. En plus elle a trouvé une variation systématique au cours

de la journée [15]. Or sur fréquence fixe à cause de l'occultation on a une variation journalière du nombre effectif des bonds [16]; il est maximum vers midi. Tenant compte de ces faits A. Stoyko a pu expliquer satisfaisamment les observations qui ont donné un maximum du délai de transmission à midi (Fig. 23). Il existe aussi un effet saisonnier avec un maximum en été [15] (Fig. 24).

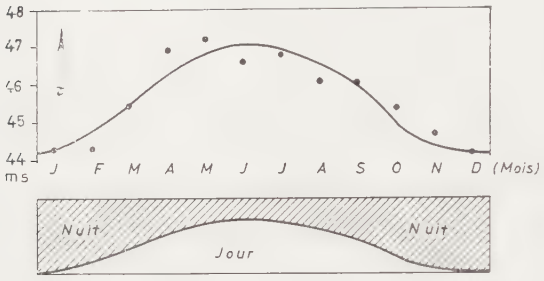

Fig. 24. – Délai de transmission (valeur totale) pour un parcours de 12 237 km (calcul, courbe et mesures: points suivant Stoyko [15]).

Une autre observation intéressante à été faite par Décaux [17]. Il a constaté que la fréquence reçue est légèrement variable en fonction des conditions de propagation. Il s'agit sans doute d'un effet Doppler introduit par la variation de la hauteur de réflexion. Or la variation de cet effet observée par Décaux et Crouzard n'est pas compatible avec l'hypothèse du même parcours effectif sur toutes les fréquences. Dans cette hypothèse on aboutirait à une augmentation de l'effet lorsque la fréquence augmente. Or le contraire est observé, l'effet est plus fort pour les basses fréquences (Fig. 25). Ceci aussi est dû à l'occultation qui a pour résultat que sur les basses fréquences on se sert de parcours dont le nombre de bonds est plus grand. Par conséquent l'effet Doppler se produit à plusieurs reprises sur les basses fréquences d'où son importance plus grande [16]. Le même résultat a été obtenu par Stoyko [15] (Fig. 23).

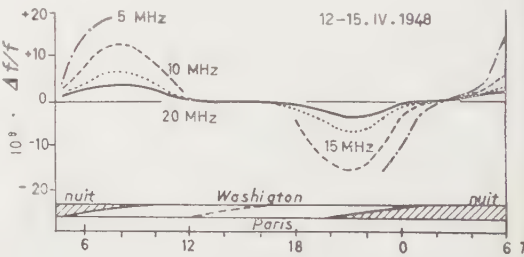

Fig. 25. – Variation de la fréquence reçue en fonction de l'heure pour la distance Paris-Washington (paramètre des courbes: la fréquence émise) suivant Décaux [17]).

3·3. *Propagation ionosphérique sur des distances supérieures à* 10 000 km. – Pour ces distances les méthodes habituelles de calcul se heurtent à des difficultés considérables. Or Harnischmacher [18] a mis au point une nouvelle méthode qui est le développement logique de notre méthode de prévision [9], Son raisonnement peut être résumé comme suit:

La propagation pour les distances inférieures se produit dans la plupart des cas dans des conditions ionosphériques qui ne son pas trop variables le long

du parcours. Pour la plus grande partie de la journée on a soit les conditions de jour soit celles de nuit sur l'ensemble du trajet. Or pour les distances très grandes ceci n'est plus vrai. On trouvera en général nuit et jour sur le trajet. Dans ces conditions les méthodes introduites par THEISSEN [19] pour les heures du crépuscule sont surtout indiquées pour les très grandes distances.

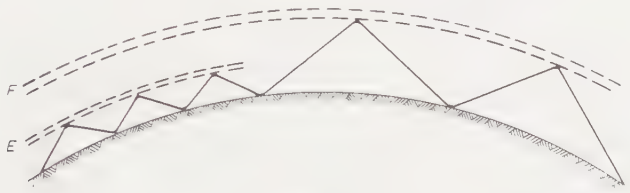

Fig. 26.

Il s'agit donc d'introduire les *parcours mixtes* du type $n \cdot \mathrm{E} + m \cdot \mathrm{F}$. Ces parcours sont prépondérants parce que du côté jour du trajet il existe une couche E bien développée; c'est là que les n bonds sur E se produisent. Par contre du côté nuit il n'y a que la couche F_2 ayant une fréquence critique relativement faible. Donc le parcours est continué par plusieurs (m) bonds réfléchis sur la région F (Fig. 26).

Ce raisonnement fait surtout allusion à l'occultation qui élimine les réflexions sur la région F du côté jour (pour les fréquences relativement basses qui sont nécessaires à cause de la plus faible ionisation en F_2 du côté nuit).

Sans entrer dans les détails de cette jolie méthode nous pouvons constater que ses résultats ont pu être vérifiés par des expériences et que ces expériences ont donné complètement satisfaction [18].

RÉFÉRENCES

[1] K. BIBL, K. RAWER et E. THEISSEN: *Rapport R 11 du Service de Prévision Ionosphérique Militaire* (1951).
[2] L. PHARABET: a paraître.
[3] K. BIBL, K. RAWER et E. THEISSEN: *Nature*, **169**, 247 (1952).
[4] K. RAWER: *Revue Scient.*, **85**, 361 (1947); **86**, 481, 585 (1948); *Nature*, **166**, 316 (1950).
[5] K. FÖRSTERLING et H. LASSEN: *Zeits. techn. Phys.*, **12**, 453, 502 (1931).
[6] La plupart des calculs numériques a été fait par M. WLASCHÜTZ.
[7] E. ARGENCE, K. RAWER et K. SUCHY: *Compt. Rend. Paris*, **241**, 505 (1955).
[8] K. RAWER: *Die Ionosphäre* (Groningen, 1953).
[9] K. RAWER: *Geofisica Pura e Applicata*, **32**, 172 (1955).
[10] K. BIBL, R. BUSCH, K. RAWER et K. SUCHY: *Journ. Atm. Terr. Phys.*, **6**, 69 (1955).

[11] K. Rawer: *Nature*, **163**, 528 (1949).
[12] R. Eyfrig: *Arch. elektr. Übertragung* (à paraître 1956).
[13] H. Neyer et K. Rawer: *Ann. de Géophys.*, **5**, 61 (1948); *Arch. elektr. Übertragung*, **5**, 215 (1951).
[14] N. Stoyko: *Compt. Rend. Paris*, **220**, 139 (1945); M. Boella: *URSI Stockholm Assembly*, 172 (1948).
[15] A. et N. Stoyko: *Compt. Rend. Paris*, **232**, 1817 (1951); A. Stoyko: *Ann. Franç. Chronométrie*, **21**, 193 (1951).
[16] K. Rawer: *Compt. Rend. Paris*, **227**, 1149 (1948).
[17] B. Décaux: *Compt. Rend. Paris*, **226**, 238 (1948); *URSI Stockholm Assembly*, 171 (1948); B. Décaux et M. Crouzard: *Compt. Rend. Paris*, **227**, 116 (1948).
[18] E. Harnischmacher: *Compt. Rend. Paris*, **237**, 1071 (1953).
[19] E. Theissen: *Rapport R 8 du Service de Prévision Ionosphérique Militaire* (1950).

OSSERVAZIONI ED INTERVENTI

— H. Bremmer:

Est-ce-que le point de disparition de la trajectoire élévé raccordant l'émetteur et le recepteur est défini clairement? Il s'agit ici du rayon de Pederson qui, théoriquement, peut atteindre tous les points de la surface de la terre sans aucune réflection intermédiaire.

— K. Rawer:

Le point d'évanouissement du rayon en question est simplement celui de la disparition numérique du champ associé.

— M. Boella:

Dans les expériences de mesure du temps de propagation des signaux horaires entre Turin et Washington sur la fréquence de 5 MHz, qu'on a fait en 1951, la comparaison des résultats des mesures du temps de propagation avec les données des stations ionosphériques qui sont sur le parcours, a montré qu'il y avait dans la majorité des cas une propagation avec un numéro de bonds assez grand (4 ou 5 sur la distance de 6 700 km environ). Ceci correspond à des angles d'arrivée des signaux entre 15° et 20°. Les mésures étaient faites pendant la nuit, à Turin et on a l'expérience seulement de deux nuits.

— K. Rawer:

De nuit on a souvent plusieurs parcours d'intensité pareille mais il se produit aussi le cas d'occultation de sorte qu'il y-ait un parcours prépondérant. Si l'on observe sur une seule fréquence et à la même heure on retrouvera assez souvent la même valeur. Nous avons eu en Allemagne des observations de Telefunken en 1938-39 qui avaient ainsi trouvé que l'angle d'arrivée entre l'Amérique et l'Europe était toujours 15° à 20°.

Or, durant la guerre on a répété ces expériences en étendant la gamme des fréquences observées ainsi que l'horaire des observations. Ainsi l'on a trouvé les résultats que j'avais indiqués.

— P. Dominici:

1) Sono assolutamente d'accordo sul maggiore significato del parametro f_{bE_s} rispetto al parametro tradizionale fE_s.

2) La statistica di f_{bE_s} è bene che sia la più corretta possibile per gli studi della geofisica. A tal fine ritengo che sia utile usare per il rilevamento dei dati sperimentali delle ionosonde a variazione continua di frequenza piuttosto che ionosonde a cambiamento di gamma, nelle quali si hanno forti variazioni della sensibilità dell'apparato in corrispondenza del cambiamento di gamma: è evidente allora che si ha un addensamento di valori f_{bE_s} nei punti del diagramma $[f_{bE_s}](f)$ corrispondenti alle frequenze di cambiamento di gamma.

SUPPLEMENTO AL VOLUME IV, SERIE X
DEL NUOVO CIMENTO

N. 4, 1956
2° Semestre

Sur l'absorption des ondes courtes dans un milieu ionisé isotrope.

E. ARGENCE

Service de Prévision Ionosphérique - Fribourg en Brisgau

1. – Considérations critiques sur la propagation dans un milieu isotrope absorbant.

1·1. – Les premiers travaux sur les milieux absorbants remontent aux études sur la réflexion métallique effectuées en 1836 par MCCULLAGH [1] et en 1838 par CAUCHY [2] qui ont introduit l'emploi de l'indice complexe: cette façon d'opérer a été critiquée récemment (1947) par ARZELIÈS qui utilise une méthode directe [3].

Les mesures de BEYNON [4] sur l'absorption à incidence oblique suivies d'une étude théorique d'APPLETON et BEYNON [5] sur le rôle joué par la réflexion partielle dans l'absorption d'une onde courte se propageant dans l'ionosphère, nous incitent à examiner de nouveau la portée du théorème de MARTYN (1935) et de façon plus étendue les conditions de propagation dans un milieu ionisé absorbant et isotrope.

D'après la définition habituelle, un milieu homogène est *isotrope* lorsque ses propriétés sont les mêmes dans toutes les directions. Cependant en ce qui concerne l'ionosphère, où il existe un gradient vertical d'ionisation, cette définition exige quelques précisions. Désignons par Σ l'intersurface (surface de séparation de deux milieux absorbants, dans tout ce qui suit nous supposerons le premier milieu diélectrique parfait, le second milieu absorbant). A l'approximation de l'optique géométrique, une onde plane décrit une trajectoire, enveloppe des normales aux plans d'onde. Deux trajectoires dont les angles d'incidence sur l'intersurface sont les mêmes seront identiques dans le cas d'un milieu stratifié — les plans de stratification étant parallèles à Σ supposée plane — et définies à une rotation ou à une translation près.

Nous pouvons donc adopter la définition suivante du milieu ionisé isotrope: « Un milieu ionisé est isotrope, lorsque la trajectoire de phase d'une onde électromagnétique, se propageant dans un tel milieu, se trouve définie à une translation ou à une rotation près et lorsque, en deux points homologues, obtenus par rotation ou translation, l'affaiblissement de l'onde est le même ».

Cependant comme nous le verrons plus loin une telle définition peut soulever quelques difficultés.

1·2. *Théorème de Martyn.* – Si nous adoptons l'hypothèse, vérifiée pratiquement pour les région E et F, que l'on a toujours

$$\omega^2 \gg \nu^2 ,$$

nous avons pour expression du décrément d'absorption à incidence normale

$$\delta = \log \varrho = \int k \, \mathrm{d}z , \tag{1}$$

avec

$$k = \frac{\nu}{2c} \frac{\omega_0^2/\omega^2}{\sqrt{1 - (\omega_0/\omega)^2}} , \qquad \text{(coefficient d'absorption)},$$

et pour l'incidence oblique,

$$\delta_M = \int k \frac{\mathrm{d}z}{\cos\varphi} = \int \frac{\nu}{2c} \frac{\omega_0^2 \omega^2}{\sqrt{\cos^2\varphi_0 - (\omega_0/\omega)^2}} \mathrm{d}z . \tag{2}$$

Le théorème de Martyn résulte de cette dernière expression. On a effectivement

$$\delta_M = \cos\varphi_0 \int_0^{z_1} \frac{\nu}{2c} \frac{\omega_0^2/\omega^2 \cos^2\varphi_0}{\sqrt{1 - (\omega_0/\omega\cos\varphi_0)^2}} \mathrm{d}z ,$$

z_1 point de « réflexion » est la plus petite racine de $1 - (\omega_0/\omega\cos\varphi_0)^2 = 0$, il en résulte:

$$\delta_M = \cos\varphi_0 \, \delta(\omega\cos\varphi_0) \qquad \text{(Théorème de Martyn [6])}.$$

Remarques. – La démonstration précédente est insuffisante.

1) Elle suppose que la loi de réfraction valable pour les milieux transparents est applicable aux milieux absorbants, c'est-à-dire que μ est indépendant de l'angle d'incidence φ_0 sur l'intersurface.

2) Le coefficient d'extinction est également indépendant de φ_0.

1·3. – Les ondes électromagnétiques les plus générales peuvent s'écrire sous la forme:

$$E_x = \mathcal{E}_x \exp[i(\omega t - \Phi) - \Phi']$$
$$\cdots\cdots\cdots\cdots$$
$$H_x = \mathcal{H}_x \exp[i(\omega t - \Phi) - \Phi']$$
$$\cdots\cdots\cdots\cdots$$

$$\Phi = \frac{2\pi}{\lambda}(\alpha x + \beta y + \gamma z), \qquad \Phi' = \frac{2\pi}{\lambda}(ux + vy + wz) .$$

sont respectivement le plans d'onde Φ et d'extinction α, β, γ les *cosinus directeurs* de la direction de propagation; u, v, w, les *paramètres directeurs* d'extinction, nous avons évidemment:

$$\alpha^2 + \beta^2 + \gamma^2 = 1 \; ; \qquad u^2 + v^2 + w^2 \neq 1 \; .$$

Le milieu étant isotrope nous pouvons choisir 2 axes arbitrairement.

Soit Oz la direction d'extinction, Oy l'intersection du plan d'onde et du plan d'extinction, la direction de propagation sera alors située dans le plan xOz et nous pourrons écrire:

$$E_x = \mathcal{E}_x \exp\left[i \left(\omega t - \frac{2\pi}{\lambda} (\alpha x + \gamma z) \right) - \frac{2\pi}{\lambda} w z \right]; \tag{3}$$

choisissons Oz normal à l'intersurface et posons

$$\alpha = \sin\varphi \; , \qquad \beta = \cos\varphi \; .$$

1·4. – Ecrivons les équations de Maxwell-Lorentz

$$\text{(I)} \quad \begin{cases} \nabla \wedge \boldsymbol{E} = -\dfrac{\varkappa}{c} \dfrac{\partial \boldsymbol{H}}{\partial t} \; . & \nabla \cdot \boldsymbol{E} = 0 \, , \\ \nabla \times \boldsymbol{H} = \dfrac{K_0}{c} \dfrac{\partial \boldsymbol{E}}{\partial t} + \dfrac{4\pi}{c^2} \varrho \boldsymbol{v} \; . & \nabla \cdot \boldsymbol{H} = 0 \, . \end{cases}$$

Nous en déduisons (*):

$$\nabla^2 \boldsymbol{E} - \frac{\varkappa K_0}{c^2} \frac{\partial^2 \boldsymbol{E}}{\partial t^2} - \frac{4\pi}{c^2} \varkappa \varrho \, \boldsymbol{\Gamma} = 0 \; . \qquad \left(\boldsymbol{\Gamma} = \frac{\mathrm{d}\boldsymbol{v}}{\mathrm{d}t} \right) . \tag{4}$$

Nous pouvons écrire pour l'élongation d'un oscillateur

$$x = \mathcal{U} \exp[i\omega t]$$
$$y = \mathcal{V} \exp[i\omega t]$$
$$z = \mathcal{W} \exp[i\omega t] \, .$$

D'où l'on déduit, au facteur $\exp[i\omega t]$ près,

$$\frac{\mathrm{d}x}{\mathrm{d}t} = i\omega \mathcal{U} \, , \qquad \frac{\mathrm{d}^2 x}{\mathrm{d}t^2} = -\omega^2 \mathcal{U} \, , \quad \text{etc.} \, .$$

(*) Dans tout ce qui suit, nous supposerons que $\varkappa = 1$, $k_0 = 1$. La vitesse des ondes électromagnétiques dans le vide est prise égale à l'unité.

D'autre part nous avons pour l'équation du mouvement d'un ion, si l'on néglige les forces de rappel et l'action du champ magnétique extérieur:

$$m\frac{\mathrm{d}^2x}{\mathrm{d}t^2} = eE_x - g\frac{\mathrm{d}x}{\mathrm{d}t}\,.$$

$$-m\omega^2\mathcal{U} = e\mathcal{E}_x - ig\omega\mathcal{U} \quad \text{etc.}$$

(g frottement dû aux collisions).

D'où

$$\mathcal{U} = \frac{e}{ig\omega - m\omega^2}\mathcal{E}_x \quad \text{etc.}\,. \tag{5}$$

Nous avons également

$$4\pi\varrho\Gamma_x = -4\pi Ne\omega^2\mathcal{U} \quad \text{etc.} \qquad (\varrho = Ne \text{ densité de charge}). \tag{5'}$$

Si nous portons ces valeurs dans l'équation (4), compte tenu de (3) nous obtenons

$$1 - \frac{\omega^2}{V^2}p\,,$$

$$2\gamma w = V^2 q\,.$$

D'où

$$V = \sqrt{1 - \frac{w^2}{p}}\,,$$

et l'on a posé:

$$\begin{cases} p = 1 - \dfrac{\omega_0^2}{\omega^2 + \nu^2}\,, \\ q = \dfrac{\nu}{\omega}\dfrac{\omega_0^2}{\omega^2 + \nu^2}\,. \end{cases} \qquad \left(\nu = \frac{g}{m}\right), \tag{6}$$

1·5. – φ_0 désignant l'angle d'incidence, φ l'angle de réfraction, par voie géométrique en établit facilement que

$$\frac{V_1}{V_2} = \mu = \frac{\sin\varphi_0}{\sin\varphi}\,. \tag{7}$$

$\mu = V_1/V_2$ définit l'indice de réfraction en milieu absorbant.

Nous supposons que le premier milieu est diélectrique parfait

$$\mu_1 = 1 , \qquad q_1 = 0 .$$

Désignons par λ_1 la longueur d'onde dans le milieu 1, par λ_2 la longueur d'onde dans le milieu 2; l'exponentielle d'extinction pourra s'écrire $\exp[-(2\pi/\lambda_2)wz]$, mais nous avons

$$V = \frac{\lambda}{T} = \sqrt{\frac{1 - w^2}{p}} , \qquad \lambda_2 = \sqrt{\frac{1 - w^2}{p}}\,\lambda_1 .$$

D'où

$$\frac{2\pi}{\lambda_2} w = \frac{2\pi}{\lambda_1} w \sqrt{\frac{p}{1 - w^2}} = \frac{2\pi}{\lambda_1}\chi , \qquad \left(\chi = w\sqrt{\frac{p}{1 - w^2}}\right). \tag{8}$$

χ est le *coefficient d'extinction.*

Par hypothèse nous avons $V_1 = 1$ dans le premier milieu pour le second milieu avons les relations

$$2\cos\varphi \cdot w = V_2^2 q , \tag{9}$$

$(\gamma_2 = \cos\varphi)$

$$1 - w^2 = V_2^2 p . \tag{10}$$

D'autre part:

$$\mu = \sqrt{\frac{p}{1 - w^2}} ,$$

de (9) et (10) nous obtenons

$$2\cos\varphi \frac{w}{1 - w^2} = \frac{q}{p} , \tag{11}$$

or

$$\mu\chi = p\frac{w}{1 - w^2} .$$

Nous en déduisons à partir de (11)

$$2\mu\chi = \frac{q}{\cos\varphi} , \tag{12}$$

de même

$$\mu^2 - \chi^2 = p . \tag{13}$$

Ainsi, dans le cas d'un milieu ionisé nous avons les relations:

$$(14)\qquad \begin{cases} \mu = \dfrac{\sin\varphi_0}{\sin\varphi}\,, \\ \mu^2 - \chi^2 = p\,, \\ 2\mu\chi = \dfrac{q}{\cos\varphi}\,, \end{cases} \qquad \text{avec} \quad \begin{cases} p = 1 - \dfrac{\omega_0^2}{\omega^2 + \nu^2}\,, \\ q = \dfrac{\nu}{\omega}\,\dfrac{\omega_0^2}{\omega^2 + \nu^2}\,. \end{cases}$$

1'6. *Méthode de l'ikonale.* – Considérons l'équation de propagation:

$$(15)\qquad \nabla^2\psi + \left(\frac{\omega}{c}\right)^2 \varepsilon\psi = 0\,, \qquad (\varepsilon, \text{ costante diélectrique}).$$

Cherchons les solutions de la forme

$$(16)\qquad \psi = Q\exp\left[-i\frac{\omega}{c}\,S\right].$$

Nous obtenons après substitution et séparation des parties réelle et imaginaire

$$(17)\qquad (\nabla S)^2 - \frac{\nabla^2 Q}{Q(\omega/c)^2}\qquad \varepsilon = 0\,,$$

$$(18)\qquad \nabla^2 S + 2\frac{(\nabla S\cdot\nabla Q)}{Q} = 0\,.$$

A l'approximation de l'optique géométrique

$$(19)\qquad \frac{\nabla^2 Q}{(\omega/c)^2 Q} \ll 1\,;$$

et l'équation (17) devient

$$(20)\qquad (\nabla S)^2 = \varepsilon \qquad \text{(Equation de l'ikonale).}$$

Cette relation peut être étendue *formellement* aux milieux absorbants. Si le vecteur $\boldsymbol{\mu}$ représente l'indice de réfraction multiplié par un vecteur unité dirigé suivant la direction des phases $\boldsymbol{\chi}$ l'indice d'extinction multiplié par un vecteur unité dirigé suivant la direction d'extinction, nous pouvons écrire

$$(21)\qquad \nabla S = \boldsymbol{\mu} - i\boldsymbol{\chi}\,,$$

$$(22)\qquad (\nabla S)^2 = \varepsilon = p - iq\,.$$

D'où

$$(\nabla S)^2 = (\boldsymbol{\mu})^2 - (\boldsymbol{\chi})^2 - 2i(\boldsymbol{\mu}\cdot\boldsymbol{\chi}) = p - iq\,. \tag{23}$$

C'est-à-dire

$$\begin{cases} \mu^2 - \chi^2 = p\,, \\ 2\mu\chi = \dfrac{q}{\cos q}\,. \end{cases} \tag{24}$$

Nous avons admis que les plans de stratification étaient parallèles à l'intersurface Σ. Nous allons montrer que la loi de Descartes, peut être étendue à un tel milieu supposé absorbant.

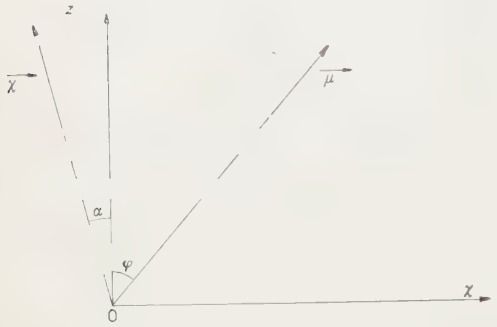

Fig. 1.

Nous avons la relation (donnée par Sommerfeld-Runge [7])

$$\nabla \times \nabla S = 0 \tag{25}$$

et les expressions suivantes (Fig. 1)

$$\begin{cases} |\boldsymbol{\mu}|\sin\varphi + i|\boldsymbol{\chi}|\sin\alpha = \mu_x + i\chi_x, \\ |\boldsymbol{\mu}|\cos\varphi + i|\boldsymbol{\chi}|\cos\alpha = \mu_z + i\chi_z. \end{cases} \tag{26}$$

Nous avons d'après (25)

$$(\nabla \times \nabla S)_y = \frac{\partial \mu_x}{\partial z} - \frac{\partial \mu_z}{\partial x} + i\left(\frac{\partial \chi_x}{\partial z} - \frac{\partial \chi_z}{\partial x}\right).$$

Or par hypothèse μ est uniquement fonction de z, il en est de même pour χ, donc

$$\frac{\partial \mu_z}{\partial x} \quad \frac{\partial \chi_z}{\partial x} \quad 0\,.$$

Par suite μ_x et χ_x ont une valeur constante. Sur l'intersurface nous devons avoir $\chi_x = 0$.

Il en résulte d'après (26) que $\alpha = 0$ et

$$\mu \sin\varphi = \mu_0 \sin\varphi_0 \qquad (\mu_0 = 1). \tag{27}$$

L'expression (25) peut être utilisée pour l'étude de milieux plus généraux (Suchy, [8]).

Les expressions (24)–(27) et (14), sont identiques.

Désignons par $d\boldsymbol{r}$ l'élément de longueur suivant la direction du rayon; la

relation

$$\mathrm{d}S = \nabla S \cdot \mathrm{d}\boldsymbol{r}$$

conduisant à l'expression

$$S = \int \boldsymbol{n} \cdot \mathrm{d}\boldsymbol{r} ,$$

valable pour les milieux transparents, peut être étendue en posant

$$\mathrm{d}S = \mathrm{d}S_1 + i\,\mathrm{d}S_2$$

$$\mathrm{d}S = \nabla S_1 \cdot \mathrm{d}\boldsymbol{r} + i\,\nabla S_2 \cdot \mathrm{d}\boldsymbol{r} .$$

D'où

$$S_2 = \int \nabla S_2 \cdot \mathrm{d}\boldsymbol{r} .$$

S_2 nous permet de définir le décrément d'affaiblissement

$$\delta = \int \nabla S_2 \, \mathrm{d}z ,$$

dont la valeur est égale, au coefficient ω/c près, à

$$\delta = \int \chi(z) \, \mathrm{d}z .$$

Remarque. – Nous avons deux surfaces des indices

$$(\Sigma_1), \qquad \mu^2(\varphi) = \frac{1}{2}\left[p + \sqrt{p^2 + \left(\frac{q}{\cos\varphi}\right)^2}\right] \qquad \text{(réfraction)} ,$$

$$(\Sigma_2), \qquad \chi^2(\varphi) = \frac{1}{2}\left[-p + \sqrt{p^2 + \left(\frac{q}{\cos\varphi}\right)^2}\right] \qquad \text{(extinction)} ,$$

de révolution autour de Oz. La méridienne est une quartique circulaire.

Suivant une remarque d'Arzeliès [9] un milieu isotrope absorbant se comporte comme un milieu anisotrope monoréfringent. De là résulte une certaine ambiguité au sujet de définition des propriétés caractéristiques concernant de tels milieux (Sect. 1°1).

1·7. – Les relations précédentes nous donnent

$$(28)\qquad \begin{cases} \mu^2 = \frac{1}{2}\left[p + \sin^2\varphi_0 + \sqrt{(p - \sin^2\varphi_0)^2 + q^2}\right] \\ \chi^2 = \frac{1}{2}\left[-(p \quad \sin^2\varphi_0) + \sqrt{(p - \sin^2\varphi_0)^2 + q^2}\right]. \end{cases}$$

Nous obtenons pour équation des trajectoires de phase

$$(29)\qquad \left(\frac{dx}{dz}\right)^2 = \frac{2\sin^2\varphi_0}{p - \sin^2\varphi_0 + \sqrt{(p - \sin^2\varphi_0)^2 + q^2}}.$$

Remarques. – Les relations (14) ont été établies par CAUCHY à partir de la notion d'indice complexe

$$n^2 = (\mu \quad i\chi)^2$$

introduit *à priori*.

La direction d'extinction en résulte. (Une démonstration très claire a été donné par STRATTON [10]).

1·8. *Polarisation et trajectoires d'énergie.* – Les équations de Maxwell-Lorentz nous conduisent au système:

$$\begin{cases} (1') & -i\mathcal{H}_x V = (i\gamma + w)\mathcal{E}_y \\ (2') & -i\mathcal{H}_y V = -(i\gamma + w)\mathcal{E}_x + i\alpha\mathcal{E}_z \\ (3') & -i\mathcal{H}_z V = -i\alpha\mathcal{E}_y \\ (4') & (i\gamma + w)\mathcal{H}_y = iV(p - iq)\mathcal{E}_x \\ (5') & -(i\gamma + w)\mathcal{H}_x + i\alpha\mathcal{H}_z = iV(p - iq)\mathcal{E}_y \\ (6') & -i\alpha\mathcal{H}_y = iV(p - iq)\mathcal{E}_z \\ (7') & i\alpha\mathcal{E}_x + (i\gamma + w)\mathcal{E}_z = 0 \\ (8') & i\alpha\mathcal{H}_x + (i\gamma + w)\mathcal{H}_z = 0, \end{cases} \qquad (V = \omega\lambda/2\pi).$$

Onde de type 1. – Supposons $\mathcal{E}_x$ réel:

$$\mathcal{E}_x = E_{0,x}.$$

Posons pour simplifier

$$E_{0,x} = E_0.$$

Nous avons d'après (7)

$$\mathcal{E} \qquad\qquad i\alpha \qquad\qquad E_0 .$$
$$\qquad\quad i\gamma \qquad w$$

et d'après (4′)

$$\mathcal{H}_y = \frac{iv(p - iq)}{i\gamma + w} E_0 .$$

Nous pouvons écrire d'autre part

$$E_x = E_0 \exp\left[-\frac{2\pi}{\lambda} wz\right] \cos\left(\omega t - \frac{2\pi}{\lambda}(\alpha x + \gamma z)\right),$$

$$E_z = E_{0,z} \exp[-i\psi] = -\frac{\alpha}{\gamma^2 + w^2}(\gamma + iw) E_0 .$$

D'où

$$\begin{cases} E_{0,z} \cos\psi = \dfrac{\alpha\gamma}{\gamma^2 + w^2} E_0 , \\ E_{0,z} \sin\psi = \dfrac{\alpha w}{\gamma^2 + w^2} E_0 . \end{cases}$$

Nous en déduisons:

$$E_{0,z} = \frac{\alpha}{\sqrt{\gamma^2 + w^2}} E_0 , \qquad\qquad \operatorname{tg}\psi = -\frac{w}{\gamma} .$$

D'où

$$E_z = \frac{\alpha E_0}{\sqrt{\gamma^2 + w^2}} \exp\left[-\frac{2\pi}{\lambda} wz\right] \cos\left(\omega t - \frac{2\pi}{\lambda}(\alpha x + \gamma z) - \psi\right).$$

Nous obtenons de même pour les composantes magnétiques ($\mathcal{H}_x = \mathcal{H}_z = 0$, définissant l'onde la plus simple)

$$\begin{cases} \mathcal{H}_y = H_{0,y} \exp[-i\theta] = \dfrac{VE_0}{\gamma^2 + w^2}((qw + p\gamma) + i(pw - q\gamma)) , \\ H_{0,y} \cos\theta = \dfrac{VE_0}{\gamma^2 + w^2}(qw + p\gamma) , \\ H_{0,y} \sin\theta = \dfrac{VE_0}{\gamma^2 + w^2}(q\gamma - pw) , \\ \operatorname{tg}\theta = \dfrac{q\gamma - pw}{qw + p\gamma} . \end{cases}$$

D'où

$$H_y = VE_0 \sqrt{\frac{p^2+q^2}{\gamma^2+w^2}} \exp\left[-\frac{2\pi}{\lambda} wz\right] \cos\left(\omega t - \frac{2\pi}{\lambda}(\alpha x + \gamma z) - \theta\right).$$

En définitive nous avons pour l'onde de type 1:

$$(30)\quad \begin{cases} E_x = E_0 \exp\left[-\dfrac{2\pi}{\lambda_1}\chi z\right] \cos\omega(t - \mu(x\sin\varphi + z\cos\varphi)), \\ E_y = E_0\mu \dfrac{\sin\varphi}{\sqrt{\mu^2\cos^2\varphi + \chi^2}} \exp\left[-\dfrac{2\pi}{\lambda_1}\chi\right] \cos\omega\left(t - \mu(x\sin\varphi + z\cos\varphi)\right. \\ H_y = E_0 \sqrt{\dfrac{p^2+q^2}{\mu^2\cos^2\varphi + \chi^2}} \exp\left[-\dfrac{2\pi}{\lambda_1}\chi\right] \cos\omega\left(t - \mu(x\sin\varphi + z\cos\varphi)\right. \\ \operatorname{tg}\psi = -\chi/\mu\cos\varphi; \qquad \operatorname{tg}\theta = \dfrac{\mu q\cos\varphi - p\chi}{q\chi + \mu p\cos\varphi}. \end{cases}$$

Nous avons tenu compte de la relation $w = \chi/\mu$.

Nous voyons que la composante H est polarisée linéairement, les composantes E elliptiquement et nous avons pour équations des ellipses de polarisation

$$(31)\quad \left(\frac{\mu^2\cos^2\varphi + \chi^2}{\sin^2\varphi_0}\right) E_z^2 + E_x^2 - 2\frac{\sqrt{\mu^2\cos^2\varphi + \chi^2}}{\sin\varphi_0}\cos\varphi E_x E_z - \\ - E_0^2 \exp\left[-\frac{4\pi}{\lambda_1} z\right] \sin^2\varphi_0 = 0.$$

Nous pouvons ainsi déterminer la polarisation en chaque point de la trajectoire.

Onde de type 2. – Dans ce cas E est polarisé linéairement et H elliptiquement, un calcul analogue à celui précédemment développé conduit aux expressions suivantes des composantes des vecteurs électrique et magnétique

$$(32)\quad \begin{cases} E_y = M_0 \exp\left[-\dfrac{2\pi}{\lambda_1}\chi z\right] \cos\omega(t - \mu(x\sin\varphi + z\cos\varphi)), \\ H_x = M_0 \exp\left[-\dfrac{2\pi}{\lambda_1}\chi z\right] \sqrt{\mu^2\cos^2\varphi + \chi^2} \cdot \\ \qquad \cdot \cos\omega\left(t - \mu(x\sin\varphi + z\cos\varphi) - \dfrac{\psi}{\omega}\right), \\ H_z = M_0 \exp\left[-\dfrac{2\pi}{\lambda_1}\chi z\right] \sin\varphi_0 \cos\omega(t - \mu(x\sin\varphi + z\cos\varphi)). \end{cases}$$

Les trajectoires d'énergie peuvent être définies à partir du vecteur de Poynting:

$$\boldsymbol{P} = \frac{1}{8\pi}[\boldsymbol{E} \cdot \boldsymbol{H}].$$

Si l'on désigne par w la densité d'énergie localisée dans le milieu ionisé (VAN MIEGHEM, [11]), on obtient pour équation différentielle des trajectoires

$$\begin{cases} \dfrac{dx}{dt} = \dfrac{\overline{\mathcal{P}}_x}{w}, \\ \dfrac{dy}{dt} = \dfrac{\overline{\mathcal{P}}_y}{w}, \\ \dfrac{dz}{dt} = \dfrac{\overline{\mathcal{P}}_z}{w}. \end{cases}$$

$\overline{\mathcal{P}}_x$, $\overline{\mathcal{P}}_y$, $\overline{\mathcal{P}}_z$ désignant les composantes du vecteur moyen de Poynting.

Pour l'onde de type 1 nous obtenons:

$$\begin{cases} \overline{\mathcal{P}}_x = -\overline{E_z H_y} \\ \overline{\mathcal{P}}_y = 0 \\ \overline{\mathcal{P}}_z = \overline{E_x H_y}. \end{cases}$$

Posons

$$\mu(x \sin\varphi + z\cos\varphi) = \frac{\Phi}{\omega}.$$

Nous avons à évaluer les intégrales:

$$I_1 = \frac{\omega}{2\pi}\int_0^{2\pi/\omega} \cos\omega\left(t - \frac{\psi + \Phi}{\omega}\right)\cos\omega\left(t - \frac{\Phi + \theta}{\omega}\right)dt,$$

et

$$I_2 = \frac{\omega}{2\pi}\int_0^{2\pi/\omega} \cos\omega\left(t - \frac{\Phi}{\omega}\right)\cos\omega\left(t - \frac{\Phi + \theta}{\omega}\right)dt.$$

Le résultat est immédiat:

$$I_1 = \tfrac{1}{2}\cos(\psi - \theta), \qquad I_2 = \tfrac{1}{2}\cos\theta.$$

D'où

$$\frac{dx}{dz} = \frac{\sin\varphi_0}{\sqrt{\mu^2\cos^2\varphi + \chi^2}}\left(\frac{\mu\cos\varphi}{\sqrt{\mu^2\cos^2\varphi + \chi^2}} + \frac{\chi}{\sqrt{\mu^2\cos^2\varphi + \chi^2}}\,\frac{\mu q\cos\varphi \quad p\chi}{q\chi + \mu p\cos\varphi}\right). \tag{33}$$

On obtient de même pour l'onde de type 2:

$$\overline{\mathcal{P}_x} = \overline{E_y H_z} = \tfrac{1}{2} E_0^2 \exp\left[-\frac{4\pi}{\lambda_1}\chi z\right] \mu \sin\varphi ,$$

$$\overline{\mathcal{P}_z} = -E_y H_x = \tfrac{1}{2} E_0^2 \exp\left[-\frac{4\pi}{\lambda_1}\chi z\right] \sqrt{\mu^2 \cos^2\varphi + \chi^2}\cos\psi .$$

D'où

$$\frac{\mathrm{d}x}{\mathrm{d}z} = \operatorname{tg}\varphi . \tag{34}$$

Dans ce cas la trajectoire d'énergie et la trajectoire de phase coïncident.

En résumé, l'jonosphère se comportant comme un milieu absorbant isotrope peut transmettre soit le type d'onde 1, soit le type d'onde 2 et l'on obtient pour chaque type d'onde, une trajectoire d'énergie. Ce résultat est valable pour des milieux absorbants plus généraux.

1·9. – *Le décrément d'affaiblissement* de l'onde a pour expression

$$\delta = 2\frac{\omega}{c}\int_0^{z_M} \chi \,\mathrm{d}z , \tag{35}$$

c'est-à-dire:

$$\delta = \sqrt{2}\,\frac{\omega}{c}\int_0^{z_M} \sqrt{-(p(z) - \sin^2\varphi_0) + \sqrt{(p(z) - \sin^2\varphi_0)^2 + q^2}}\,\mathrm{d}z . \tag{36}$$

z_M étant la plus petite racine de $p - \sin^2\varphi_0 = 0$.

Nous remarquons que pour

$$(p(z) - \sin^2\varphi_0)^2 \gg q^2(z) .$$

Nous avons:

$$\delta \simeq \delta_M .$$

δ_M désignant le décrément de Martyn.

Dans le cas des milieux fortement absorbants

$$\delta > \delta_M .$$

Remarques:

a) Certains auteurs calculent l'absorption *suivant la direction des phases.* Dans ce cas:

$$\delta = 2\frac{\omega}{c}\int_0^{z_M} \chi \, ds \,, \tag{37}$$

et nous avons pour les milieux faiblement absorbants:

$$\delta = \int_0^{z_1 - \Delta z_1} \frac{\nu}{c} \frac{(\omega_0^2/\omega^2)\sqrt{1-(\omega_0/\omega)^2}}{\cos^2\varphi_0 - (\omega_0/\omega)^2}\, dz + \int_{z_1-\Delta z_1}^{z_1} \Delta \, dz \,, \tag{38}$$

(z_1 étant la plus petite racine de $\cos^2\varphi_0 - (\omega_0/\omega)^2 = 0$) et

$$1 = \frac{\omega}{c}\frac{q}{\mu\cos^2 q} \,.$$

Les limites $(0,\ z_1 - \Delta z_1)$ sont relatives à la région pour laquelle

$$(p - \sin^2\varphi_0)^2 \gg q^2 \,.$$

Nous voyons que dans ce cas

$$\delta \simeq \delta_M \,.$$

b) A incidence normale nous avons:

$$\delta \simeq \int_0^{z_1-\Delta z_1} \frac{\nu}{c}\sqrt{\frac{(\omega_0/\omega)^2}{1-(\omega_0/\omega)^2}}\, dz + \int_{z_1-\Delta z_1}^{z_1} \Delta \, dz; \qquad \left(\Delta = 2\frac{\omega}{c}\sqrt{\frac{p}{2}\left[1+\sqrt{\left(\frac{p}{2}\right)^2+\left(\frac{q}{2}\right)^2}\right]}\right). \tag{39}$$

Dans le cas de régions très faiblement absorbantes ($\omega^2 \gg \nu^2$) la seconde intégrale est négligéable ($\Delta z_1 \simeq 0$).

1·10. – *a*) Etudiant la propagation d'une onde plane dans un milieu absorbant EPSTEIN [12] a été conduit dans le cas où l'on suppose le milieu ionisé isotrope et stratifié à la relation suivante:

$$(\nabla S)^2 = \left(\frac{\partial S}{\partial x}\right)^2 + \left(\frac{\partial S}{\partial z}\right)^2 = n^2 = p - iq \,, \tag{40}$$

et à poser

$$\frac{dx}{dz} = \frac{\sin\varphi_0}{\sqrt{n^2 - \sin^2\varphi_0}} = \frac{dx_1}{dz} + i\frac{dx_2}{dz}. \tag{41}$$

Par suite:

$$\begin{cases} \dfrac{dx_1}{dz} = \mathrm{Re}\,\dfrac{\sin\varphi_0}{\sqrt{n^2 - \sin^2\varphi_0}}, \\ \dfrac{dx_2}{dz} = \mathrm{Im}\,\dfrac{\sin\varphi_0}{\sqrt{n^2 - \sin^2\varphi_0}}. \end{cases} \tag{41'}$$

Ce qui nous donne:

$$\begin{cases} \dfrac{dx_1}{dz} = \pm\sin\varphi_0 \sqrt{\dfrac{(p - \sin^2\varphi_0) - \sqrt{(p - \sin^2\varphi_0)^2 + q^2}}{2((p - \sin^2\varphi_0)^2 + q^2)}}, \\ \dfrac{dx_2}{dz} = \dfrac{q\sin\varphi_0}{\pm\sqrt{2((p - \sin^2\varphi_0)^2 + q^2)(p - \sin^2\varphi_0 + \sqrt{(p - \sin^2\varphi_0) + q^2})}}. \end{cases} \tag{42}$$

dx_1/dz peut être considéré comme définissant la trajectoire de phase; dx_2/dz la trajectoire d'extinction; en ce qui concerne la méthode utilisée plus haut, il est aisé de voir que les trajectoires d'extinction se réduisent à des droites normales à l'intersurface.

b) A notre point de vue la méthode d'Epstein est arbitraire. En effet, la relation

$$(\nabla S)^2 = p - iq$$

implique

$$\nabla S = \boldsymbol{P} - i\boldsymbol{A} \tag{43}$$

(il n'est pas nécessaire pour l'instant de préciser la signification des vecteurs $\boldsymbol{P}$ et $\boldsymbol{A}$), nous avons d'autre part

$$\nabla \times \nabla S = 0 \tag{44}$$

qui ainsi que nous l'avons vu plus haut conduit à la relation

$$P\sin\varphi = P_0\sin\varphi_0 \qquad (P_0 = 1). \tag{45}$$

Donc P joue le rôle d'un indice de réfraction, de même A celui d'on indice d'extinction.

(43) entraîne les relations (Sect. 6)

$$46) \qquad \begin{cases} P^2 - A^2 = p\,, \\ 2PA = \dfrac{q}{\cos q}\,. \end{cases}$$

La trajectoire de phase est ainsi définie, de ce fait résulte le caractère arbitraire des équations (41) et (41').

1·11. *Conclusion.* – Nous avons examiné dans ce travail, un certain nombre de propriétés des milieux ionisés isotropes absorbants et stratifiés. La notion d'Ikonale permet de caractériser simplement ces milieux et d'aborder l'étude des trajectoires d'une onde électromagnétique. A de tels milieux se trouve attaché un décrément d'affaiblissement fonction de l'angle d'incidence. Le théorème d'équivalence de Martyn reste valable dans certaines conditions réalisées pour les régions E et F de l'ionosphère.

Signalons que l'étude de l'équation de propagation permet de formuler d'autres théorèmes d'équivalence (Argence, Rawer, Suchy, [13]).

La région D peut être étudiée à l'aide de la méthode exposée ici, lorsque l'on suppose que la fréquence critique locale de la région est constante, ce qui permet d'étendre la théorie des lames optiques et de déterminer le flux d'énergie à la sortie de la région. Cette question sera abordée dans un autre travail.

2. – Influence de la constitution des couches sur l'absorption.

2·1. – Une étude générale de ce problème a été donnée antérieurement par Nicolet et Bossy [14] et par Argence, Mayot, Rawer [15]. Nous nous limitons ici à l'étude de l'absorption sélective à incidence normale, dans le cas où l'on suppose $\omega^2 \gg \nu^2$ (régions E et F).

2·2. *Décrément d'absorption.* – Nous avons à incidence normale:

$$\delta_2 \cong \frac{M}{c}\,\frac{1}{f^2}\int_{\xi_0}^{\xi_1} \frac{f_0^2(\xi)\nu(\xi)\,\mathrm{d}\xi}{\sqrt{1-(1/x^2)(N(\xi)/N_m)}}\,.$$

L'indice a été écrit sous la forme:

$$\mu^2 = 1 - \frac{1}{x^2}\left(\frac{f_0}{f_c}\right)^2 = 1 - \frac{1}{x^2}\,\frac{N(\xi)}{N_m}\,, \qquad \left(x = \frac{f}{f_c}\right),$$

ξ désignant l'altitude, f la frequence du signal et f_c la frequence critique.

2·3. *Absorption dans une région non-isotherme et dans une région isotherme.*

A) Cas d'une région non-isotherme.

Nous négligeons la séparation par diffusion des molécules, de telle sorte que l'atmosphère puisse être considérée comme homogène. Nous supposons d'autre part, ce qui est en accord avec les mesures les plus récentes, que pour la région E, T est fonction linéaire de l'altitude. Nous avons pour expression definissant la pression p

$$\frac{\mathrm{d}p}{\mathrm{d}z} = -g\varrho\,, \qquad (\varrho, \text{ densité}), \tag{1}$$

g, constante de gravité est supposée indépendante de l'altitude.

L'équation des gaz parfaits nous donne d'autre part:

$$p = nkT \tag{2}$$

(k, constante de Boltzmann, n concentration moléculaire), d'où nous tirons

$$\frac{\mathrm{d}p}{p} = \frac{\mathrm{d}n}{n} + \frac{\mathrm{d}T}{T} = -\frac{\mathrm{d}z}{H}; \quad \left(H = \frac{kT}{mg}, \text{ échelle des hauteurs}\right). \tag{3}$$

Le gradient de température étant une fonction de l'altitude:

$$\frac{\mathrm{d}T}{T} = \frac{\mathrm{d}H}{H}\,.$$

Or par hypothèse:

$$\frac{\mathrm{d}H}{\mathrm{d}z} = \beta\,.$$

Nous avons par suite les relations:

$$\frac{\mathrm{d}p}{p} = \frac{\mathrm{d}n}{n} + \frac{\mathrm{d}T}{T} = -\frac{1}{\beta}\frac{\mathrm{d}H}{H}\,, \tag{4}$$

$$\frac{\mathrm{d}n}{n} = -\frac{\mathrm{d}H}{H} - \frac{1}{\beta}\frac{\mathrm{d}H}{H} = -\left(\frac{1+\beta}{\beta}\right)\frac{\mathrm{d}H}{H}\,. \tag{5}$$

D'où

$$\frac{p}{p_0} = \left(\frac{H}{H_0}\right)^{-1/\beta}, \qquad \frac{n}{n_0} = \left(\frac{H}{H_0}\right)^{-(1+\beta)/\beta}. \tag{6}$$

Si nous désignons par Q_ν le flux quantique par unité de surface, σ_ν la section

efficace de photoionisation, nous avons, P_ν désignant la production ionique,

$$P_\nu = n\sigma_\nu Q_\nu ,$$
$$\mathrm{d}Q_\nu = -P_\nu \mathrm{d}s,$$

$\mathrm{d}s$ exprimant l'élément de longueur du rayon ionisant, avec $\mathrm{d}s = -\mathrm{d}z/\cos\chi$ (χ distance zénithale solaire).

D'où,

$$Q_\nu(z) = Q_\infty \exp\left[-\sigma_\nu \sec\chi \int_z^{z_1} n(z)\,\mathrm{d}z\right]. \tag{7}$$

Dans le cas d'une variation linéaire de température:

$$\begin{cases} T = T(1+bz) & H = H_0(1+bz) \\ n = n_0(1+bz)^{-(1/bH_0)-1} & \text{avec } bH_0 = \beta. \end{cases} \tag{8}$$

Dans le cas d'une recombinaison directe, nous avons pour l'état d'équilibre

$$\frac{\mathrm{d}N}{\mathrm{d}t} = P - \alpha N^2 \simeq 0 ,$$

(α, coefficient de recombinaison, N densité électronique). D'où

$$N = \left(\frac{\sigma Q_\infty}{\alpha(z)}\, n(z)\right)^{\frac{1}{2}} \exp\left[-\frac{\sigma_\nu}{2} \sec\chi \int_z^{z_1} n(z)\,\mathrm{d}z\right]. \tag{9}$$

Nous pouvons prendre comme limites d'intégration $(z;\infty)$ d'où:

$$\int_z^\infty n\,\mathrm{d}z = \frac{n_0}{\beta}\int_z^\infty \left(\frac{H}{H_0}\right)^{-(1+\beta)/\beta} \mathrm{d}H = nH ,$$

par conséquent:

$$N = \left(\frac{\sigma Q_\infty}{\alpha(z)}\, n(z)\right)^{\frac{1}{2}} \exp\left[-\frac{\sigma}{2} \sec\chi nH\right].$$

Supposons α constant ($\alpha = \alpha_0$), alors

$$N = \left(\frac{\sigma_\nu Q_\infty n_0}{\alpha_0}\right)^{\frac{1}{2}} (1+bz)^{-(1/2bH_0)-1} \exp\left[-\frac{\sigma_\nu}{2} \sec\chi n_0 H_0 (1+bz)^{-(1/bH_0)}\right]. \tag{10}$$

Variations de la fréquence de collisions. – Si nous désignons par D le diamètre moléculaire, m_e la masse de l'électron, la théorie cinétique nous conduit à l'expression:

$$\nu_{e,n} \simeq \left(\frac{\pi k D^4}{2m_e}\right)^{\frac{1}{2}} n T^{\frac{1}{2}} .$$

L'indice (e, m) précisant qu'il s'agit de chocs entre électrons et molécules neutres, ν_0 étant le nombre de chocs correspondant à la température T_0, ν le nombre de chocs pour la température T, nous obtenons la relation

$$\frac{\nu}{\nu_0} = \left(\frac{T}{T_0}\right)^{\frac{1}{2}} \frac{n}{n_0} . \tag{11}$$

a) Dans le cas d'une région isotherme:

$$\begin{cases} T = T_0, \qquad n = n_0 \exp\left[-\displaystyle\int_0^z \frac{dz}{H}\right], \\ n = n_0 \exp\left[-\dfrac{z}{H}\right], \\ \dfrac{\nu}{\nu_0} = \exp\left[-\dfrac{z}{H}\right] . \end{cases} \tag{12}$$

b) Dans le cas d'une région non-isotherme, compte tenu des hypothèses précédentes (8),

$$\frac{\nu}{\nu_0} = (1 + bz)^{-(1/bH_0)-1} . \tag{13}$$

Calcul du décrément d'affaiblissement. – Compte tenu de (6), nous avons pour expression du décrément

$$\delta_2 = \frac{\nu_0}{c} \frac{N_0}{N_m} \eta^2 \int \frac{(1 + bz)^{-\frac{3}{2}\gamma - 1} \exp[-k(1 + bz)^{-\gamma}]\, dz}{\sqrt{1 - \eta'^2 (1 + bz)^{-\frac{1}{2}\gamma - \frac{1}{2}} \exp[-K(1 + bz)^{-\gamma}]}} , \tag{14}$$

avec les notations suivantes:

N_m = densité électronique au maximum de la couche;

$$N_0 = \left(\frac{\sigma_v Q_\infty n_0}{\alpha}\right),$$

$$\eta = f_c/f; \qquad \eta' = \eta \frac{N_0}{N_m}; \qquad K = \frac{\sigma}{2} \sec \chi \, n_0 H_0; \qquad \frac{1}{bH_0} = \gamma .$$

Effectuons le changement de variable

$$x = K(1 + bz)^{-\gamma} .$$

Nous obtenons pour nouvelle expression de l'intégrale:

$$(15) \qquad -\frac{1}{b\gamma} K^{-\frac{3}{2}} \int \frac{x^{\frac{1}{2}} \exp[-x]\,dx}{\sqrt{1 - \eta'^2 K^{-\frac{1}{2}-\frac{1}{2}\gamma} x^{\frac{1}{2}+\frac{1}{2}\gamma} \exp[-x]}} .$$

Dans le cas où l'on admet pour le coefficient de recombinaison une loi de variation de la forme

$$\alpha = \alpha_0 \left(\frac{n}{n_0}\right)^m ,$$

nous sommes conduits à une intégrale de même forme générale,

$$(16) \qquad A = \int \frac{x^h \exp[-x]\,dx}{\sqrt{1 - g x^k \exp[-x]}} .$$

Calcul de l'intégrale A, valeurs numériques. – Dans le cas de la traversée ($\eta < 1$) les limites sont 0 et ∞; dans le cas de la réflexion x et ∞; x_1 désignant la plus grande racine de l'équation transcendante

$$1 - g x^k e^{-x} = 0 .$$

Développant l'expression précédente nous obtenons:

$$(17) \qquad A = \int x^h \exp[-x]\,dx + \\ + \sum_{n=1}^{\infty} \frac{1 \cdot 3 \ldots (2n-1)}{2 \cdot 4 \ldots 2n} g^n \frac{1}{(n+1)^{nk+h+1}} \int X^{nk+h} \exp[-X]\,dX ,$$

où l'on a posé:

$$X = (n+1)x .$$

Dans le cas de la traversée:

$$\int_0^{\infty} X^{nk+h} \exp[-X]\,dX = \Gamma(nk+h+1)\,. \tag{18}$$

Dans le cas de la réflexion:

$$\int_{(n+1)x_1}^{\infty} X^{nk+h} \exp[-X]\,dX = Q[(n+1)x_1, nk+h+1]\,, \tag{19}$$

$Q(x, p)$ désignant la fonction de Prym

$$Q(x, p) = \int_x^{\infty} \exp[-t]t^{p-1}\,dt\,. \tag{20}$$

Nous avons supposé jusqu'ici que la couche était intiniment étendue, en réalité nous devons admettre l'existence, imposée par les données expérimentalesr de deux limites finies a et b pour la variation de x, et α_n et β_n définies pa,

$$\alpha_n = (n+1)a$$

$$\beta_n = (n+1)b$$

pour la variation de X. Les intégrales pourront être exprimées dans ce cas à l'aide des fonctions de Whittaker ou comme différence de fonctions de Prym.

Dans tous les cas le radical

$$R = \frac{1}{\sqrt{1 - g \exp[-x]x^k}}\,,$$

peut être développé en série, puisque $|gx^k e^{-x}| \leqslant 1$ et l'on intègre terme à terme la série ainsi obtenue.

Notons que la variation de l'expression

$$G = 1 - ge^{-x}x^k$$

présente l'allure suivante en fonction du paramètre g (Fig. 2).

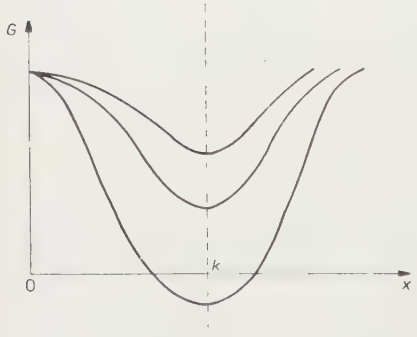

Fig. 2.

Le minimum a lieu pour

$$\frac{\partial G}{\partial x} = 0\,.$$

Soit

$$\quad \frac{2\gamma - 1}{2\gamma} .$$

quelque soit g.

Nous sommes conduits à calculer les intégrales:

$$J_\nu(\alpha, \beta) = \int_\alpha^\beta X^{p-1} \exp[-X] \, dX ,$$

et l'on peut poser:

$$\alpha = (n+1)a ; \qquad \beta = (n+1)b ; \qquad p = nk + h + 1$$

$$J_\nu(\alpha, \beta) = Q_\nu(\alpha) - Q_\nu(\beta)$$

$Q_p(x)$ désignant la fonction de Prym.

Les tables de Pearson permettent alors d'effectuer les calculs.

Cependant il est plus commode d'effectuer le calcul direct; on peut procéder ainsi:

a) Pour y faible devant p,

$$Q_p(y) = \Gamma(p) - \frac{1}{p} \exp[-y] y^p A(y) , \tag{21}$$

$A(y)$ désignant la série convergente

$$A(y) \quad 1 \quad \frac{y}{p-1} + \frac{y^2}{(p-1)(p-2)} + \ldots + \frac{y^p}{(p+1)\ldots(p+n)} ,$$

$\Gamma(p)$ désignant la fonction d'Euler

$$\Gamma(p) = \int_0^\infty \exp[-x] x^{p-1} \, dx .$$

b) Pour y grand devant p,

$$Q_p(y) = y^{p-1} \exp[-y] B(y) ,$$

où $B(y)$ désigne le développement asymptotique

$$B(y) = 1 + \frac{p-1}{y} + \frac{(p-1)(p-2)}{y^2} + \ldots + \frac{(p-1)\ldots(p-n)}{y^n} .$$

On peut utiliser également la relation de récurrence:

$$Q_{p+1}(y) = y^p \exp[-y] + pQ_{p-1}(y) .$$

— *Valeurs numériques.*

Nous considérons les trois cas suivants:

Cas considerés	b	γ	K
A	0.0222	6.45	9.51
B	»	»	18.5
C	»	»	64.0

On obtient ainsi dans le cas de la *traversée* les limites

$$A\begin{cases} z_2 & -26.1 & x_2 = 0.4987 \\ z_1 & -10 & x_1 = 48.0134 \end{cases}$$

$$B\begin{cases} z_2 & 16.8 & x_2 = 2.3949 \\ z_1 & -10 & x_1 = 93.401 \end{cases}$$

$$C\begin{cases} z_2 & 7.64 & x_2 = 23.298 \\ z_1 & -10 & x_1 = 323.118 \end{cases}$$

et les valeurs de $g = \eta'^2 K^{-k}$

A; $(K^{-k} = 0.3723)$		B; $(K^{-k} = 0.1854)$		C; $(K^{-k} = 0.9055)$	
η'	g	η'	g	η'	g
0.162	0.007 147	0.261	0.012 632	72.5	475.963
0.324	0.028 587	0.522	0.050 527	75.2	512.074
1.140	0.353 910	1.740	0.561 414	95.5	825.855
1.945	1.030 201	3.130	1.816 659	334	10 101.990
2.590	1.826 763	3.650	2.470 418	8 840	7 076 220
2.920	2.321 926	4.170	3.224 459	72.1	470.725
3.000	2.450 898	4.250	3.349 366	70.0	443.704
		4.330	3.476 646	61.8	345.839
		4.770	4.219 116		

Cas C (traversée).

Nous avons à utiliser la formule:

$$A = I_0 + I_1 + I_2 + \ldots + I_n$$

avec

$$p_n = nk + \tfrac{3}{2}; \quad k = 0.5775; \quad \alpha_n = (n+1)a; \quad \beta_n = (n+1)b \begin{cases} a = 23.298, \\ b = 323.118, \end{cases}$$

$$I_n = \frac{1\cdot 3 \ldots (2n-1)}{2\cdot 4 \ldots 2n}\, g^n \frac{1}{(n+1)^{nk+\frac{3}{2}}} \left(Q_{p_n}(\alpha_n) - Q_{p_n}(\beta_n)\right).$$

Pour calculer $Q_p(y)$ on peut utiliser le développement asymptotique

$$Q_p(y) = y^{p-1} \exp[-y] B_p(y)$$

et nous avons

$$Q_{p_n}(\alpha_n) \gg Q_{p_n}(\beta_n)$$

$$\frac{Q_{I_n}(\beta_n)}{Q_{p_n}(\alpha_n)} \cong \frac{(\beta_n)^{p_n-1} \exp[-\beta_n]}{(\alpha_n)^{p_n-1} \exp[-\alpha_n]} \cong$$

$$\simeq \binom{b}{a} \exp[-(n+1)(b-a)] \cong (14)^{nk+\frac{1}{2}} \exp[-(n+1)300],$$

valeur négligeable.

Il en résulte

$$(22) \qquad I_n = a^{\frac{1}{2}} \exp[-a] \frac{B_n}{n+1} \frac{1\cdot 3 \ldots (2n-1)}{2\cdot 4 \ldots 2n} \exp[-n(a - k \log a - \log g)],$$

et

$$\frac{I_{n-1}}{I_n} \cong \exp[-(a - k \log a - \log g)] = \exp[-\lambda].$$

C'est-à-dire, pour le cas considéré,

$$\exp[-\lambda] < 0.002.$$

Donc nous avons sensiblement

$$A \simeq I_0$$

avec

$$(23) \qquad I_0 = Q_{\frac{3}{2}}(a), \qquad p_0 = \frac{3}{2} \qquad a = 23.298,$$

résultat indépendant de g.

Ce qui nous conduit à la valeur de δ_2,

$$\delta_2 = \frac{\nu_0}{2c} \eta'^2 \left(\frac{1}{b\gamma} k^{-\frac{3}{2}}\right) 3.75 \cdot 10^{-10}.$$

Cas B (traversée).
$K = 18.5$ et nous obtenons

$$z_2 = 16.8\,, \qquad x_2 = 2.3949\,,$$
$$z_1 = 10\,, \qquad x_1 = 93.401\,.$$

Là encore on utilise l'expression asymptotique

$$(24)\qquad Q_p(y) = y^{p-1}\exp[-y]\left(1 + \frac{p-1}{y} + \frac{(p-1)(p-2)}{y^2} + \ldots\right),$$

et nous obtenons le tableau suivant:

$$I_0 = 0.1665$$

η'	0.261	0.522	1.740	3.130	3.650	4.170	4.250	4.330	4.770
A	0.1666	1.6881	0.1702	0.1793	0.1851	0.1928	0.1942	0.1957	0.2054

et ensuite

$$\delta_2 = \frac{\nu_0}{2c}\eta'^2\,\frac{1}{b\gamma}\,k^{-\frac{3}{2}}A\,,$$

avec

$$\frac{1}{b\gamma}\,k^{-\frac{3}{2}} \qquad 0.087767\,.$$

Cas A.
$K = 9.51$, et nous obtenons:

$$z_2 = 26.1 \qquad x_2 \qquad 0.4987$$
$$z_1 = 10 \qquad x_1 = 48.013\,.$$

Nous avons également:

$$(25)\qquad \begin{cases} Q_{p_n}(\alpha_n) \quad Q_{p_n}(\beta_n) \sim Q_{p_n}(\alpha_n)\,, \\ I_n = \dfrac{1\cdot 3 \ldots (2n-1)}{2\cdot 4 \ldots 2n}\;\dfrac{g^n}{(n+1)^{nk+\frac{3}{2}}}\,Q_{p_n}(\alpha_n)\,, \end{cases}$$

avec

$$p_n = nk + \tfrac{3}{2} \qquad \alpha_n = (n+1)a$$
$$k = 0.5775 \qquad a = 0.4987 \cong 0.5\,.$$

Dans ce cas on utilise l'expression:

$$(26) \qquad Q_p(y) = \int_x^\infty y^{p-1} \exp[-y]\,dy = \Gamma(p) - \frac{y^p \exp[-y]}{p} A(y)\,,$$

et l'on a

$$\frac{Q_{p_n}(\alpha_n)}{(n+1)^{p_n}} = \frac{\Gamma(p_n)}{(n+1)^{p_n}} - a^{\frac{3}{2}} \exp[-a] \frac{A_n}{nk + \frac{3}{2}} \exp[-n(a - k \log a)]\,.$$

Il est à noter que la convergence des séries est très lente:
Nous obtenons le tableau suivant:

$$I_0 = 0.7106$$

η'	0.162	0.324	1.140	1.945	2.590	2.920	3.000
A	0.7113	0.7133	0.7466	0.8407	1.055	1.38	1.58

Cas de la réflexion.
La variable x est liée à l'altitude z par la relation

$$x = k(1 + b_0 z)^{-\gamma} \qquad z_1 < \bar{z},\ x_1 < \bar{x}.$$

Considérons l'intégrale positive

$$1 - \int_a^b \frac{x^h \exp[-x]\,dx}{\sqrt{1 - g x^k \exp[-x]}}\,. \qquad (a = \bar{x},\ b = x_1,\ a < b),$$

Avec

$$h = \tfrac{1}{2}\,, \qquad k = 0.5775\,,$$
$$g = \eta'^2 K^{-k}\,, \qquad b = 0.0222\,.$$

La variation de l'expression $(f(x) = 1 - ge^{-x}x^k)$ présente l'allure indiqué par la figure 3, a est la plus grande racine de $f(x) = 0$ et quel que soit x on a:

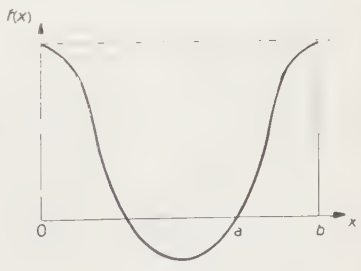

Fig. 3.

$$a > k = 0.05775\,.$$

Dans le cas A et B on obtient les valeurs suivantes:

A ($K = 9.51$)					B ($K = 18.5$)				
$\bar{z}$	η'	g	$a=\bar{x}$	$b=x_1$	$\bar{z}$	η'	g	$a=\bar{x}$	$b=x_1$
22.7	3.01	2.4673	0.6826	18.013	16.8	5.95	6.5648	2.3948	93.402
20	3.09	2.6002	0.8891	—	15	7.24	9.7200	2.8975	—
15	3.59	5.3097	1.4815	—	10	18.6	64.152	5.0765	—
10	5.40	7.9409	2.6096	—	5	132.3	3245.67	9.3825	—
8.5	6.55	11.6833	3.1186	—					
5	13.60	50.3687	4.8231	—					
0	116.1	3670.685	9.51	—					

1) b étant relativement grand, on remplace l'intégrale

$$A = \int_a^b \varphi(x)\,dx\,,$$

par

$$A = \int_a^\infty \varphi(x)\,dx;$$

la différence

$$\int_b^\infty \varphi(x)\,dx \simeq \int_b^\infty x^{\frac{1}{2}} \exp[-x]\,dx\,,$$

est négligeable devant

$$\int_a^\infty x^{\frac{1}{2}} \exp[-x]\,dx\,,$$

et *a fortiori* devant

$$\int_a^\infty \varphi(x)\,dx\,.$$

Nous considérons donc l'intégrale

$$A = \int_a^\infty \frac{x^{\frac{1}{2}} \exp[-x]\,dx}{\sqrt{1 - gx^k \exp[-x]}}\,. \tag{27}$$

2) L'expression $f(x)$ peut s'écrire:

$$f(x) = (x - a)h(x)$$

$$h(x) = \frac{1}{x - a} \quad g x^{k} \exp[- x] .$$

Sous cette forme on peut utiliser la méthode de Gauss généralisée:

$$(28) \qquad A = \int_{a}^{\infty} \frac{x^{\frac{1}{2}} \exp[-x]\,dx}{\sqrt{(x-a)h(x)}} .$$

Ce qui nous permettra d'obtenir une convergence plus rapide.

La substitution $x = a + (t^2/2)$ nous conduit au calcul de

$$A = \sqrt{2} \exp[-a] \int_{0}^{\infty} \frac{(a + t^2/2)^{\frac{1}{2}}}{\sqrt{H(t)}} \exp\left[-\frac{t^2}{2}\right] dt ,$$

$$A = \frac{\sqrt{2}}{2} \exp[-a] \int_{-\infty}^{+\infty} \frac{(a + t^2/2)^{\frac{1}{2}}}{\sqrt{H(t)}} \exp\left[-\frac{t^2}{2}\right] dt = \frac{\sqrt{2}}{2} \exp[-a] \int_{-\infty}^{+\infty} \exp\left[-\frac{t^2}{2}\right] F(t)\,dt .$$

En complétant la fonction $H(t)$ dans l'intervalle $(-\infty, 0)$ par

$$H(-t) = H(t)$$

la fonction

$$F(t) = \frac{(a + t^2/2)^{\frac{1}{2}}}{\sqrt{H(t)}} ,$$

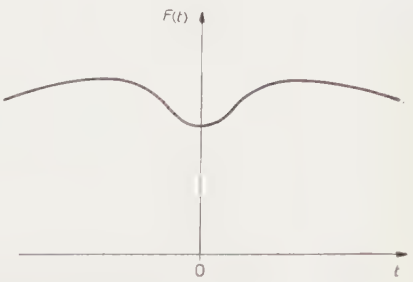

Fig. 4.

est ainsi une fonction paire.

On remplace $F(t)$ par un polynome de degré pair orthogonal par rapport à $\exp[-t^2/2]$ (HERMITE).

On obtient une approximation suffisante (10^{-3} à 10^{-4} en valeur relative) en prenant 6 valeurs de t (2 à 2 opposées),

$$(29) \qquad \int_{-\infty}^{+\infty} F(t) \exp\left[-\frac{t^2}{2}\right] dt = 2(M_1F_1 + M_2F_2 + M_3F_3) .$$

alors

t_1: 0.616 707 M_1: 1.024 781

t_2: 1.889 176 M_2: 0.222 127

t_3: 3.324 257 M_3: 0.006 406

et nous avons les resultats numériques suivants:

A ($K = 9.51$)				B ($K = 18.5$)			
$\bar{z}$	η'	$a=\bar{x}$	Δ	$\bar{z}$	η'	$a=\bar{x}$	Δ
22.7	3.01	0.6826	1.698	16.8	5.95	2.3949	0.3393
20	3.09	0.8892	1.339	15	7.24	2.8975	0.2194
15	3.59	1.4895	0.7520	10	18.6	5.0765	0.043260
10	5.40	2.6086	0.2986	5	132.3	9.3825	0.000539
8.5	6.55	3.1187	0.1913				
5	13.60	3.8231	0.04147				
0	116.1	9.510	0.000431				

B) Cas d'une région isotherme.

Dans le cas où la région traversée par l'onde est isotherme, nous pouvons utiliser pour la variation de la fréquence de collisions la relation (12) et nous pouvons supposer que la loi de variation de la densité électronique est du type quadratique, ce qui d'une part est une bonne approximation de la formule générale de Chapman et ce qui d'autre parte se trouve sensiblement vérifié dans le cas d'une région inosphérique normale.

Nous désignerons par ξ l'altitude calculée à partir du maximum d'ionisation et par ξ_m la demi-épaisseur de la couche, nous avons pour loi de variation de l'indice en fonction de l'altitude:

$$\mu^2 = 1 - \left(\frac{f_c}{f}\right)^2 \left(1 - \left(\frac{\xi}{\xi_m}\right)^2\right), \tag{30}$$

et pour loi de variation du nombre de chocs:

$$\nu = \nu_m \exp\left[-\frac{\xi}{H}\right].$$

D'où l'expression du décrément:

$$\delta_2 = \frac{\nu_m}{2c}\left(\frac{f_c}{f}\right)^2 \int_{\xi_0}^{\xi_1} \frac{\exp\left[-\xi/H\right]\left[1-(\xi/\xi_m)^2\right] d\xi}{\sqrt{1-(f_c/f)^2(1-(\xi/\xi_m)^2)}}. \tag{31}$$

Pour la commodité des calculs nous poserons:

$$\frac{f_c}{f} = \eta .$$

Calcul de l'intégrale $F(\eta)$.

Cas de la réflexion ($\eta = f_c/f > 1$).
Le décrément peut s'écrire:

$$\delta_2 = \frac{\nu_m}{2c}\,\eta^2 \xi_m \int_{\sqrt{\eta^2-1}/\eta}^{1} \frac{\exp\left[\xi_m u/H\right](1-u^2)\,\mathrm{d}u}{\sqrt{1-\eta^2(1-u^2)}} ; \qquad u = -\frac{\xi}{\xi_m} . \tag{32}$$

Si nous effectuons le changement de variable

$$v = \lambda u = -\lambda \frac{\xi}{\xi_m} ,$$

et en posant

$$\lambda = \frac{\eta}{\sqrt{\eta^2-1}} ,$$

le décrément δ_2 a pour expression

$$\delta_2 = \frac{\nu_m}{2c}\,\xi_m F(\eta) , \tag{33}$$

avec

$$F(\eta) = \eta \int_1^{\lambda} \frac{\exp\left[\alpha(v/\lambda)\right](1-v^2/\lambda^2)\,\mathrm{d}v}{\sqrt{v^2-1}} . \tag{34}$$

Pour l'intégration nous pouvons utiliser les fonctions de Legendre de deuxième expèce. En effet on peut écrire:

$$F(\eta) = \eta \exp\left[\alpha\right] \int_1^{\lambda} \frac{\exp\left[-\alpha(1-v/\lambda)\right](1-v^2/\lambda^2)\,\mathrm{d}v}{\sqrt{v^2-1}} .$$

C'est-à-dire en développant en série entière de α et en posant $g = 1/\lambda$,

$$G(\lambda) = \int_1^{1/g} \frac{\mathrm{d}v}{\sqrt{v^2-1}}\,(1-g^2v^2)\left[1 - \frac{\alpha}{1}(1-gv) + \ldots + (-1)^n \frac{\alpha^n}{n!}(1-gv)^n + \ldots\right],$$

$$G(\lambda) = G_0 - \alpha G_1 + \frac{\alpha^2}{2!} G_2 - \frac{\alpha^3}{3!} G_3 + \ldots ,$$

avec

$$G_n = \int_1^{1/g} \frac{(1-gv)^n(1+g^2v^2)}{\sqrt{v^2-1}}\,\mathrm{d}v\,.$$

Les fonctions $G_n(\lambda)$ peuvent être calculées une fois pour toutes; on en déduira $G(\lambda)$ pour une valeur quelconque de α. On peut écrire:

$$1-g^2v^2 = (1-gv)(2-(1-gv))$$

et si l'on pose

$$H_n = \int_1^{1/g} \frac{(1-gv)^n}{\sqrt{v^2-1}}\,\mathrm{d}v\,,$$

nous avons la relation de récurrence

$$G_n = 2H_{n+1} - H_{n+2}\,.$$

La fonction H_n s'exprime à l'aide de la fonction de Legendre de seconde espèce.

En effet,

$$H_n = \frac{1}{\eta^n}\int_1^{\eta/\sqrt{\eta^2-1}} \frac{(\eta-\sqrt{\eta^2-1}\,v)^n}{\sqrt{v^2-1}}\,\mathrm{d}v\,,$$

ou en posant

$$H_n(\eta) = \frac{1}{\eta^n}\int_0^{\log\sqrt{(\eta+1)/(\eta-1)}} (\eta-\sqrt{\eta^2-1}\cosh\theta)^n\,\mathrm{d}\theta = \frac{Q_n(\eta)}{\eta}\,. \tag{35}$$

L'intégrale est une forme intégrale classique de la fonction de Legendre de deuxième espèce.

Il existe des tables de la fonction Q_n, donnant les valeurs de la fonction avec six chiffres significatifs.

Pour les valeurs $\eta > 10$ un calcul direct à partir de l'expression hypergéométrique de Q_n est facile.

Cas de la traversée, $\eta < 1$; $(f_c/f < 1)$.

Nous sommes ramenés au calcul de l'intégrale:

$$\varphi(\eta) = \eta\int_{-\mu}^{+\mu} \frac{\exp[-\alpha(w/\mu)](1-w^2/\mu^2)\,\mathrm{d}w}{\sqrt{w^2+1}}\,, \tag{36}$$

avec

$$\mu = \frac{\eta}{\sqrt{\eta^2 - 1}}; \qquad w = \mu \frac{\xi}{\xi_m}.$$

Le développement de l'exponentielle nous donne:

$$\varphi(\eta) = \eta \int_{-\mu}^{+\mu} \frac{(1 - w^2/\mu^2)\,\mathrm{d}w}{\sqrt{w^2 + 1}} \left(1 - \frac{\alpha w}{\mu} + \frac{\alpha^2 w^2}{2!\mu^2} - \ldots\right),$$

$$\varphi(\eta) = \varphi_0(\eta) + \frac{\alpha^2}{2!}\varphi_2(\eta) + \frac{\alpha^4}{4!}\varphi_4(\eta) + \ldots,$$

puisque

$$\varphi_1 = \varphi_3 = \ldots = \varphi_{2n+1} = 0,$$

avec

$$\varphi_{2n}(\eta) = \eta \int_{-\mu}^{+\mu} \frac{(1 - w^2/\mu^2)(w/\mu)^{2n}\,\mathrm{d}w}{\sqrt{w^2 + 1}} = 2\eta \int_0^{\mu} \frac{(1 - w^2/\mu^2)w^{2n}\,\mathrm{d}w}{\sqrt{w^2 + 1}\,\mu^{2n}}.$$

Cette intégrale peut s'écrire:

$$\varphi_{2n}(\eta) = 2(L_{2n} - L_{2n+2})$$

en posant

$$L_{2n} = \eta \int_0^{\mu} \frac{w^{2n}\,\mathrm{d}w}{\sqrt{w^2 + 1}\,\mu^{2n}},$$

ce qui donne pour développement de $\varphi(\eta)$

$$\varphi(\eta) = 2\left((L_0 - L_2) + \frac{\alpha^2}{2!}(L_2 - L_4) + \frac{\alpha^4}{4!}(L_4 - L_6) + \ldots\right), \tag{37}$$

avec

$$L_0 = \frac{\eta}{2}\log\left(\frac{1 + \eta}{1 - \eta}\right); \qquad 2nL_{2n} = 1 - \frac{2n - 1}{\mu^2} L_{2n-2}.$$

RÉFÉRENCES

[1] McCullagh: *Proc. Roy. Irish Acad.*, I, 22 (1836); II, 376 (1843).
[2] A. Cauchy: *Compt. Rend. Paris*, **7**, 953 (1838); **8**, 553, 658, 961 (1838).
[3] H. Arzeliès: *Ann. de Phys.*, **2**, 154 (1947).
[4] W. J. G. Beynon: *Proc. Inst. Electr. Eng.*, **101**, III, 15 (1954).
[5] E. V. Appleton and W. J. G. Beynon: *Journ. Atm. Terr. Phys.*, **6**, 141 (1955).
[6] D. F. Martyn: *Proc. Phys. Soc.*, **47**, 323 (1938).
[7] A. Sommerfeld et I. Runge: *Ann. der Phys.*, **35**, 277 (1911).
[8] K. Suchy: *Ann. der Phys.*, **11**, 113 (1952).
[9] H. Arzeliès: *Compt. Rend. Paris*, **235**, 421 (1952).
[10] J. A. Stratton: *Electromagnetic Theory* (London, 1941).
[11] J. Van Mieghem: *Propagation des ondes* (Paris, 1944) pg. 73.
[12] P. S. Epstein: *Proc. Nat. Ac. Sci. Washington*, **16**, 40 (1930).
[13] E. Argence K. Rawer et K. Suchy: *Compt. Rend. Paris*, (1955), sous presse.
[14] M. Nicolet et L. Bossy: *Ann. de Geoph.*, **5**, 275 (1949).
[15] E. Argence M. Mayot et K. Rawer: *Ann. de Geophys.*, **6**, 242 (1950).

OSSERVAZIONI ED INTERVENTI

— P. Dominici:

Dal punto di vista fisico, una notevole limitazione nel calcolo dell'assorbimento ionosferico, è che, con le approssimazioni usuali, l'attendibilità delle formole finali è buona solo nel caso di onde di frequenza sufficientemente elevata: già nel caso di onde decametriche per lunghezze di cammino dell'onda dell'ordine di λ si possono avere notevoli variazioni della densità elettronica, e non valgono più le considerazioni dell'ottica geometrica.

— E. Argence:

Le problème a été examiné dans le cadre de l'Optique Physique dans un travail antérieur effectué en collaboration avec K. Rawer et K. Suchy ainsi que nous l'avons indiqué au cours de cet exposé.

— D. Graffi:

I risultati ottenuti possono estendersi anche nella ipotesi di una ionosfera stratificata sfericamente?

— E. Argence:

L'estensione non è possibile.

SUPPLEMENTO AL VOLUME IV, SERIE X
DEL NUOVO CIMENTO

N. 4, 1956
2° Semestre

Sur la détermination du nombre de chocs relatif à la région F_2 de l'ionosphère.

E. Argence et K. Rawer

Service de Prévision Ionosphérique - Fribourg en Brisgau

1. – Effet de focalisation.

1·1. – L'amplitude des échos ionosphériques a été mesurée dès le début des recherches concernant l'ionosphère dans le but de déterminer l'absorption due aux couches.

Durant la journée les couches basses sont à l'origine d'une forte absorption. De nuit ces couches ayant à peu près disparu, l'absorption due à la couche F_2 peut être déterminée. Cette détermination offre cependant quelques difficultés car l'absorption est faible.

Une étude théorique à la fois simple et élégante de ces expériences a été donnée par Ratcliffe [1].

Les formules correspondantes ont été discutées antérieurement par l'un de nous [2]. Les limites imposées au raisonnement par suite de l'existence de *fading* ont également été indiquées. Nous devons chercher à éliminer leur influence lors du dépouillement; l'action des *fading* rapides dus surtout aux changement de l'état de polarisation est facile à éliminer; on doit alors répéter plusieurs fois la même mesure et effectuer le calcul à l'aide de la médiane des observations.

Contrairement à une opinion assez souvent répandue l'influence de ces effets de polarisation n'est pas très gênante et n'est pas une cause importante d'erreurs.

Par contre la présence d'une houle ionosphérique joue un rôle beaucoup plus important. Ce point de vue est également celui de Piggott [3].

Ces influences font perdre beaucoup de leur valeur aux mesures isolées. C'est l'ensemble des mesures qui peut donner une information significative. Seule la statistique d'un grand nombre d'expériences possède une signification précise et l'on peut déduire l'absorption médiane de la médiane des mesures.

De la dispersion des valeurs mesurées on peut chercher à mettre en évidence la « houle » responsable de l'effet perturbateur [4].

Cette façon de procéder revient à une perte d'information due au fait que les mesures isolées ne peuvent pas être exprimées dans les termes d'une théorie simplifiée. Il nous a donc semblé utile de considérer une théorie plus complète, tenant compte de l'action de la houle.

1·2. – La hauteur effective de réflexion z, peut être représentée par

$$z = z_0 + A \cos \frac{2\pi x}{\Lambda}, \tag{1}$$

où A représente l'amplitude et Λ la longueur d'onde de la houle considérée.

D'après une estimation due à PIERCE et MIMNO [5] on sait que pour la région F, $\Lambda \cong 100$ km et $A \cong 100$ m. Ce qui nous permet de négliger les termes d'ordre supérieur de A/Λ et de A/z.

D'autre part l'inclinaison est toujours faible et par conséquent les parcours demeurent sensiblement verticaux. Les calculs ont été effectués compte tenu de ces hypothèses.

Soit un émetteur placé en x_0. Considérons le premier écho reçu nous trouvons pour valeur du coefficient angulaire au point de réflexion x_{11} (Fig. 1)

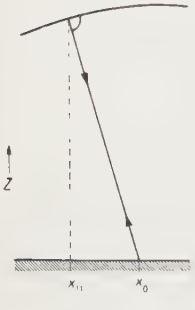

Fig. 1.

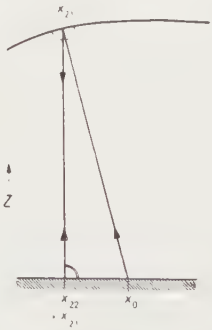

Fig. 2.

$$\left(\frac{dz}{dx}\right)_{11} = \frac{x_0 - x_{11}}{z(x_{11})}. \tag{2}$$

D'où l'on obtient à l'aide de (1) ($A \ll z_0$)

$$x_{11} - x_0 \simeq z_0 \frac{2\pi A}{\Lambda} \sin \frac{2\pi x_0}{\Lambda}. \tag{3}$$

Quant au deuxième écho (Fig. 2) la condition de réflexion est donnée par

$$\left(\frac{dz}{dx}\right)_{21} = \frac{1}{2} \frac{x_0 - x_{21}}{z(x_{21})}. \tag{4}$$

Nous en déduisons:

$$x_{21} - x_0 \simeq z_0 \frac{4\pi A}{\Lambda} \sin \frac{2\pi x_0}{\Lambda} = -2 z_0 \left(\frac{dz}{dx}\right)_0. \tag{5}$$

Le déplacement du point de réflexion est négligeable étant donné que la houle peut être considérée comme faible.

Dans ces conditions pour déterminer la valeur du champ il suffit de considérer l'effet dû à la courbure de l'ionosphère au point de réflexion. Consi-

dérons une ionosphère incurvée (rayon ϱ) et une terre plane (la courbure terrestre est négligeable par rapport à celle de la houle). Le décrément « photométrique », $\delta_1^{(p)}$, pour un écho à p bonds est fonction du diamètre d'un faisceau mince réfléchi p fois par l'ionosphère (et $p-1$ fois par le sol) [6]. A l'aide de la Fig. 3 on déduit par voie géométrique (α, β, φ étant petits)

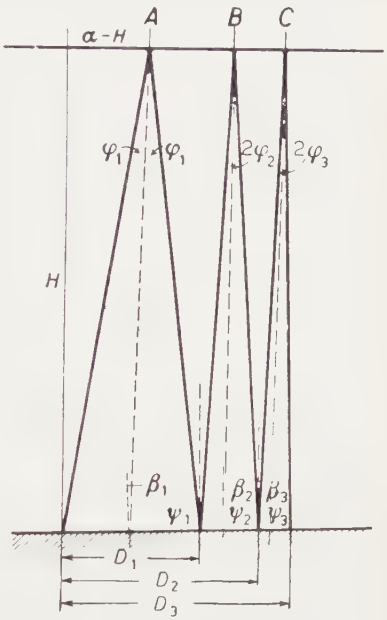

Fig. 3.

$$\beta_1 = \alpha - \varphi_1; \qquad \varphi_1 = \alpha\left(1 - \frac{H}{\varrho}\right), \tag{6}$$

d'où

$$\frac{D_1}{\alpha} = 2H\frac{\varphi_1}{\alpha} = 2H\left(1 - \frac{H}{\varrho}\right). \tag{7}$$

D_1 est le diamètre du faisceau après une réflexion sur l'ionosphère. Pour calculer D_2 (le diamètre aprés deux réflexions) on peut écrire

$$\psi_1 = \pi - \varphi_1 + \beta; \qquad \beta_2 = [\alpha - (\pi - 2\psi_1)]\frac{H}{\varrho}; \qquad \varphi_2 = \frac{\pi}{2} - \psi_1 - \beta_2, \tag{8}$$

et l'on trouve

$$\frac{D_2}{\alpha} = \frac{D_1 - 2H\varphi_2}{\alpha} = 4H\left[1 - \frac{3H}{\varrho} + 2\left(\frac{H}{\varrho}\right)^2\right]. \tag{9}$$

La suite des calculs nous amène au système suivant:

$$\left\{\begin{aligned}
&\frac{D_1}{\alpha} = 2H\left(1 - \frac{H}{\varrho}\right),\\
&\frac{D_2}{\alpha} = 4H\left(1 - \frac{H}{\varrho}\right)\left(1 - 2\frac{H}{\varrho}\right),\\
&\frac{D_3}{\alpha} = 6H\left(1 - \frac{H}{\varrho}\right)\left(1 - \frac{4}{3}\frac{H}{\varrho}\right)\left(1 - 4\frac{H}{\varrho}\right),\\
&\frac{D_4}{\alpha} = 8H\left(1 - \frac{H}{\varrho}\right)\left(1 - 2\frac{H}{\varrho}\right)\left(1 - \frac{4}{2+\sqrt{2}}\frac{H}{\varrho}\right)\left(1 - \frac{4}{2-\sqrt{2}}\frac{H}{\varrho}\right).
\end{aligned}\right. \tag{10}$$

Il y a focalisation lorsque le diamètre s'annule et l'on a toujours la solution $H/\varrho = 1$. Pour les échos multiples on trouve pour les valeurs critiques de la

courbure

Ordre de réflexion	Valeurs critiques de la courbure H/ϱ			
1	1			
2	1	0.5		
3	1	0.75	0.25	
4	1	0.5	0.853	0.147

Le décrément photométrique s'écrit alors:

$$(11)\qquad \begin{cases} \delta_1^{(1)} = 20 \log (2H) + L_1 \\ \delta_1^{(2)} = 20 \log (4H) + L_1 + L_{\frac{1}{2}} \\ \delta_1^{(3)} = 20 \log (6H) + L_1 + L_{\frac{3}{4}} + L_{\frac{1}{4}} \\ \delta_1^{(4)} = 20 \log (8H) + L_1 + L_{\frac{1}{2}} + L_{0,853} + L_{0,147} \end{cases}$$

où

$$(11a)\qquad L_q = 10 \log \left| 1 - \frac{1}{q} \frac{H}{\varrho} \right| ,$$

dans le cas d'une houle cylindrique. Le facteur est 20 au lieu de 10 pour une houle sphérique.

Dans le cas d'une courbure concave de l'ionosphère les fonctions L sont presque toujours négatives. L'affaiblissement est plus faible que celui dû à une couche plane. Par contre pour une courbure convexe ($H/\varrho < 0$) l'affaiblissement est plus fort.

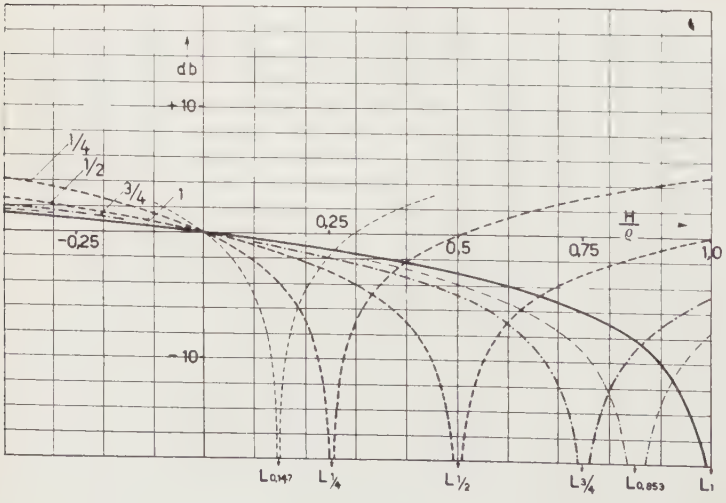

Fig. 4.

Les fonctions L sont représentées sur la Fig. 4. Nous remarquons que l'influence de la houle est nettement dissymétrique. L' effet reste faible dans le cas d'une courbure convexe, il

ne devient important que pour les valeurs positives de H/ϱ voisines des valeurs critiques de focalisation.

1·3. – Dans le but d'évaluer la « perte de transmission » P, [7] il faut faire entrer en ligne de compte le décrément d'absorption δ_2 et la perte due au sol δ_T. De sorte que nous pouvons écrire pour la perte correspondant aux échos successifs

$$P^{(p)} = \langle E_0 \rangle - \langle E_p \rangle = \delta_1^{(p)} + p\delta_2 + (p-1)\delta_T \; ; \tag{1.12}$$

E_p étant le champ en db au dessus de 1 μV/m, $\langle E_0$ le champ de référence à 1 km au dessus de l'émetteur.

Par comparaison nous déduisons

a) de l'amplitude du premier et du deuxième écho:

$$\begin{cases} \delta_2 - \delta_T = \Delta_{12} - L_{\frac{1}{2}} \\ \Delta_{12} = \langle E_1 \rangle - \langle E_2 \rangle - 20 \log 2 \; ; \end{cases} \tag{13}$$

b) de l'amplitude du premier et du troisième écho:

$$\begin{cases} \delta_2 + \delta_T = \Delta_{13} - \tfrac{1}{2}(L_{\frac{3}{4}} + L_{\frac{1}{4}}) \\ 2\Delta_{13} = \langle E_1 \rangle - \langle E_3 \rangle - 20 \log 3 \; . \end{cases} \tag{14}$$

Les Δ sont les valeurs du décrément dans l'hypothèse où la couche est supposée plane.

De l'observation de trois échos successifs on peut déterminer trois paramètres; le rayonnement caractérisé par $\langle E_0$, le décrément d'absorption δ_2, et la courbure H/ϱ.

Le procédé le plus simple consiste à effectuer d'abord l'évaluation abituelle c'est-à-dire de calculer Δ_{12} et Δ_{13}. Nous obtenons

$$G = \Delta_{12} - \Delta_{13} = L_{\frac{1}{2}} - \tfrac{1}{2}(L_{\frac{1}{4}} + L_{\frac{3}{4}}) \; . \tag{15}$$

Cette fonction est représentée par la Fig. 5 (cas d'une houle cylindrique; les ordonnées doivent être multipliées par 2 dans le cas d'une houle sphérique).

Nous avons séparé ainsi les effets d'absorption et de focalisation. Si l'on suppose connu le rayonnement vertical (« force cymomotrice ») du sondeur, les mesures relatives à deux échos suffisent (équations (12) et (13)).

Dans le cas des échos multiples on doit considérer la perte au sol. De jour cette influence est faible comparée à celle de l'absorption; de nuit elle n'est pas négligeable. A première vue il semble que l'on puisse envisager la déter-

mination directe de δ_T, δ_2 et de H/ϱ à l'aide des mesures relatives aux trois premiers échos, cependant l'incertitude numérique demeure trop grande.

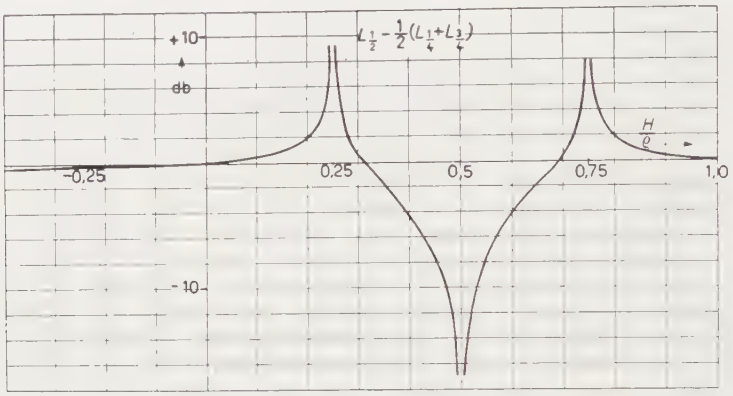

Fig. 5.

Il nous a paru préférable de calculer δ_T à partir des formules de Fresnel. Nous avons considéré les valeurs des paramètres relatives à un « bon » et à un « très bon » sol (constante diélectrique relative $\varepsilon = 25$ et 4, conductibilité $\sigma = 0.03$ et $0.01\ \Omega^{-1}\,m^{-1}$). Le résultat pour le cas de l'incidence normale est donné dans le Table ci-dessous.

Table I.

Fréquence en MHz		1	2	3	4	5	6
Valeurs de δ_T (db)	Bon sol	1.0	1.4	1.8	2.2	2.5	2.8
	Très bon sol	0.6	0.8	1.0	1.2	1.4	1.6

Notre connaissance des qualités du terrain ne nous permet pas d'obtenir une précision supérieure, il semble toutefois que les valeurs les plus élevées de δ_T figurant dans la première ligne sont plus proches de la réalité et en accord avec les expériences effectuées près de Fribourg en Brisgau.

2. – Calcul du décrement d'absorption dans le cas d'une fréquence de collisions électrons-ions.

2·1. – Le calcul de la fréquence de collision électrons-ions (ν_{ei}) (*) s'est montré d'une grande importance dans les études de radio-astronomie, il a fait

(*) Le nombre de chocs entre électrons et ions est indiqué indifféremment par ν_{ei} ou ν.

l'objet des travaux de MAJUMDAR [7], GINSBURG [8], CHAPMAN et COWLING [9], SMERD et WESTFOLD [10] et DENISSE [11].

Les différentes expressions ainsi obtenues sont pratiquement équivalentes. Nous utiliserons l'expression de Majumdar:

$$\nu = 1.8 \frac{Z^2 N}{T^{\frac{3}{2}}} [\log (kT\alpha - C - 1)] , \tag{16}$$

(Z nombre de charges du noyau; k constante de Boltzmann; N densité ionique, sensiblement égale à la densité électronique).

Nous avons

$$kT\alpha \gg C + 1 ,$$

de sorte que nous sommes en droit d'écrire

$$\nu \simeq 1.8 \frac{Z^2 N}{T^{\frac{3}{2}}} \log (kT\alpha) . \tag{17}$$

C'est-à-dire en explicitant:

$$\alpha = 6.63 \cdot 10^{27} b^2 ; \qquad b = \tfrac{1}{2}\bar{a} ; \qquad \bar{a} = (N)^{-\frac{1}{3}}$$

$$\nu \cong \beta_1 (N \log \beta_2 - \tfrac{2}{3} N \log N), \tag{18}$$

où

$$\beta_2 = 1.66 \cdot 10^{27} kT$$

$$\beta_1 = \frac{1.8 Z^2}{T^{\frac{3}{2}}} \ \text{cm}^3 \ \text{s}^{-1}.$$

Puisque

$$\log \beta_2 \gg \tfrac{2}{3}$$

nous négligerons le second terme de (18) et nous écrirons

$$\nu \simeq \beta_1 \log \beta_2 N . \tag{19}$$

2·2. – *Cas d'une variation parabolique de la densité électronique.*

a) N_m désignant la valeur maximum de la densité électronique nous pouvons écrire:

$$N = N_m (1 - Y^2) \qquad \text{avec} \quad Y = z/z_m .$$

D'où nous déduisons pour la valeur du décrément:

$$\delta_2 \simeq z_m\lambda_1 \int \frac{(1-Y^2)^2\,\mathrm{d}Y}{\sqrt{1-(1/u^2)(1-Y^2)}} + z_m\lambda_2 \int \frac{(1-Y^2)^2 \log(1-Y^2)\,\mathrm{d}Y}{\sqrt{1-(1/u^2)(1-Y^2)}},$$

avec

$$\lambda_1 = \frac{1}{u^2}\cdot\frac{1}{2c}\,\beta_1 N_m \log\left(\frac{\beta_2}{N_m^{\frac{2}{3}}}\right), \qquad \lambda_2 = \frac{1}{u^2}\,\frac{1}{3c}\,\beta_1 N_m,$$

$$u = \frac{f}{f_c}.$$

Si nous effectuons le changement de variable

$$1-Y^2 = u^2\eta,$$

nous obtenons

$$\delta_2 \simeq \frac{z_m u^6}{2}\left[(\lambda_1 + 2\lambda_2 \log u)I_1 - \lambda_2 I_2\right], \tag{20}$$

et nous avons à évaluer les intégrales

$$I_1 = \int_{\eta_0}^{\eta_1} \frac{\eta^2\,\mathrm{d}\eta}{\sqrt{(1-\eta)(1-u^2\eta)}}; \qquad I_2 = \int_{\eta_0}^{\eta_1} \frac{\eta^2 \log\eta\,\mathrm{d}\eta}{\sqrt{(1-\eta)(1-u^2\eta)}}. \tag{21}$$

Les limites ayant respectivement pour valeurs

$$\begin{cases} \eta_0 = 0 \\ \eta_1 = 1 \end{cases} \quad \text{(réflexion)},$$

$$\begin{cases} \eta_0 = 0 \\ \eta_1 = 1/u^2 \end{cases} \quad \text{(traversée)}.$$

On établit facilement que la contribution de l'intégrale I_2 est négligeable devant celle de I_1.

D'où il résulte que l'on peut écrire:

$$\delta_2 \simeq \frac{z_m}{4c}\,u^4\beta_1 N_m \log\left(\frac{\beta_2}{N_m^{\frac{2}{3}}}\right) I_1. \tag{22}$$

b) Nous pouvons procéder au calcul de l'intégrale I_1 :

1) Cas de la réflexion:

$$I_1 = \int_0^1 \frac{\eta^2\,\mathrm{d}\eta}{\sqrt{(1-\eta)(1-u^2\eta)}},$$

d'où

$$I_1 = -\frac{1}{u}\left(\frac{1+u^2}{2u^2}\right)^2 \varphi_1(u)\,, \tag{23}$$

avec

$$\varphi_1(u) = \left[1 + \frac{1}{2}\left(\frac{1-u^2}{1+u^2}\right)^2\right] \log\frac{1+u}{1-u} - \frac{3u}{1+u^2}\,.$$

2) Cas de la traversée:

$$I_1 = \frac{2u}{u^2-1}\int_0^{1/u^2} \frac{\eta^2\,\mathrm{d}\eta}{\sqrt{\left(\dfrac{((1+u^2)/2u^2)-\eta}{(u^2-1)/2u^2}\right)-1}}\,.$$

Ce qui nous donne

$$I_1 = \frac{1}{u}\left(\frac{1+u^2}{2u^2}\right)^2 \varphi_2(u)\,,$$

avec

$$\varphi_2(u) = \left[1 + \frac{1}{2}\left(\frac{u^2-1}{u^2+1}\right)^2\right] \log\frac{1+u}{u-1} - \frac{3u}{1+u^2}\,.$$

2·3. *Cas d'une distribution de Chapman.* – Posons avec les notations habituelles

$$\begin{cases} z = \dfrac{h - h_0}{H}\,, \\ H = \dfrac{kT}{mg}\,. \end{cases}$$

Nous avons pour expression de la loi de variation de la densité électronique

$$N = N_m \exp\left[\tfrac{1}{2}(1 - z - \sec\chi e^{-z})\right]$$

et

$$\delta_2 \simeq \int \frac{\nu}{2c}\,\frac{1-\mu^2}{\mu}\,\mathrm{d}z\,.$$

Effectuons le changement de variable

$$x = (\tfrac{1}{2}\sec\chi)\exp\left[-\frac{z}{2}\right].$$

Nous obtenons

$$\delta_2 = \delta_0\left[\int x\exp[-2x^2]\,\mathrm{d}x + \sum_{n=1}^{\infty}\frac{1\cdot3\cdot5\ldots(2n-1)}{2\cdot4\ldots2n}\,\alpha^n\int x^{n+1}\exp[-(2+n)x^2]\,\mathrm{d}x\right],$$

avec

$$\delta_0 = -\frac{\beta_1}{c} \log \beta_2 N_m \sqrt{2e} (\cos \chi)^{\frac{1}{2}} \alpha H ,$$

$$\left(\alpha = \left(\frac{f_c'}{f} \right)^2 \sqrt{2e}; \quad f_c' = f_c \cos^{\frac{1}{2}} \chi \right).$$

Pour le cas de la réflexion, les limites sont x_1 et ∞, x_1 étant la plus grande racine de

$$1 - \alpha x e^{-x^2} = 0 \qquad (f < f_c').$$

Pour le cas de la traversée les limites sont 0 et ∞ $(f > f_c')$. Examinons le second cas en premier lieu.

Traversée:

$$\delta_2 = \delta_0 I_1 \left(\frac{f_c'}{f} \right),$$

$$I \left(\frac{f_c'}{f} \right) = \int_0^\infty x \exp[-2x^2] \, dx + \sum_{n=1}^{\infty} \frac{1 \cdot 3 \cdot 5 \ldots (2n-1)}{2 \cdot 4 \ldots 2n} \chi^n \int_0^\infty x^{n-1} \exp[-(2-n)x^2] \, dx .$$

Effectuons le changement de variable

$$x = \frac{t}{\sqrt{2(n+2)}} .$$

Nous obtenons

$$\int_0^\infty x^{n+1} \exp[-(2+n)x^2] \, dx = \frac{1}{[2(n+2)]^{(n+2)/2}} \int_0^\infty t^{n+1} \exp\left[-\frac{t^2}{2}\right] dt .$$

Nous devons finalement calculer

$$I_p = \int_0^\infty t^p \exp\left[-\frac{t^2}{2}\right] dt .$$

Nous obtenons ainsi les relations

$$\frac{d}{dt}\left(t^p \exp\left[-\frac{t^2}{2}\right] \right) = p t^{p-1} \exp\left[-\frac{t^2}{2}\right] - t^{p+1} \exp\left[-\frac{t^2}{2}\right],$$

$$p I_{p-1} - I_{p+1} = 0,$$

d'où nous déduisons respectivement pour les cas $p = 2m$ et $p = 2m + 1$

$$I_{2m} = 1 \cdot 3 \cdot 5 \ldots (2m - 1) \sqrt{\frac{\pi}{2}},$$

$$I_{2m+1} = 2 \cdot 4 \cdot 6 \ldots 2m .$$

Réflexion:

$$\delta_2 = \delta_0 A_2 \left(\frac{f'_c}{f}\right),$$

$$A_2\left(\frac{f'_c}{f}\right) = \int_{x_1}^{\infty} x \exp[-2x^2]\,dx + \sum_{n=1}^{\infty} \frac{1 \cdot 3 \cdot 5 \ldots (2n-1)}{2 \cdot 4 \ldots 2n} \alpha'' \int_{x_1}^{\infty} x^{n+1} \exp[-(n+2)x^2]\,dx.$$

Le même changement de variable que précédemment nous conduit aux intégrales

$$J_p = \int_{t_1}^{\infty} t^p \exp\left[-\frac{t^2}{2}\right] dt, \qquad (t_1 = x_1\sqrt{2(n+2)}).$$

La relation

$$\frac{d}{dt}\left(t^p \exp\left[-\frac{t^2}{2}\right]\right) = pt^{p-1} \exp\left[-\frac{t^2}{2}\right] - t^{p+1} \exp\left[-\frac{t^2}{2}\right],$$

nous donne la nouvelle relation de récurrence

$$J_{p+1} = pJ_{p-1} + \overline{\omega}_p, \qquad \left(\overline{\omega}_p = t_1^p \exp\left[-\frac{t_1^2}{2}\right]\right).$$

J_{2m} se calcule à partir de

$$J_0 = \int_{t_1}^{\infty} \exp\left[-\frac{t^2}{2}\right] dt,$$

c'est-à-dire

$$J_0 = \sqrt{2} \int_{x_1\sqrt{n+2}}^{\infty} \exp[-\theta^2]\,d\theta,$$

et J_{2m+1} à partir de

$$J_1 = \int_{t_1}^{\infty} t \exp\left[-\frac{t^2}{2}\right] dt = \exp\left[-\frac{t_1^2}{2}\right].$$

Nous avons d'autre part

$$J_0 = \sqrt{2}\left[\frac{\sqrt{\pi}}{2} - E_{rf}(x_1\sqrt{n+2})\right],$$

$E_{rf}(v)$ désignant la fonction de Gauss

$$E_{rf}(v) = \int_0^v \exp[-v^2]\,\mathrm{d}v\,.$$

3. – Les mesures.

3·1. – Nous avons effectué un certain nombre d'observations durant les nuits d'hiver 1949-50. Un rapport préliminaire a déjà été publié [12]. Nous allons utiliser les résultats théoriques que nous venons d'exposer en vue de déterminer le nombre de chocs relatif à la région F_2.

Après avoir mesuré la fréquence critique de la couche F_2, nous avons choisi un certain nombre de fréquences, les mesures ont été effectuées à partir de la plus basse des fréquences, l'intervalle de lecture étant de 10 secondes. L'amplitude de chaque écho a été évalué sur l'écran gradué d'un oscilloscope étalonné avec le récepteur à impulsion en tension d'entrée [2]. Après une douzaine de lectures nous avons opéré avec une nouvelle fréquénce et la médiane des amplitudes mesurées a été utilisée pour l'évaluation suivante. Une fois mesurées les amplitudes sur les fréquences choisies, compte tenu du brouillage, nous avons déterminé de nouveau le « passage » de la fréquence critique, de façon à procéder une nouvelle fois à la détermination de cet important paramètre.

3·2. *Interprétation.* – L'interprétation des résultats présente un certain nombre de difficultés dûes au caractère ambigu du phénomène de focalisation.

Nous mesurons la valeur moyenne du champ au sol, de sorte que la distinction entre rayons divergents et rayons convergents est impossible.

L'ambiguité peut cependant être levée dans la plupart des cas si l'on tient compte des faits suivants:

a) Les valeurs négatives du décrément d'absorption n'ont pas de réalité physique. La valeur de la courbure déduite de ces mesures aberrantes doit être rejetée.

b) La force cymomotrice du sondeur (champ E_0) est connue avec une assez bonne exactitude; si les valeurs observées conduisent à une valeur inadmissible de E_0, la valeur correspondante du rayon de courbure est incompatible avec les mesures et doit être abandonnée.

c) La courbure de la houle de la région F_2 étant relativement faible on pourra dans le cas où les conditions *a*) et *b*) ne suffisent pas à lever l'ambiguité, choisir la plus faible des valeurs en question.

Pour la plus grande partie des mesures (environ les 2/3) une interprétation satisfaisante des résultats ne peut être obtenue que si l'on admet l'existence d'une surface réfléchissante incurvée. L'indétermination relative aux mesures étant de l'ordre de 2 db, nous avons appliqué la correction de courbure chaque fois que la différence entre les valeurs de Δ était supérieure à 2 db.

Nous avons donc opéré de la façon suivante:

1) Nous déterminons Δ_{12}, Δ_{13} et $\langle E_0 \rangle$ à partir de $\langle E_1 \rangle$, $\langle E_2 \rangle$, $\langle E_3 \rangle$.

2) La différence $\Delta_{12} - \Delta_{13} = G$ nous permet de déterminer la courbure (H/ϱ).

La fonction G nous donnera deux valeurs de (H/ϱ), si la différence est négative et quatre si elle est positive. Des valeurs ainsi obtenues on peut déduire les fonctions de correction de E_0 et de Δ_{12}. De cette façon nous pouvons déterminer deux tables nous donnant les valeurs de E et de δ_2 et sélectionner les valeurs par l'application des critères *a*) et *b*) données plus haut.

Nous voyons maintenant que pour chaque courbure il existe quatre possibilités (classes).

1) L'ambiguité est de faible importance, $|G| < 2$ db. Dans ce cas il n'y a pas d'effet de courbure, on utilise comme valeur de δ_2 la moyenne des valeurs de Δ_{12} et Δ_{13}.

2) L'ambiguité disparaît si l'on utilise les critères *a*) ou *b*) ou *a*) et *b*).

3) Après avoir éliminé les cas non conformes à ces deux conditions il nous reste encore un certain nombre de valeurs, et nous appliquons le critère *c*).

4) Il n'esiste pas un choix satisfaisant entièrement aux conditions *a*) et *b*). On est conduit alors à chercher le choix le meilleur, compte tenu de l'imprécision des mesures, ce qui revient à retenir parfois quelques valeurs faiblement négatives de δ_2; compte tenu de l'imprécision, toutefois on a toujours $|\delta_2| < 2$ db. Cependant des cas *trés rares* conduisent à une valeur inadmissible de δ_2 et E_0 et échappent à notre analyse.

La présentation directe des décrément $(\delta_2 + \delta_r)$ obtenus suivant les règles données précédemment en fonction de la fréquence ne donne aucun résultat. Par contre si la représentation est effectuée en fonction de f_c/f, on peut mettre en évidence une certaine régularité (Fig. 6). Cette figure montre nettement la diminution de dispersion à laquelle nous sommes arrivés après avoir effectué

la correction nécessaire. La méthode habituelle aurait introduit un décrément négatif pour un tiers des cas.

La dispersion standard de nos résultats définitifs est de l'ordre de ± 3 db. Cette dispersion est relativement importante, toutefois elle permet d'indiquer le sens de la variation globale de δ_2 en fonction de f_c/f mais il semble difficile d'en déduire une relation fonctionnelle en toute rigueur. D'autre part la structure de la houle est encore mal connue. En introduisant le modèle d'une houle sphérique nous aboutissons à des valeurs de (H/ϱ) plus faibles donnant des corrections différentes.

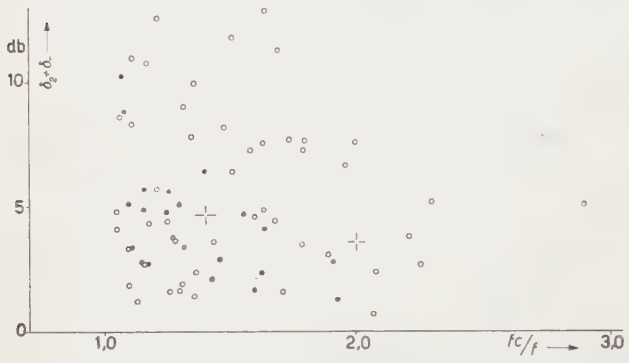

Fig. 6.

Ce qui demeure possible, c'est une confrontation de nos valeurs avec les résultats théoriques obtenus d'après l'étude de l'absorption ionosphérique, telle que nous l'avons développée plus haut.

La variation du décrément d'absorption diffère suivant les hypothèses envisagées.

Etant donnée la forte dispersion des valeurs nous ne retenons que les deux couples correspondant à la médiane des observations pour $f_c/f < 1.7$, et $f_c/f > 1.7$ est obtenu après soustraction de l'absorption due à la réflexion au sol. Cette dernière (voir Sect. 1) a été déterminée théoriquement (nous avons introduit la fréquence moyenne des différentes mesures). La variation en fonction de $1/u = f_c/f$ est très faible. Nous avons effectué l'évaluation à titre d'exemple (Table II). Seul l'ordre de grandeur peut être retenu.

Table II.

f_c/f	1.4	2.0
$\bar{f}$ (moyenne en MHz)	3.0	2.1
$\delta_2 + \delta_T$ (db) (*)	4.7	3.6
δ_T (db) (**)	1.8	1.5
δ_2 (db)	2.9	2.1

(*) Valeurs médianes observées.
(**) Bon sol.

Pour déduire des valeurs numériques satisfaisantes un très grand nombre d'observations est nécessaire.

4. – Discussion des résultats.

a) *Cas où l'on considère la contribution due aux chocs moléculaires.* – Si l'absorption ionosphérique est due aux chocs entre les électrons et molécules neutres on peut supposer une variation presque exponentielle du nombre des chocs ν_{em} en fonction de l'altitude. Le calcul de l'absorption correspondante a été effectué rigoureusement pour le cas d'une répartition parabolique de l'ionisation dans un travail antérieur [13, 14]. Si nous utilisons la formule

$$\delta_2 = 20N \cdot \Delta_3^* \qquad \text{où} \qquad N = \nu_0 Y_m \frac{\log_{10} e}{c}, \tag{24}$$

(Y_m demiépaisseur, c vitesse de la lumière) avec les valeurs numériques [15] nous obtenons la Table III.

TABLE III.

f_c/f	1.4	2.0
δ_2 (db)	2.9	2.1
Δ_3^* (db)	3.04	1.74
N	0.0476	0.0603

Nous en déduisons une valeur médiane de $N = 0.054$, d'où

$$\nu Y_m = 3.7 \cdot 10^4 \text{ km s}^{-1}. \tag{25}$$

Avec $Y_m = 80$ km on obtient

$$\nu_0 \simeq 500 \text{ s}^{-1}.$$

Cette valeur est relative au nombre de chocs au centre de la couche F_2 dont l'altitude est sensiblement égale à 300 km.

Cette valeur semble très élevée si on la compare aux mesures obtenues par fusées [16]. Ces mesures donnant la densité d et la température T permettent une évaluation de ν.

On a pour valeur du nombre de chocs avec les molécules d'ogxyène où d'azote

$$\nu_{em} = 4.7 \cdot 10^{-16} \cdot n\sqrt{T} \text{ m}^{-3} \text{ s}^{-1} \text{ °K}^{-1} \tag{26}$$

(n nombre des particules par m^3 [13]).

Le coefficient numérique dépend de la section efficace des molécules, il peut être légèrement différent pour le cas des atomes libres O et N dont nous admettons l'existence à l'altitude de 300 km.

Les mesures par fusées ont été effectuées dans d'excellentes conditions jusqu'à une altitude de 220 km, on a trouvé à cette altitude [16]

$$H = 28.43 \text{ km}\,, \qquad T = 455.5\ ^{\circ}\text{K}\,; \qquad d = 7.014 \cdot 10^{-14}\ \text{g cm}^{-3}\,,$$

(H échelle des hauteurs).

De ces valeurs on obtient à partir de (3) un nombre de chocs très faible, $\nu_{en} \simeq 30\ \text{s}^{-1}$ à 220 km. Or notre valeur $\sim 500\ \text{s}^{-1}$ correspond à une altitude supérieure de presque 3 H. Nous voyons ainsi que le nombre de chocs correspondant à une altitude de 300 km est le centième environ du nombre que nous avons pu déduire de nos mesures, il semble donc que la théorie des chocs neutres soit sujette à critiques.

Cas des chocs ioniques.

Une évaluation du décrément correspondant a été donnée dans la Sect. 2. Pour le modèle parabolique de répartition de l'ionisation nous avons trouvé:

$$\delta_2 \simeq 1.448 \cdot Y_m w u^4 I_1(u)\ \text{s km}^{-1}\,. \tag{27}$$

(Pour les valeurs numériques de $u^4 I_1(u)$ voir Appendice). En comparant avec nos mesures nous obtenons la Table IV.

Table IV.

$u = f/f_c$	0.714	0.500
δ_2 (db)	2.9	2.1
$u^4 I_1(u)$	0.282	0.086
$\delta_2 u^{-4} I_1^{-1}(u)$ (db)	10.3	24.4
$Y_m W$ (10^5 km s^{-1})	7.1	16.9

Nous en déduisons une valeur moyenne de

$$Y_m w = 1.2 \cdot 10^6\ \text{km s}^{-1}\,.$$

Avec $Y_m = 80$ km on obtient $w = 1.5 \cdot 10^4\ \text{s}^{-1}$. Or

$$w = \frac{1.8}{T^{\frac{3}{2}}} N_m [\log (1.6575 \cdot 10^{27} kT) - \tfrac{2}{3} \log N_m]\,, \tag{28}$$

(k constante de Boltzmann, N_m nombre d'électrons par m^3, au maximum de la couche).

La valeur moyenne de N_m relative à nos expériences peut être déduite de la fréquence critique moyenne 4.18 MHz, d'où nous déduisons $N_m = 2.17 \cdot 10^{11} m^{-3}$. On obtient ainsi une valeur de la température T de l'ordre de 100°.

Cette valeur correspondant à l'altitude de 300 km est sans aucun doute trop faible. Une température plus élevée est vraisemblable, les observations par fusées donnant ~ 600 °K.

Il peut être utile de faire entrer en ligne de compte la contribution dûe aux chocs entre électrons (électrons-électrons, (ν_{ee})) mais une évaluation exacte de cette contribution effective est difficile.

Une estimation récente de RAWER et SUCHY [17] pour la région F_2 donne

$$\frac{\nu_{ei} - \nu_{ee}}{\nu_{ei}} \simeq 5 . \tag{29}$$

Donc si l'on fait intervenir la contribution électron-électrons le nombre ν_{ei} est le cinquième environ de la valeur déduite des observations

$$\nu_{ei} = 3 \cdot 10^3 \, s^{-1} .$$

Et l'on aboutit à une température de 200 °K. Cette valeur plus proche des mesures déduites des observations effectuées par fusées est encore trop faible.

Enfin il ne semble pas impossible qu'entre en ligne de compte une contribution des couches basses durant la nuit. Une évaluation due à celle-ci, en vue de la détermination du décrément d'absorption peut être estimée.

Une couche E ayant une fréquence critique de 0.5 MHz et une épaisseur nocturne équivalente à l'épaisseur diurne donnerait une absorption par chocs neutres de l'ordre de grandeur de 0.5 db (pour 2.5 MHz).

Cette contribution est trop faible pour pouvoir influencer sérieusement nos résultats.

5. – Conclusion.

Les résultats donnés ici sont provisoires, il serait sans doute fort utile, d'effectuer un grand nombre d'observations s'échelonnant sur une intervalle de temps beaucoup plus court et d'étendre les méthodes statistiques mises au point par ALPERT [18] et BRAMLEY [19].

Appendice

Convergence des développements dans le cas où l'on considère une région de Chapman.

a) *Cas de la traverseé.* – Le terme général a pour expression:

$$u_n = \frac{1\cdot 3\cdot 5 \ldots (2n-1)}{2^n \cdot n!}\,\alpha^n \int_0^\infty x^{n+1} \exp\left[-(2+n)x^2\right] \mathrm{d}x\,.$$

Considérons la série de terme général

$$U_n = \frac{1\cdot 3\cdot 5 \ldots (2n-1)}{2^n \cdot n!}\,\alpha^n x^{n+1} \exp\left[-(2+n)x^2\right] \qquad (x \geqslant 0).$$

Le maximum du terme $x^{n+1}\exp\left[-(2+n)x^2\right]$ a pour valeur:

$$\left[\frac{1+n}{2(n+2)}\right]^{(1+n)/2} \exp\left[-\frac{1+n}{2}\right].$$

De sorte que la série U_n est majorée par la série

$$V_n = \frac{1\cdot 3\cdot 5 \ldots (2n-1)}{2^n \cdot n!}\,\alpha^n \left[\frac{1+n}{2(n+2)}\right]^{(1+n)/2} \exp\left[-\frac{1+n}{2}\right],$$

$$U_n < V_n\,.$$

Pour que U_n soit uniformément convergente, V_n doit converger. L'application du critère de d'Alembert nous montre que

$$\left|\frac{V_{n+1}}{V_n}\right| \to \alpha \exp\left[-\tfrac{1}{2}\right] 2^{-\frac{1}{2}}\,.$$

D'où

$$\left|\alpha \exp\left[-\tfrac{1}{2}\right] 2^{-\frac{1}{2}}\right| < 1\,,$$

c'est à dire

$$\alpha < \sqrt{2e}\,.$$

Si cette condition est satisfaite, on a d'après un théorème classique que la série u_n est convergente.

b) *Cas de la réflexion.*

α) n pair. – La série (*)

$$u_n = \frac{1\cdot 3\cdot 5 \ldots (2n-1)}{2^n \cdot n!} \cdot \frac{1}{2(n+2)t^n} \exp\left[\frac{nt^2}{2(n+2)}\right] 2^{n/2}\left(\frac{n}{2}\right)! \exp\left[-\frac{t^2}{2}\right] \exp_n\left[-\frac{t^2}{2}\right],$$

est majorée par la série de terme général

$$U_n = \frac{1\cdot 3\cdot 5 \ldots (2n-1)}{2^n \cdot n!} 2^{n/2}\left(\frac{n}{2}\right) \exp\left[\frac{nt^2}{2(n-2)}\right],$$

puisque l'on a toujours $\exp_n[t^2/2] < \exp[t^2/2]$.

L'application du critère de d'Alembert montre que

$$\frac{u_{n+1}}{u_n}\Big|_{n\to\infty} = \frac{n+2}{t^2} < 1 .$$

Nous devons donc avoir

$$t^2 > n+2 \qquad \text{c'est-à-dire} \qquad x > 1/\sqrt{2}$$

β) n impair. – Dans ce cas:

$$u_n = \frac{1\cdot 3\cdot 5 \ldots (2n-1)}{2^n \cdot n!} \frac{2^{n/2}(n+2)^{n/2}}{t^n} \exp\left[\frac{nt^2}{2(n+2)}\right] \frac{1}{2^{(n/2)+1}(n+2)^{(n/2)+1}} \Phi_1(t) .$$

On a posé

$$\Phi_1(t) = 3\cdot 5\cdot 7 \ldots n\left[\int_t^\infty \exp\left[-\frac{t^2}{2}\right] dt + \varphi_n(t) \exp\left[-\frac{t^2}{2}\right]\right],$$

avec

$$\varphi_n(t) = t + \frac{t^3}{3} + \frac{t^5}{3.5} + \ldots + \frac{t^n}{3\cdot 5 \ldots n} .$$

Lorsque $n \to \infty$ la série φ est solution de l'équation différentielle

$$y' - ty - 1 = 0 ,$$

(*) Nous avons posé

$$\exp_n[x] = 1 + \frac{x}{1} + \frac{x^2}{2!} + \ldots + \frac{x^n}{n!} .$$

admettant pour solutions

$$y_1 = \exp\left[\frac{t^2}{2}\right]\int_0^t \exp\left[-\frac{t^2}{2}\right]dt + C\exp\left[\frac{t^2}{2}\right],$$

ou bien

$$y_2 = -\exp\left[\frac{t^2}{2}\right]\int_t^\infty \exp\left[-\frac{t^2}{2}\right]dt + C\exp\left[\frac{t^2}{2}\right].$$

La fonction $\psi(t)$ ainsi définie

$$\psi(t) = \exp\left[\frac{t^2}{2}\right]\int_t^\infty \exp\left[-\frac{t^2}{2}\right]dt.$$

s'apparente à la fonction de Radau:

$$\Theta(t) = \exp[t^2]\int_t^\infty \exp[-t^2]dt.$$

Lorsque $n \to \infty$

$$\exp\left[-\frac{t^2}{2}\right]\varphi_n(t) \to \int_0^\infty \exp\left[-\frac{t^2}{2}\right]dt = \sqrt{\frac{\pi}{2}},$$

et

$$\varphi_n(t) < \exp\left[\frac{t^2}{2}\right]\int_0^t \exp\left[-\frac{t^2}{2}\right]dt;$$

$$\Phi_1(t) < 3\cdot 5\cdot 7 \ldots n\left[\int_0^\infty \exp\left[-\frac{t^2}{2}\right]dt\right];$$

$$\Phi_1(t) < 3\cdot 5\cdot 7 \ldots n\sqrt{\frac{\pi}{2}}.$$

Comme pour n pair, la série converge uniformément pour $x > 1/\sqrt{2}$.

RÉFÉRENCES

[1] J. A. Ratcliffe: *Proc. Roy. Soc.*, A **151**, 370 (1935).
[2] K. Rawer: *Journ. Atm. Terr. Phys.*, **2**, 38 (1951).
[3] W. R. Piggott: *Journ. Inst. Electr. Eng.*, **10**, III, 61 (1953).
[4] E. Argence et K. Rawer: *Compt. Rend. Paris*, **239**, 1066 (1954).
[5] J. A. Pierce et H. R. Mimno: *Phys. Rev.*, **57**, 95 (1940).
[6] K. Rawer: *Rev. Scient.*, **86**, 585 (1948).
[7] R. C. Majumdar: *Zeits. f. Phys.*, **107**, 599 (1937).
[8] V. Ginzburg: *Journ. Phys. USSR*, **8**, 255 et 383 (1944).
[9] S. Chapmann et T. G. Cowling: *The Mathematical Theory of Non Uniform Gases* (Cambridge, 1953).
[10] S. F. Smerd et K. C. Wetsfold: *Phil. Mag.*, **40**, 831 (1949).
[11] J. F. Denisse: *Thèse* (Paris, 1949).
[12] K. Rawer, K. Bibl et E. Argence: *Mém. Soc. Roy. Liège*, **12**, 269 (1952).
[13] E. Argence, M. Mayot et K. Rawer: *Ann. de Geophys.*, **6**, 242 (1950).
[14] E. Argence: sous presse.
[15] K. Bibl et K. Rawer: *Journ. Atm. Terr. Phys.*, **2**, 51 (1951).
[16] H. E. Newell: *High Altitude Rocket Research Academic Press*, no. 4 (1953).
[17] K. Rawer et K. Suchy: *Ann. der Phys.* (à paraître).
[18] J. L. Alpert et A. A. Ainberg: *Abhand. aus der Sowjetischen Phys.*, **8**, 274 (1954).
[19] E. N. Bramley: *Proc. Inst. Electr. Eng.*, B **102**, 533 (1955).

SUPPLEMENTO AL VOLUME IV, SERIE X
DEL NUOVO CIMENTO

N. 4, 1956
2° Semestre

Echo Sounding Experiments with Variable Frequency at Oblique Incidence.

W. DIEMINGER and H. G. MÖLLER

Institut für Ionosphärenforschung - Lindau über Northeim

(Presented by W. DIEMINGER)

It is well known that radio propagation conditions over any distance may be deduced from the results of observations at vertical incidence by simple calculations [1-2]. However, these calculations imply some assumptions, which are not completely certain and, perhaps as a result of those assumptions, the observations of radio communication conditions do not completely agree with the calculations. Therefore it seems more desirable to compare radio communication conditions with direct observations of the different modes of propagation.

Perhaps the most efficient system to achieve this task is to use the pulse method not at vertical incidence but to observe the pulses by a receiver in the wanted distance from the transmitter. Experiments of that kind on fixed frequencies were carried out all over the globe and gave valuable information about paths of propagation. Much more information may be obtained by using the sweep frequency method between the sender and a remote receiver.

A few experiments of that nature were carried out in Canada, Great Britain, Japan, USA and Germany, and some results were published recently [3-6]. The scarcity of those experiments is caused without any doubt by the technical difficulties of synchronisation between the transmitter and the receiver.

1. – Experiments.

To get useful records perfect synchronism is necessary between the pulse recurrency frequency of the transmitter and the time base of the recorder at the location of the receiver. In addition exact tuning between transmitter and receiver must be maintained during the whole frequency sweep. The basic

idea of the equipment used in Germany is to derive every control from a pair of crystal clocks granting a relative stability of frequency which is of the order of 10^{-8}.

The complete equipment consists of a self consistent vertical sounding station which is located at LINDAU in the middle of Germany. In addition there is an independent receiver, which may be located at any wanted distance from the vertical sounding station. Both sets are build in such a way that, starting the movement of the tuning condensers at exactly the same time and rotating them with exactly the same velocity, the deviation in tuning between both stations is less than 2 kHz in any part of the frequency range. In practice the start of the movement is controlled by a signal derived from the crystal clock and the accuracy of revolution is guaranteed by a synchronous motor fed from the crystal clock through an amplifier. The pulse recurrency frequency of the sender and the time bases of the oscilloscopes and recorders are derived from the crystal clocks in a conventional manner.

The equipment covers a frequency range between 1 and 16 MHz within 8 minutes. The initial setting of the crystal clocks is achieved by a special time signal sent out from LINDAU. Minor corrections during the course of the experiments may be obtained by operating a fine trimmer of the crystal clock at the far end so that the remaining phase shift of the echo traces on the recording film will become a minimum.

The most delicate problem of the experiments is the antenna. The vertical rhombic which is used for vertical incidence mostly, is not suitable for long distance experiments because the radiation is concentrated to high angles of departure. A horizontal rhombic on the other side is not very convenient because its vertical polar diagram has one or several minima which may spoil certain modes of propagation. During our experiments the problem of antennas was not solved completely. On the transmitting end mostly a V shaped cage dipole of a length of 2×45 m was used. At the receiver for distances up to 400 km two double doublets and for the experiments over a path of 1300 km a combination of two horizontal rhombics of different size gave rather satisfactory results.

For the shorter distances a power of 10 kW and a pulse length of 100 μs was used, for the 1300 km path the power was increased to 50 kW and the pulse length reduced to 50 μs.

Information about the technical details will be given elsewhere.

2. – Results.

It is not possible for limitations of time to discusse here fully the results of the experiments carried out with the equipment described above over dis-

tances between 200 and 1300 km. Moreover the very cumbersome reduction of the records is by far not yet finished. So I shall confine myself to the most

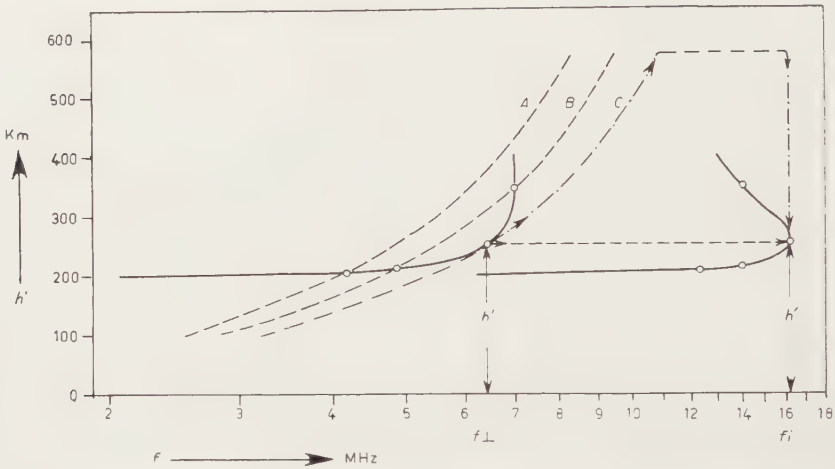

Fig. 1. – Graphical derivation of oblique incidence conditions from vertical incidence measurements. (After N. Smith).

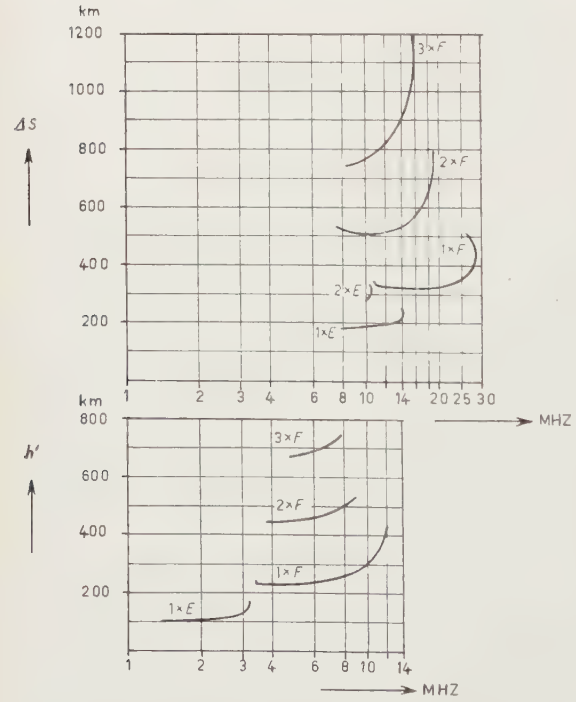

Fig. 2. Propagation paths over 2 000 km deduced theoretically from vertical incidence record.

spectacular results. The common method to derive propagation conditions from the results at vertical incidence is a graphical one given by Newbern Smith [2]. A curve $\cos i = f(h')^p$ representing the angle of incidence as a function of the virtual height of reflection for a given distance (« Transmission-curve »), is superimposed to a $h'f$-curve plotted on semilogarithmic paper (Fig. 1). The intersection-points of both curves will give the virtual height for the so called equivalent frequency $f_i = f_1/\cos i$. By shifting the transmission curve parallel to the abscissa the virtual height is obtained

for every equivalent frequency. It may be understood from Fig. 1 that, for certain positions of the transmission curve (e.g. B) there exist two intersection points corresponding to two possible modes of propagation. The lower one corresponds to a ray reflected at a relatively flat angle, the upper one to a ray impinging on the ionosphere at a steeper angle. In addition it may be seen, that the maximal usable frequency is determined by the position C of the transmission curve where the latter is the tangent of the $h'f$-curve. The appropriate value of $1/\cos i$ is called MUF-factor and the corresponding equivalent frequency MUF (maximal usable frequency).

Using that method, in Fig. 2 the upper diagram is deduced theoretically from the vertical $h'f$-curves in the lower part. The characteristic features of the oblique diagram are: 1) The critical frequency of the $1\times F$ path is shifted considerably towards higher frequencies. That shift decreases with increasing order of the reflection. 2) Near the critical frequency there are two branches corresponding to the normal and the high angle ray. Those theoretical results agree generally with the records obtained in oblique incidence experiments (Fig. 3). However, the high angle ray, for example, is extended over a frequency range which is much larger than expected by theory. This

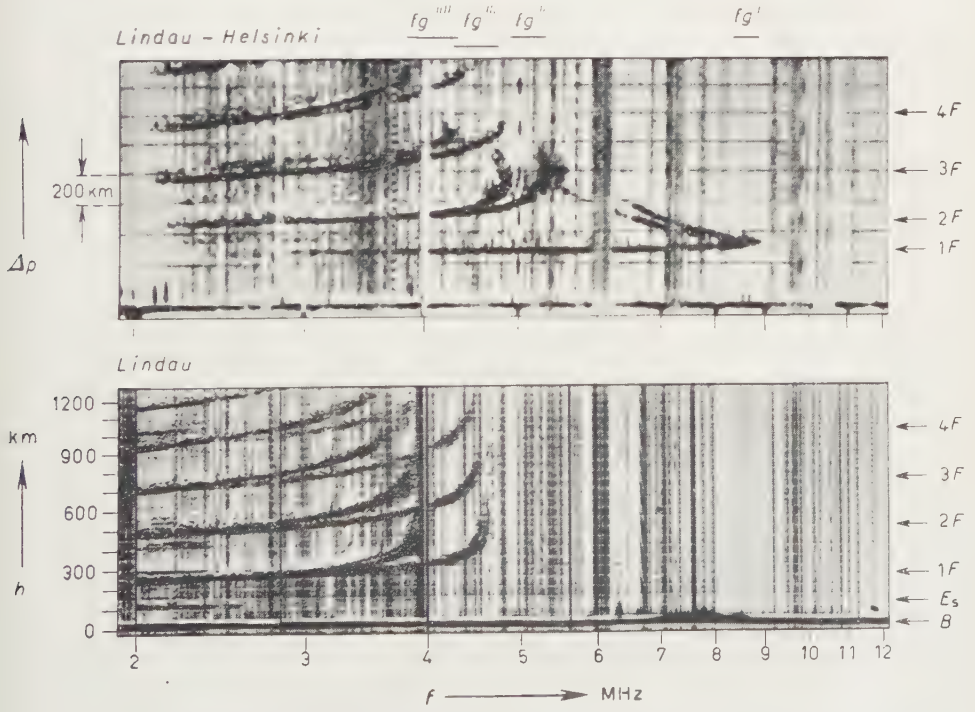

Fig. 3. – Comparison of an oblique incidence ionogram (distance 1 300 km) with a simultaneous vertical incidence ionogramm.

special result agrees well with the observations made in Canada and USA in similar experiments [4, 6]. There also was found a very strong high angle ray.

That strong high-angle ray has some interesting consequences as to the propagation over long distances. Considering the low-angle ray only, it is found that the maximum distance for a single hop F-path is 3000 ÷ 4000 km, depending on the height of reflection. For greater distances the single hop

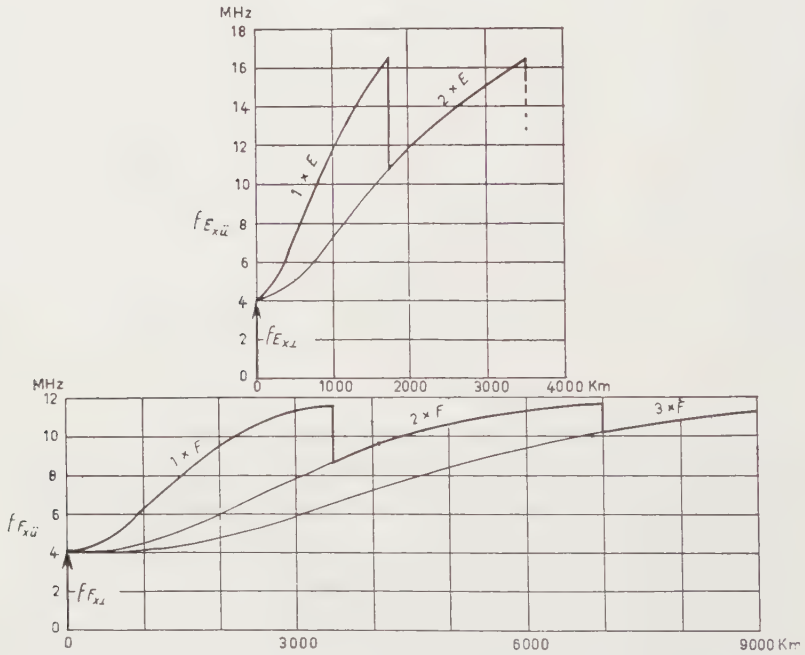

Fig. 4. – MUFs for E- and F-reflection as a function of distance between sender and receiver.

will be screened off by the horizont. A point which is a little farther than the limiting distance will be reached by multiple hops only. Since the angle of incidence for the two-hop path is steeper than that of the single hop, the MUF-factor will decrease suddenly as soon as the limiting distance is reached (Fig. 4). That is no longer true when the high angle ray is taken into account. Even for a distance for which the single hop low-angle ray is screened off, the high angle ray is still possible. So the MUF will be controlled by the high angle ray which leaves the earth tangentially. It can be shown easily that for that reason the MUF-factor does not drop suddenly as soon as the limiting distance for single-hop transmission is reached.

On an oblique incidence $P'f$-diagram one might expect the following phe-

nomena (Fig. 5): For the limiting distance the single hop and the double hop are fully developed (*a*). At a somewhat greater distance the low-angle ray and a part of the high-angle ray are screened off by the horizont (*b*). Next only a little bit of the high-angle ray remains (*c*). For the limiting distance of the double hop finally nothing but the 2*F* trace survives (*d*). The MUF however remains nearly constant for all distances. (*) Some indications of these « high-angle tails » are present on records made on fixed frequencies between Germany and USA in 1948.

Another interesting question is the field strength of the high-angle tail. Without any doubt the strength of the high-angle ray will be less than that of the low angle ray. In addition the amplitude will decrease towards the top of the « tail » owing to the polar diagram of the radiating antenna. So we might expect a more or less steady decrease of the amplitude when moving from the junction of the low- and high-angle two-hop ray towards higher frequencies. That corresponds well with observations of BECKMANN on long distance communication [8]. He found that, in the average, the field strength as a function of frequency does not fall suddenly as soon as the theoretical MUF is reached but decreases slowly in a range of several MHz. Presumably that is caused, at least partly, by the high-angle tails.

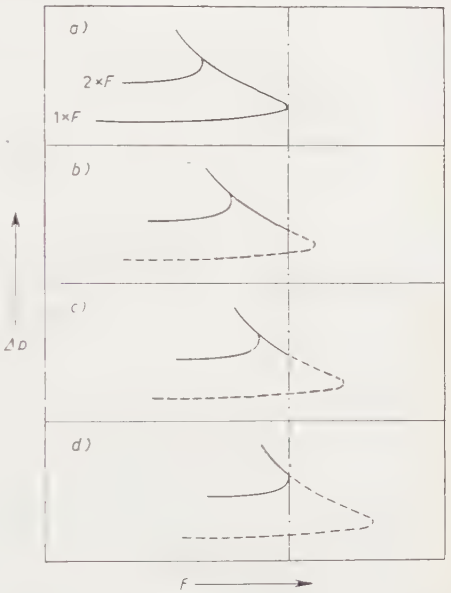

Fig. 5. – Screening off-effect of 1F-path with increasing distance. The high angle ray is less affected than the low angle ray.

Obviously the value of the MUF factor depends, apart from the distance, on the virtual height of the reflecting layer (Fig. 4). The value for the E-layer raises much steeper than that for the F-layer. That is illustrated by the records shown in Fig. 6. The upper record is taken over a distance of 220 km, the lower one is the simultaneous record at vertical incidence. The critical frequency of the E-reflection is shifted much more to higher frequencies than that of the F-reflection. The corresponding MUF-factors are 1.02 for F-reflection and 1.19 for E-re-

(*) *Note added on proof:* Fig. 5 is a rough sketch only. A more thorough investigation shows that the MUF decreases gradually as soon as the limiting distance is reached. The decrease however is much less than assumed formerly.

flection in excellent agreement with the theoretical values. That effect is considerably enlarged for medium distances. For a distance of 1300 km, for ex-

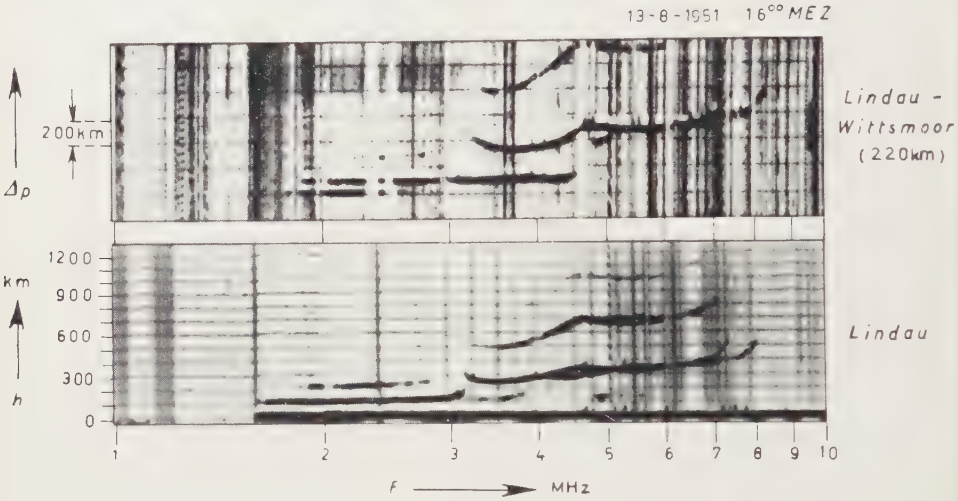

Fig. 6. – Comparison of an oblique incidence ionogram (distance 220 km) with a vertical incidence ionogramm. The E-MUF is shifted much more towards higher frequencies than the F-MUF.

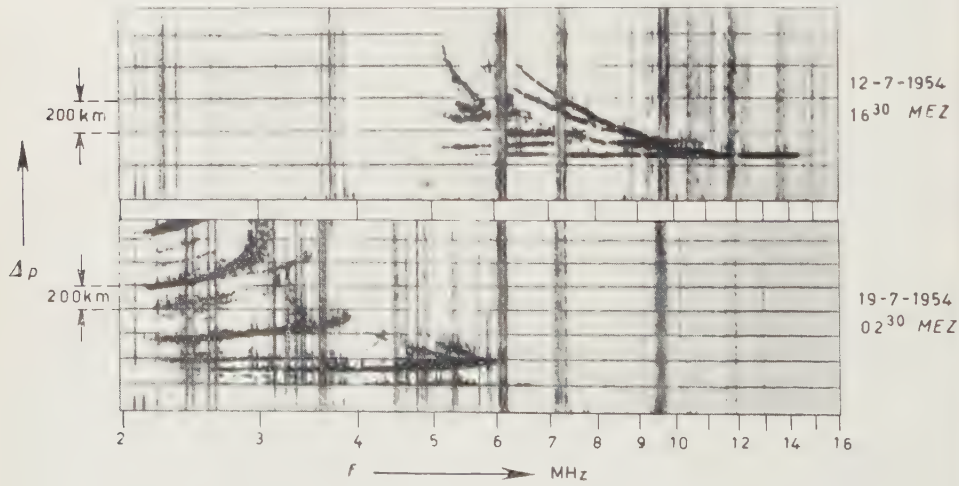

Fig. 7. – Day and night ionogramms at oblique incidence (Lindau-Helsinki, 1300 km).

ample the MUF-factor for E is 3.8, whereas the MUF-factor for F is 1.8 only. That means that on summer days when the critical frequency of F_2 is relatively low, the MUF is controlled by the E-layer instead of the F_2-layer. That is illustrated by the upper part of Fig. 7. The lowest trace corresponding to

E-reflection extends to much higher frequencies than the next one, which corresponds to the single-hop F-path. During night time (Fig. 7 lower part) when sporadic E is absent, the MUF is controlled by single F-hop obviously.

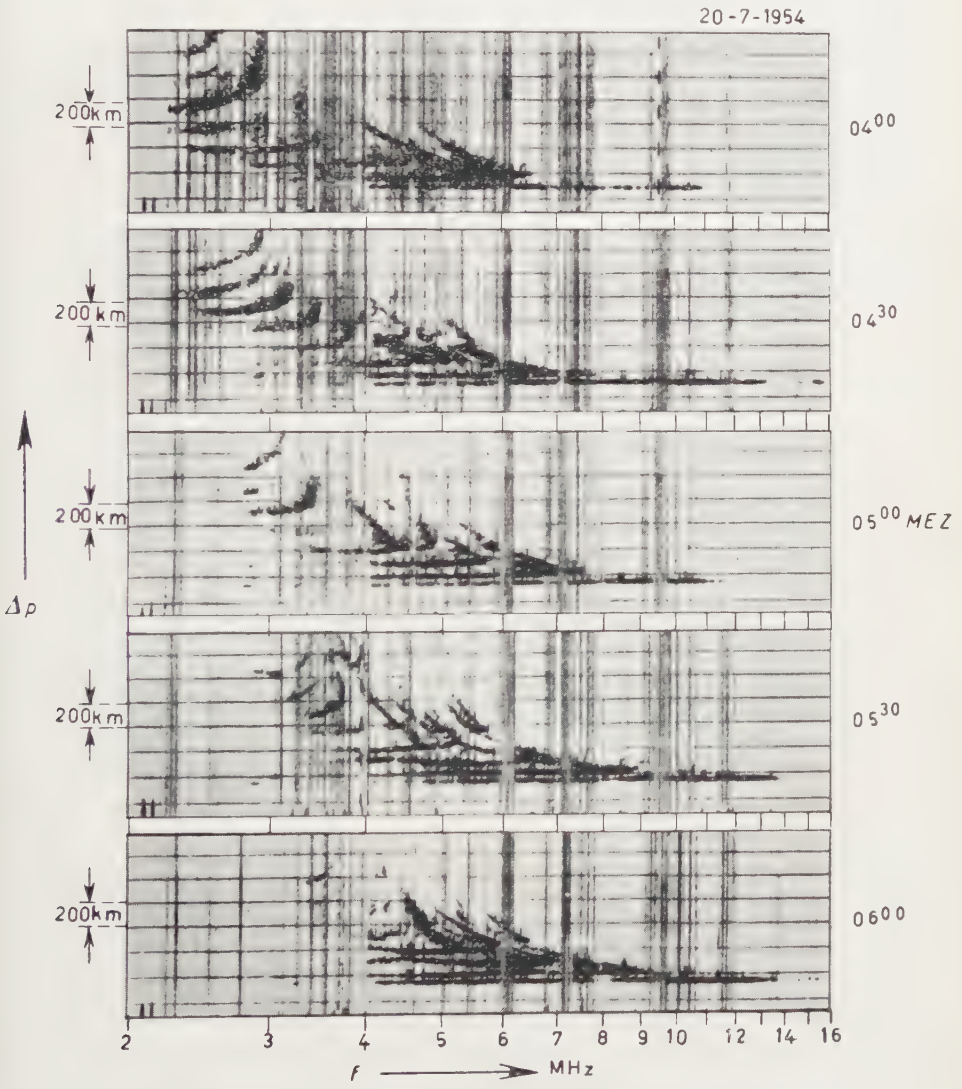

Fig. 8. – Oblique incidence ionograms at sunrise (Lindau-Helsinki, 1 300 km).

It is much more to be learnt from those records. With raising sun the lower frequencies are cut-off by absorption and blanketing (Fig. 8). It is interesting to note that the paths corresponding to low angles of elevation are more affected than the higher ones. Another feature may be of practical im-

portance. The number of paths is less numerous near the MUF. In addition the time delay of the first echo is a minimum somewhat below the MUF, and increases for lower frequencies. On the record of 0500 h for example, the

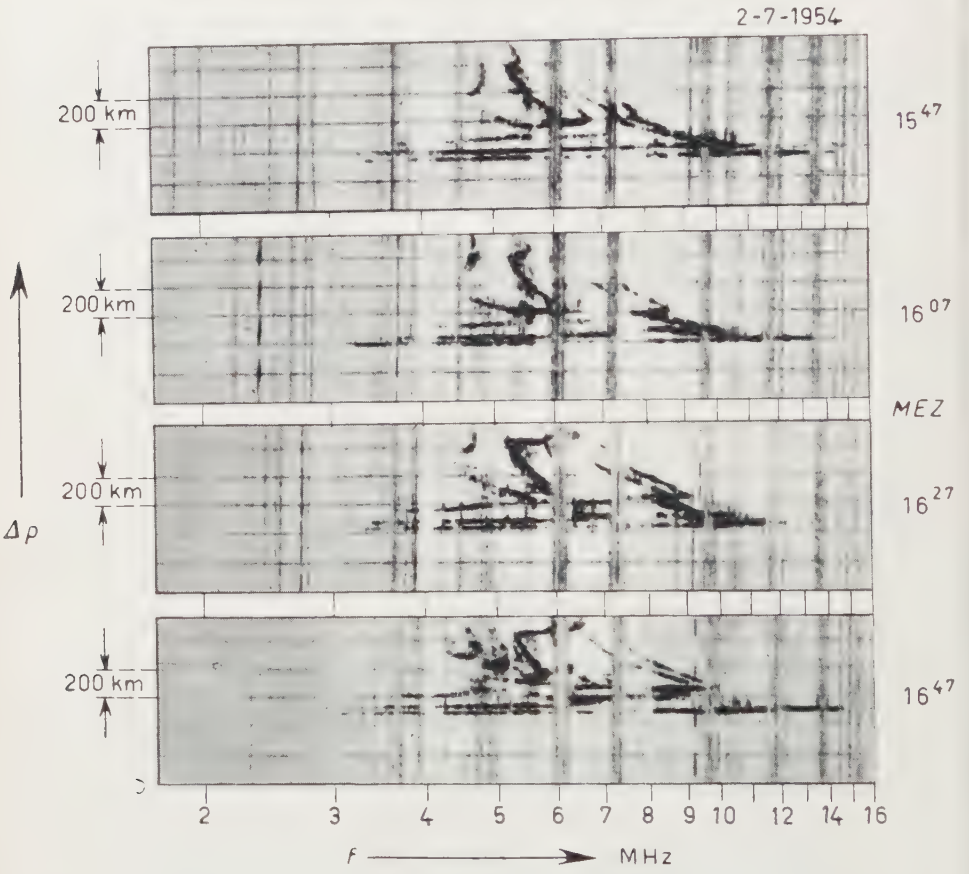

Fig. 9. – Oblique incidence ionograms during the last phase of an ionospheric storm (Lindau-Helsinki, 1 300 km).

first signal on 3 MHz is 0.2 ms later than on 6 MHz. That perhaps explains an observation reported by Boella, that the delay of a time signal may be greater on lower frequencies.

By the next series of records (Fig. 9) a special case is illustrated which arises during ionospheric storms, when the critical frequency of F_2 drops and the virtual height raises. Then on medium to long distances the MUF of F_1 will become higher than that of F_2, and the propagation will be controlled by F_1 mainly. So the influence of the ionospheric storm will be not as bad as expected from the effect in F_2.

Finally I shall discuss the following question. It is always found that, for medium latitudes the MUF observed in radio communication service is higher than that predicted by theory, or in other words: predictions are pessimistic. As far as it may be seen from our experiments over 1300 km that is caused by several effects: 1) For many periods the MUF is controlled by sporadic E, which cannot be predicted exactly for well known reasons. Such an effect is illustrated by Fig. 10. On the first record the MUF is controlled

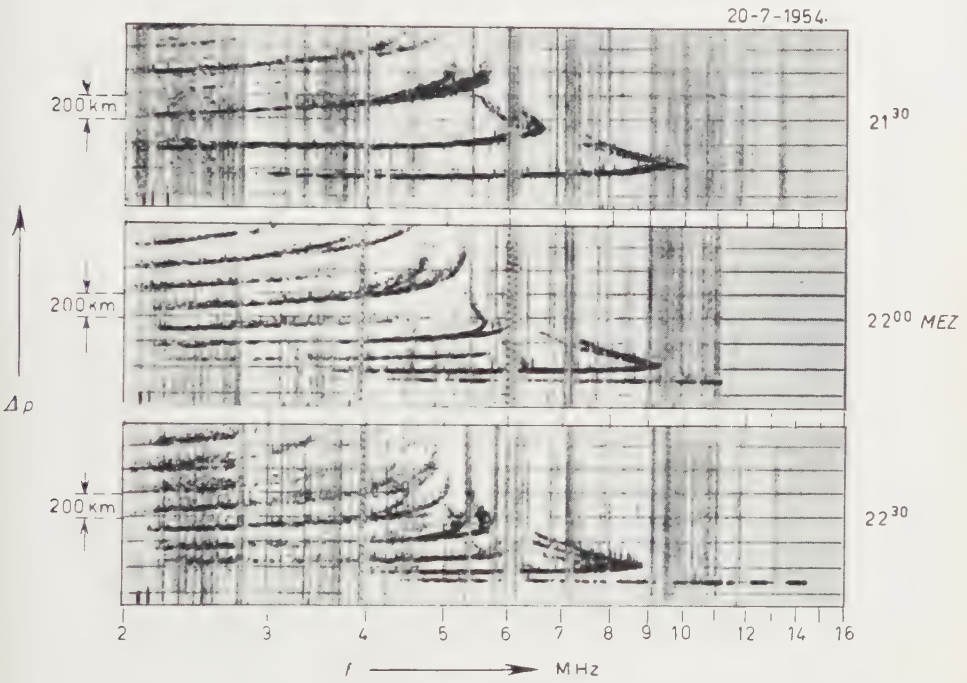

Fig. 10. – Effect of sporadic E on effective MUF (Lindau-Helsinki, 1300 km).

by the F-layer. In the next record, however, the MUF has been raised from 9.5 to 11 MHz and in the third one from 8.8 to 14.7 MHz by sporadic E. 2) It has been found that on many occasions there is a « nose » of echoes extending well beyond the junction of the high- and low-angle ray. It may be seen on Fig. 11 that that nose is present on 3 of the 5 records. The shape of the nose is rather variable. Sometime it covers a frequency range of 2 MHz. It was found also in experiments carried out by the Bureau of Standards in USA [9, 10]. It should be stressed that the phenomenon is not at all a regular one. It is present for about 30% of the time at night. We have no figures yet for daylight conditions because during day time the $1 \cdot F_1$ hop coincides with the $2 \times E$ hop so that no clear distinction is possible whether

there exists a « nose » or not. For night time conditions however it can be stated that the nose is not a regular phenomenon but is bound to some special

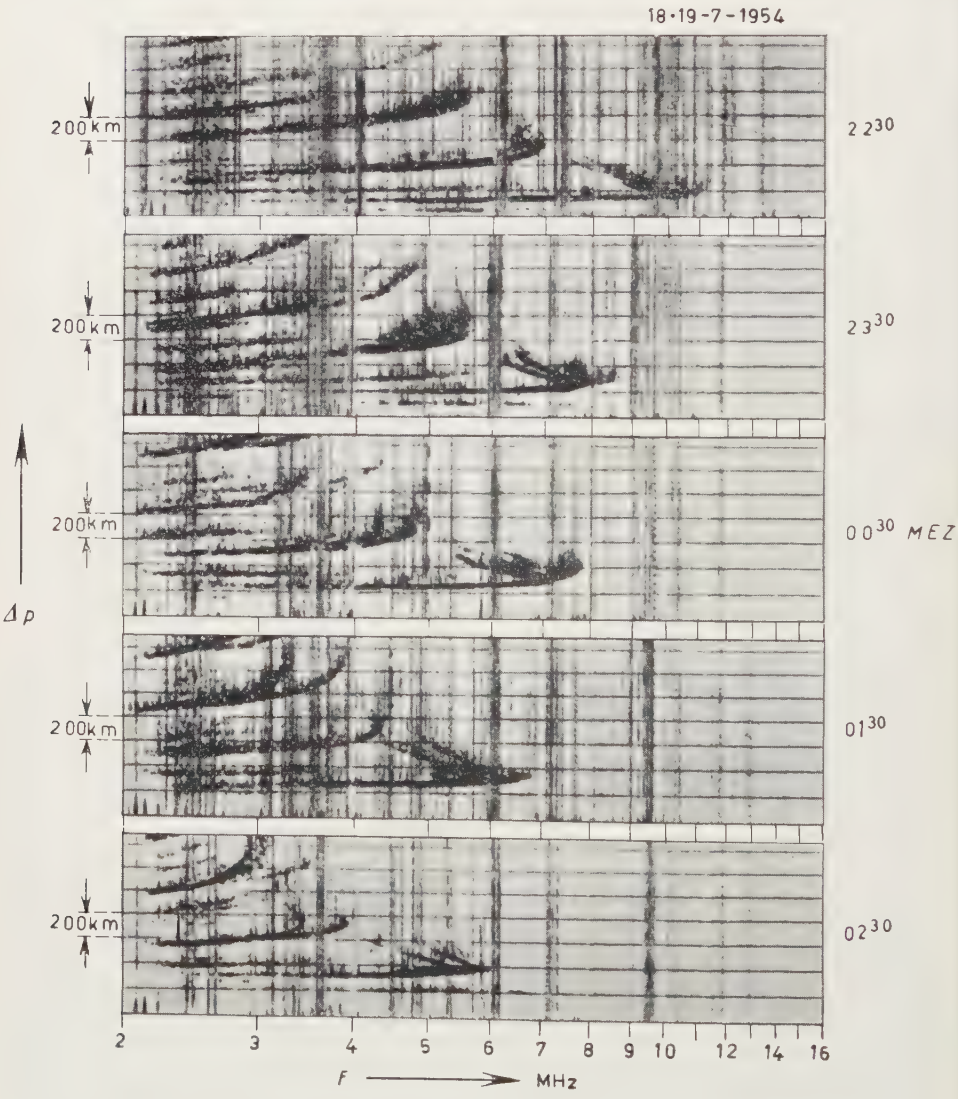

Fig. 11. – « Nose » in front of 1×F-MUF (Lindau-Helsinki, 1 300 km).

conditions in the ionosphere. We do not know yet those conditions. No correlation has been found till now with sporadic E, spread F-echoes or rapid changes in reflection height. 3) On nearly all records which where reduced till now, the junction between high- and low-angle ray is higher than that calculated from vertical incidence soundings at the midpoint of the trajectory.

That effect is shown in Fig. 12. The record on the top (*a*) is taken at Ekenäs which is only 25 km off the midpoint of the circuit Lindau-Helsinski. Using

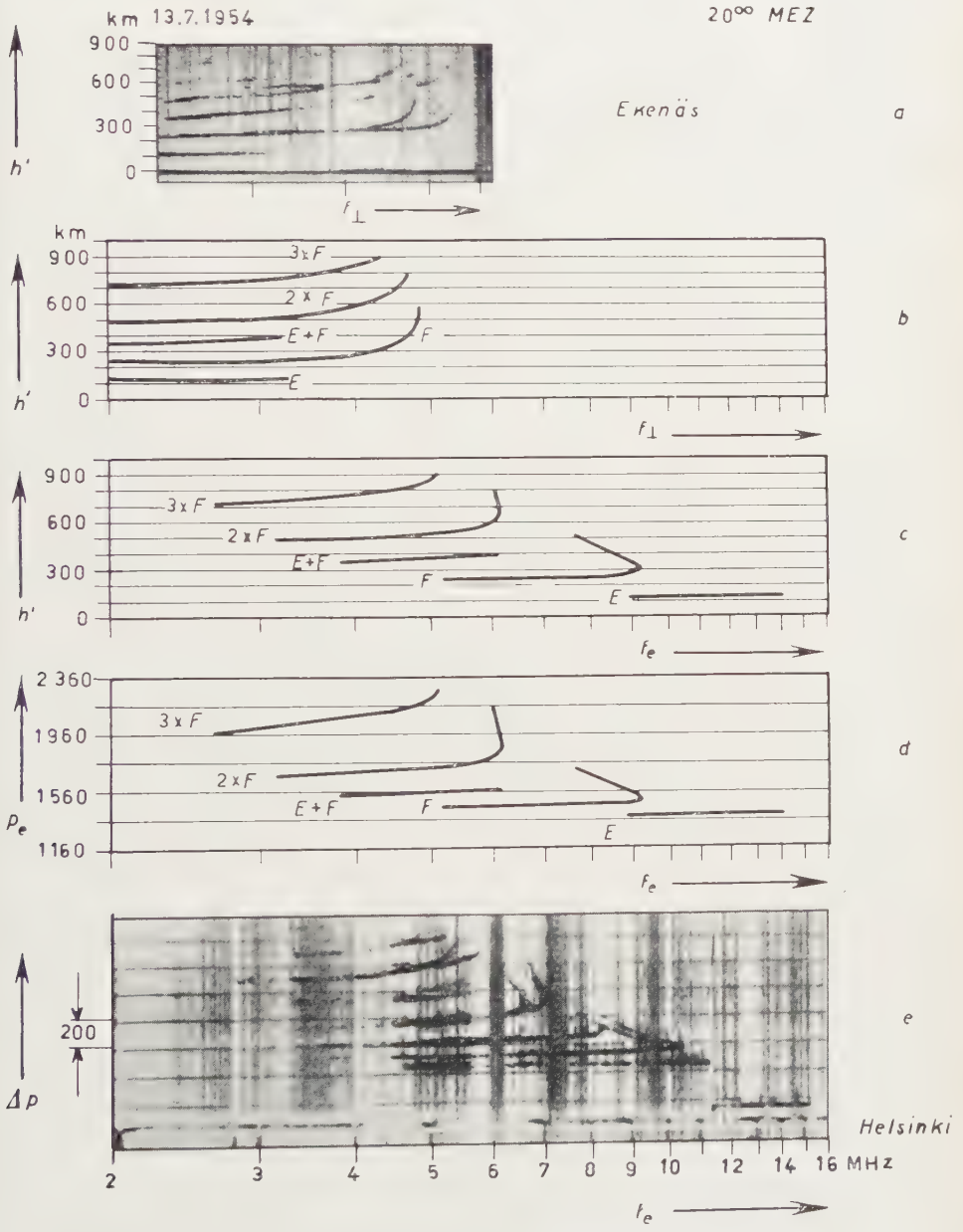

Fig. 12. – Comparison between propagation conditions deduced theoretically from vertical soundings at the midpoint of the trajectory with actual propagation conditions. (Ionogram of Ekenäs by courtesy Mr. STOFFREGEN, Upsala Ionospheric Observatory).

the method of Smith, the equivalent oblique record for the ordinary ray is constructed in *b*), *c*), *d*). The lowest row finally shows the record taken simultaneously on the path Lindau-Halsinski. In spite of general agreement of the different curves the observed MUF of the single hop ordinary F-path is 0.7 MHz higher than the calculated one. For the double hop the difference is 0.4 MHz approximately. Considering all results obtained till now it may be stated that the observed ordinary MUF over the path of 1300 km is $0 \div 16\%$ higher than the calculated one. The observed median value is 4% higher than the calculated one. That result is somewhat contradictory to the publications of other investigators stating that the calculated and observed values « usually agree rather well » [6, 9]. On has to wait for more data to explain that discrepancy. There are very few cases when the observed value was well below the calculated one. It has been found, however, that in all those occasions, the virtual height of the oblique path was distinctly higher that that of the equivalent vertical record taken in the middle of the path. That may be caused by retardation anywhere along the oblique trajectory which cannot be chequed by the observation in the midpoint alone. To get conclusive results a series of vertical sounding stations would be necessary spread along the whole path.

From the point of view of prediction service it may be concluded that the method of conversion commonly used is at least safe. The overwhelming part of the observations give higher values than the calculations, leaving a safety margin in practical use.

Summing up it may be stated that the oblique incidence sweep frequency method is well able to solve problems which cannot be explained either by vertical incidence measurement or operational observations alone. By misfortune Europe is not a suitable field for such experiments because really long distance experiments are badly hampered by very efficient barriers set up by customs and administrations.

OSSERVAZIONI ED INTERVENTI

— K. Rawer:

J'ai trois remarques à ajouter à ce très intéressant exposé de Mr. Dieminger:

1) En ce qui concerne la distance maximum de transmission d'un bond il est vrai que le rayon de Pedersen permet en principe une liaison sur une plus grande distance. J'ai une fois calculé le décrément géometrique correspondant; j'ai ainsi trouvé une portée de 5000 km dans le cas d'une puissance de l'ordre de 1 kW. Mais dans la realité pratique, le diagramme des antennes joue ici un role prépondérant. Les angles de départ bien faible sont difficils à réaliser. J'ai l'impression que la distance maximum supposée par le CRLP américain (4000 km) est nettement trop grande pour la plupart

des applications. Nous avons effectué des essais entre Tananarive (Madascar) et Djibouti (Somalie). Sur cette distance de 7 000 km aucune liaison a pu etre établie sur les fréquences corréspondantes au parcours $2F$ mais seulement sur celles de $3F$. Ceci montre que 3 500 km est souvent une trop grande distance pour etre parcourue dans un seul bond. Ce problème de l'influence des antennes devrait encore etre étudié en détail.

2) Quant à la comparaison entre les résultats pratiques et les prévisions il semble pourtant exister quelque cas où les prévisions sont trop optimistes. M. Mc-Allcock de New Zeeland m'a cité un cas très net de ce genre dans la région équatoriale. Il est possible que dans cette région la méthode américaine des « points directeurs » soit mal adaptée aux faits.

3) Enfin nous avons aussi essayé une vérification du calcul de la MUF. Nous avions une liaison en impulsion (fréquence fixe) sur une distance de 1 200 à 1 300 km avec una statio de sondage au milieu. Les heures de coupure des échos $1F$ ont été fixées des enregistrements à la minute près. On a après déterminé la MUF théorique de cet instant à partir des ionogrammes du point milieu. Cette comparaison a été effectuée par le Dr. Eyfrig. Nous avons trouvé que les prévision étaient trop pessimistes meme avec la méthode exacte de N. Smith. Comme correction de la méthode abituelle (où l'on prend M-3000 et un coéfficient de réduction pour obtenir le facteur de la distance intéressante) on arrive à environ 6%. Cette correction a été introduite récemment dans nos prévision de routine.

SUPPLEMENTO AL VOLUME IV, SERIE X
DEL NUOVO CIMENTO

N. 4, 1956
2° Semestre

On a Correlation between the Electronic Density of the E-Layer and the 500 mb Surface Position.

A. NAPOLETANO

Centro di Studi di Radiopropagazione
Istituto di Fisica Tecnica dell'Università - Napoli

1. – Premise.

At the international Congress of Physics held at Bologna on September 1950, the author gave a report on the results obtained by a correlation of the depth of modulation in the effect of gyro-interaction (for which the values are regulated by the ionization condition of the E-layer) and the barometric pressure on land using the data obtained in the gyro-interaction studies of May-June 1950. In order to avoid the moderating action of the earth surface on atmospheric pressure, the author extended his study also to high level pressures using charts representing the isobaric surfaces of 500 mb.

An inverse correlation at ground was then found; whilst at high levels a lowering of the 500 mb surface, which was due to an increased density of the air mass, corresponded to a higher depth of modulation.

The results indeed were far from being satisfactory because of the scarce and uncertain data available. It was then thought that a retrospective examination should be made using the data of measurements made in the gyro-interaction studies of 1948 and 1949, which, although not many in number, were however more numerous than those obtained in the studies of 1950.

2. – Experiments.

The author decided to leave definitely out of his studies the data of pressure at ground as these are influenced in various ways by the air masses which are immediately in contact with the earth surface, and to carry out an exclusive study of the isobaric surface of 500 mb. He then used absolute

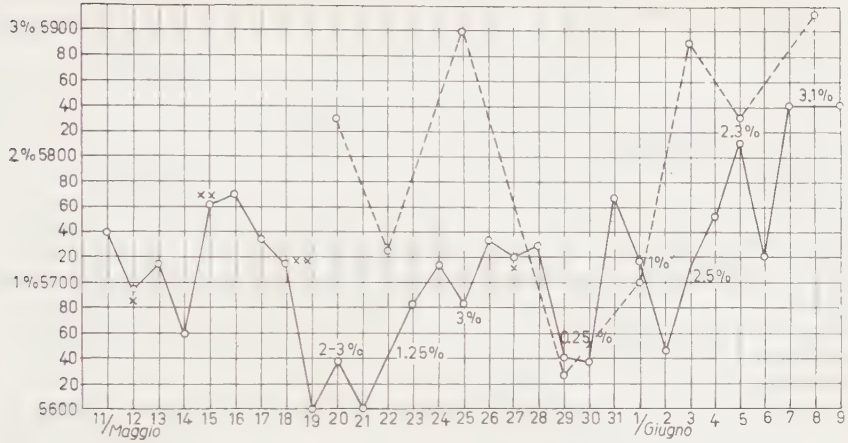

Fig. 1. – x Phenomenon which was not noted; xx Phenomenon which was noted without being registered. – 1948: Heights of the 500 mb surface in mgp and modulation depths.

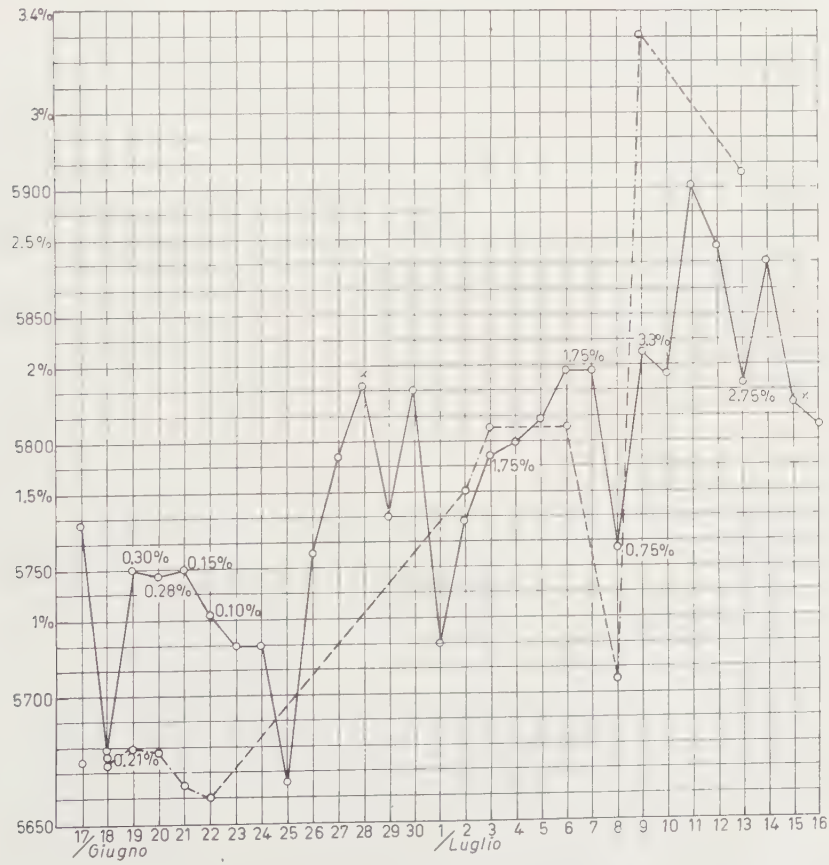

Fig. 2. – 1949: Height of the 500 mb surface in mgp and modulation depths.

topographical charts developed at 0300 G.M.T. and from these, with a good approximation, the height of 500 mb expressed in geopotential metres were calculated on Foligno's vertical where the reflection of the radio-waves occurred.

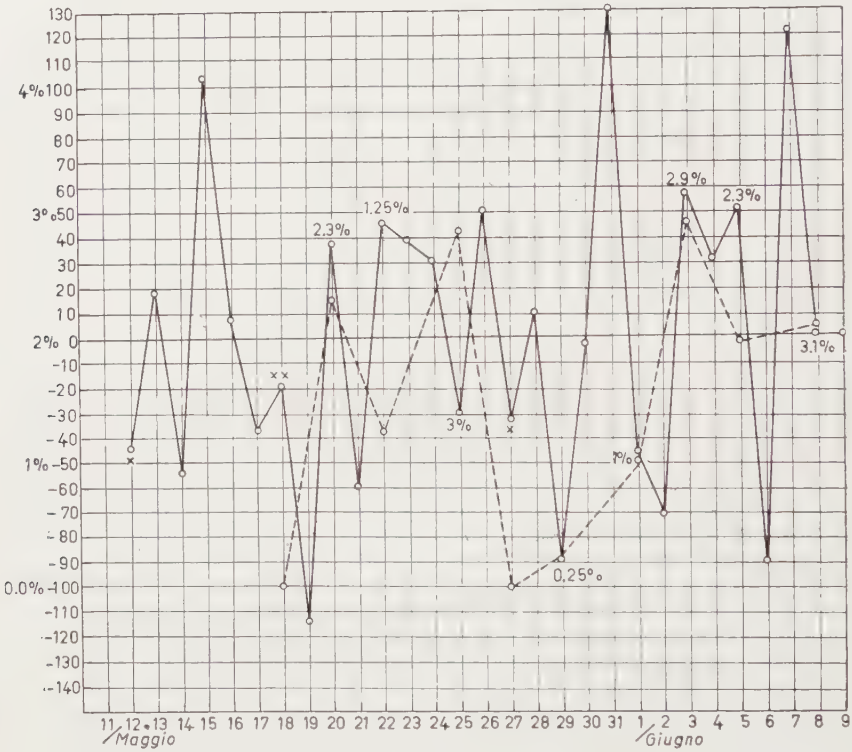

Fig. 3. – x Phenomenon which was not noted; xx Phenomenon which was noted without being registered. - 1948: Variations in 500 mb surface heights in mgp and modulation depths.

As a first approximation, a graphical method was used to compare the series of figures including the height of the 500 mb surface and the parasitic modulation depth (Fig. 1-2) and those including the variations of the 500 mb surface height during 24 hours and the same modulation depths (Fig. 3-4). After examining the diagrams a relation between the series of parasitics which had been compared was thought likely to exist. It was then decided to use a mathematical method to estimate the significance of the correlations.

For a practical calculation of the « correlation coefficient » the equivalent formula was used

$$r = \frac{\Sigma XY - n\alpha\beta}{\sqrt{(\Sigma X^2 - n\alpha^2)(\Sigma Y^2 - n\beta^2)}}.$$

In which α and β indicate, as usual, the mean values of X and Y, respectively. It can be seen that the present expression is preferable to the usual one, in-

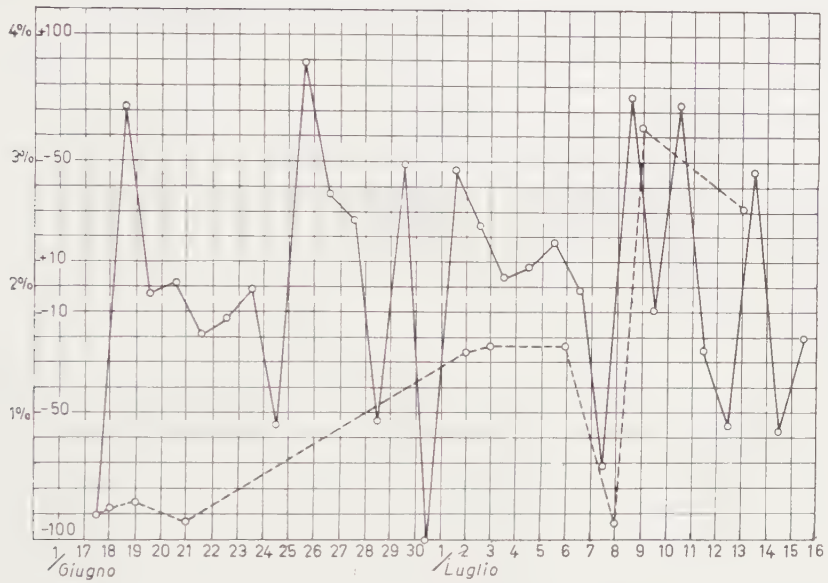

Fig. 4. — 1949: Variations in 500 mb surface heights in mgp and modulation depths.

sofar as the X and Y terms of the given series are directly used. The scheme suggested by PHILIPS [1] was used by the author as a layout for the calculations.

3. – Results.

The first relation found was a direct correlation between the surface heights and the modulation depth, with a correlation coefficient of over 52% when $\Delta h/\Delta t$, namely, the variation in height during the 24 hours preceding the day of the experiments and the modulation depths, were correlated, also in this case a direct correlation with a correlation coefficient of about 50% was found.

From these first results it was possible to deduce that, when the value of the surface height increases, in the majority of the cases observed, the modulation depth is higher. This means that the decrease in density accompanying the increase in height, insofar as the weight of the surface remains the same, is related to the increase in modulation depth; and vice versa when the surface decreases.

4. – Conclusions.

The higher modulation depths occurring when the 500 mb surface density decreases, leads one to think that there is a relation between the electron density of the E-layer and the air density at the 500 mb surface. This happens because gyro-interaction depends directly on the electron density of the E-layer.

The electronic structure of the ionosphere is for the greater part governed by the sun radiations which act also in the lower atmosphere. Their action on the ionosphere is, however, almost instantaneous, whilst on the lower atmosphere it is considerably delayed; in the case of the daily variations, for instance, by about one hour.

Moreover, it is not the same parts of the solar spectrum that act on the ionosphere and the lower atmosphere. The ionosphere, as we know, depends on the ultraviolet radiation, which is absorbed long before it reaches the earth; in addition, needless to say, it is affected by corpuscular radiation, which has no bearing on lower atmosphere phenomena.

Thus it is evident that the possibility to explore the condition of the ionosphere—in our case the E-layer—offers a mean to deduce, with some anticipation, what the behaviour of the atmosphere layers not immediately in contact with the Earth is going to be.

In particular, furthermore, some reactions by the meteorological atmosphere on the ionosphere might be revealed; this is possible if one takes into consideration the fact that very large masses play an important role as stated by the *Bureau*. The increases in electron density in the area might be interpreted under this point of view; they should also be attributed to an intensive ionization process by an exterior ionizing agent which, aided by the condition of low density in the atmosphere above the earth surface, reaches the level of the E-layer.

If followed with some continuity and by using adequate means, the effect of gyro-interaction might have a wide practical scope, insofar as registration during the hours of night would make it possible to foresee, with a certain anticipation, the fluctuations of the atmosphere at various levels (it is in fact not to be excluded that the same correlations might be found, for example, at the level of 200 mb, that is to say, at about 12 km). This being the case, a surface with a positive $\Delta h/\Delta t$ will indicate a decreased density and the same time show the presence at that level of a flow of warm moist air, whilst, with a negative $\Delta h/\Delta t$, it would indicate an increased density and show a flow of cold dry air.

If an adequate number of stations were distributed, for example, throughout Europe, we would be in a position to build some charts with given constant pressure which could be used for altimetrical navigation.

* * *

The author wishes to thank Prof. M. CUTOLO for the material provided and the assistance and useful advice kindly given during the course of this study.

REFERENCE

[1] F. M. PHILIPS: *Short method of obtaining a Pearson coefficient of correlation etc.*, in *Monthly Weath. Rev.* March 1922.

SUPPLEMENTO AL VOLUME IV, SERIE X
DEL NUOVO CIMENTO

N. 4, 1956
2° Semestre

Remarks on the Connection between Mode Theory and Ray Theory.

H. BREMMER

Philips Research Laboratory - Eindhoven

1. – Introduction.

The theories dealing with the propagation of radio waves via the ionosphere are based either on the concept of rays or on that of characteristic functions (also known as eigenfunctions, or modes). The former theories result in an expansion each term of which corresponds to a ray that reaches the receiver after a special number (r) of reflections in the ionosphere (r-hop transmission), whereas the expansions of the latter theories are of the same type as those describing the field in wave guides. The convergence of the ray expansions is best at short distances from the transmitter, that of mode expansions is best at great distances. In this paper the connection between both types of expansions is shown for a model based on simplifying conditions which do not concern the essential features of the problem.

2. – The Assumptions Defining the Model under Consideration.

Two simplifications will be introduced, viz.

a) The effect of the curvature of the earth and the surrounding ionosphere is accounted for by using the modified refractive index $M(r) = r\mu(r)/a\mu(a)$ instead of the actual refractive index $\mu(r)$ (r = distance from the centre of the earth to the point of observation in the atmosphere, a = radius of the earth). The role of the quantity M is well known for troposheric propagation. In the case of ionospheric propagation however, the small difference between M and μ is less important since the relative variation of these quantities rather than that of r is most pronounced there.

b) The effect of the electrical behaviour of the earth is accounted for by the approximative boundary condition

$$\frac{\partial \Pi}{\partial z} = \gamma \Pi \,, \tag{1}$$

at the earth's surface for the amplitude of the Hertzian vector. In the two representative cases of a vertical electric-dipole transmitter (antenna of length l short compared to the wavelength) and of a vertical magnetic dipole (realized by a small loop antenna in an horizontal plane) this Hertzian vector is directed vertically throughout, and the field components can be derived from it by differentiations. If k_0 and k_1 represent, for a given frequency, the wave number in the air surrounding the transmitter, and the corresponding complex wavenumber in the earth, the constant γ reads as follows for the two above types of transmitter.

$$\gamma_e = -i \frac{k_0^2}{k_1^2} \sqrt{k_1^2 - k_0^2}; \qquad \gamma_m = -i \sqrt{k_1^2 - k_0^2} \,.$$

A physical interpretation of the boundary condition (1) involves that all plane waves penetrating from the air into the earth are refracted in one and the same direction, namely the limiting direction corresponding to grazing incidence. The validity of (1) as an approximation is therefore made plausible by observing that the nearly horizontal plane waves dominate in the propagation over distances which are not too small. Moreover, it has been shown by Hufford [1] that the well known approximative theory of Sommerfeld for the propagation through a homogeneous atmosphere above a plane earth can be based on the condition (1).

The two above simplifications lead to the following formulation of our problem. In the space $z > 0$ above the earth the three-dimensional wave equation

$$\left\{\nabla^2 + k_0^2 M(z)\right\} \Pi = 0 \,, \tag{2}$$

has to be solved under the following conditions, $M(z)$ being the modified refractive index at a height z above the flattened earth: *a*) the boundary condition (1) at $z = 0$, *b*) the radiation condition concerning the vanishing at infinity ($z = +\infty$), *c*) the condition of a singularity proportional to R^{-1} near the transmitter (R = distance from the transmitter to the point of observation).

3. – The Determination of the Ray-Theory Solution.

For simplicity's sake we shall restrict ourselves to a vertical electric dipole at the point $(0, 0, h)$ at a height h above the earth's surface. The amplitude of the Hertzian vector for the free-space field of such a dipole reads

$$\Pi_{pr} = \frac{I_0 l}{c} \frac{\exp[ik_0 R]}{R},$$

in which the dipole moment $I_0 l$ is the product of the current amplitude I_0 and the antenna length l. The equivalent integral

$$\Pi_{pr} = \frac{I_0 l}{c} \int_0^\infty \mathrm{d}\lambda \frac{\lambda}{\sqrt{\lambda^2 - k_0^2}} J_0(\lambda\varrho) \exp[-\sqrt{\lambda^2 - k_0^2}\,|z-h|], \tag{3}$$

($\varrho = \sqrt{x^2 + y^2}$ distance from the transmitter in horizontal direction) can be interpreted as a superposition of cylindrical waves

$$J_0(\lambda\varrho) \exp[\mp\sqrt{\lambda^2 - k_0^2}\, z] \tag{4}$$

characterized by the parameter λ.

With the aid of the asymptotic expression of the Bessel function J_0 we find that each of these cylindrical waves propagates at great distances in directions making an angle $\tau(\lambda) = \arcsin(\lambda/k_0)$ with the vertical axis $\varrho = 0$ through the transmitter; these propagation directions are complex for $\lambda > k_0$. Further, the waves with a negative sign in (4) propagate in an oblique upward direction, those with a positive sign in an oblique downward direction; the square root in (4) is defined as having a positive real part. According to (3) the transmitter emits upward cylindrical waves into the space above the level $z = h$, and downward cylindrical waves into the space below this level.

We now assume the transmitter as situated in a homogeneous layer $0 < z < z_1$ (while $z_1 > h$) between the surface $z = 0$ of the earth and the bottom $z = z_1$ of the stratified atmosphere characterized by $M(z)$. In order to obtain the total field in the homogeneous layer we first investigate what happens to a special downward cylindrical wave $W_0 = J_0(\lambda\varrho) \exp[\sqrt{\lambda^2 - k_0^2}\, z]$ leaving the transmitter. On its arrival at the earth's surface this wave produces a reflected cylindrical wave propagating upwards. The ratio of both waves at $z = 0$ constitutes a reflection coefficient $R(\lambda)$ so that the reflected wave can be represented by

$$W_1 = R(\lambda) J_0(\lambda\varrho) \exp[-\sqrt{\lambda^2 - k_0^2}\, z].$$

The reflection coefficient R can be derived from the requirement that (1) should apply at $z=0$ to the sum of W_0 and W_1. We thus obtain the expression

$$R(\lambda) = \frac{\sqrt{\lambda^2 - k_0^2} - \gamma}{\sqrt{\lambda^2 - k_0^2} + \gamma} . \tag{5}$$

The reflected wave W_1 will reach the bottom $z = z_1$ of the stratified atmosphere and generate in the latter a rising and a downcoming wave the sum of which can be represented by $J_0(\lambda\varrho)\cdot f_\lambda(z)$. This function has to satisfy the threedimensional wave equation (2); this involves the one-dimensional wave equation

$$\frac{d^2 f_\lambda}{dz^2} + \{k_0^2 \cdot M^2(z) - \lambda^2\} f_\lambda = 0 , \tag{6}$$

for $f_\lambda(z)$. The downward waves produced in the stratified medium due to its inhomogeneity result into another downward cylindrical wave W_2 when passing the bottom level $z = z_1$. The ratio at $z = z_1$ of the new wave W_2, and of the wave W_1 producing it, again constitutes a reflection coefficient, $T(\lambda)$ say; hence:

$$W_2 = R(\lambda)\, T(\lambda) \cdot J_0(\lambda\varrho) \exp\{-\sqrt{\lambda^2 - k_0^2}(z - 2z_1)\} .$$

The new atmospheric reflection coefficient $T(\lambda)$ has to be determined from the condition that the transition at $z = z_1$ from the sum $W_1 + W_2$ into the function $J_0(\lambda\varrho)\cdot f_\lambda(z)$ (in which f_λ is characterized, apart from a constant, as being a solution of (6) satisfying the radiation condition) has to be continuous both for the wave function itself, and for its derivative with respect to z. The value of $|T(\lambda)|$ will be very small if the ray trajectory corresponding to the elevation angle $\tau(\lambda)$ should traverse the atmosphere (ionosphere) instead of being bent downwards.

The down-coming wave W_2 in its turn produces a rising wave W_3 on its arrival at the earth's surface; the wave W_3 once again splits at the level $z = z_1$ into a wave penetrating into the stratified atmosphere, and another down-coming wave W_4, and so on. Similar waves are generated by the upward cylindrical waves contained in the primary field (3). All the rising and down-coming cylindrical waves, thus produced in succession in the homogeneous layer $0 < z < z_1$, are to be added in order to obtain the total field there. The expression obtained after the summation is simplest in the limiting case $z = z_1 = h = 0$. This reduction of the homogeneous layer to a zero thickness implies that the stratification starts right at the earth's surface while both transmitter and receiver are to be assumed on the latter.

A final integration over λ according to (3) then yields the expression:

$$(7) \qquad (H)_{z=h=0} = \frac{I_0 l}{c} \int_0^\infty \mathrm{d}\lambda \, \frac{\lambda}{\sqrt{\lambda^2 - k_0^2}} J_0(\lambda \varrho) \left\{ 1 + R + (1+R)^2 \sum_{r=1}^{\infty} R^{r-1} T^r \right\}.$$

4. – Interpretation of the Ray-Theory Solution (7).

Obviously the contribution due to the first part $1+R$ of the form in brackets of (7) describes the ground wave since only this contribution remains in the absence of a stratified atmosphere ($T = 0$). The structure of the remaining r terms constituting the skywave indicates the production of such a term by r successive atmospheric reflections, and $r-1$ intermediate reflections against the earth's surface.

One of the two factors $1+R$ occurring in each sky-wave contribution arises from the fact that each primary rising cylindrical wave leaving the transmitter is accompanied by a secondary rising wave; the latter is produced by the reflection against the earth of the down-coming wave that is the image of the primary rising wave with respect to the transmitter level $z = h$. Both rising waves only differ by a factor R in view of the infinitesimal thickness of the homogeneous layer $0 < z < z_1$, which was assumed in (7). An additional factor $1+R$ is due to a corresponding situation at the receiver, which is also in accordance with the reciprocity theorem. The occurrence of the factor $(1+R)^2$ in (7) has thus been explained.

The ray-theory expansion (7) is the rigorous solution for the problem defined in Sect. 2. This solution should not be confused with the geometric-optical approximation of the ray theory. The latter approximation can be derived from (7) with the aid of the saddlepoint theory for exponential integrals while replacing $T(\lambda)$ by its W.K.B. approximation.

5. – Expansions into Characteristic Functions.

The first expansion of this type was given in WATSON's [2] paper dealing with a spherical homogeneous ionosphere limited by a sharp boundary. Other expansions were given by RYDBECK [3] and SCHUMANN [4]. The possibility of such expansions of the wave guide type is very plausible; in fact, the guiding effect of the ionosphere can be explained roughly by the property that the cross-dimension of the wave guide formed by the space between the earth and the ionosphere is larger than the wavelengths of all radio frequencies. SCHUMANN's publications concern the particular modes which occur if the wavelength becomes of the same order of magnitude as the mentioned cross-section;

these modes play a role at the very low frequencies which may be excitated by thunderstorms.

6. – The Transition from the Ray-Solution (7) to an Expansion in Terms of Eigenfunctions.

This transition can be performed by the following steps. First we evaluate the sum of the geometric series which is represented by the sky-wave terms in (7). The convergence of this series is guaranteed by the fact that $|R|$ and T should be smaller than unity in view of their role of reflection coefficients. Next we can transform the integration path along the positive axis of the λ-plane into a path along the complete real axis provided we replace the Bessel function J_0 by half the corresponding Hankel function $H_0^{(1)}$. We thus arrive at

$$(\Pi)_{z=h=0} = \frac{I_0 l}{2c} \int_{-\infty}^{\infty} \mathrm{d}\lambda \, \frac{\lambda}{\sqrt{\lambda^2 - k_0^2}} \, H_0^{(1)}(\lambda \varrho) \, \frac{(1+R)(1+T)}{(1-RT)} \,. \tag{8}$$

In its turn the new integration path can be transformed into that of a contour around the complete half plane $\mathrm{Im}\,\lambda > 0$ since the integrand vanishes exponentially at the infinite points of this contour. The only singularities of the integrand in the domain enclosed by the contour are the poles at the zeros of the denominator $1 - RT$. The multi-valuedness of the square root in (8) is compensated by the other factors as may be verified by the substitution of the proper value (8) for R and the corresponding value

$$T(\lambda) = \frac{\sqrt{\lambda^2 - k_0^2} + f'_{\lambda s}(0)/f_{\lambda s}(0)}{\sqrt{\lambda^2 - k_0^2} - f'_{\lambda s}(0)/f_{\lambda s}(0)} \,. \tag{9}$$

for the atmospheric reflection coefficient. The integral (8) therefore reduces to the sum of the residues at the poles λ_s; the latter are to be determined as those zeros of the equation

$$1 - R(\lambda_s) \cdot T(\lambda_s) = 0 \tag{10}$$

that are situated above the real axis of the λ-plane.

The equation (10) can be interpreted as a resonance condition. It expresses that the (complex) propagation direction $\tau_s = \arcsin(\lambda_s/k_0)$ is such that the corresponding cylindrical waves (4) are unchanged after a combined atmospheric reflection (multiplication by T) and reflection against the earth (mul-

tiplication by R) in the infinitesimal layer $0 < z < z_1$. The determination of the roots λ_s thus amounts to a quantization of angular directions. The final expression for the sum of the residues becomes, after some reduction with the aid of (5) and (9):

$$(11) \qquad (\Pi)_{z=h=0} = \frac{2\pi}{ic} I_0 l \sum_s \lambda_s \frac{H_0^{(1)}(\lambda_s \varrho)}{\left\{\frac{\partial}{\partial \lambda} f_\lambda'(v)\right\}_{\lambda_s}} .$$

7. – Final Remarks.

The above derivations show the fundamental significance of the integral (8). In fact, it comprises both the ray-theory treatment and the expansion in eigenfunctions; the former is obtained by developing the denominator into a geometric series, the latter by taking the sum of the residues of the corresponding contour integral.

We further mention that the eingenvalues λ_s to be derived from (10) constitute a discrete spectrum. This is a consequence of the boundary condition (1). For more complicated boundary conditions the field inside the earth has to be determined simultaneously with that in the atmosphere; as shown by FRIEDMAN, the continuous contribution to the λ_s-spectrum than only disappears for a perfectly conducting earth.

REFERENCES

[1] G. A. HUFFORD: *Quarterly Applied Math.*, **9**, 391 (1952).
[2] G. WATSON: *Proc. Roy. Soc., London*, A **95**, 546 (1919).
[3] O. E. H. RYDBECK: *On the propagation of radio waves* (Göteborg, 1944).
[4] W. O. SCHUMANN: *Zeits. angew. Phys.*, **4**, 474 (1952).

SUPPLEMENTO AL VOLUME IV, SERIE X
DEL NUOVO CIMENTO

N. 4, 1956
2° Semestre

On Some Characteristics of the F_2 Region in South America.

I. RANZI

Istituto di Fisica dell'Università - Firenze

1. – Pre-Sunrise Shrinkage of the F_2 Region, followed by Rapid Expansion.

One of the most interesting phenomena observed at Buenos Aires is a contraction of the F_2 layer, which begins 3-4 hours before sunrise and is followed by a very rapid expansion: it is remarkable that the expansion occurs always with an anticipation of about two hours with regard to the morning minimum of f_{0F_2}.

As an example, in Fig. 1 are reproduced some records of March 30th, 1950.

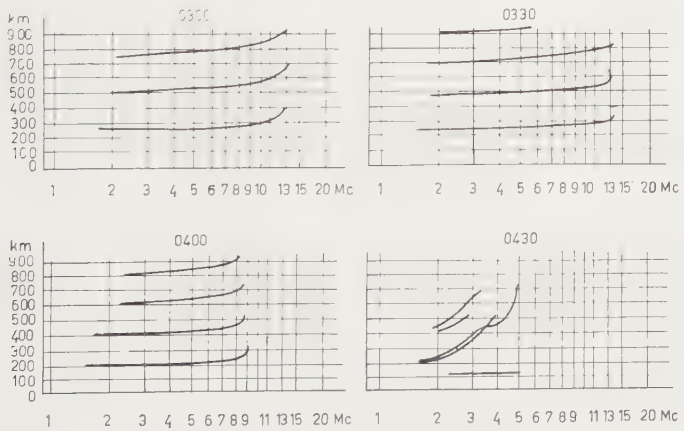

Fig. 1. – Shrinkage of the F_2 region, followed by a rapid expansion, as observed at Buenos Aires on March 30th, 1950. Sunrise occurred at 0606 (60° W M.T.).

In some cases, the minimum virtual height has become so low as 190 km, less than the minimum in the afternoon, and the semithickness was reduced

to 20 km. The expansion is so rapid that the semithickness may increase from 20 km to 130 km in 30 min.

Just before the expansion occurs, the f_{0F_2} begins to decrease rapidly, while, during the contraction, it remain constant or increases.

The phenomenon shows a greater amplitude when the critical frequency remains high after midnight and when the magnetic activity is low.

D. F. Martyn [1], in a recent development of his theory, has suggested the existence, at low latitudes, of horizontal drifts of ionization, which are directed westward by day and eastward by night; thus there will be a considerable convergence of ionization on the dawn meridian; this convergence is more intense at the lower levels in the F_2 region.

It is well known that, in relation with the anomalous behaviour of the magnetic diurnal variation in the western hemisphere, the dynamo currents must be more intense in the southern part of the western hemisphere: we may exspect that the convergence of ionization, which depends on the dynamo currents, will be more remarkable in the same region.

2. – Midday Decrease of f_{0F_2} in Western Antarctics.

As I referred [2], the f_{0F_2} presents, at the Deception Island (63 0 S; 60 7 W), a very pronounced summer midday decrease, so that the maximum occurs about at 23 hours of the local time. Subsequent observations confirmed the phenomenon. In the Arctics and in the eastern Antarctics we do not observe a similar behaviour of f_{0F_2}.

The western Antarctics presents the lowest magnetic dip, as compared to other zones at the same geographic latitude: so that, to the normal increase of the tidal velocity with the latitude, is associated a very low decrease of the horizontal component of the earth magnetic field; consequently, the vertical drift of ionization, which depends on this component and on the tidal velocity, will be more intense in that region.

According to Martyn's theory, we must expect more pronounced midday decrease of f_{0F_2}.

REFERENCES

[1] D. F. Martyn: *Report of the Conference on the Physics of the Ionosphere* (Cambridge, September 1954), p. 260.

[2] I. Ranzi: *Geofisica Pura e Applicata*, **23**, 65 (1952).

OSSERVAZIONI ED INTERVENTI

— K. Rawer:

Je ne rappelle pas avoir vu un cas d'une variation si nette que celui qui nous a été présenté. Néanmoins le phénomène ne me parait pas tout à fait exceptionnel. Il est malheureux que la station de Huancayo est toujours considérée comme étant typique pour la région tropicale. Ceci n'est pas vrai: sur l'équateur magnétique où se trouve Huancayo les couches F_2 ainsi que E_s ont un caractère tout à fait exceptionnel. Buenos Aires ne se trouve pas trop loin du maximum d'ionisation qui se produit, de jour en F_2, au sud de l'équateur magnétique. Or, nous retrouvons à Dakar qui est située sur l'endroit correspondant au nord de l'équateur des phénomènes comparables. On y a souvent cette distension rapide d'un couche assez fortement ionisée durant les dernières deux ou trois heures de la nuit. Le maximum d'ionisation que l'on obtient est souvent inférieur à celui qui est observé en Europe centrale. Nos anciennes idées suivant lesquelles existait un maximum d'ionisation sur l'équateur avec une diminution progressive vers le nord et vers le sud doivent être complètement revisées. Une théorie plus complète tenant compte de tout ces phénomènes est désirable.

SUPPLEMENTO AL VOLUME IV, SERIE X
DEL NUOVO CIMENTO

N. 4, 1956
2° Semestre

The Ionized Aurora.

N. C. GERSON

Geophysics Research Directorate, AF Cambridge Research Center
Air Research and Development Command
Cambridge, Mass.

1. – Introduction.

Although radio wave probings of the ionosphere have become routine during the past two decades, similar scientific studies of the aurora are very recent. As with radio astronomy, the use of radio waves introduces a new and potentially powerful tool in the research. Much additional information concerning the physics and mechanisms of the aurora, and its production, decay and changes will result from these studies. Further, data on the use of the ionized aurora for communication purposes will arise from examinations now in progress or yet to be undertaken. For purely statistical purposes, radio wave observations on the aurora remove the continual limitation imposed by inclement weather and cloudiness on luminous auroral observations.

The ionized aurora is associated with the visual aurora. It usually accompanies the visual aurora although it does not seem to be coincident with it in space or possibly even in time. As the visual and the ionized aurorae presumably are both formed by the same group of bombarding particles, they undoubtedly bear some relationship to each other as well as to the energy of the auroral primaries. This aspect of the ionized aurora has scarcely been investigated and constitutes an important problem in auroral physics and communications research.

This paper will present some results obtained during an examination of the ionized aurora. Most of the data were obtained at a radio frequency of 50 MHz.

2. – Description of Method.

Generally, two methods have been utilized in investigating the ionized aurora. The first involves single station operation using radar methods, and is analogous to the vertical incidence, fixed frequency probing technique employed in ionospheric studies. The second method requires two stations, with a transmitter at one site and a receiver at the second. The latter method is similar to the oblique incidence propagation measurements made on the ionosphere. Both methods have their utility and effectively supplement each other as in the case of ionospheric studies.

The investigations described in this paper, were made with the two-station method. A frequency of 50 MHz was employed although in a few cases 144 MHz was utilized. The study took place in the three-year period from January 1949 to December 1951 inclusive. In the great majority of cases, the average radiated power was about 80 W. The observations were made on a co-operative basis by over 300 radio amateurs located in Canada, the United States and Mexico. However, most reports on the existence of the ionized aurora were obtained from northern United States and Canada; no auroral were observed at the Mexican stations.

Two amateurs were usually involved for each observation. Towards the end of the program, several continuously operating beacons were established. The beacons emitted signals which the radio amateurs sought during unusual propagation conditions.

It had been noted for some time that the reception of signals reflected from the ionized aurora generally required that the antennas of both the receiver and transmitter point somewhere in the direction of the visual aurora. It was found that this condition should be satisfied irrespective of the actual bearing of one station with respect to the second. In the co-operative radio amateur newtork, the two stations which established radio contact by means of reflections from the ionized aurora, were separated so that they could not communicated with each other during normal ionospheric conditions. When the ionized aurora was present, however, these stations could establish contact by directing their antennas towards the aurora.

Identification of the aurorally reflected radio waves could be made by the peculiar modulation impressed upon the transmitted signals. This modulation, which has been termed « auroral interaction », has several distinct aspects. The sound has been variously described as a « hissing », « garbling », « fluttering », etc., superimposed upon the wanted signal. Fading is common. When auroral interaction is severe, it is impossible to use radiotelephone; recourse must be made to continuous wave transmissions, and even then, the returned signals may be completely unintelligible. On other occasions, how-

ever, the signal has been very steady, indicating that the magnitude of auroral interaction was rather small.

The modulation impressed on the signal presumably arises from the rapid and random motion of electrons present in the ionized aurora. The auroral primaries bombard the atmosphere with speeds in excess of 10^8 cm/s. Some of this energy is imparted to the free electrons which are torn from the atmospheric particles during ionizing collisions. Each auroral primary could initiate a small « avalanche » of electrons. The resulting electron density in the ionized aurora reaches $10^8/cm^3$ and during strong displays may reach 10^9 to 10^{10} cm^3. The energetic, randomly moving electrons in the ionized aurora impress a noise modulation upon the desired signal which at times cause the severe interference.

In any event, the characteristic fading and the peculiar hissing which are noticed in signals reflected from the aurora generally allow an unambiguous determination of the propagation mode at the receiver site. Thus, aurorally propagated radio waves may be distinguished from those propagated by means of sporadic E, intense F_2 layer ionization, tropospheric (or ducting) effects, or meteor produced ionization.

In the study described here the data, after being received from the radio amateurs, were care screened, cross checked, and tabulated by hours of the day. This tabulation provided the basis for most of the results discussed below.

3. – Location of Ionized Aurora.

Before describing the statistical results, a possible method for locating an ionized aurora in space will be given.

Echoes should be received from the ionized aurora as long as it is visible from both the receiver and transmitter; i.e., as long as a sufficient number of Fresnel zones are illuminated by the transmitter and simultaneously visible from the receiver. To a first approximation, ray theory may be invoked.

In analyzing the data, it is clear that the greatest possible path from a given station to the ionized aurora is the tangent ray. Visual observations show unmistakeably that by far the most common altitude of the lower border of the aurora lies at an altitude of 100 km and that the most intense portions of the aurora are located close to this altitude. This condition will also be assumed for the ionized aurora; i.e., that the most common lower altitude is at 100 km and that the most intense ionization also occurs there. With this assumption, the tangent ray from the earth reaches the aurora at a distance of 1 100 km.

It will be assumed that the southernmost stations able to communicate by the aurora do so by means of the tangent ray from the lowest latitude station

of the station pair. This procedure allows a delineation of the southern extent of the ionized aurora which undoubtedly lies somewhat close, spacially, to the visual aurora.

Employing this method, the southern extent of an ionized aurora was located for the aurora of November 19, 1949. Fig. 1 indicates the location of some of the radio amateur station pairs (connected by a line) which were able

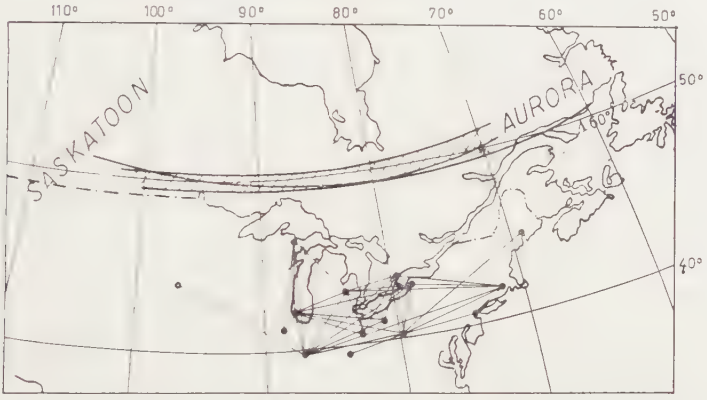

Fig. 1. Location of an ionized aurora by radio probing method.

to establish radio contact by means of the ionized aurora. The tangent ray from the lowest latitude station and Snell's law were employed to find a probable location of the ionized aurora. Also shown is the 60° N geomagnetic latitude. At Saskatoon, Canada, a visual aurora was observed « through the clouds. »

The above procedure, which may be materially improved, indicates one method for locating the ionized aurora. In the present study, broad beamed antennas were employed and antenna directions were but roughly reported. For a more accurate determination of the aurora, narrow beam antennas would be utilized and all angles carefully noted. A rotating or oscillating directive antenna is quite feasible and when used at a a grid of stations could effectively pinpoint the ionized aurora unambiguously.

4. – Seasonal Distribution.

From the hourly tabulations, the frequency of occurrence of the ionized aurora by months was prepared. A graph of the results is shown in Fig. 2. As would be expected, most ionized aurorae appear during the equinoctial

periods and least appear during the solstices. The greatest number of reported instances was found in April, and the next greatest number in October.

Some variation from the general conclusions given above for the entire period 1949-1951 is fuond in the curves for individual years. During 1949, for example, little increase in the occurrence of the ionized aurora took place during spring, whereas during fall a marked maximum was found. As individual years undoubtedly vary from a mean value or trend, these differences are not considered to be significant. A long series of data plotted by individual years, however, should indicate a gradual increase in auroral activity with increasing solar activity and vice versa. In any event, the consolidated results obtained during the study period are considered to be fairly representative of auroral conditions for this portion of the sunspot cycle.

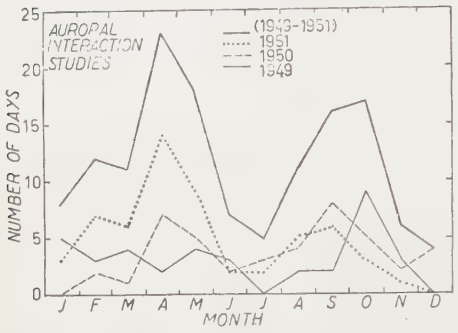

Fig. 2. – Seasonal distribution of the ionized aurora.

A comparison with statistics found for the visual aurora reveals the similarity in occurrence of the ionized and visual aurorae. Fig. 3 portrays the annual variation in appearance of the visual aurora for both the northern hemisphere (upper curve) and southern hemisphere (lower curve).

The strong correlation between the occurrence of the ionized and visual aurorae confirms the initial expectation; if found otherwise the results would perhaps be difficult to clarify. If it is postulated that the incoming auroral primaries both excite and ionize the atmospherie particles, then the excited and ionized volumes should bear some relationship to each other.

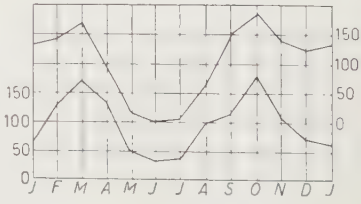

Fig. 3. – Seasonal distribution of the visual aurora.

If the bombarding auroral primaries produced cylinders of excitation and ionization, then the ratio of the radii of the two cylinders should equal some quantity, A, whose magnitude is as yet unknown. It is quite possible that the quantity A is energy dependent, but additional studies are required.

5. – Diurnal Variation of the Ionized Aurora.

It has frequently been assumed that strong auroral displays persisted consecutively for several days, but only being visible on successive nights.

Presumably they were not observed during daylight because the intense scattering by the lower atmosphere prevented their observation. It was generally believed that radio wave observations on the ionized aurora would reveal its presence during daylight.

The radio method, of course, allows the aurora to be kept under surveillance throught the twenty-four hour period. The results which the radio probings revealed were somewhat unexpected; the ionized aurora occurred during some daylight hours, but the frequency of occurrence was a minimum during the morning. The greatest number of reported cases was found during darkness.

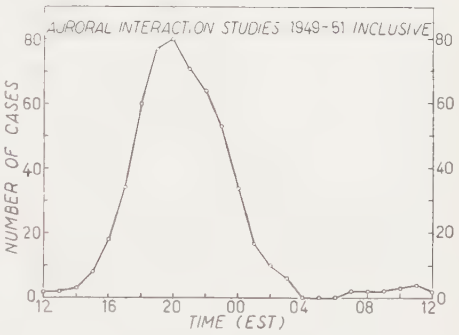

Fig. 4. — Diurnal distribution of the ionized aurora.

Graphed on Fig. 4 are the results of all data obtained during the period under study. A rather sharp maximum of occurrence is found near 2000 Local Standard Time. By far the greatest number of occurrences was reported in the interval from 1600÷2400 LST. The period from about 0400 LST to about 1400 LST had a minimum of aurorae. On the average, ionized aurorae first made their appearance at about 1400 LST, with a maximum about six hours later. Conditions on any given night, however, may depart considerably from this average. During the interval from 0400–0600 LST no cases were reported. It is believed, however, that the co-operating observers were not active during this interval and that additional observations are necessary before definite conclusions may be reached.

It is felt that the results after 0100÷0200 LST may be somewhat misleading for the same reason. In any event, considerably more observations are required in the interval from 0000÷1200 LST before the tentative results shown in Fig. 4 may be accepted with confidence.

While some fine details yet require resolution, there is no doubt regarding the very low frequency of occurrence of aurorae during daylight. This decrease has been observed by other investigators and seems somewhat typical for the (low) sunspot activity period from 1949 to the present.

Some interesting speculations may be made regarding the relatively small occurrence of ionized aurorae during the morning hours. Essentially, it would seem that some mechanism operates to prevent intense auroral ionization during the morning. Undoubtedly, the precession of the geomagnetic pole around the geographic pole changes the orbits of the incoming particles; however, whether this action is strong enough to deflect the auroral primaries from

the morning side of the planet, is not known. With homoenergetic solar particles, the precession could alter the size and shape of the zone of avoidance, and so cause the morning minimum actually observed. Another possibility concerns the ionizing action of solar radiation, which may act as a « poisoning agent » in the high atmosphere. In this sense, the presence of the shorter wavelength radiation from the sun raises the atmospheric atoms and molecules to higher energy states which may be more difficult to ionize by collision. This aspect of the problem—the « bite out » effect or the minimum of auroral activity during the morning hours—requires more intensive investigation.

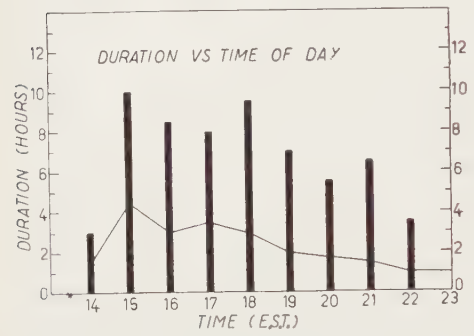

Fig. 5. – Duration of the ionized aurora beginning at the hour (LST) indicated.

Some remarks may also be made on the duration of individual ionized aurorae. The total time of their appearance is shown in Fig. 5. The solid vertical bars indicate the maximum duration of an ionized aurora for the hour shown as ordinate. The broken curve joining the bars is the median value of the duration for the hour concerned. In general, it appears that the duration of an ionized aurora may be somewhat related to the time it first appears. It would seem that aurorae forming in the early afternoon last longer than those appearing later in the day. If the medians alone are considered, the duration appears to decrease from about four hours at 1500 LST to about one hour at 2300 LTS.

It should be emphasized that the duration chart (Fig. 5) is very tentative and must be accepted as a graph of *minimum duration*. It is felt that the true duration of most ionized aurora is greater than that portrayed in this figure. Many of the co-operating amateurs went to bed after about 0200 LST, limiting the apparent duration of ionized auroral. Nevertheless, the graph is useful in that it presents lower limits to the duration. Future studies will clarify this aspect.

6. – Communication Possibilities of the Ionized Aurora.

On most occasions the occurrence of the aurora has been considered to signify the onset of a polar blackout condition. Radio communication on usual frequencies was disrupted, and the radio disturbance so common to the polar regions were initiated. It now seems clear, however, that radio propagation at the higher frequencies is quite feasible during these disturbed

conditions, provided an ionized aurora is present. The general effect is diagrammatically illustrated very simply in Fig. 6. -As is well known, under normal conditions broadcast and somewhat higher radio frequencies are reflected from the (E or) F_2 ionic layer, as shown by the solid ray from the transmitter to the ionic layer and thence to the receiver R_2. To very high radio frequencies, the ionosphere is transparent, and the radio ray from T escapes into space,

When an ionized aurora exists, however, marked changes may occur in the reflexion and scattering conditions. The presence of the aurora is revealed by the streamers of Fig. 6. They may cause strong absorption of the radio waves at broadcast frequencies; insufficient energy is returned to be detected by the receiver. Thus, in Fig. 6, the broadcast ray essentially stops at its intersection with the ionized aurora.

VHF frequencies also behave differently. Rather than escaping into space, as before the existence of the aurora, they are reflected or scattered to some site on the ground not previously in the « zone of contact » from station T. This site is indicated as R_1 on Fig. 6. In essence, the appearance of the ionized aurora has eliminated the radio contact between station T and receiver R_2, using normal frequencies, but has opened a new communication channel from T to R_1.

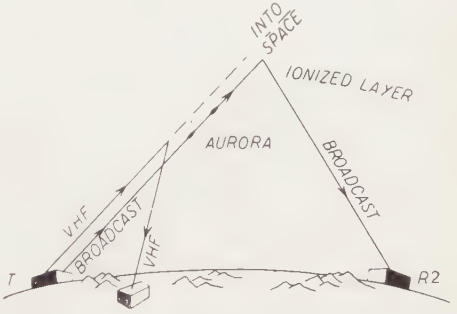

Fig. 6. – Simplified version indicating the effect of the aurora on radio ray paths. With no aurora present, and undisturbed polar ionospheric conditions, the broadcast ray is returned earthward after refraction by an ionic layer while a VHF ray escapes into space. With an ionized aurora (or disturbed polar conditions) the broadcast ray is absorbed, but the VHF ray is scattered earthward.

In general, the communication possibilities of the ionized aurora have scarcely been utilized. During periods of disturbed conditions, they open alternative channels for communication purposes, and even under normal conditions, they may allow new circuits to be employed.

It is known that the location of the brightest luminous aurora is not the location of the most intensely ionized auroral region. Nevertheless, directive antennas searching over the luminous aurora or in its vicinity may find the sufficiently dense ionization volumes needed to allow communication with predetermined relay stations.

It would be expected that the intensity of ionization when maximum solar activity is approaced would increase, thereby allowing higher radio frequencies to be employed. During periods of sunspot minimum, radio frequencies up to 220 MHz, reflected from the ionized aurora, have been used successfully for

communication purposes. At sunspot maximum, it is felt that the upper frequency limit should increase to 100 MHz or even considerably higher. During the period of maximum solar activity, however, the auroral primaries would probably be more energetic and more numerous, so that the disturbing effects of auroral interaction may be severe. In general, a greater number of new communication circuits probably could be established and operated even though the impressed noise modulation may increase. On a percentage basis, the trouble someness may be rather small.

In employing the aurora for the reflection of radio waves, the use of directive antennas would increase the signal to noise ratio. It may prove necessary to change the direction of the receiving and transmitting antennas to maximize signal strength. It may also be necessary, during sustained transmission, to again search for an optimum antenna bearing. In any event, better results may be expected if oscillating directive antennas are employed.

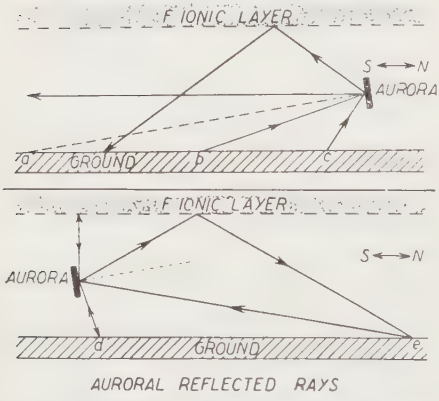

Fig. 7. Radio ray path from the ground to the ionized aurora, which is assumed to be oriented along the magnetic lines of force. Upper diagram, stations located south of the aurora; lower diagram, stations located north of the aurora.

It should be noted that the present study was conducted with rather low power, about 80 W. An increase in radiated power would of course improve the signal to noise ratio.

Undoubtedly, the best propagation results occur when both transmitting and receiving stations lie south of the auroral zone. This conclusion arises solely from a consideration of the dip of the magnetic lines of force in the auroral zone. Fig. 7 indicates the location of an ionized auroral sheet along the magnetic lines of force. The expected ray paths are indicated when transmitters are located (*a*) north and (*b*) south of the auroral zone. The upper half of the figure illustrates conditions for a transmitter located south of the aurora. The ionized aurora is inclined to the earth along the magnetic lines of force. The normal to the ionized aurora is shown dotted. Several ray paths are possible. A ray could be reflected along the normal to the ionized volume; it could proceed as a critical ray, or it could be multiply reflected by some ionic layer and the aurora. The actual ray path depends upon the transmission point. The lower section of Fig. 7 indicates corresponding conditions when the transmitter is located north of the ionized aurora. In this instance, it is much more difficult for an incident ray to be returned to the ground.

The optimum time for communication by means of the ionized aurora

seems to be from about 1600–2200 LST. The best time of the year for auroral propagation occurs during the equinoctial periods.

The use of scatter circuits, together with more widespread use of the ionized aurora will allow greater inroads to be made on positive communication conditions in the polar regions. The presence of the ionized aurora allows the attainment of propagation circuits not yet fully exploited.

BIBLIOGRAPHY

A. Aspinwall and G. S. Hawkins: *Journ. Brit. Astron. Ass.*, **60**, 130 (1950).
B. W. Currie and H. W. Edwards: *Terr. Mag. Atmos. Elec.*, **39**, 293 (1934).
B. W. Currie, P. A. Forsythe and F. Vawter: *Journ. Geophys. Res.*, **58**, 179 (1953).
N. C. Gerson: *Nature*, **167**, 804 (1951).
N. C. Gerson: *Journ. Atmos. Terr. Phys.*, **4**, 81 (1954).
N. C. Gerson: *Journ. Atmos. Terr. Phys.*, **6**, 263 (1955).
N. C. Gerson: *Proc. Phys. Soc.*, B **68**, 408 (1955).
G. Hallgran and J. Meos: *Tellus*, **4**, 249 (1955).

SUPPLEMENTO AL VOLUME IV, SERIE X
DEL NUOVO CIMENTO

N. 4, 1956
2° Semestre

Some Observations on the Influence of a Solar Eclipse upon the Ionosphere.

P. DOMINICI

Istituto Nazionale di Geofisica - Roma

It is well known that a solar eclipse offers important information on the phenomena controlling the development of the ionospheric layers.

The most general equation of the electron equilibrium in the ionosphere,

$$\frac{\mathrm{d}N}{\mathrm{d}t} = q(t) - l(t) ,$$

where N is the electron density, $q(t)$ and $l(t)$ are the rates of electron production and of electron loss respectively, and t is the time, is generally writen in one of the two following forms:

$$\frac{\mathrm{d}N}{\mathrm{d}t} = q(t) - \alpha N^2 ; \qquad \frac{\mathrm{d}N}{\mathrm{d}t} = q(t) - BN .$$

if one assumes as the principal process for the electron loss the ionic recombination (α is the effective recombination coefficient) or the attachment to neutral atoms and molecules (B is the attachment coefficient).

Assuming that: *a*) the principal ionizing agent in the upper atmosphere is the ultra-violet solar radiation; *b*) the ionizing power of the sun is uniformly distributed over its visible disk, we write

$$q(t) = q_M S \cos \chi ,$$

where χ is the zenith angle of the sun, S is the visible fraction of the area of the solar disk, q_M is the value of q when $\chi = 0$ and $S = 1$.

If one knows the astronomical « magnitude » m (eclipsed fraction of the solar diameter) of the eclipse, the minimum value d of the distance between

the centers of the disks of the sun and of the lunar shadow is $d = 1 - m$, and this distance, measured in solar diameters, is, during the eclipse:

$$D = \sqrt{d^2 + \left(\frac{t_2 - t}{t_2 - t_1}\right)^2 (1 - d^2)},$$

where t_1 is the commencement time of the eclipse and t_2 the time of greatest occultation. The visible fraction of the solar disk is

$$S = \frac{2}{\pi}(\arcsin D + D\sqrt{1 - D^2}) = \frac{4}{\pi} D \left(1 - \frac{D^2}{6} - \frac{D^4}{40} - \ldots\right).$$

We now considered the ionospheric conditions about the maximum of the eclipse. The electron equilibrium in the ionosphere is not instantaneous, and the maximum electron density N of a particular layer attains its minimum N_m at the time $(t_2 + \Delta t)$ instead of t_2.

We indicate with the indexes n, 1, 2, m the values of the « normal » magnitudes (i.e. in absence of eclipse), at the time t_1, at the time t_2, at the minimum of electron density respectively.

If $(dN/dt)_n \cong 0$ when $t = t_2$, we may write, for example in the recombination case,

$$\begin{cases} \alpha_m N_m^2 = q(t_2 + \Delta t) \cong q_M \left[S_2 \cos \chi_2 + (\cos \chi_1 - S_2 \cos \chi_2) \dfrac{\Delta t}{t_2 - t_1} \right] \\ \alpha_n N_n^2 = q_M \cos \chi_2 . \end{cases}$$

Putting: $K = S_2 + \{(\cos \chi_1 / \cos \chi_2) - S_2\} \Delta t / (t_2 - t_1)$ and if $\alpha_m = \alpha_n$, we have

$$1 = \frac{K}{(N_m/N_n)^2}, \qquad \text{(recombination)},$$

Analogously for the attachment case,

$$1 = \frac{K}{N_m/N_n}. \qquad \text{(attachment)}.$$

We may write at the instant t_2,

$$\begin{cases} \dfrac{N_2 - N_m}{\Delta t} \cong q_M S_2 \cos \chi_2 - \alpha_2 N_2^2, \\ 0 = q_M \cos \chi_2 - \alpha_n N_n^2, \end{cases}$$

and, if $\alpha_2 = \alpha_n = \alpha$, we have:

$$\alpha \sim \frac{N_2 - N_m}{\Delta t (N_2^2 - S_2 N_n^2)}.$$

Analogously for the attachment case,

$$K \sim \frac{N_2 \cdot N_m}{\left|t(N_2 - S_2 N_\ldots)\right|}.$$

We have applied this simple analysis of first approximation to the ionospheric data obtained at Rome during the partial solar eclipse of June 30, 1954 (Fig. 1), and moreover to data obtained by others in some past eclipses [1], which occurred in calm geomagnetic conditions and for which $(dN/dt)_{\ldots} \simeq 0$ when $t = t_2$.

The results appear in Fig. 2 and in Fig. 3. In Fig. 2 the ratios $K/(N_m/N_n)$ and $K'(N_m/N_n)^2$ are plotted with the zenith angle of the sun; the encircled values, which are strangley out of place, are the values calculated for the F_2 layer from data obtained in high-latitude stations during the eclipse of July 9, 1945 [2], for which we suppose an anomaly of local origin.

The examination of these figures leads one to the following conclusions:

(*a*) In the E and F_1 layers, the rate of electron loss varies with the second power of the electron density, as if the process of electron removal the ionic recombination.

(*b*) In the F_2 layer, the rate of electron loss varies with the first power

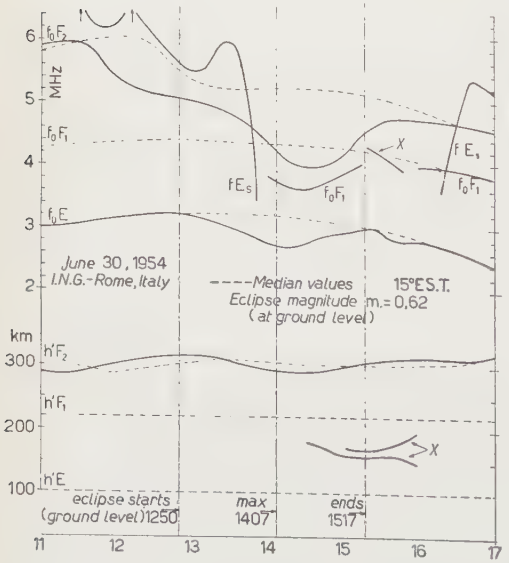

Fig. 1

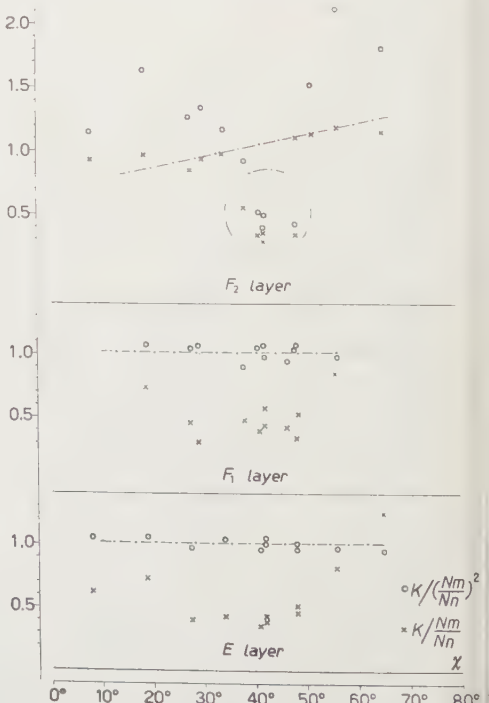

Fig. 2

of the electron density, as if the process of electron removal were the attachment to neutral atoms and molecules.

(*c*) In the F_2 layer, the decrease of electron density during a solar eclipse is, for identical conditions, more important in winter eclipses than in summer eclipses.

(*d*) The recombination and attachment coefficients decrease with the height.

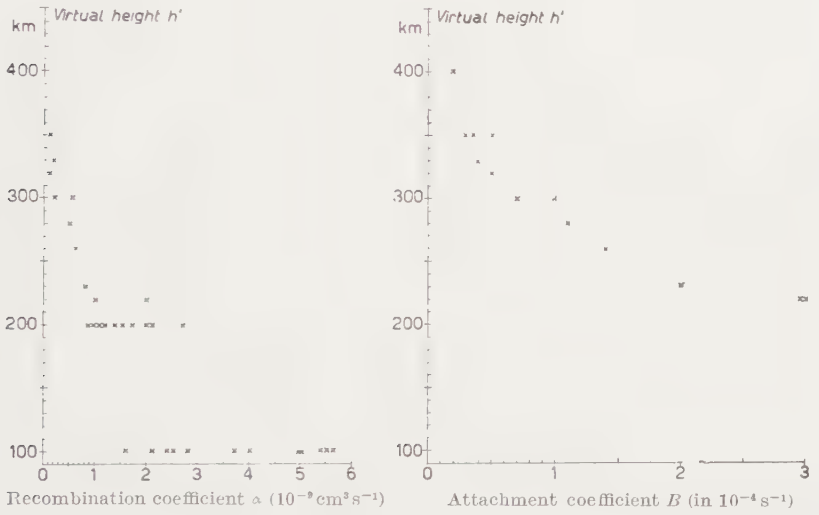

Fig. 3

The seasonal anomaly of the eclipse-effect in the F_2 layer can be explained, perhaps, with a superposition hypothesis of the two layers of the F region, as suggested many years ago by L. V. Berkner [3]. The cooling of the ionosphere during the eclipse has the result of raising the level of maximum electron density in each layer towards zones with lower electron loss; the raising is greater for a smaller vertical density-gradient of the ionizable molecules, i.e. the F_2 layer tends to separate itself from the F_1 layer. If the critical frequency of F_2 is due to the superposition zone between the F_1 and the « true » F_2, one understands that the eclipse-effect upon this frequency depends on the vertical movements of the two layers and also on their « degree of superposition », and is stronger in conditions of large superposition, i.e. in winter months. Unfortunately we are not able to test this hypothesis with the data obtained at Rome during the eclipse of February 25, 1952 [4], the F_1 data are missing due to interferences, and we hence leave the question for further study.

Besides, referring to Fig. 1, we have noted three interesting phenomena

of enough general character in the ionospheric eclipse of June 30, 1954 observed at Rome: the existence of secondary minima of critical frequency outside the limits of the optical eclipse in the E, F_2 and, perhaps, F_1 layers; a marked eclipse-effect upon the sporadic E ionization; the appearance of a sub-stratification (*X* in Fig. 1) between the E and F_1 layers.

On the first question, it is necessary to consider the eclipse of the « ionizing » sun instead of the « visible » sun in order to explain this fact. The « ionizing » sun, which includes the corona and the corpuscolar emissions, is more ample than the disk of the « visible » sun, and is not uniform, strong ionizing sources being localized in particularly active zones of the solar surface and atmosphere. The secundary minima of electron density observed shortly before and after the optical eclipse may be explained in terms of coronal occultation [5], and the minima observed far outside the limits of the photon eclipse, in terms of corpuscolar eclipse; the occultation of active zones of solar surface may explain the irregularities sometimes observed in ionospheric characteristics during a solar eclipse. These questions are all of great interest, and it is hence necessary to sistematically integrate in the next eclipses the ionospheric data with heliophysical data.

On the second question, also in the eclipses of February 14, 1934 in Southern Seas [6], of June 19, 1936 in Japan [7] and of July 9, 1945 in Northern Sweden [2], a strong decrease of the E sporadic frequency has been observed. These facts and some regularities in the seasonal and diurnal behaviour of the sporadic E, leads one to suppose some relation between the formation of the sporadic E and the activity of the normal layers, for example by electron photo-detachment processes from negative ions [8], or/and, as suggested by D. F. Martyn, by the descent of banks of charges from the F_1 layer to the E level [9]. The sometimes observed decrease in the E sporadic ionization during a solar eclipse may be consequently due to a real eclipse-effect.

On the third question, the appearance of a sub-stratification between the E and F_1 layers during the eclipse of June 30, 1954 may be ascribed, perhaps, to the phenomenon suggested by Martyn, that is the formation of the sporadic E also by descent of charges from the F_1 layer. One sees in Fig. 2 that this short-lived stratification has the form of two nigh, thin layers, one disappearing by descent to E level, the other by ascent to F_1 level. Something like that has been observed in other eclipses [10], with the appearance of a new layer between the F_1 and the F_2 layers, that is perhaps explicable as a particular case of partial merging of the two layers; in fact, if the maximum electron density of the superposition zone has a value comprised between the maximum value of the F_1 and « true » F_2 densities, one can observe three critical frequencies in the F region.

Concluding Remarks.

If one examines the available data on ionospheric eclipses, one is, in general, able to deduce from this examination only conclusions of very generical character, already known, in part, by other ways, as: (*a*) that the principal ionizing agents of the upper atmosphere are electromagnetic radiations from the sun; (*b*) that the rate of electron removal is proportional to the second power of electron density in the E and F_2 layers, to the first power in the F_2 layer.

The actual situation of the ionospheric physics on the contrary requires a more stringent investigation of the experimental facts. For example, we in practice have no information on the behaviour of the level of maximum electron density of each ionospheric layer during a solar eclipse, and hence we cannot study effects due to hypothetical vertical movements of the ionosphere during the eclipse.

We think that our work in the future could be improved in order to establish:

(i) a common standard for obtaining and presenting the ionospheric data regarding a solar eclipse;

(ii) a common method, at least to first approximation, for the reduction of the experimental curves $h'(f)$ to curves of electron density with geometrical heights, for studying at the various sites and in comparable conditions the eclipse-effects at the heights at which they effectively occur.

(iii) a common method, at least to first approximation, for the correlation between the ionospheric data and some heliophysical magnitudes during a solar eclipse.

REFERENCES

[1] *The effect of solar eclipses upon the ionosphere*, bibliography by Netherlands Postal and Telecommunications Services, n. 768 (1954).

[2] L. Harang: *Terr. Mag. Atm. Elec.*, **50**, 307 (1945); W. Stoffregen: *Terr. Mag. Atm. Elec.*, **51**, 495 (1946); S. Geier and P. Akerlind: *Terr. Mag. Atm. Elec.*, **52**, 479 (1947); O. E. H. Ridbeck: *Trans. Chalmers Univ. Techn.*, n. 53 (1946).

[3] J. A. Fleming: *Terrestrial Magnetism and Electricity* (Washington, 1938), p. 462.

[4] G. Zanotelli: *Ann. Geof.*, **6**, 367 (1953).
[5] H. W. Wells and A. H. Shapley: *Terr. Mag. Atm. Elec.*, **51**, 401 (1946).
[6] T. Minohara, Y. Ito and K. Maeda: *Rep. Rad. Res. Jap.*, **4**, 51 (1934).
[7] K. Maeda and Y. Isagawa: *Rep. Rad. Res. Jap.*, **6**, 91 (1936).
[8] B. Chatterjee: *Journ. Atm. Terr. Phys.*, **3**, 229 (1953).
[9] *URSI, Mixed Comm. Ion., Proc. II Meet.*, p. 44 (1951).
[10] P. G. Ledig, M. W. Jones, A. A. Giesecke and E. J. Chernosky: *Terr. Mag. Atm. Elec.*, **51**, 411 (1946); Y. Nakata: *Rep. Ion. Res. Jap.*, **4**, 21 (1950).

SUPPLEMENTO AL VOLUME IV, SERIE
DEL NUOVO CIMENTO

N. 4, 1956
2° Semestre

Some Considerations on Temperature Effects in the Upper Atmosphere.

F. MARIANI

Istituto Nazionale di Geofisica - Roma

It is well known that the problem of the temperature effects on the electronic density in the F region of the ionosphere is not satisfactorily solved. Part of the noticeable uncertainties are in the experimental method of ionospheric measurements which give $h'(f)$ curves of the « virtual » (*not geometrical*) height; other very important uncertainties concern the knowledge of some parameters which are considered in the fundamental theory (temperature, its vertical gradient, etc.).

The following considerations refer to the F region (particularly to the F_2 layer); they are essentially qualitative for, at this stage, the numerical results are widely incomplete. Final results and a complete discussion shall be published, as soon as possible, on *Annali di Geofisica*.

BATES and MASSEY [1] have shown that, neglecting the diffusion, the electronic density N at a particular level is given by the equation

$$\frac{\partial N}{\partial t} = I(z) - \alpha N^2 , \tag{1}$$

where $I(z)$ = ionization intensity;

$$\alpha = \bar{\alpha} + \frac{1}{NT}\frac{\mathrm{d}T}{\mathrm{d}t} + \frac{1}{N(1+\lambda)}\frac{\mathrm{d}\lambda}{\mathrm{d}t} ;$$

$\bar{\alpha} = \alpha_e + \lambda\alpha_i$; $\alpha_e =$ electronic recombination coefficient; $\alpha_i =$ ionic recombination coefficient; $T =$ absolute temperature and λ is a complicate function for which we here assume $\mathrm{d}\lambda/\mathrm{d}t = 0$, so that we reduce to consider the equation

$$\frac{\partial N}{\partial t} = I(z) - \bar{\alpha}N^2 - \frac{N}{T}\frac{\mathrm{d}T}{\mathrm{d}t} . \tag{2}$$

If we, in an elementary form, consider only the process of the attachment, the equation (2) is substituted by the equation

$$\frac{\partial N}{\partial t} = I(z) - \bar{\beta} N - \frac{N}{T}\frac{\mathrm{d}T}{\mathrm{d}t}, \tag{3}$$

where $\bar{\beta}$ is the attachment coefficient.

Concerning the dependence of $\bar{\alpha}$ and $\bar{\beta}$ on the temperature, it is generally assumed that $\bar{\alpha} \propto 1/T^n$ with $n = \frac{1}{2}, 1, 2, 3$ and $\bar{\beta} \propto 1/T$.

The results of DOMINICI [2] and of other authors suggest that the correct equation for the F_2 layer may be an equation of the type (3).

If we write $\nu = N/N_0$, where N_0 is the maximum electronic density when the zenithal angle of the sun has the value $\chi = 0°$; $I(z) = I_0 F(z, t)$, where I_0 is the maximum ionization intensity when $\chi = 0°$; $t = (86400/2\pi)\Phi$, where Φ is the time expressed in radiants; and if we assume, for sake of simplicity, constant values of $\bar{\alpha}$ and $\bar{\beta}$, we obtain from (2) and (3) the equations

$$\sigma \frac{\partial \nu}{\partial \Phi} = F - \nu^2 - \sigma \varrho \nu, \tag{4}$$

where

$$\sigma = \frac{1}{1.37 \cdot 10^4 (I_0 \bar{\alpha})^{\frac{1}{2}}}; \qquad \varrho = \frac{1}{T}\frac{\mathrm{d}T}{\mathrm{d}t},$$

and

$$\sigma \frac{\partial \nu}{\partial \Phi} = F - \nu - \sigma \varrho \nu, \tag{5}$$

where

$$\sigma = \frac{1}{1.37 \cdot 10^4 \bar{\beta}}.$$

The complete solutions of the equations (4) and (5) have to be periodic with the period 2π. If we consider only the meridian hours and assume that σ is rather small (for example $\leqslant 1/5$) we can consider the stationary case and to apply, as a better approximation, the perturbation theory; writing $\nu = \nu_0 + \sigma\nu_1$ we obtain from (4) and (5) the solutions

$$\begin{cases} \nu_0 = \sqrt{F}, \\ \nu_1 = -\frac{1}{2}\dfrac{\partial \log \sqrt{F}}{\partial \Phi} - \dfrac{\varrho}{2}, \end{cases} \tag{4'}$$

and

$$(5') \qquad \begin{cases} \nu_0 = F\,, \\ \nu_1 = -\dfrac{\partial F}{\partial \Phi} - \varrho\,. \end{cases}$$

The ionization intensity $I(z)$, if one puts $T = T_0(1 + pz)$, is proportional to

$$(6) \qquad \exp\left[-k(1+pz)^{-1/pH_0}\sec\chi\right]\cdot(1+pz)^{-1-1/pH_0}$$

where k is a constant parameter; H_0 the scale height at $z = 0$.

If one wants to explain the anomalous diurnal behaviour of f_0F_2 it is necessary to assume large time variations of the temperature: for example, AKASOFU [3], who considers grad $T \propto \cos\chi$ in the F_1 layer, in order to obtain in the F_2 layer a ionization intensity less at noon than at 11^h is forced to assume a ratio 5 : 4 of the grad T at noon and grad T at 11^h very larger than the corresponding ratio of the cos χ; with another scheme, KAMIYAMA [4] is forced to assume

$$T = T_0 \exp\left[\gamma_0 z\,(\cos\chi)^{\frac{1}{2}}\right],$$

where

$$\gamma_0 = 0{,}0072\ \mathrm{km}^{-1}$$

With these (or others) « a priori » assumptions one may attempt the explanation of the anomalous behaviour of f_0F_2; however, the required time variations of the temperature may seem excessive so that we think more interesting, at this stage, to consider another aspect of the problem.

In the equation (2) the term $-(N/T)\,\mathrm{d}T/\mathrm{d}t$ expresses the contraction or expansion effects caused by time variation of the temperature; indeed this term has to be substituted [5] by the term $(N/n)\,\mathrm{d}n/\mathrm{d}t$ (n is the particle concentration) that reduces to $-(N/T)\,\mathrm{d}T/\mathrm{d}t$ only if one considers the isobaric case, i. e., if one considers that the F_2 layer lies on an isobaric surface [6].

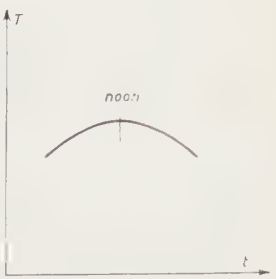

Fig. 1.

The time dependence of the terms $-(N/T)\,\mathrm{d}T/dt$ and $(N/n)\,\mathrm{d}n/dt$ is very different: let us consider a time variation of the temperature having a maximum value at noon (Fig. 1); the term $-(N/T)\,\mathrm{d}T/\mathrm{d}t = -N\varrho$, assuming $t = 0$ at noon, is

$$(7) \qquad N\varrho \begin{cases} < 0 & \text{for} \quad t < 0 \\ > 0 & \text{for} \quad t > 0\,; \end{cases}$$

from equation (4) we thus see that, if $F(z)$ is a minimum at noon, the density ν may have two maxima: one before, the other after noon, this being larger than the former; instead if one considers the term $(N/n)\,\mathrm{d}n/\mathrm{d}t$ it is, for height larger than a minimum value which is rather small in relation to the normal assumed values of the involved parameters,

$$\frac{N}{n}\frac{\mathrm{d}n}{\mathrm{d}t}\begin{cases} < 0 & \text{for} \quad t > 0, \\ > 0 & \text{for} \quad t < 0. \end{cases} \tag{8}$$

This behaviour of $(N/n)\,\mathrm{d}n/\mathrm{d}t$ is such that the two eventual maxima of the electronic density are the antimeridian one larger than the postmeridian one (normally this effect is not statistically observed). If the ionospheric temperature is a maximum after noon, this difference of the maxima is emphasized.

The Figs. 2, 3, 4 show the results obtained, in the stationary case, for some particular cases, respectively considering the term $-(N/T)\,\mathrm{d}T/\mathrm{d}t$ (Figs. 2, 3) or the term $(N/n)\,\mathrm{d}n/\mathrm{d}t$ (Fig. 4); we have indicated with ν_m the

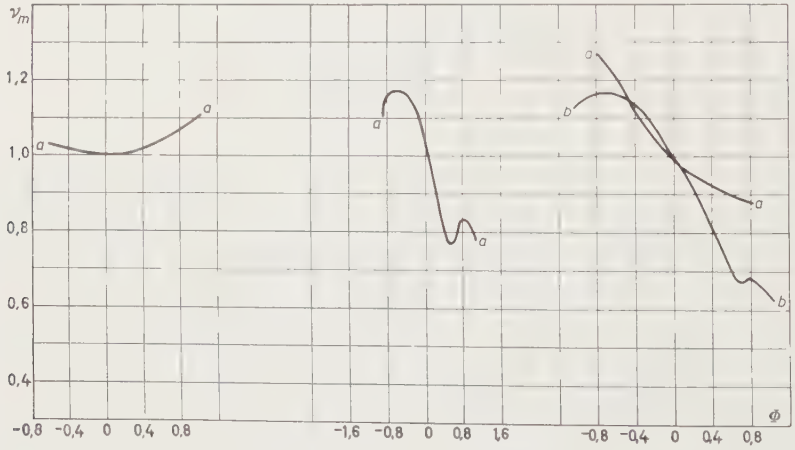

Fig. 2. Fig. 3. Fig. 4.

maximum value of ν, putting $\nu_m=1$ at noon. Curves aa in Figs. 2, 3 show the behaviour of ν_m in the case of KAMIYAMA and, in the case in which grad T/T_0 has a constant value with the height but depends on the time in the form

$$\operatorname{grad}\frac{T}{T_0} = \operatorname{grad}\left(\frac{T}{T_0}\right)_{\Phi=\Phi_1} \exp[h(\Phi-\Phi_1)],$$

where $\Phi_1=0.4$; $\operatorname{grad}[(T/T_0)]_{\Phi=\Phi_1}=0.0316\ \mathrm{km}^{-1}$, $h=\begin{cases} 0.577 & -2 \leqslant \Phi \leqslant 0.4 \\ -0.357 & \text{other values of } \Phi. \end{cases}$

Curves *aa* and *bb* in Fig. 4 show the corresponding behaviour of ν_m considering the term $(N/n)\,\mathrm{d}n/\mathrm{d}t$.

The different behaviour of the electronic density in the two cases must be considered if one wants to explain the anomalous diurnal behaviour of the F_2 layer; we think that it is more correct the use of the term $(N/n)\,\mathrm{d}n/\mathrm{d}t$ but in this case the postmeridian maximum of f_0F_2 may eventually be larger than the antemeridian one only if the maximum value of the temperature occurs during the morning: this fact does not seem quotable so that we conclude that, if the isobaric scheme is not valid, the diurnal time variations of the temperature in the F_2 layer must be rather small; hence the anomalies of the layer cannot be caused by temperature effects of the type considered.

This negative conclusion agrees with the results that GERSON [6] has obtained by different considerations. We think that the diurnal variations of the temperature are small except those occurring near sunrise and sunset or, possibly, during the night.

If one wants to explain the anomalies of the F_2 layer it is necessary to consider some different hypotheses: let us consider the possibility that both F_1 and F_2 layers are originated by the same ionization process (considered for example by MITRA [7]); the formation of the F_2 layer is determined by a sudden height diminution of the recombination coefficient: MITRA does not consider the cause of this diminution.

Concerning this fact the author has studied [8] the electron production in an atmosphere in which the temperature gradient is

$$\text{(9)} \qquad \text{grad } T \begin{cases} = \text{a constant} \neq 0 & \text{for} \quad z \leqslant c \\ = 0 & \text{for} \quad z > c\,, \end{cases}$$

where c is a reference level. This model may be suggested by the experimental observation [9] that the ionospheric temperature at the heights of $600 \div 700$ km is $1000 \div 1500$ °K, smaller than or equal to the values normally assumed in the F_2 layer. One could explain the cusp A (Fig. 5) observed in the ionograms (expecially in the summer ones) saying that it is caused by the discontinuity of the temperature gradient; the scheme may give an interpretation of the hypothesis of MITRA; the different dependence law of the recombination coefficient with the height in the lower and in the upper parts of the F region (F_1 and F_2 layers, respectively) may be attributed to the different behaviour of the

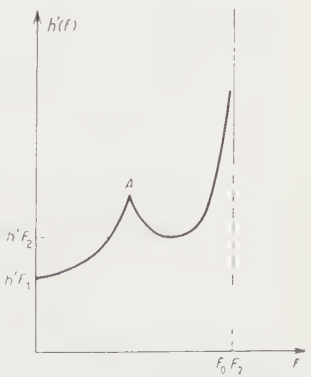

Fig. 5.

temperature in the two parts of the F region below and above the height c corresponding to the sudden temperature variation.

We write equations (2) and (3) neglecting, during the daylight, the term including the time variations of the temperature; we assume a scheme of the ionosphere in which the generalized recombination coefficient α has the form

$$\alpha \propto \frac{n}{TN}; \tag{10}$$

if we assume that at a certain height c (the height of the temperature discontinuity) the coefficient α has a constant value α_0 during the meridian hours, the height dependence of α is of the type

$$\alpha = \alpha_0 \frac{n/n_c}{(T/T_c)(N/N_c)}, \tag{11}$$

where n_c, T_c, N_c are the values of n, T, N at the height c.

With these assumptions we obtain the following height dependence of the recombination coefficient

$$\alpha = \alpha_0 \frac{1}{(T/T_c)^{2+1/pH_0}} \frac{N_c}{N}, \qquad \text{for } z \leqslant c, \tag{12}$$

and

$$\alpha = \alpha_0 \exp\left[-\frac{z-c}{H_1}\right] \cdot \frac{N_c}{N}. \qquad \text{for } z > c. \tag{13}$$

where H_1 is the scale height for $z > c$.

It is noticeable that we can write the equation (2), respectively for the F_1 and F_2 layers, in the following form.

$$\sigma \frac{\partial v}{\partial \Phi} = F - \frac{\nu_c}{(T/T_c)^{2+1/pH_0}} v, \tag{14}$$

$$\sigma \frac{\partial v}{\partial \Phi} = F - \nu_c \exp\left[-\frac{z-c}{H_1}\right] \cdot v. \tag{15}$$

We draw attention to the fact that at the height c equation (14) is written in the form

$$\sigma \frac{\partial v}{\partial \Phi} = F - v^2. \tag{16}$$

i. e., in the form corresponding to a recombination scheme; this fact agrees with the results of DOMINICI: indeed these results, showing that the process effective in the F_1 layer is the recombination one, are obtained for heights near the height of reflection of the frequency f_0F_1.

We have calculated the behaviour of the electron density in the stationary case, for some particular values of the zenithal angle χ; this preliminary study shows some interesting features:

a) the electron density in the region $z > c$ has a minimum value at noon and its maximum value increases for increasing values of the zenithal angle χ;

b) the density in the region $z \leqslant c$ has a maximum at noon and it decreases approximately as $(\cos \chi)^{\frac{1}{2}}$, for increasing values of χ;

c) the cusp A is vanishing for increasing values of χ: this fact explains the disappearence of the F_1 layer in not meridian hours and during the night;

d) the height $h'F_1$ is a minimum at noon and it slightly increases in not meridian hours; on the contrary the height of the maximum electron density seems to increase in meridian hours.

With regard to nocturnal conditions the equation (15) easily shows that the decreasing of f_0F_2 is slower than according to the Chapman theory, for the decreasing value of the recombination coefficient; this effect, at least qualitatively, agrees with the experimental observations.

The conclusions we have drawn seem to agree with the more complete numerical analysis we are carrying out.

REFERENCES

[1] D. R. BATES and H. S. W. MASSEY: *Proc. Roy. Soc.*, **187**, 261 (1946).
[2] P. DOMINICI: in this issue pag. 1572.
[3] S. AKASOFU: *Sci. Rep. Tok. Univ.*, V series **5**, 123 (1953).
[4] H. KAMIYAMA: *Sci. Rep. Tok. Univ.*, V series **6**, 11 (1954).
[5] N. C. GERSON: *Nature*, **163**, 491 (1941).
[6] N. C. GERSON: *Rep. Progr. Phys.*, **14**, 316 (1951).
[7] A. P. MITRA: *Indian Journ. Phys.*, **35**, 79 (1952).
[8] F. MARIANI: *Ann. Geofis.*, **8**, 59 (1955); **9**, 43 (1956)..
[9] G. P. KUIPER: *The atmospheres of the earth and planets* (Chicago, 1949).

SUPPLEMENTO AL VOLUME IV, SERIE X
DEL NUOVO CIMENTO

N. 4, 1956
2° Semestre

Diffusion in a Not Isothermal Ionosphere.

F. MARIANI

Istituto Nazionale di Geofisica - Roma

We briefly consider the diffusion effects in the ionosphere; this problem has been recently studied by FERRARO [1] for an isothermal atmosphere: we here want to extend the study to a not isothermal atmosphere applying the results of the general diffusion theory including the thermal diffusion.

We assume that the ionosphere is a binary mixture of a ion-electron gas and of a molecular gas, so that we can write, if external forces are not present,

$$(1) \qquad \boldsymbol{c}_1 - \boldsymbol{c}_2 = -\frac{n^2}{n_1 n_2} D_{12}\left[\frac{\partial}{\partial z}\frac{n_1}{n} + \frac{n_1 n_2}{n\varrho P}(m_2 - m_1)\frac{\partial P}{\partial z} + k_T \frac{\partial}{\partial z}\log T\right],$$

where

z = vertical height

$\boldsymbol{c}_1$ = mean velocity of the ion-electron gas

$\boldsymbol{c}_2$ = mean velocity of the molecular gas

n_1, n_2 = number density of the two gases

$n = n_1 + n_2$; n_0 = its value at $z = 0$

m_1, m_2 = mean ion-electron and molecular masses

ϱ_1, ϱ_2 = matter density of the two gases

$\varrho = \varrho_1 + \varrho_2$

P = pressure

T = absolute temperature; T_0 = its value at $z = 0$

$k_T = \alpha_T (n_1/n)(n_2/n)$ = thermal diffusion coefficient; α_T = a constant

$D_{12} = D_0 (T/T_0)^{\frac{1}{2}} (n/n_0)^{-1}$ = diffusion coefficient; D_0 = its value at $z = 0$.

The fundamental equation may be written in the form

$$(2) \qquad \frac{\partial n_1}{\partial t} = I(z) - \alpha n_1^2 - \operatorname{div}(n_1 \boldsymbol{c}_1), \qquad \text{(recombination case)},$$

or

$$\frac{\partial n_1}{\partial t} = I(z) - \beta n_1 - \operatorname{div}(n_1 \boldsymbol{c}_1) \,. \qquad \text{(attachment case).} \tag{3}$$

If we assume a constant value pT_0 of grad T, from (1), (2), (3) and $n_1\boldsymbol{c}_1 + n_2\boldsymbol{c}_2 = 0$ we deduce the equation

$$\frac{\partial n_1}{\partial t} = I(z) - \varphi(n_1) + D_{12}\left[\frac{\partial^2 n_1}{\partial z^2} - Q(z,t)\frac{\partial n_1}{\partial z} + R(z,t)n_1\right], \tag{4}$$

where $\varphi(n_1)$ is αn_1^2 or βn_1, respectively in the recombination and in the attachment case;

$$Q = \frac{G_1}{1 + pz}; \qquad G_1 = \left[\left(\frac{5}{2} + \alpha_T\right)p + \frac{1}{H_{10}} + \frac{1}{H_{20}}\right],$$

$$R = \frac{G_2}{(1 + pz)^2}; \qquad G_2 = \left[(1 + \alpha_T)\frac{p^2}{2} + \frac{1}{2}\frac{p}{H_{10}} + (1 + \alpha_T)\frac{p}{H_{20}} + \frac{1}{H_{10}H_{20}}\right];$$

and H_{10}, H_{20} are the scale heights of the ion-electron gas and of the molecular gas for $z = 0$; we see that if $p \to 0$, the equation (4) identifies with that considered by Ferraro.

If one moreover assumes a constant recombination coefficient α_0 during the daylight, the equation (4) is written, with usual notations, in the form

$$\sigma\frac{\partial v}{\partial \Phi} = F - v^2 + \tau x^{\frac{3}{2}+1/pH_{20}}\left[\frac{\partial^2 v}{\partial x^2} + \frac{G_1}{px}\frac{\partial v}{\partial x} + \frac{G_2}{p^2x^2}v\right], \quad \text{(recombination case)}, \tag{5}$$

where

$$x = 1 + pz; \quad \tau = \frac{D_0 p^2}{N_0\alpha_0}; \quad N_0 = \text{maximum value of } n_1 \text{ for } \chi = 0^\circ;$$

$$\chi = \text{zenithal angle of the Sun}; \quad \Phi = (2\pi/86\,400)t \,.$$

The diffusion effects are small in the E and F_1 layers for the parameter τ is vanishing; instead in the F_2 layer they may be rather important: if we put, for example,

$$N_0 = \frac{5}{1.37}\cdot 10^6 \text{ cm}^{-3}; \; D_0 = 4.85\cdot 10^7 \text{ C.G.S.}; \; \frac{1}{pH_{20}} = 2;$$

$$H_{20} = 13 \text{ km}; \; \alpha_0 = 10^{-10} \text{ C.G.S.},$$

the value of the parameter τ is,

$$\tau = 0.0196 \,.$$

If one considers the term

$$\tau x^{\frac{3}{2}+1/pH_{20}}\left[\frac{\partial^2 \nu}{\partial x^2}+\frac{G_1}{px}\frac{\partial \nu}{\partial x}+\frac{G_2}{p^2x^2}\nu\right],$$

as a perturbative one it is possible to write the solution of the equation (5) in the form $\nu = \nu_0 + \tau\nu_1$ where ν_0 is the solution of the equation $\sigma(\partial\nu/\partial\Phi) = F - \nu^2$ and ν_1 is the solution of the equation

$$\sigma\frac{\partial \nu}{\partial \Phi} = -2\nu_0\nu + \tau x^{\frac{3}{2}+1/pH_{20}}\left[\frac{\partial^2 \nu_0}{\partial x^2}+\frac{G_1}{px}\frac{\partial \nu_0}{\partial x}+\frac{G_2}{p^2x^2}\nu_0\right], \tag{6}$$

having the period 2π.

The numerical results, although incomplete, seem to show that the diffusion effects on f_0F_2 are rather small; on the contrary the effects on the electronic density may be important expecially in the lower part of the layer. These results agree, at least qualitatively, with those obtained by FERRARO. If the temperature gradient is larger the perturbation theory does not give proper results: we must solve the equation (5) in the complete form, but this possibly is not the case.

These results and those of FERRARO show that the diffusion effects are small also in the more complicated model of ionosphere we have considered in the preceding paper.

REFERENCES

[1] V. C. A. FERRARO: *Terr. Magn. Atmos. Electr.*, **50**, 215 (1945).

SUPPLEMENTO AL VOLUME IV, SERIE X
DEL NUOVO CIMENTO

N. 4, 1956
2° Semestre

Some Critical Considerations on the Parameters h' and f_0 of the Ionospheric Layers.

P. Dominici and F. Mariani

Istituto Nazionale di Geofisica - Roma

It is well known that the physical interpretation of the behaviour of the F_2 layer is very difficult and that the questions connected with the singularities of this behaviour are very interesting for further progress of the ionospheric physics.

Our actual knowledge of the ionosphere is based almost only on the data obtained by standard methods in the various Observatories by vertical radiosoundings. The behaviour of the ionospheric layers is obtained from the behaviour of the two parameters h' (minimum virtual height of reflection) and f_0 (critical frequency of the ordinary ray).

The « anomalies » of the F layer are in the fact that the behaviour of $h'F_2$ and f_0F_2 is quite different than the behaviour of $h'E$, $h'F_1$, f_0E, f_0F_1. Since the behaviours of the E and F_1 layers agree, at least qualitatively, with the Chapman's theory, one must explain why this theory does not apply to the F_2 layer, if for the action of perturbative effects or if for reasons relating to the nature of the layer itself.

We so have some theories based on the hypothesis that the « true » F_2 layer is substantially a Chapman's layer and that the diurnal and annual anomalies of the critical frequency are due to the effects of expansion or contraction of the layer, or to the superposition of the F_1 and the « true » F_2 layers with the formation of a region of high electron density (« apparent » F_2 layer) or to the dynamo-magnetic effects of lunar and solar tides in the upper atmosphere; on the other side we have the theories based on the hypothesis that the F_2 layer is produced as a continuation of the F_1 caused by a sudden variation of the recombination coefficient.

A critical examination of these theories leads one to the conclusion that, at this stage, it is impossible to give a model of the F_2 layer satisfactorily

describing the physical facts, if one does not assume some convenient « a priori » hypothesis: it is the case of the theories based on thermal effects, which can explain, at least qualitatively, the most important anomalies of the F_2 layer by the assumption of a convenient law of height or time variation of the temperature. We have already pointed out some critical considerations on these theories in a preceding paper [1]; here we want to consider the possibility that the method of analysis of the experimental data may, in any way, determine difficulties of physical interpretation.

We notice that, unfortunately, the experimental data are not always very reliable; however, in our opinion, the greater difficulty is in the fact that their interpretation is rather doubtful, as we now will show.

This interpretation is essentially based upon the consideration of minimum virtual heights and of critical frequencies; let us consider, at first, the virtual height: it is well known that the virtual height is proportional to the « transmission time » and that the velocity of propagation of the exploring wave is not constant in the ionosphere. Hence, the consideration of virtual heights can determine noticeable errors in the questions of ionospheric physics. For example, if the virtual height increases, one is led to think that the layer rises; indeed, in some particular cases, one can show that an effective lowering of the F_2 layer is accompanied by an increase of the minimum virtual height: we have calculated the virtual height $h'(f)$, for a summer day at the latitude 45°, in a F region constituted by a F_1 layer and a « true » F_2 layer exactly overlapping at 7 o'clock; we have moreover assumed that the two layers are chapmanian and that they have maximum electronic density N_0 and ν_0, and different semi-thickness z_0 and ζ_0.

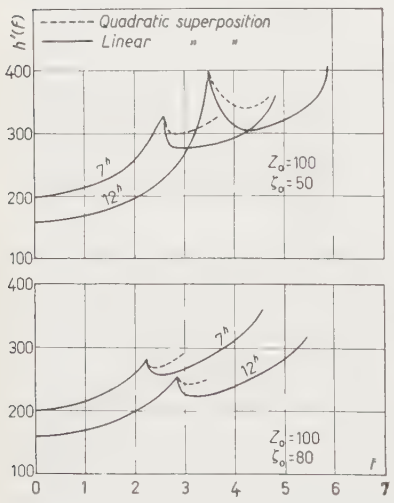

Fig. 1. – $h'(f)$ in km; f in MHz.

Considering the case of linear superposition, or as a better approximation, the case of quadratic superposition and putting $N_0 = 1.12 \cdot 10^5$ cm^{-3}, $\nu_0 = 1.97 \cdot 10^5$ cm^{-3} we have obtained the two pairs of curves (Fig. 1), respectively for a semithickness $z_0 = 100$ km (F_1 layer), $\zeta_0 = 50$ km (F_2 layer) or $z_0 = 100$ km, $\zeta_0 = 80$ km.

In the first case $h'F_1$ decreases during the meridian hours and $h'F_2$ increases, although the F_2 layer lowers as a whole. In the second case, instead, both $h'F_1$ and $h'F_2$ decrease.

These results indicate that, although they are obtained in some particular case and by some particular hypothesis, we cannot always assure that the

effective behaviour of the lower part of the F_2 layer is identical to the behaviour of the minimum virtual height $h'F_2$.

In regard to the other ionospheric parameter, the critical frequency, we think that, although it is a parameter having an unambiguous physical meaning, however we may put some reserve: in effects the maximum electronic density (corresponding to the critical frequency f_0) occurs at variable heights during the day and the year so that it depends not only on the zenithal angle of the Sun but also on the (generalized) recombination coefficient which is a function of the height. This fact may limit or alter the physical meaning of some results obtained in the study of the behaviour of f_0, for example when one considers the results of the harmonical analysis of the experimental data.

We conclude that the parameters h' and f_0 may have a not clear physical meaning, even if for different reasons. In the radiopropagation problems this question has not a great importance since other noticeable uncertainties greatly influence the experimental facts so that a great precision is not required. Instead, from the physical point of view, it is very important, at this stage, to examine carefully the experimental data.

As a first step to further progress, one must obtain the distribution of the electronic density N with the *geometrical* height z from the experimental curves $h'(f)$; many authors have studied this problem and many solutions have been proposed, some based on very approximative methods. A great accuracy is instead necessary in the reduction of the experimental curves $h'(f)$ to the $N(z)$ curves; this accuracy is possible by numerical integration of the integral equation $h'(f) = \int \mu'[f, N(z)]\,dz$, including the effect of the geomagnetic field on the ionospheric refraction index μ' [2, 3].

The time required by this numerical analysis is largely compensated by some essential advantages: we can obtain a complete scheme of the behaviour of the electronic density at *every* geometrical height so that we can study the time variation of N at *every* particular level, independently on « a priori » models of ionosphere. Consequently from the usual equation $\partial N/\partial t = I - \alpha N^2$ we can deduce the time and the height dependence of the (generalized) recombination coefficient α.

In this manner it is possible to have an unambiguous experimental basis so that we can put more close conditions which the theory must satisfy.

The numerical analysis of the experimental data may be accomplished rather easily for nocturnal conditions, when $I = 0$ and the E and F_1 layers are absent or very reduced; this preliminary study shall be then very useful in order to extend the analysis to the diurnal data.

REFERENCES

[1] P. Dominici and F. Mariani: *Ann. Geofis.*, **8**, 103 (1955).
[2] D. H. Shinn and H. A. Whale: *Journ. Atmos. Terr. Phys.*, **2**, 85 (1952).
[3] J. M. Kelso: *Journ. Atmos. Terr. Phys.*, **5**, 11 (1954).

OSSERVAZIONI ED INTERVENTI

I. Ranzi:

È veramente lodevole la serietà con cui i due giovani ricercatori dell'Istituto Nazionale di Geofisica hanno condotto i loro lavori; particolarmente interessanti appaiono i risultati relativi al fenomeno di sovrapposizione delle regioni F_1 ed F_2.

Una sola riserva mi sembra si debba fare circa l'attendibilità delle determinazioni dei valori del coefficiente di ricombinazione nella regione F_2, dato che vari fatti stanno a dimostrare che questa regione deve le sue variazioni a movimenti ionici più che alla diretta azione delle radiazioni solari. Non va trascurato il fatto, che, secondo le ultime misure con razzi, le varie regioni ionosferiche non appaiono separate da minimi netti: in tali condizioni, acquistano importanza gli studi sugli effetti di sovrapposizione, quali sono stati iniziati dai due relatori.

— P. Dominici:

Effettivamente una tale ipotesi era stata da me considerata. Se α_m ed α_n sono i valori del coefficiente di ricombinazione generalizzato corrispondenti rispettivamente alla fase massima dell'eclisse ed allo stato « normale », è facile vedere che il rapporto α_m/α_n è dato da $K/(N_m/N_n)^2$, cioè dalle quantità riportate nel grafico della Fig. 2 della mia nota *Some Observations on the Influence of a Solar Eclipse upon the Ionosphere* presentata a questo Convegno (in questo fascicolo a pag. 1572). Da tale figura risulta che questo rapporto si mantiene negli strati E ed F_1 praticamente uguale all'unità; nello strato F effettivamente c'è una variazione, cooperante con il generale movimento di salita assunto dallo strato.

SUPPLEMENTO AL VOLUME IV, SERIE X
DEL NUOVO CIMENTO

N. 4, 1956
2° Semestre

Spettroscopia molecolare dell'ossigeno per mezzo di microonde. Forma delle righe di assorbimento (*).

N. CARRARA

Centro di Studio per la Fisica delle Microonde - Firenze

Introduzione.

Durante la seconda guerra mondiale, BERINGER [1] osservò che l'ossigeno, alla pressione atmosferica, assorbe energia elettromagnetica nella gamma dei 5 mm. Questo fatto apparve sorprendente, poichè la molecola dell'ossigeno non è elettricamente polare e, nel caso di molecole non polari, le risonanze capitano molto lontano dalla gamma delle microonde. Ma VAN VLECK [2], osservando che la molecola dell'ossigeno è paramagnetica, potè attribuire l'assorbimento dell'ossigeno nella gamma delle microonde a transizioni di dipolo magnetico, fra le componenti di struttura fine dei livelli rotazionali della molecola. Secondo VAN VLECK [3] l'assorbimento osservato da BERINGER a pressione atmosferica doveva risultare dalla sovrapposizione di numerose righe nella gamma dei 5 mm, più una riga isolata, corrispondente alla lunghezza d'onda di circa 2.5 mm, e le righe avrebbero dovuto separarsi a pressione convenientemente ridotta. Egli potè anche effettuare un primo calcolo delle frequenze delle medesime righe.

Le ricerche sperimentali successive di LAMONT [4], STRANDBERG, MENG e INGERSOLL [5] confermarono e precisarono i risultati di VAN VLECK. Successivamente BURGHALTER e altri [6] riuscirono a risolvere completamente, a bassa pressione, le righe della gamma dei 5 mm e più tardi ANDERSON e altri [7] osservarono la riga di 2.5 mm.

VAN VLECK [2] si riferì, per il calcolo teorico delle frequenze di assor-

(*) Questo scritto si riferisce ad una ricerca resa possibile grazie ad un contratto con l'« European Office Air Research and Development Command, United States Air Force ».

bimento a studi precedentemente compiuti da KRAMERS [8], HEBB [9] e SCHLAPP [10], per giustificare la scomposizione dei livelli rotazionali della molecola in tripletti (rho-type-triplet). Sebbene l'accordo fra le previsioni teoriche e i risultati sperimentali fosse assai buono, rimanevano — e rimangono ancora — alcuni punti oscuri che hanno indotto ad approfondire sia gli studi teorici, sia le determinazioni sperimentali.

Una prima correzione fu apportata da BURGHALTER e altri [11]; successivamente MILLER e TOWNES [12], MIZUSHIMA e HILL [13], TINKHAM e STRANDBERG [14] hanno ulteriormente approfondito la questione.

Le righe non sono mai monocromatiche. Vari fattori intervengono infatti a determinarne la forma e la larghezza (distanza fra i due punti della riga corrispondenti a metà potenza).

Le cause più comuni che producono l'allargamento delle righe sono l'effetto Doppler, lo smorzamento della radiazione e le interruzioni derivanti dalle collisioni. Quest'ultima causa, che predomina nella gamma delle microonde, è stata studiata in un lavoro fondamentale di VAN VLECK e WEISSKOPF [15]. La teoria di Van Vleck e Weisskopf è un perfezionamento delle antiche teorie di LORENTZ [16] e DEBYE [17].

L'argomento è stato successivamente trattato da moltissimi autori e ha dato luogo a gran numero di ricerche sperimentali; tuttavia ancora molte questioni rimangono aperte, e sopratutto perchè, mentre non mancano misure di alta precisione delle frequenze di risonanza, le misure della forma e della intensità delle righe sono relativamente poche e generalmente di scarsa precisione. Poichè la conoscenza della forma e della intensità delle righe sarebbe estremamente utile per la determinazione delle forze molecolari, molte ricerche sperimentali e teoriche sono state compiute in questi ultimi tempi in tale direzione, sia su gas puri sia su mescolanze gassose.

Le ricerche sperimentali hanno visto un progressivo e prodigioso affinarsi delle tecniche sperimentali. Una nuova tecnica è stata elaborata anche presso il Centro Microonde, in collaborazione con l'Istituto di Fisica della Università di Pisa, dalla quale speriamo interessanti risultati (GOZZINI). Anche una analisi critica dei risultati forniti da queste tecniche è stata compiuta (CARRARA).

1. – Rho-Type-Triplet.

Lo spettro di assorbimento a microonde della molecola di ossigeno è dovuto allo stato fondamentale della molecola stessa $^3\Sigma_g^-$. È noto il significato di questo simbolo.

In una molecola biatomica il campo nucleare, nel quale sono situati gli elettroni, non ha simmetria sferica, ma assiale. Ne segue che soltanto la com-

ponente del momento orbitale angolare degli elettroni nella direzione dell'asse internucleare è una costante del moto. Nel campo elettrostatico determinato dai nuclei, ha luogo una precessione del momento orbitale elettronico L attorno all'asse internucleare, in modo che la componente lungo il medesimo asse, M può presentare uno dei valori: $M = L,\ L-1,\ L-2 \ldots L$. Poichè nel campo elettrostatico, invertendo il moto degli elettroni, l'energia del sistema non cambia, ma M si cambia in $-M$, stati che differiscono solo per il segno di M hanno la stessa energia (sono degenerati). Invece stati con diverso M hanno energie notevolmente diverse. Pertanto si classificano gli stati delle molecole biatomiche, in base al diverso valore di $|M|$, che viene indicato con Λ e può assumere i valori 0, 1, 2, ..., L. Per $\Lambda = 0$ il simbolo dello stato è Σ, per $\Lambda = 1$ è Π, per $\Lambda = 2$ è Δ, ecc.

Ma gli elettroni hanno anche un proprio spin, che viene indicato con S. Lo stato fondamentale della molecola dell'ossigeno è uno stato Σ, cioè $\Lambda = 0$. D'altra parte, conformemente al fatto che la molecola di ossigeno è paramagnetica, lo spin elettronico è $S = 1$. Pertanto i livelli rotazionali K (con K indichiamo il momento angolare orbitale, escluso lo spin), livelli Σ come si è detto, si compongono con lo spin $S = 1$, scindendosi ciascuno in tre livelli di eguale K e diverso J (momento angolare totale compreso lo spin) dando luogo a $J = K+1$, K, $K-1$; queste terne di livelli sono dette Rho-Type-Triplet. Occorre anche avvertire, che, per le simmetrie derivanti dalla costituzione nucleare ed elettronica dell'ossigeno, risulta che i livelli con K pari non esistono. La composizione fra K ed S viene compiuta con la regola di Hund, caso *b*).

Sono possibili transizioni fra i livelli di diverso J ed uguale K; tale possibilità deriva dal fatto che la molecola è paramagnetica; la separazione fra le componenti di un medesimo tripletto è così piccola che le transizioni fra di esse appartengono alla gamma delle onde millimetriche. Poichè J non può cambiare di più di una unità, non sono possibili transizioni fra componenti $J = K+1$ e $J = K-1$, le quali apparterrebbero alla gamma delle onde decimetriche. La scissione di ogni livello K in un tripletto viene indicata dal numero 3 scritto in alto a sinistra del simbolo Σ.

In una molecola biatomica ogni piano attraverso l'asse internucleare è un piano di simmetria. Perciò l'autofunzione elettronica di uno stato non degenerato (Σ) o rimane inalterato o cambia segno, per una riflessione rispetto ad ogni piano passante attraverso i due nuclei. Nel primo caso lo stato viene detto Σ^+, nel secondo Σ^-. Se i due nuclei hanno anche la stessa carica, come accade per la molecola di ossigeno $^{16}O_2$, oltre a questa simmetria, vi è anche la simmetria centrale, in conseguenza della quale le autofunzioni devono rimanere inalterate o cambiare segno per una riflessione attraverso il centro. Nel primo caso lo stato viene detto pari, nel secondo dispari; tali stati vengono indicati rispettivamente con le lettere *g* (gerade) e *u* (ungerade). Avremo dunque stati Σ_g e Σ_u.

In conclusione il simbolo dello stato fondamentale dell'ossigeno $^3\Sigma_g^-$ significa: componente del momento orbitale totale elettronico lungo l'asse internucleare $\Lambda = 0$ (stato Σ); spin elettronico totale 1, cioè scissione dei livelli fondamentali in tre componenti (stato $^3\Sigma$); l'autofunzione elettronica cambia segno per una riflessione attraverso un piano passante per i nuclei (stato $^3\Sigma^-$); e non cambia segno per una riflessione attraverso il centro della molecola (stato $^3\Sigma_g^-$).

La separazione dei livelli nelle tre componenti è prodotta principalmente, secondo KRAMERS [8] dalla interazione fra gli spin degli elettroni non appaiati; tenendo conto anche dell'accoppiamento fra lo spin elettronico e la rotazione molecolare, SCHLAPP [9] potè calcolare con notevole approssimazione i termini rotazionali ottenendo le formule:

$$(1)\qquad \begin{cases} F_1 = BK(K+1) + (2K+3)B - \lambda - \sqrt{(2K+3)^2B^2 + \lambda^2 - 2\lambda B} + \mu(K+1) \\ F_2 = BK(K+1) \\ F_3 = BK(K+1) - (2K-1) \quad -\lambda + \sqrt{(2K-1)^2B^2 + \lambda^2 - 2\lambda B} - \mu K \end{cases}$$

in cui le F si riferiscono rispettivamente ai livelli $J=K+1$; $J=K$; $J=K-1$; inoltre λ, μ sono costanti e $B = h/8\pi^2cI$ è la costante rotazionale della molecola, di cui I è il momento di inerzia rispetto all'asse di rotazione.

La struttura fine dei livelli rotazionali dà luogo, secondo SCHLAPP, alle seguenti frequenze (numeri d'onda) d'assorbimento:

$$(2)\qquad \begin{cases} \nu_+(K) = \lambda - \mu(K+1) - (2K+3)B + [\lambda^2 - 2\lambda B + (2K+3)^2B^2]^{\frac{1}{2}} \\ \nu_-(K) = \lambda + \mu K \qquad + (2K-1)B - [\lambda^2 - 2\lambda B + (2K-1)^2B^2]^{\frac{1}{2}}, \end{cases}$$

dove ν^+ corrisponde alle transizioni fra $J=K+1$ e $J=K$; e ν_- a quelle fra $J=K-1$ e $J=K$. Come mostrò VAN VLECK, nella molecola di ossigeno, che non è polare, sono infatti possibili transizioni per dipolo magnetico, e queste seguono, per le proprietà di simmetria $+$, $-$, le seguenti regole di selezione:

$$+ \longleftrightarrow +\,, \qquad - \longleftrightarrow -\,, \qquad + \not\longleftrightarrow -$$

$$\Delta J = 0\,, \quad \pm 1\,, \quad \text{con la restrizione } J = 0 \not\to J = 0\,; \qquad \Delta K = 0\,.$$

Le risonanze che ne seguono capitano nella gamma dei 60 000 MHz (circa 5 mm di lunghezza d'onda) con una eccezione, quando $K = 1$, in cui la frequenza è circa 120 000 MHz (lunghezza d'onda circa 2.5 mm).

Dalle formule precedenti si deduce:

$$(3)\qquad \nu_+(K-2) + \nu_-(K) = 2\lambda + \mu = \text{costante}\,.$$

Ora, mentre le osservazioni sperimentali di BURGHALTER e altri [11] sull'assorbimento dell'ossigeno a bassa pressione furono in buon accordo con le frequenze fornite dalla formula di Schlapp, emerse tuttavia che la (3) non era soddisfatta.

MILLER e TOWNES rilevarono che nelle formule di Schlapp sono omessi termini di secondo ordine in μ [12]. I due autori rielaborarono le formule di Schlapp e pervennero a formule per le F più complesse, senza per altro modificare la (3).

MIZUSHIMA e HILL [13] ripresero in esame la questione, partendo dalla Hamiltoniana del Rho-Type-Triplet, e trovarono ancora nuove formule più complesse per le F, e un'espressione per la (3), in cui appare una dipendenza da K.

Ultimamente M. TINKHAM e P. STRANDBERG [14], traendo profitto da una recente pubblicazione di MECKLER [18] nella quale è esposta una soluzione elettronica dello stato fondamentale della molecola di ossigeno e sono forniti dati sufficientemente precisi sui livelli energetici, applicano alla molecola di ossigeno l'approssimazione di Born-Oppenheimer e pervengono a nuove formule, invero molto complesse, per le frequenze ν_+ e ν_-, da cui discende che la somma $\nu_+(K-2) + \nu_-(K)$ è di tipo parabolico in K.

In conclusione si può affermare che la questione della determinazione e della giustificazione delle frequenze di risonanza di assorbimento della molecola di ossigeno è oggi risolta con grande precisione e che l'accordo con i dati sperimentali è veramente soddisfacente. Per i valori numerici delle frequenze calcolate ed osservate, rimandiamo alle pubblicazioni originali citate.

2. – Forma delle righe di assorbimento.

Come è stato detto nella introduzione, le righe spettrali non sono mai perfettamente monocromatiche; esse si presentano allargate e l'allargamento, nella gamma delle microonde, dipende essenzialmente dalle collisioni.

VAN VLECK e WEISSKOPF, considerando le molecole distribuite fra i vari stati secondo la legge di Boltzmann, ottennero la seguente fondamentale espressione per il coefficiente di assorbimento:

$$\alpha = \frac{8\pi^3 \nu N}{6hc} \frac{h}{kT} \frac{\sum_i \sum_j |\mu_{ij}|^2 \nu_{ij} f(\nu_{ij}, \nu) \exp[-E_j/kT]}{\sum_j \exp[-E_j/kT]}, \tag{4}$$

dove $\nu_{ij} = (E_j - E_i)/h$, μ_{ij} è l'elemento di matrice, che dipende dal momento dipolare magnetico e $f(\nu_{ij}, \nu)$, detto fattore di forma, è dato da

$$f(\nu_{ij}, \nu) = \frac{1}{\pi} \frac{\nu}{\nu_{ij}} \left[\frac{\Delta\nu}{(\nu_{ij} - \nu)^2 + \Delta\nu^2} + \frac{\Delta\nu}{(\nu_{ij} + \nu)^2 + \Delta\nu^2} \right], \tag{5}$$

in cui $\Delta\nu$ exprime la semilarghezza della riga ed è

$$\Delta\nu = 1/2\pi\tau \; ; \qquad \tau = 1/N\bar{v}\sigma \; ; \tag{6}$$

dove τ è l'intervallo medio di tempo che separa due collisioni successive di una molecola, N il numero di molecole per unità di volume, $\bar{v}$ la velocità media relativa delle molecole che vengono in collisione e σ la sezione efficace di urto.

Per una riga isolata, la (4) può essere convenientemente modificata per mettere in evidenza la dipendenza del coefficiente di assorbimento dalla frequenza, dalla temperatura e dalla pressione. Per prima cosa si può ammettere che N sia proporzionale al rapporto fra la pressione e la temperatura, cioè a P/T; poi la somma che compare a denominatore della (1), detta funzione di ripartizione, si può considerare proporzionale ad una potenza di T da determinare, il cui esponente indicheremo con m; inoltre l'elemento di matrice μ_{ij} si può considerare indipendente dalla temperatura. Pertanto, per una riga isolata si può scrivere:

$$\alpha = C \frac{\nu^2 P \exp[-E_j/kT]}{T^{2+m}} \left[\frac{\Delta\nu}{(\nu_{ij}-\nu)^2 + \Delta\nu^2} + \frac{\Delta\nu}{(\nu_{ij}+\nu)^2 + \Delta\nu^2} \right], \tag{7}$$

dove C è una opportuna costante ed m dipende dal tipo di molecola (per l'O_2, $m = 1$). Ma anche $\Delta\nu$ dipende dalla temperatura e dalla pressione. Sembra che la migliore approssimazione sia di ritenere $\Delta\nu$ proporzionale a $P \cdot T^{-\frac{1}{2}}$. Infine, se si suppone che $\Delta\nu < 0.2\nu_{ij}$ si può anche trascurare nella precedente il secondo termine fra parentesi quadra. Tenendo conto di tutto ciò la (7) può essere ulteriormente semplificata nel modo seguente:

$$\alpha = C_1 \frac{\nu_{ij}^2 \exp[-E_j/kT]}{T^{\frac{3}{2}+m}}, \qquad \text{per } \nu = \nu_{ij}, \tag{8}$$

$$\alpha = 2C_1 \frac{P^2 \exp[-E_j/kT]}{T^{\frac{5}{2}+m}}, \qquad \text{per } \nu \gg \nu_{ij}, \tag{9}$$

$$\alpha = 2C_1 \frac{P^2 \exp[-E_j/kT]}{T^{\frac{5}{2}+m}} \left(\frac{\nu}{\nu_{ij}}\right)^2, \qquad \text{per } \nu \ll \nu_{ij}. \tag{10}$$

Le formule precedenti mettono in evidenza la dipendenza del coefficiente di assorbimento dalle grandezze indicate, nei casi considerati. Per esempio, nell'intorno di una risonanza (formula (8)) α è indipendente dalla pressione, come è stato verificato sperimentalmente da Townes e da Bleaney e Penrose [19, 20]. Nel secondo caso invece l'assorbimento risulta indipendente dalla frequenza e proporzionale al quadrato della pressione, come è stato verificato sperimentalmente da Bleaney e Loubser [21] e da Loubser, Klein e Townes [22].

Infine nel terzo caso, α è proporzionale al quadrato della pressione e al quadrato della frequenza. Anche questa dipendenza dalla pressione è stata verificata per l'ammoniaca da Birnbaum, Kryder e Lyons [23].

Approssimativamente il massimo dell'assorbimento si presenta per $\nu = \nu_{ij}$; considerazioni più approfondite portano, per il valor massimo del coefficiente di assorbimento alla seguente espressione:

$$\alpha_m = C \frac{\exp[-E_j/kT]}{T^{2+m}} \left(\frac{\nu_{ji}^2 P}{\Delta\nu} + P\Delta\nu \right), \tag{11}$$

che mostra come al crescere della pressione, α_m aumenta con legge di tipo parabolico. Anche questa conclusione sembra confermata in base alle misure di Townes e Merrit [24] e di Becker e Autler [25].

Nell'ipotesi che ogni singola riga sia lontana dalle altre e che $\Delta\nu < 0.2\nu_{ij}$ la formula di Van Vleck-Weisskopf predice con sufficiente approssimazione l'intensità del massimo della riga e la sua indipendenza dalla pressione; predice la struttura generale della riga nell'intorno della frequenza di assorbimento e la dipendenza dell'assorbimento dalla frequenza e dalla pressione nelle ali della riga stessa, lontano dalla frequenza corrispondente al massimo. La forma della riga può considerarsi rappresentata accuratamente nell'intervallo di frequenze di ampiezza doppia di quella che corrisponde a $2\Delta\nu$, e forse anche in un intervallo triplo. Invece, molto lontano dalle frequenze di risonanza, nelle ali lontane dalla riga, nella maggior parte dei casi, le misure di assorbimento danno valori notevolmente maggiori di quelli prevedibili in base alla formula di Van Vleck-Weisskopf.

Il confronto fra l'assorbimento osservato e quello calcolato lontano dalla frequenza di risonanza costituisce un severo esame della validità di qualsiasi teoria dell'assorbimento stesso. Tuttavia è un confronto difficile da eseguire; infatti, se la frequenza di risonanza è molto lontana da quella inviata nel gas e la pressione è sufficientemente bassa per poter considerare le singole righe completamente separate, l'assorbimento è troppo piccolo per poter ottenere misure attendibili; d'altra parte se si investiga l'assorbimento ad alta pressione, derivante da una banda costituita dalla sovrapposizione di molte righe, rimane la difficoltà di sceverare gli effetti derivanti dalle righe singole.

Nel fondare la loro teoria, Van Vleck e Weisskopf partono da semplici considerazioni sulla natura delle collisioni molecolari. Essi distinguono fra collisioni forti e deboli. Una collisione è forte quando, dopo l'urto, una molecola non conserva alcun «ricordo» delle condizioni in cui si trovava prima dell'urto; la collisione è invece debole, quando l'effetto delle collisioni diventa apprezzabile solo dopo un numero rilevante di collisioni. Essi inoltre definiscono «adiabatiche» le collisioni che avvengono in un tempo trascurabile in confronto con il periodo delle oscillazioni del campo elettromagnetico esterno, cui il gas è sottoposto. La loro teoria dell'allargamento delle righe per colli-

sione parte dal presupposto che le collisioni siano forti ed adiabatiche nel senso precedentemente detto. Ma la teoria di Van Vleck-Weisskopf, o una qualunque teoria dello stesso tipo, non lascia completamente soddisfatti, perchè la semilarghezza $\Delta\nu$, o il parametro di allargamento $\Delta\nu/P$ vengono introdotti como parametri empirici. Una teoria più completa dovrebbe esprimere il medesime parametro in base alle forze intermolecolari. D'altra parte i valori di $\Delta\nu$ che si possono ottenere in base alla teoria cinetica classica sono sempre più piccoli di quelli che si determinano sperimentalmente.

Un trattamento completo dell'allargamento derivante dalla pressione e la valutazione di $\Delta\nu$ sono così complessi che hanno permesso trattamenti diversi fra loro e con diversa approssimazione; alcuni sono adatti per lo spettro ottico ed infrarosso, altri per la regione delle microonde.

Le forze intermolecolari, che intervengono nel determinare l'allargamento sono le forze di Van der Waals. I diversi tipi di forze intermolecolari sono esaminati ed elencati nell'opera di Townes e Schawlow: *Microwave Spectroscopy*, p. 348 [26].

Tutti i trattamenti sull'allargamento per effetto della pressione, possono essere suddivisi in: teorie basate sulle collisioni e teorie statistiche.

Le teorie basate sulle collisioni suppongono che durante la maggior parte del tempo le molecole siano sufficientemente lontane fra di loro, così da poter essere considerate libere. Casualmente una molecola si avvicina tanto ad un'altra o a un gruppo di altre molecole, che il campo intermolecolare perturba apprezzabilmente i suoi livelli energetici. Dopo la collisione, la molecola può ritornare nello stato precedente, però con un cambiamento nella fase della radiazione emessa, oppure subisce una transizione in un livello energetico diverso. Ambedue i tipi di collisione contribuiscono all'allargamento delle righe per effetto della pressione. Le teorie delle collisioni ammettono che la radiazione abbia luogo soltanto mentre la molecola è indisturbata, essendo le collisioni di durata brevissima e infrequenti.

Le teorie statistiche considerano le molecole sempre sotto l'azione del campo internucleare, e suppongono che la frequenza radiata dipenda dall'ammontare dell'interazione durante la radiazione.

Le prime forniscono un'approssimazione insufficiente a pressioni tali che le molecole siano molto vicine e quindi le collisioni molto frequenti, perchè trascurano l'irraggiamento durante le collisioni; le seconde sono accettabili soltanto quando le velocità molecolari sono sufficientemente piccole e non sono accurate nel campo delle microonde.

Se ora consideriamo il caso che la pressione sia sufficientemente bassa perchè si possa ammettere che le collisioni avvengano fra due sole molecole (e non fra più molecole), possiamo supporre che a un certo momento una molecola, che ruota od oscilla, e quindi irradia una determinata frequenza, collida con un'altra. Se non vi è perdita di energia per effetto della collisione, dopo la

collisione la molecola oscilla con la stessa frequenza di prima, ma con un cambiamento nella fase, derivante dal fatto che, durante la collisione, la frequenza subisce variazioni in conseguenza dell'interazione fra le molecole. Queste collisioni vengono dette da TOWNES (l. c.) adiabatiche; l'intensità dell'onda irradiata è eguale a quella prima della collisione, e siccome il brusco cambiamento della fase può essere interpretato come uno spettro di frequenze di Fourier, rimane giustificato l'allargamento della riga. Ma può anche accadere che la collisione sia così forte, da determinare un cambiamento di energia, tale da provocare una transizione fra due diversi stati. Collisioni di questo tipo sono state denominate da TOWNES «diabatiche»: dopo una collisione diabatica, le caratteristiche della molecola radiante risultano non correlate con quelle che la molecola possedeva prima dell'urto. È poi possibile mostrare [26], che, quando il cambiamento di fase in una collisione adiabatica è di almeno un radiante, l'energia richiesta per tale cambiamento è, nel campo delle microonde, più grande di quella necessaria per una transizione. Per questa ed anche per altre ragioni, consegue che nel campo delle microonde le collisioni di maggior significato sono quelle diabatiche [27].

Una teoria che tiene adeguato conto delle collisioni diabatiche, e quindi è applicabile nel caso delle microonde, è stata elaborata da ANDERSON [28], la quale, in alcuni casi, può utilmente servire, in unione con i dati sperimentali, a determinare l'ampiezza di alcune forze intermolecolari. La teoria di Anderson parte dalle seguente ipotesi fondamentali:

a) Le molecole che entrano in collisione seguono traiettorie classiche definite.

b) La durata di ogni singola collisione è piccola in confronto al tempo che intercorre fra due collisioni consecutive.

La teoria stessa conduce ad espressioni per il coefficiente di assorbimento e quindi per la forma delle righe, molto simili a quella di Van Vleck-Weisskop, e fornisce espressioni generali per la larghezza delle righe stesse.

Per quanto riguarda la molecola dell'ossigeno $^{16}O_2$, fra tutte le forze di Van der Waals che possono in generale intervenire a determinare l'allargamento delle righe per effetto della pressione, solo alcune vanno prese in considerazione [29]. Intanto la molecola dell'ossigeno non ha momento dipolare elettrico; pertanto le interazioni di Van der Waals a grande raggio d'azione non si presentano. Quelle che rimangono sono quelle dovute al dipolo magnetico, a quadrupolo elettrico molecolare, alla dispersione di London (gli elettroni nella molecola inducono un momento dipolare elettronico) e quelle di scambio (dovute alla interazione diretta delle distribuzioni elettroniche nelle due molecole).

L'interazione per momento dipolare magnetico, nel caso dell'ossigeno, non contribuisce apprezzabilmente all'allargamento delle righe, perchè il diametro di collisione valutato in base a questo solo effetto (stimato in base alla distanza

minima per la quale il cambiamento di fase è un radiante) è troppo piccolo (0.238 Å).

L'allargamento delle righe dell'ossigeno dovuto alla sola azione di quadrupolo elettrico molecolare è stato calcolato da MIZUSHIMA [30] col metodo delle collisioni adiabatiche; il diametro di collisione calcolato col metodo delle collisioni diabatiche, più approssimato (ANDERSON) risulta in questo caso minore di 1.71 Å.

ANDERSON ha calcolato anche l'allargamento provocato dalle forze di dispersione di London; anche questo risulta troppo piccolo, ma fornisce tuttavia il contributo più importante. Per questo solo effetto il coefficiente di allargamento $\Delta\nu/P$ risulta 1.27 MHz/mm (invece di circa 1.92 MHz/mm di Hg, come determinato sperimentalmente).

Un ulteriore contributo è dato anche dalle forze di scambio, dovute all'interazione delle funzioni d'onda.

Tenendo conto solo di questi ultimi due tipi di forze di Van der Waals, ARTMANN e GORDON hanno calcolato il coefficiente di allargamento anzidetto per l'ossigeno, ottenendo risultati generalmente in buon accordo con l'esperienza [29].

In conclusione, con le più recenti teorie si è cercato di dare giustificazione in base alle forze intermolecolari del parametro di allargamento $\Delta\nu/P$, introdotto da VAN VLECK e WEISSKOPF come un parametro sperimentale.

Da quanto precede emerge chiaramente che il problema della determinazione delle frequenze di assorbimento nella gamma delle microonde, per la molecola dell'ossigeno, può considerarsi esaurientemente risolto. Similmente esistono teorie molto approfondite sulla forma delle righe di assorbimento, in dipendenza della frequenza, della pressione e della temperatura, e possiamo aggiungere, in dipendenza della presenza di gas estranei. Tuttavia rimangono ancora oscuri i seguenti punti, che sono oggetto di indagine presso il Centro Microonde.

A) L'assorbimento nelle ali di ogni singola riga, lontano dalla frequenza centrale della riga stessa, appare molte volte maggiore di quello prevedibile in base alle trattazioni teoriche.

B) La forma e la semilarghezza di ogni singola riga, determinata a bassa pressione, quando ogni riga può considerarsi isolata dalle altre, dipendono dalla pressione con una legge nota che è ben confermata dall'esperienza. Quando la pressione aumenta le singole righe si allargano e a poco a poco si fondono, dando luogo ad una unica banda di assorbimento che, per pressioni convenientemente elevate, assume un aspetto simile a quello di una riga isolata. Tuttavia l'andamento di questa banda, come deriva dalla composizione delle singole righe la cui forma sia calcolata con la legge precedentemente indicata, non corrisponde all'esperienza. Da ciò risulta che o le misure sono in errore,

o la dipendenza della larghezza delle righe dalla pressione, a pressioni elevate è diversa da quella fin qui nota per le teorie che sono state elaborate.

Sebbene in questi ultimi tempi siano comparsi lavori che hanno assai attenuato queste discrepanze, sono necessarie ancora approfondite ricerche sia teoriche sia sperimentali per appurare queste questioni, specialmente quella indicata al punto *B*).

3. – Tecniche sperimentali.

L'assorbimento delle microonde nei gas è generalmente rilevato inviando le microonde, generate da un oscillatore adeguato, entro un tratto di guida d'onda contenente il gas alla pressione voluta, e misurando l'energia trasmessa in funzione della frequenza. Il generatore è costituito da un klystron o anche, nel caso di onde millimetriche, da un moltiplicatore di frequenza con cristallo di silicio o di germanio, alimentato da un klystron per onde centimetriche. L'energia trasmessa dal gas investe generalmente un diodo rivelatore, pure costituito da un cristallo semiconduttore. Se la pressione del gas è sufficientemente bassa, così che la larghezza delle righe è dell'ordine del megahertz, è conveniente che la frequenza dell'oscillatore varî periodicamente intorno alla frequenza centrale della riga; ciò può essere semplicemente ottenuto applicando al repulsore del klystron una tensione a denti di sega, sovrapposta alla tensione per la quale il klystron eroga la frequenza centrale della riga. La variazione della frequenza del klystron prodotta da questa tensione (tensione di sweep) può essere dell'ordine di circa 50 MHz. L'uscita del cristallo rivelatore, convenientemente amplificata, può essere direttamente applicata alle placche di deviazione verticale di un oscillografo catodico, mentre alle placche di deviazione orizzontale può essere applicata la tensione usata per la modulazione in frequenza del klystron in modo da ottenere l'asse dei tempi. La rappresentazione oscillografica dell'uscita del cristallo in opportune condizioni di funzionamento dà una rappresentazione della potenza emergente dal gas, e quindi anche della riga di assorbimento.

Infatti per potenze dell'ordine del microwatt, usate nella spettroscopia, il cristallo funziona da rivelatore quadratico, inoltre se la polarizzazione base del repeller del klystron è tale da far oscillare il klystron nella regione centrale del modo, la frequenza erogata dal klystron varia linearmente con la tensione del repeller. Allora la rappresentazione oscillografica della tensione ai capi del cristallo in funzione della tensione del repeller dà la rappresentazione della potenza trasmessa dal gas in funzione della frequenza.

Un simile apparato, corredato delle convenienti strutture a microonde (attenuatori, ondametri ecc.) costituisce il tipo più semplice ed elementare di spettrografo per microonde.

Le limitazioni di tali spettrografi sono assai notevoli. Essi sono adatti per l'osservazione di righe di assorbimento solo quando esso è forte, cioè determina una riduzione della potenza di almeno il 0.1 %. Inoltre il rumore di fondo è notevole.

Un miglioramento considerevole nel rapporto segnale disturbo si ottiene sovrapponendo alla tensione a denti di sega una tensione a media frequenza (per esempio, dell'ordine di 100 kHz) di ampiezza molto piccola, e facendo seguire al cristallo rivelatore un amplificatore accordato su tale media frequenza, un secondo rivelatore, un ulteriore amplificatore video e finalmente l'oscillografo.

Se l'ampiezza della tensione a media frequenza è molto piccola in confronto con quella della tensione a denti di sega, e la frequenza di quest'ultima è molto minore della media frequenza, si può ritenere che, per la prima tensione, la frequenza erogata dal klystron varî rapidamente (100 kHz) in un piccolo intervallo intorno ad un valore centrale, che, lentamente e periodicamente, si sposta per effetto della tensione a denti di sega. Ne segue che ai capi del cristallo rivelatore, che riceve la potenza trasmessa dal gas, sarà presente una tensione alternata, di frequenza pari alla media frequenza e di ampiezza proporzionale alla variazione della potenza trasmessa dal gas nel piccolo intervallo sopra accennato. Pertanto l'ampiezza della tensione a media frequenza ai capi del cristallo rappresenta, con approssimazione tanto migliore quanto più piccola è l'ampiezza della tensione a media frequenza applicata al repeller del klystron, il valore assoluto della derivata della potenza trasmessa in funzione della frequenza. Per la presenza dell'oscillatore accordato sulla frequenza intermedia, solo le componenti di rumore prossime a tale frequenza (nell'esempio 100000 Hz) sono amplificate, da cui consegue il notevole miglioramento del rapporto segnale disturbo.

La modulazione a frequenza intermedia può essere ottenuta, invece che applicando al repulsore del klystron una tensione di pari frequenza, in altro modo, per esempio per effetto Stark. Infatti se un campo elettrico è applicato ad una molecola polare, esso sposta le frequenze di assorbimento; pertanto se a un certo istante la frequenza erogata dal klystron coincide con la frequenza del picco di assorbimento di una riga, l'applicazione al gas di un campo elettrico fa decrescere l'assorbimento. Se il campo elettrico è variabile a frequenza intermedia, ne conseguirà la modulazione desiderata. Un simile sistema non è applicabile all'ossigeno, la cui molecola non è polare.

Nel caso di molecole paramagnetiche si può invece ricorrere all'effetto Zeeman, sottoponendo il gas ad un campo magnetico variabile, come diremo in seguito. Una simile disposizione può essere adottata per la molecola di ossigeno.

Molti altri tipi di spettrografi a microonde sono stati attuati, per i quali rimandiamo alla letteratura. Vogliamo qui piuttosto interessarci alla inter-

pretazione delle rappresentazioni che in generale vengono da essi fornite.

Quando la riga di assorbimento è sufficientemente sottile (circa 1 MHz) e intensa, la forma può essere osservata direttamente sulla rappresentazione oscillografica fornita dal più semplice tipo di spettrografo di cui sopra abbiamo fatto cenno. Occorre naturalmente che la rappresentazione oscillografica sia fedele. Non debbono quindi intervenire distorsioni per effetto della velocità della tensione a denti di sega, della banda degli amplificatori ecc. Ammesso che la rappresentazione sia fedele, in una prima approssimazione, quando le righe sono molto sottili, la larghezza della riga $2\Delta\nu$ può essere determinata in base alla distanza in frequenza fra i punti di flesso della riga stessa. Se questa è $2\delta\nu$, si può dimostrare che è approssimativamente $2\Delta\nu = \sqrt{3}\cdot 2\delta\nu$. Con migliore approssimazione scritta la formula di Van Vleck nella forma semplificata $\alpha = \alpha_1\big(\Delta\nu/((\nu-\nu_0)^2+\Delta\nu^2)\big)$, ove α_1 è una costante le cui dimensioni sono $(\text{s cm})^{-1}$, è:

$$\Delta\nu = \sqrt{3}\delta\nu - \tfrac{1}{4}\alpha_1 l + \frac{1}{16\sqrt{3}\delta\nu}(\alpha_1 l)^2 ,$$

ove l è la lunghezza della cella che contiene il gas.

Il riconoscimento dei punti di flesso sulla rappresentazione della curva di assorbimento non è cosa agevole. Molto più comoda è la determinazione dei punti di flesso quando lo spettrografo è a doppia modulazione e quindi fornisce la rappresentazione del modulo della derivata della curva di assorbimento, che naturalmente, anche in questo caso dovrà essere fedele.

Per quanto riguarda la fedeltà della rappresentazione occorre prendere in considerazione l'ampiezza e la frequenza di sweep, in relazione alla larghezza della riga. Se tali grandezze sono eccessive, la rappresentazione risulta distorta: tali distorsioni sono state studiate [31] e sono state riconosciute le condizioni sotto le quali esse possono considerarsi trascurabili.

Un notevole miglioramento del rapporto segnale disturbo si ottiene se in luogo del secondo rivelatore di tipo comune, che rileva il modulo della derivata della curva di assorbimento, si fa uso di un rivelatore sensibile alla fase (lock-in detector), con il quale si ottiene la rappresentazione della stessa derivata in grandezza e segno e la banda passante risulta estremamente ridotta.

La separazione Zeeman delle righe dell'ossigeno è stata ultimamente studiata da Hill e Gordy [32], da Henry [33] e da Tinkham e Strandberg [34]. Uno spettrografo Zeeman per l'ossigeno consiste essenzialmente in un generatore a klystron, seguito eventualmente da un dispositivo per la moltiplicazione di frequenza; la cella è costituita da uno spezzone di guida d'onda, circondato da un solenoide per generare il campo magnetico. Lo spezzone è convenientemente tagliato per l'eliminazione delle correnti parassite conseguenti alle variazioni del campo magnetico. Variando la corrente nel solenoide, il campo magnetico, orientato nella direzione dell'asse della guida, provoca la separazione di

livelli rotazionali. Si ottengono così le righe Zeemann, la cui separazione dipende dalla intensità del campo. Poichè tale separazione è indipendente dal verso del campo, le righe vengono modulate ad una frequenza doppia di quella del campo; per evitare ciò ed ottenere una modulazione della stessa frequenza f_c del campo, basta che la componente della corrente alternativa che lo genera sia sovrapposta ad una componente continua di conveniente intensità, in modo che la legge di variazione del campo sia [35] della forma $1+\cos 2\pi f_c t$. Inoltre, poichè i detti campi magnetici sono dello stesso ordine del campo magnetico terrestre (ordine del gauss), è necessario compensare l'effetto Zeemann prodotto da quest'ultimo. La compensazione si ottiene orientando l'asse della cella e del solenoide nella direzione del campo magnetico terrestre e introducendo nel solenoide una opportuna corrente.

Generalmente la rivelazione è fatta con un rivelatore sensibile alla fase, con segnale di riferimento alla stessa frequenza del campo, e con banda passante di circa 1 Hz, e quindi con minimo rumore di fondo. La frequenza intermedia, cioè la frequenza del campo magnetico è generalmente bassa, circa 4000 Hz; pertanto occorre che la frequenza della tensione a denti di sega sia molto bassa, ciò che esclude la possibilità dell'impiego di oscillografi catodici e impone l'adozione di registratori meccanici.

Le curve che si ottengono con questo tipo di modulazione sono la derivata seconda della curva di assorbimento [36].

Fin qui si è supposto che il campo magnetico sia molto debole, dell'ordine del gauss, tanto che si rende necessaria la compensazione del campo magnetico terrestre. Esistono tuttavia disposizioni in cui si è fatto uso di campi magnetici molto intensi; tanto intensi che le frequenze di risonanza paramagnetiche (Zeeman) risultano molto inferiori delle frequenze normali di assorbimento, in assenza del campo [37].

Una tecnica assai diversa è stata recentemente messa a punto da Artmann e Gordon [29], che hanno eseguito determinazioni sull'ossigeno sia a bassa sia ad alta pressione. Essi hanno fatto uso del metodo così detto a cavità non accordata, che è adatto per misure di allargamento e di intensità assoluta. Purtroppo la precisione di tale disposizione non sembra sufficiente per eliminare le discrepanze fra teoria ed esperienza tuttora in discussione.

Le microonde sono introdotte, in questo tipo di spettrografo, in una cavità di grandissime dimensioni in confronto con la lunghezza d'onda, così che gran numero di modi possono essere contemporaneamente presenti. Un ventilatore, nell'interno della cavità funziona da mescolatore di modi, in quanto le sue pale, agitandosi, mutano continuamente le condizioni al contorno. La radiazione viene modulata in ampiezza a bassa frequenza (20 Hz) tramite un attenuatore mosso da un motore. Nella cavità è disposta una catena di bolometri, la cui risposta risulta modulata alla stessa frequenza; la risposta stessa viene inviata ad un amplificatore accordato ad alto guadagno e a banda stretta; l'uscita

di tale amplificatore viene infine rettificata e misurata con un convenzionale dispositivo a potenziometro. Le misure vengono così ottenute per punti, ma è possibile l'impiego di dispositivi registratori.

Le osservazioni da ARTMANN e GORDON sono state compiute per pressioni comprese fra 2 e 10 mm_{Hg}; il parametro di allargamento $\Delta\nu/P$ e l'intensità di picco risultarono indipendenti dalla pressione, ciò che conferma che l'allargamento è essenzialmente dovuto agli urti. L'andamento delle righe di assorbimento fu trovato entro i limiti degli errori sperimentali conforme alla formula di Van Vleck-Weisskopf. Col medesimo metodo fu determinato anche l'assorbimento dell'ossigeno in aria secca e alla temperatura ambiente alle pressioni di $\frac{1}{4}$ e $\frac{1}{2}$ atmosfera, al fine di determinare se l'assorbimento ad alta pressione, possa essere determinato in base alle misure compiute a bassa pressione. Anche in questo caso l'incertezza sperimentale è stata maggiore degli errori probabili statistici.

Nonostante dunque l'alto livello del lavoro compiuto in questi ultimi tempi, le questioni indicate non sono ancora chiarite. Come già detto presso il Centro Microonde ci si sta attrezzando per tali ricerche (in relazione ad un contratto sollecitato dalle Forze Aeree Americane). Con la collaborazione dell'Istituto di Fisica dell'Università di Pisa (dott. GOZZINI) è stata elaborata una nuova tecnica per le misure ad alta pressione, che sono le più discusse, mentre al Centro è attualmente quasi pronto uno spettrografo a doppia modulazione per l'ossigeno.

Tale tecnica permette lo studio della dispersione e dell'assorbimento dell'$^{16}O_2$, in funzione della pressione, fino a pressioni dell'ordine di una atmosfera, ed in un intervallo assai vasto di frequenze.

Si determina, ad una pressione prefissata, la differenza del coefficiente di assorbimento e dell'indice di rifrazione a due frequenze diverse, confrontando direttamente la variazione prodotta dal gas del Q e delle frequenze di risonanza di due cavità, risonanti a frequenze diverse [38].

REFERENZE

[1] R. BERINGER: *Phys. Rev.*, **70**, 53 (1946).
[2] Y. H. VAN VLECK: *Phys. Rev.*, **71**, 412 (1947).
[3] Y. H. VAN VLECK: *Astrophys. Journ.*, **80**, 161 (1934).
[4] H. R. LAMONT: *Phys. Rev.*, **74**, 353 (1948).
[5] M. W. P. STRANDBERG, C. Y. MENG and Y. G. INGHERSOLL: *Phys. Rev.*, **75**, 1526 (1949).
[6] Y. H. BURGHALTER, R. S. ANDERSON, W. V. SMITH and W. GORDY: *Phys. Rev.*, **77**, 152 (1950).
[7] R. S. ANDERSON, C. M. JOHNSON e W. GORDY: *Phys. Rev.*, **83**, 1061 (1951).
[8] H. A. KRAMERS: *Zeits. f. Phys.*, **53**, 422 (1929).

[9] M. H. Hebb: *Phys. Rev.*, **49**, 610 (1936).
[10] R. Schlapp: *Phys. Rev.*, **51**, 342 (1937).
[11] Y. H. Burghalter, R. S. Anderson, W. V. Smith e W. Gordy: *Phys. Rev.*, **79**, 651 (1950).
[12] S. L. Miller e C. H. Thownes: *Phys. Rev.*, **90**, 537 (1953).
[13] M. Mizushima e R. M. Hill: *Phys. Rev.*, **93**, 745 (1954).
[14] M. Tinkham e M. W. P. Strandberg: *Phys. Rev.*, **97**, 937 (1955).
[15] Y. H. Van Vleck e W. F. Weisskopf: *Rev. Mod. Phys.*, **17**, 227
[16] H. A. Lorentz: *Proc. Amst. Akad. Sci.*, **8**, 591 (1906).
[17] P. Debye: *Polar Molecules* (New York, 1929).
[18] A. Meckler: *Journ. Chem. Phys.*, **21**, 1750 (1953).
[19] G. H. Townes: *Phys. Rev.*, **70**, 665 (1946).
[20] B. Bleaney e R. P. Penrose: *Proc. Phys. Soc.*, **60**, 83 (1948).
[21] B. Bleaney e Y. N. Loubser: *Proc. Phys. Soc.*, A **63**, 483 (1950).
[22] Y. H. N. Loubser, Y. Klein e C. H. Townes: *Quart. Progr. Rep. Columbia. Rad. Lab., Phys. Dep. Columbia University.*
[23] G. Birmbaum, S. Y. Kryder e H. Lyons: *Journ. Appl. Phys.*, **22**, 95 (1951).
[24] C. H. Townes e F. R. Merritt: *Phys. Rev.*, **70**, 558 (1946).
[25] G. E. Becker e S. H. Autler: *Phys. Rev.*, **70**, 300 (1946).
[26] C. H. Townes e A. L. Schwalow: *Microwave Spectroscopy* (New York, 1955), p. 351.
[27] C. H. Townes e A. L. Schawlow: *Microwave Spectroscopy* (New York, 1955), p. 355.
[28] P. W. Anderson: *Phys. Rev.*, **76**, 647 (1949).
[29] Y. O. Artman e Y. P. Gordon: *Phys. Rev.*, **96**, 1237 (1954).
[30] M. Mizushima: *Phys. Rev.*, **83**, 94 (1951).
[31] N. Carrara, M. Schaffner e F. Verzocchi: *Technical Report* no. 9, Conctract no. AF 61 (514) 433 USAF ARDC.
[32] M. Hill e W. Gordy: *Phys. Rev.*, **93**, 1019 (1954).
[33] A. Henry: *Phys. Rev.*, **80**, 396 (1950).
[34] M. Tinkham e M. W. P. Strandberg: *Phys. Rev.*, **97**, 937 (1955).
[35] R. S. Anderson, W. V. Smith e W. Gordy: *Phys. Rev.*, **87**, 561 (1952).
[36] Y. H. Burghalter, R. S. Anderson, W. V. Smith e W. Gordy: *Phys. Rev.*, **79**, 651 (1950), Appendix A.
[37] R. Beringer e Y. G. Castle: *Phys. Rev.*, **81**, 82 (1951).
[38] A. Battaglia e A. Gozzini: *Technical Report* no. 8, Contract no. AF 51 (514) 43 USAF ARDC; *Onde Electrique*, Maggio 1955; *Nuovo Cimento* (in corso di stampa).

PROPRIETÀ LETTERARIA RISERVATA

Direttore responsabile: G. POLVANI Tipografia Compositori - Bologna

Questo fascicolo del *Supplemento* è stato licenziato dai torchi il 22-XII-1956.